

On Nitrogen in Aromatic Frameworks: Studies of Especially Electron-Deficient 1,1-
Diarylhydrazines and their Derivatives

By

Joël Poisson

*A thesis submitted to McGill University in partial fulfillment of the requirements of the
degree of*

Doctor of Philosophy

Department of Chemistry

McGill University

Montreal, Quebec

Canada

© Joël Poisson August 2015

To my grandmaman Claire N. Déziel.

Abstract

The synthesis of stable aromatic compounds containing nitrogen that is in some way electron-deficient for use as ligands is a relatively unexplored area of Chemistry. Recent coordination of triazolium cations to transition metals has shown that these compounds should be useful in synthesis and materials chemistry. The study of electron-deficient nitrogen in aromatic frameworks will permit the assessment of its properties in comparison to the triazolium species and offer a route to the synthesis of N-heterocycles that are inherently electron-poor.

To illustrate the typical reactivity of N-heterocycles, the triphenyl-metal-pyrrolides and indolides of the group 14 metals (Ph_3MR , $\text{M} = \text{Si}, \text{Ge}, \text{Sn}$, $\text{R} = \text{C}_4\text{H}_4\text{N}$ or $\text{C}_8\text{H}_6\text{N}$) have been synthesized by N-lithiation and subsequent nucleophilic substitution. The two groups of compounds are contrasted, showing the increase in thermal stability and decrease in N-Metal lability in going from the pyrrole to the indole analogues. The reactive nature of the pyrrole unit is also noted, with yields increasing for longer reaction times and lower temperatures due to suppression of pyrrole self-polymerization. Structural data on $\text{Ph}_3\text{Si}(\text{Pyr})$ show it to be disordered in the crystal lattice.

1-(2-nitrophenyl)-1-phenylhydrazine was prepared by Hofmann rearrangement under oxidative conditions and the key intermediates in the rearrangement were structurally characterized by single-crystal X-ray diffraction. The reaction from the starting amine with chlorosulfonyl isocyanate to give the urea proceeds through an isolable sulfimidate intermediate, which is held together by a hydrogen-bonding network. Inhibition of these bonds results in the decomposition of the sulfimidate to give the corresponding urea. Use of calcium hypochlorite in lieu of the more variable sodium salt in the final Hofmann rearrangement results in high yields of the corresponding hydrazine, which can be isolated in crystalline form.

Reaction of 1-(2-nitrophenyl)-1-phenylhydrazine with carbonyl compounds allowed the production of several derivatives, which could be used to study the electronics at nitrogen in 1,1-diarylhydrazine N-N bonds. Single-crystal diffraction data show that depending on the substituents on either side of the hydrazine N-N bond, the interaction can range from reactive and sp^3-sp^3 to stable and sp^2-sp^2 in nature. Examination of the substituent orientations in these compounds reveals the strength of these N-N bonds is due primarily to σ -bonding effects, with little to no π -contribution. From this information, a new formal description of N-N bonding in 1,1-diarylhydrazines is proposed.

Analogous reactions of carbonyl compounds with 9-aminocarbazole show the importance of phenyl ring mobility with respect to π -overlap disruption in 1,1-diarylhydrazines. These compounds contain consistently shorter N-N bonds than their analogues derived from 1-(2-nitrophenyl)-1-phenylhydrazine. Enforcement of planarity by the carbazole ring system facilitates π -contributions to the N-N bonding by extending the aromaticity over the entire -diaryl moiety. The stability granted by these contributions; however, is found to be minimal and σ -effects continue to dominate the bonding interaction.

To evaluate the properties of the synthesized 1,1-diarylhydrazines as ligands and as N-heterocyclic precursors, their reactions with metals were examined. Cadogan cyclization of 1-(2-nitrophenyl)-1-phenylhydrazine results in the formation of 1-phenylbenzotriazole in high yield and purity, with no evidence of formation of the 2-regioisomer. The reaction of the Schiff base from salicylaldehyde of 9-aminocarbazole with $Ru(H)(Cl)(CO)(PPh_3)_3$ was performed. X-ray diffraction data shows the compound to be sterically encumbered, resulting in exceptionally long Ru-phosphine, Ru-N, Ru-O and N-N bonds. These characteristics are attributed to a lack of π -backbonding from the metal centre coupled with a complete disruption of π -delocalization of the ligand N-

lone pairs, resulting in increased N-N repulsion. The analogous reaction with the Schiff base derived from 1-(2-nitrophenyl)-1-phenylhydrazine was unsuccessful.

Résumé

La synthèse de composés aromatiques qui contiennent un atome d'azote ayant, d'une manière ou d'une autre, une déficience sur sa densité électronique qui pourrait être utilisé en tant que ligand est un domaine de la chimie qui demeure encore inexploré. La coordination des triazoliums cationiques à des métaux de transition a démontré que ce type de composés devrait être utile en synthèse ainsi que dans la chimie des matériaux. Nous avons axé la recherche sur la chimie des atomes d'azotes ayant une carence sur leur densité électronique dans des systèmes aromatiques afin de savoir si de tels systèmes manifestaient des caractéristiques propres aux triazoliums et s'ils pourraient être utilisés dans la synthèse de composés N-hétérocycliques qui soient intrinsèquement en déficience électronique.

Les triphénylpyrroles et triphénylindoles des éléments de la colonne 14 du tableau périodique (Ph_3MR , $\text{M} = \text{Si, Ge, Sn}$, $\text{R} = \text{C}_4\text{H}_4\text{N}$ or $\text{C}_8\text{H}_6\text{N}$) ont été préparés à partir de substitutions nucléophiles des sels de lithium des hétérocycles avec les chlorures métalliques correspondantes. Une comparaison des pyrrolides et de leurs indolides correspondants montre un gain de stabilité en passant de pyrrole à indole. La réactivité innée du pyrrole est notée, avec un meilleur rendement lorsque le temps de réaction est augmenté et quand la température est maintenue à un minimum en raison de la répression de son auto-polymérisation. L'analyse de la structure du $\text{Ph}_3\text{Si}(\text{Pyr})$ en état cristallin confirme que ce composé est en treillage désordonné.

Le composé 1-(2-nitrophényle)-1-phénylhydrazine a été préparé par réarrangement de Hofmann sous des conditions oxydantes et les structures des intermédiaires de la séquence ont été déterminées par diffraction de rayons-X. La réaction de l'amine de départ avec l'isocyanate de chlorosulfonyl menant à l'urée passe par un sulfimidé isolable qui est maintenue par un réseau de liaisons hydrogène. L'interruption de ce réseau entraîne une décomposition du sulfimidé en son urée correspondante. L'utilisation de l'hypochlorite de calcium, au lieu de son analogue à

base de sodium qui est plus variable en composition durant le réarrangement final, donne un plus grand rendement de l'hydrazine et permet de l'isoler à l'état cristallin.

La réaction du 1-(2-nitrophényle)-1-phénylhydrazine avec des composés carbonylés a donné plusieurs dérivées qui ont pu être utilisées afin d'étudier le comportement électronique de l'azote en ce qui concerne les liaisons N-N des 1,1-diarylhydrazines. L'analyse structurale de ces cristaux par diffraction de rayons-X démontre que la longueur de cette liaison dépend des propriétés des substituants sur les deux atomes d'azote et qu'elle peut varier d'une liaison sp^3-sp^3 qui est relativement longue à une liaison sp^2-sp^2 qui est beaucoup plus forte et plus courte. Une interprétation de l'orientation des substituants dans ces composés révèle que la puissance de ces liaisons azotées résulte d'un renforcement du chevauchement σ avec une contribution π qui est négligeable. D'après cette information, un schéma par rapport aux liaisons N-N dans les 1,1-diarylhydrazines est formulé.

Certains des carbonylés qui ont été utilisés pour faire les dérivées du 1-(2-nitrophényle)-1-phénylhydrazine ont réagis avec le 9-aminocarbazole. Les dérivées ainsi produites démontrent l'importance de la mobilité des regroupements aromatiques sur l'interruption du chevauchement π chez les 1,1-diarylhydrazines. Ces composés possèdent des liaisons N-N systématiquement plus courtes que leurs dérivées correspondantes venant du 1-(2-nitrophényle)-1-phénylhydrazine. L'imposition d'un arrangement planaire au niveau géométrique/structural de la molécule par le carbazole facilite une contribution π aux liaisons N-N en renforçant l'aromaticité de la molécule. Le gain de stabilité attribué à celle-ci est subitement plus faible et l'interaction σ domine toujours.

Afin d'évaluer les caractéristiques des 1,1-diarylhydrazines qui ont été préparés en tant que ligands et précurseurs à des hétérocycles-N, leurs interactions avec des métaux de transition ont été étudiées. Le 1-(2-nitrophényle)-1-phénylhydrazine, sous conditions de cyclisation de Cadogan, donne le 1-phénylbenzotriazole de haute pureté

avec un bon rendement sans aucune preuve d'une quelconque production de l'isomère substitué à la 2^e position. Les bases de Schiff venant de la réaction du 9-aminocarbazole ou du 1-(2-nitrophényle)-1-phénylhydrazine ont été réagis avec le $\text{Ru(H)(Cl)(CO)(PPh}_3)_3$. L'analyse par diffraction de rayons-X révèle que le composé dérivé du carbazole possède un grand encombrement stérique qui se manifeste par un rallongement des liaisons Ru-phosphine, Ru-N, Ru-O et N-N. Ces caractéristiques sont attribuées à un manque de rétrodonation π de la part du centre métallique ainsi qu'une interruption de la délocalisation des doublets non liants des azotes, qui engendre une augmentation de la répulsion entre ceux-ci. Une tentative pour exécuter la même réaction avec la base de Schiff provenant du 1-(2-nitrophényle)-1-phénylhydrazine s'est révélée infructueuse.

Acknowledgements

What an experience! The only comparison I can draw to describe the doctoral journey is that of a very challenging marathon. As with any big race, there are many people to thank at the end. First and foremost, the coaches. My sincere thanks to both of my supervisors, Profs. Ian S. Butler and D. Scott Bohle. Their steadfast guidance and patience and their free-spirited philosophies made relevant Chemistry a treat by adding an air of exploration to the equation in addition to the quest for practically useful results. Next, I must thank the numerous teammates I've had throughout this particular race. Between the never-ending encouragement from members of the Bohle lab past and present, particularly Wei Gu, Laura Brothers, Inna Perepichka, Kris Rosadiuk, Zhijie Chua, Mirna Paul and Cassidy Vanderschee during one of my inevitable rants, to the plethora of interesting and knowledgeable people that made up the shifting sands of the Butler lab, particularly Dr. Mirela Barsan, I was always in great company. I must also thank the department of Chemistry. Because of the numerous lab moves throughout my studies, I was able to forge strong relationships with many different groups of people covering all areas of the chemical sciences. These numerous moves also taught me invaluable time management and leadership skills that I will carry with me forever. Thanks to the Kakkar group, specifically Tina Lam, for many, many helpful discussions. I must also thank Prof. Amy S. Blum for giving me a permanent home on the 3rd floor of pulp and paper where I learned so much having been surrounded by such a diverse group of people all working on fields far removed from my exploratory reactions with colourful nitrogen compounds.

I would like to give a special thanks to Prof. Ivor Wharf for teaching me all of the practical tricks of the trade. His patience as I learned to set up distillations without causing a fire was a godsend. He also imparted on me an appreciation of not only how to do good Chemistry, but recognize that it should be done elegantly. I would not have come this far had it not been for him.

As with any race, there is no game without the organisers. In this case, that means the tireless work of Nadim Saddé and Dr. Alexander Wahba in the mass spectrometry department as well as Dr. Fred Morin for help with difficult NMR experiments. Special thanks to Richard Rossi and Weihua of the electronics shop for assisting with numerous moves of the Raman microscope, Jean-Philippe Guay for doing the groundwork on finding gaskets for the diamond anvil cell and Claude Perriman and Mario Perrone for keeping an eye on our budget. On the administrative side, I must thank the tireless staff of the departmental offices, specifically Chantal Marotte for her never-ending understanding and encouragement, especially in the months following my car accident. I could not have fared nearly as well without her. Thanks to Karen Turner for all of her help and patience and also to Linda Del Paggio for somehow keeping track of all of my keys over my 8 years in the department. Last but not least, a big thanks to Elena Nadezhina of the Laboratoire d'analyse élémentaire for all of her hard work over the years. These talented people made seemingly arduous experimental and practical endeavours so much easier and they all contributed invaluable to a truly great experience.

Lastly, I would like to thank the supporters. The list is long. I would like to first thank my family, both immediate and extended. Mom, Dad, Christian, Claire, Peter, Conor and Dylan, your continued support and encouragement were the best fuel one could ask for. Through moves, accidents, obstacles, training and lastly writing, you somehow always kept my spirits up and focused on the finish line. Then, of course there's the cheering squad throughout the race, my friends and esteemed co-workers. Katalin Korpany, Omar Zahr, Julia Del Re, Josh Lucate, Julia Bayne, Emily Hopkins, Angelica Gopal, Alexei Kazarine, Laure Devigne, Mohini Ramkaran, Beccah Frasier, Andrea Hill, Marc Travers, Samantha Stratton, Elizabeth Ladd, Joe McLaughlin, Nissa LeBaron and Steve. You all really made my time in Montréal truly unforgettable and I wait on bated breath for the next of our awesome adventures.

Contribution of Authors

This dissertation is comprised of 3 papers presented in chapters 2-4 and 2 chapters of unpublished work (Chapters 5 and 6). Chapters 2 and 3 have already been published and chapter 4 has been submitted for publication. A thorough introduction to the thesis subject is presented in Chapter 1. The work presented in this thesis was performed in the laboratories of Professors Ian S. Butler and D. Scott Bohle. Contributions of the authors are detailed below.

Statement of originality and contribution to knowledge

In all instances, conception, setup and execution of experiments, as well as purification of synthesized compounds and data analysis in each chapter were performed by the author. The author was involved in interpretation of results and direction of the investigations in conjunction with Professors I. S. Butler and D. Scott Bohle. All work presented in this thesis, with the exception of the introductory literature review, is declared by the author to be original scholarship and distinct contributions to knowledge as is mandatory for doctoral theses. Co-authors were responsible for making the following contributions:

In Chapter 2, the crystal structure of compound **5** was obtained and refined by Yuxuan Gu. Dr. Ivor Wharf assisted with training the author in manipulation of the air-sensitive reagents and products as well as in performing complicated manipulations. Mirela M. Barsan aided in the acquiring and analysis of the Raman spectra of the pyrrolides.

In Chapter 3, the structure of sodium 1-(2-nitrophenyl)-1-phenylcarbamoylsulfimide pentahydrate was elucidated in collaboration with Cheryl D. Bain. The initial preparation of Methyl 4-((2-nitrophenyl)amino)benzoate was carried out by Julia M. Bayne under the guidance of the author. Professor D. Scott Bohle was responsible for the section on Density Functional Theory calculations.

In Chapters 3 to 5 Professor D. Scott Bohle performed the DFT calculations and aided in the interpretation of the results.

TABLE OF CONTENTS

PAGE

1	1
1.1	DEFINITIONS OF ELECTRON-DEFICIENT NITROGEN 1
1.2	GEOMETRIC AND ELECTRONIC STRUCTURE 3
1.3	SYNTHESIS OF ISOLABLE ELECTRON-DEFICIENT NITROGEN SPECIES 10
1.4	COORDINATION CHEMISTRY OF TRIAZOLIUM CATIONS 12
1.5	REACTIVITY OF 1,2,3-TRIAZOLIUM AND -BENZOTRIAZOLIUM CATIONS 15
1.6	GENERATION AND REACTIVITY OF NITRENE INTERMEDIATES 16
1.6.1	FROM $ArINT_s$ SYSTEMS 16
1.6.2	FROM AZIDES 20
1.6.3	REARRANGEMENTS INVOLVING NITRENE INTERMEDIATES 27
1.6.3.1	THE CURTIUS REARRANGEMENT 27
1.6.3.2	THE LOSSEN REARRANGEMENT 28
1.6.3.3	THE HOFMANN REARRANGEMENT 31
1.6.3.4	THE SCHMIDT REACTION 33
1.6.4	REACTIVITY OF NITRENE INTERMEDIATES 36
1.6.5	CATALYZED AZIRIDINATION REACTIONS 38
1.6.6	COORDINATION CHEMISTRY OF NITRENES 43
1.7	CONCLUSION 44
1.8	REFERENCES 45
2	64
2.1	PREAMBLE 64
2.2	INTRODUCTION 65
2.3	RESULTS AND DISCUSSION 66
2.3.1	NMR SPECTRA 68

2.3.2	MASS SPECTRA	68
2.3.3	RAMAN SPECTRA	70
2.3.4	SINGLE-CRYSTAL X-RAY DIFFRACTION STUDY OF (5)	71
2.4	CONCLUSIONS	72
2.5	EXPERIMENTAL	73
2.5.1	GENERAL METHODS	73
2.5.2	SYNTHESES	74
2.6	ACKNOWLEDGEMENTS	76
2.7	REFERENCES	77
3		80
3.1	PREAMBLE	80
3.2	INTRODUCTION	82
3.3	RESULTS AND DISCUSSION	83
3.4	CONCLUSIONS	99
3.5	EXPERIMENTAL	99
3.5.1	GENERAL METHODS	99
3.5.2	SYNTHESES	100
3.5.3	X-RAY CRYSTALLOGRAPHY	104
3.5.4	THEORETICAL METHODS	104
3.6	ACKNOWLEDGEMENTS	105
3.7	REFERENCES	105
4		110
4.1	PREAMBLE	110
4.2	INTRODUCTION	112
4.3	RESULTS AND DISCUSSION	113

4.4	CONCLUSIONS	128
4.5	EXPERIMENTAL	129
4.5.1	GENERAL METHODS	129
4.5.2	SYNTHESES	130
4.5.3	X-RAY CRYSTALLOGRAPHY	133
4.5.4	THEORETICAL METHODS	134
4.6	ACKNOWLEDGEMENTS	134
4.7	REFERENCES	134

5		139
----------	--	------------

5.1	PREAMBLE	139
5.2	INTRODUCTION	140
5.3	RESULTS AND DISCUSSION	143
5.4	CONCLUSIONS	154
5.5	EXPERIMENTAL	154
5.5.1	GENERAL METHODS	154
5.5.2	SYNTHESES	155
5.5.3	X-RAY CRYSTALLOGRAPHY	159
5.5.4	THEORETICAL METHODS	159
5.6	ACKNOWLEDGEMENTS	160
5.7	REFERENCES	160

6		164
----------	--	------------

6.1	PREAMBLE	164
6.2	INTRODUCTION	165
6.3	RESULTS AND DISCUSSION	170
6.4	CONCLUSIONS	175

6.5	EXPERIMENTAL	176
6.5.1	GENERAL METHODS	176
6.5.2	SYNTHESES	177
6.5.3	X-RAY CRYSTALLOGRAPHY	178
6.6	ACKNOWLEDGEMENTS	178
6.7	REFERENCES	178
7		185
7.1	SUMMARY	185
7.2	FUTURE WORK	188
7.3	REFERENCES	188
APPENDICES		190
APPENDIX A		190
APPENDIX B		192
APPENDIX C		202
APPENDIX D		209
APPENDIX E		218

LIST OF FIGURES

Page

Chapter 1

Figure 1-1: Electronic ground-state configurations of electron-deficient carbon and nitrogen-based analogues.	2
Figure 1-2 : Triplet and singlet electron configurations.	3
Figure 1-3: General structure of benzotriazolium and triazolium cations.	5
Figure 1-4: Resonance-stabilized classical nitrene transfer reagents.	6
Figure 1-5: Intramolecular bonding in early PhINTs reagents.	7
Figure 1-6: Synthesis of stabilized ArINTs derivatives.	8
Figure 1-7: Generation of benzotriazolium cations by N-alkylation.	10
Figure 1-8: Synthesis of 1,3-diaminotriazolium tosylate.	11
Figure 1-9: Selected examples of coordinated NHC and triazolium-based ligands.	13
Figure 1-10: Use of triazolium cations in catalysis.	15
Figure 1-11: Representative triazolium salt as a redox bridge.	16
Figure 1-12: Silver-catalyzed nitrene generation and C-H bond insertion using linear amines.	18
Figure 1-13: Use of ArINTs-based systems for the synthesis of novel boranes.	19
Figure 1-14: Rearrangement upon photolysis of alkyl azides.	20
Figure 1-15: Photo-rearrangement of di-substituted derivatives of 2-biphenylmethyl azide.	21
Figure 1-16: Processes in the photochemistry of α -benzoyl- ω -azidoalkenes.	22
Figure 1-17: Competitive processes upon photolysis of carbonyl-containing azides.	23
Figure 1-18: Photodecomposition pathways of phenyl azide.	25
Figure 1-19: Curtius rearrangement of a suitable urea.	27
Figure 1-20: Schematic representation of the Lossen rearrangement.	29

Figure 1-21: Heck reaction resulting in Lossen rearrangement.	30
Figure 1-22: Preparation of a small-molecule GCS inhibitor by a scalable Lossen rearrangement.	31
Figure 1-23: Nitrene generation from the Hofmann rearrangement of urea.	31
Figure 1-24: Hofmann rearrangement vs. intramolecular C-H insertion.	32
Figure 1-25: Nitrene generation during the Schmidt reaction.	33
Figure 1-26: Intra-molecular trapping of isocyanate generated <i>via</i> Schmidt reaction.	34
Figure 1-27: Synthesis of phenanthridines from biphenylazides.	35
Figure 1-28: Possible decomposition routes for intermediates in the Schmidt reaction.	36
Figure 1-29: Typical reactions of nitrenes.	37
Figure 1-30: Mechanisms of reactions of singlet and triplet nitrenes with alkenes.	38
Figure 1-31: Lewis base-catalyzed ring expansion of aziridinofullerenes (1) with heterocumulenes.	40
Figure 1-32: Copper-catalyzed aziridination of olefins.	41
Figure 1-33: Equality of azide and PhINTs-derived nitrenes.	42
Figure 1-34: Isolation of bridging and di-imido complexes derived from nitrenes.	43

Chapter 2

Figure 2-1: General structure of pyrrolides and indolides.	66
Figure 2-2: Mass spectrum decomposition of group 14 pyrrolides and indolides.	69
Figure 2-3: ORTEP representation of the asymmetric unit of Ph ₃ Si(Pyr).	71

Chapter 3

Figure 3-1: ORTEP representation of the solid structure of the dianion in 1-(2-nitrophenyl)-1-phenylcarbamoysulfimidate pentahydrate (1)	85
Figure 3-2: ORTEP representations of 1-(2-nitrophenyl)-1-phenylurea and methyl-4-(1-(2-nitrophenyl)ureido)benzoate.	87

Figure 3-3: ORTEP representations of 1-(2-nitrophenyl)-1-phenylhydrazine.	89
Figure 3-4: Optimized structures for the intermediates for the Hofmann rearrangement of 1,1-diphenylurea.	94
Figure 3-5: Density functional theory results.	97

Chapter 4

Figure 4-1: ORTEP representation of one molecule in the asymmetric unit of compound 1.	116
Figure 4-2: ORTEP representation of compound 2.	117
Figure 4-3: ORTEP representation of compound 3.	119
Figure 4-4: ORTEP representation of compound 4.	122
Figure 4-5: Intra-molecular hydrogen bonding in 4.	122
Figure 4-6: ORTEP representation of compound 5.	123
Figure 4-7: Variation in C-N bond length with N-N separation.	125
Figure 4-8: Calculated orbital compositions in 5.	128

Chapter 5

Figure 5-1: Structures and acidity constants of N-heterocycles.	140
Figure 5-2: ORTEP representation of AC.	144
Figure 5-3: ORTEP representation of one molecule in the asymmetric unit of compound 1.	147
Figure 5-4: ORTEP representation of compound 2.	149
Figure 5-5: ORTEP representation of compound 3.	150
Figure 5-6: Variation in C-N bond length with N-N separation.	152

Chapter 6

Figure 6-1: Reactivity of phenylhydrazines with carbonyl-containing alkynes.	165
--	-----

Figure 6-2: NAr ₂ substituent effects on C-T bands in hydrazido metal complexes.	166
Figure 6-3: Synthesis of 1-hydroxybenzotriazole.	167
Figure 6-4: Typical N-alkylation of benzotriazole resulting in a mixture of 1- and 2-alkyl substitution products.	168
Figure 6-5: Synthetic routes to 1-(2-nitrophenyl)-1-phenylhydrazine.	169
Figure 6-6: Synthesis of 1-phenylbenzotriazole <i>via</i> Cadogan cyclization of NDPH.	170
Figure 6-7: Possible mechanisms for benzotriazole formation from NDPH.	171
Figure 6-8: New polymorph of 1-phenylbenzotriazole.	172
Figure 6-9: ORTEP representation of (1).	174

Appendix B

Figure S1: Hydrogen bonding and salt network for the sulfimidate dianion in 1.	192
--	-----

Appendix C

Figure S1: NOESY spectrum of compound 1.	202
--	-----

Appendix D

Figure S1: Calculated structure of 9-aminocarbazole in the gas phase.	209
Figure S2: Calculated structure for N-(9 <i>H</i> -carbazol-9-yl)acetamide (1) <i>E</i> and <i>Z</i> isomers with relative energies.	212
Figure S3: Calculated frontier orbitals for N-(9 <i>H</i> -carbazol-9-yl)acetamide (1).	213

LIST OF SCHEMES

Page

Chapter 3

Scheme 3-1: Amination by the reductive nitration sequence of 1,1-diarylamines.	82
Scheme 3-2: Synthetic route to 1,1-diarylureas.	83
Scheme 3-3: Reaction sequence in the hypochlorite-promoted Hofmann rearrangement of ureas.	88
Scheme 3-4: Reaction mechanism for formation of hydrazines from ureas (R = alkyl or aryl).	92
Scheme 3-5: Proposed nitrene intermediate and transition state in the Hofmann rearrangement.	93
Scheme 3-6: Related mechanisms for the Hofmann rearrangement (R = aryl).	99

Chapter 4

Scheme 4-1: Synthesis of 1,1-diarylhydrazine derivatives.	114
Scheme 4-2: Isomerism in N'-(2-nitrophenyl)-N'-phenylacetohydrazide.	115

Chapter 5

Scheme 5-1: Synthesis of 9-aminocarbazole derivatives.	145
Scheme 5-2: Isomerism in N-(9 <i>H</i> -carbazol-9-yl)acetamide.	146

Chapter 6

Scheme 6-1: Formation of salicylaldehyde ruthenium complexes of synthesized hydrazine derivatives.	173
--	-----

LIST OF TABLES

Page

Chapter 1

Table 1-1: Singlet-triplet energy gaps in substituted nitrenium ions [NR ¹ R ²] ⁺ .	4
Table 1-2: Average parameters for structurally characterized NHCs and triazolium cations.	9
Table 1-3: Geometric comparison of structurally characterized triazolium and benzotriazolium cations with analogous NHCs.	10
Table 1-4: Tabulated M-C _{carbene} and M-N _{nitrene} for known phosphine chelate transition metal complexes.	14

Chapter 2

Table 2-1: Comparison of arylsilane unit cell dimensions.	72
---	----

Chapter 3

Table 3-1: Comparison of geometry around N(1) in 1-(2-nitrophenyl)-1-phenyl derivatives.	86
Table 3-2: Theoretical results for the Hofmann intermediates and transition states (G).	95

Chapter 4

Table 4-1: X-ray diffraction structural parameters for derivatives of NDPH.	118
Table 4-2: Comparison of bond lengths in dimethyl- and (diarylhydrazono)methylphenol derivatives.	121
Table 4-3: Closest intermolecular interactions in NDPH derivatives.	124

Table 4-4: Lowest energy UV-visible absorption bands for NDPH derivatives.	124
Table 4-5: Formal description of bonding in Ar_2NNR_2	127

Chapter 5

Table 5-1: Possible bonding interactions in 1,1-diarylhydrazines.	142
Table 5-2: X-ray diffraction structural parameters for derivatives of 9-aminocarbazole.	148
Table 5-3: Closest intermolecular interactions in AC derivatives.	152
Table 5-4: Lowest energy absorption bands for AC derivatives.	153

Appendix A

Table S1: Comparison of theoretical isotope patterns for pyrrolides and indolides with observed values.	190
---	-----

Appendix B

Supplementary table 1.	197
Table S2: Crystallographic data for compound 1.	198
Table S3: Crystallographic data for compound 2a.	199
Table S4: Crystallographic data for compound 2b.	200
Table S5: Crystallographic data for compound 3.	201

Appendix C

Table S1: Parameters for the $\text{N}(\text{C}(\text{O})\text{Me})_2$ Nitrogen of Structurally Characterized N,N-Diacetylhydrazines.	203
Table S2: Crystallographic data for compound 1.	204
Table S3: Crystallographic data for compound 2.	205
Table S4: Crystallographic data for compound 3.	206
Table S5: Crystallographic data for compound 4.	207

Table S6: Crystallographic data for compound 5.	208
---	-----

Appendix D

Table S1: Crystallographic data for AC.	214
Table S2: Crystallographic data for compound 1.	215
Table S3: Crystallographic data for compound 2.	216
Table S4: Crystallographic data for compound 3.	217

Appendix E

Table S1: Crystallographic data for 1-Phenylbenzotriazole.	218
Table S2: Crystallographic data for compound 1.	219

1

Concepts, Generation and Reactivity of Electron-Deficient Nitrogen

1.1 Definitions of electron-deficient nitrogen

Compounds of nitrogen spanning all eight oxidation states, even and odd alike, are known. Particularly interesting are compounds that contain nitrogen centres that are electron-deficient, which have been identified for several decades¹. The definition of what exactly constitutes electron-deficiency when it comes to the nitrogen atom, however, has been the subject of some debate. Typically, the discussion of nitrogen electron-deficiency revolves around the central theme of nitrenes and nitrenium ions (Figure 1-1), the analogues of carbenes and carbocations, respectively.

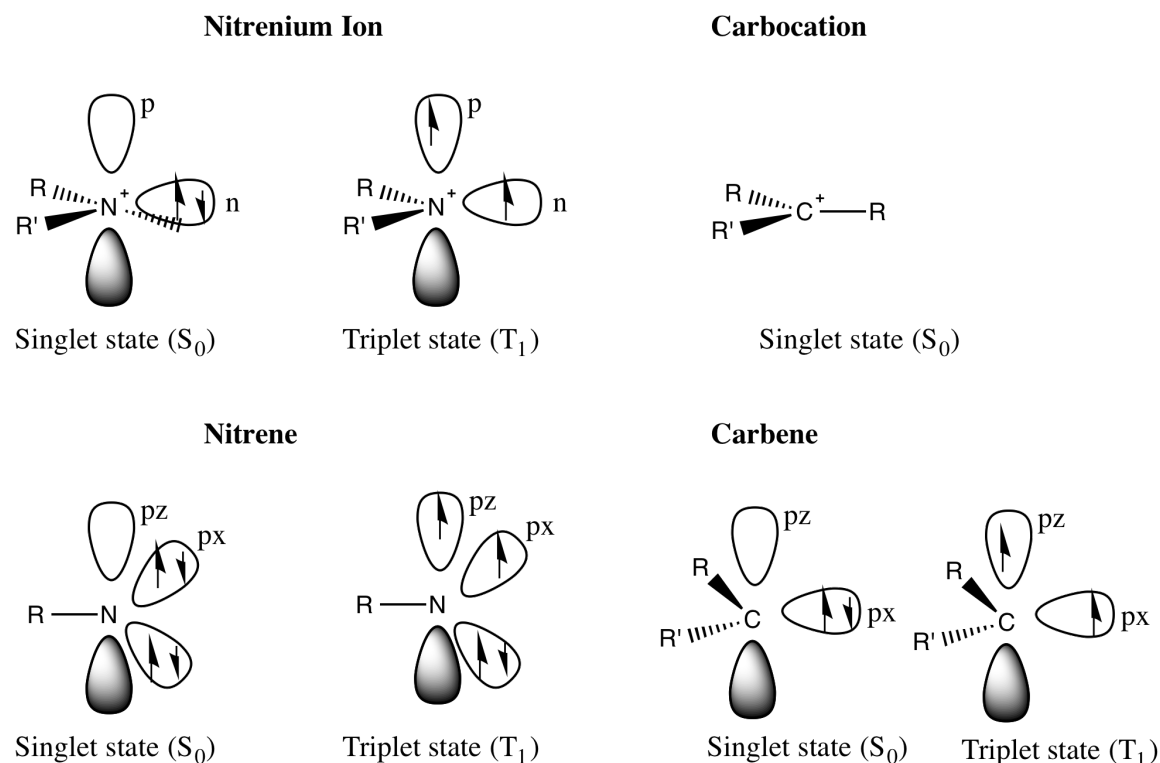


Figure 1-1: Electronic ground-state configurations of electron-deficient carbon and nitrogen-based analogues.

Examination of Figure 1-1 leads to several similarities, yet some important distinctions that must be made. Firstly, all of the above species formally contain six valence electrons. The nitrenium ion has been defined by Falvey² as “any species that can, through valence bond representations, be depicted as having a di-coordinate positively charged nitrogen” and is the nitrogen analog to the carbocation. A group of isoelectronic electron-deficient nitrogen compounds that possesses 6 valence electrons at nitrogen, but that do not comply with the definition put forth by Falvey since they are not formally cations is the nitrenes, which are the nitrogen analogs to the carbenes. While the carbenes and carbocations are well known with 29878 and 3826 SciFinder reports directly related to their study and chemical transformations, respectively, the nitrenes and nitrenium ions are only sparsely mentioned in the scientific literature with a

combined total of just over 1000 references. As such, the study of reactions involving these species is a comparatively unexplored field of Chemistry.

1.2 Geometric and Electronic Structure

In addition to electron count, the distinction between singlet versus triplet states of electron-deficient nitrogen³ must be made. As seen in Figure 1-2, the singlet state of these electron-deficient species leaves a lone pair in a non-bonding atomic orbital. As a result, there is Columbic repulsion between them and the energy of the LUMO is therefore slightly higher. For the triplet case, there are no electron pairs.

Each electron is in a singly occupied orbital, resulting in lower Columbic repulsion and hence a lower energy state for the molecule if the singlet-triplet energy gap is small.

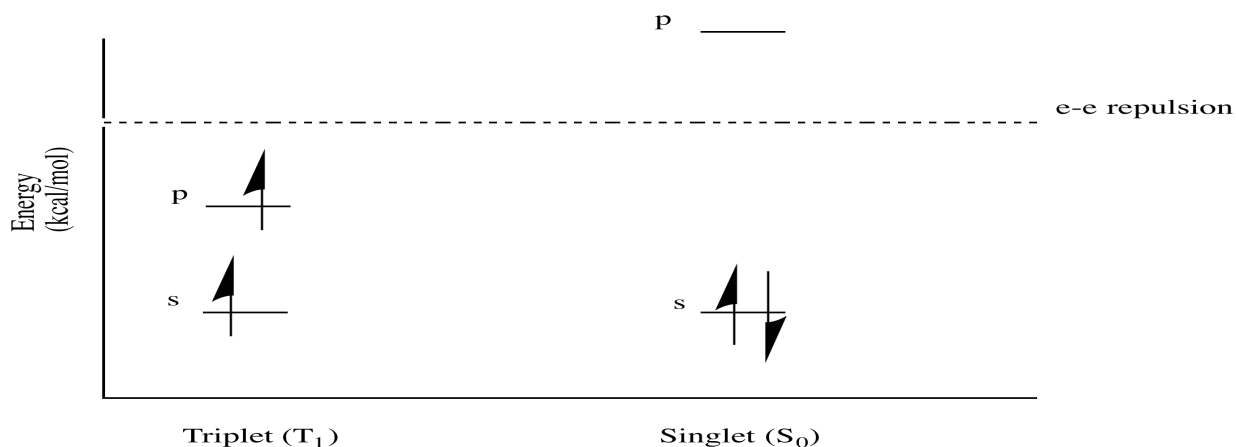


Figure 1-2: Triplet and singlet electron configurations.

This is also due in part to a favourable exchange interaction between parallel electrons that can occur if they are of similar energy according to Hund's rule⁴. The singlet state is only accessed when the surrounding environment raises the energy of the non-bonding p-orbital on nitrogen or stabilizes the σ -orbital so as to give rise to a greater energy difference than the energy of the Columbic repulsion between the electrons.

This energy difference, called the singlet-triplet gap (ΔE_{ST}), is a useful tool for predicting reactivity.

Table 1-1: Singlet-triplet energy gaps in substituted nitrenium ions $[NR^1R^2]^+$.

R ¹	R ²	ΔE_{ST} (kcal/mol)
H	H	+ 33.6
Me	H	+ 20.8
Me	Me	+ 22.5
-(CH ₂) ₄ -		+ 4.3
-(CH ₂) ₅ -		+ 9.6
CN	H	+ 27.5
Cl	H	- 1.2
F	H	- 4.69
F	F	- 57.3
F	Cl	- 25.6
Cl	Cl	- 19.8
NH ₂	H	- 32.4
NH ₂	CHO	- 38.8
OH	H	- 21.8
OH	CHO	- 12.0
Ph	H	- 18.8
4-nitrophenyl	H	- 16.8
4-methoxyphenyl	H	- 26.7
bis-(2,6-di-t-butyl)phenyl	bis-(2,6-di-t-butyl)phenyl	+ 7.3
3,5-(NH ₂) ₂ Ph	H	+ 7.7

The ΔE_{ST} in various nitrenium ions has been studied theoretically (Table 1-1)⁵. It can be seen that π -donor substituents, such as amines and phenyl-containing substituents are predicted to be more stable ground-state singlets with more N=X (X = C, N, etc) character due to delocalization. As a result of such π -donor stabilization from N-lone

pairs, the triazolium and benzotriazolium cations (Figure 1-3) are predicted⁶ to be more stabilized by these interactions than will the related N-heterocyclic carbenes.

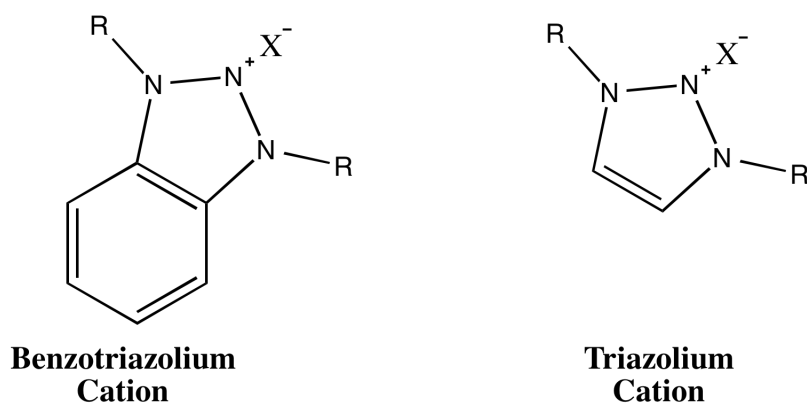


Figure 1-3: General structure of benzotriazolium and triazolium cations.

This stabilization, due to neighbouring heteroatoms with lone pairs was quantified by Falvey and co-workers⁷ using flash photolysis in 1,3-dimethylbenzotriazolium perchlorate, showing the singlet-triplet energy gap in that system to be -66 kcal/mol, greater than any stabilization seen in any of the entries in table 1-1. In comparison, the analogous carbene was calculated⁸ to have a ΔE_{ST} value of +78.9 kcal/mol, showing a marked preference of carbon for the singlet state while nitrogen, with proper stabilization from aromaticity, favours the triplet state.

Also of interest is the solid-state structure of electron-deficient nitrogen and its precursors to understand how to control its reactivity. Of particular interest are the primary nitrene transfer reagents derived from the hypervalent iodine class of compounds known as tosyl(iminoiodo) arenes (ArINTs)⁹, from which electron-deficient nitrogen can be extruded (Figure 1-4).

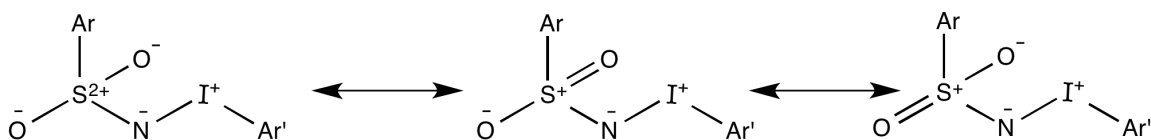


Figure 1-4: Resonance-stabilized classical nitrene transfer reagents.

These resonance-stabilized, highly polarized iodine(III) compounds have been examined as nitrene transfer reagents since 1974, when Abramovitch first hypothesized they could be used as sources of electron-deficient nitrogen¹⁰. Important structural features highlighted by Cicero¹¹ include the acute angle at the imino group, coupled with equal bond orders of approximately unity in these systems, suggesting a highly polarized I----N----S triad with considerable electron density at nitrogen. In fact, the average I-N bond length for the crystallographically characterized compounds of this type (CCDC¹²) is 2.146 Å and the average N-S distance is 1.623 Å. Solubility issues¹² involved in early ArINTs chemistry for broad synthetic applications resulted in low yields and poor nitrene transfer specificity. These difficulties were explained by structural data for early ArINTs reported by Boucher¹³ and co-workers that showed these compounds form polymeric networks in the solid state with average intermolecular I---N and I---O bonds of 3.073 Å and 3.166 Å, respectively (Figure 1-5). These intermolecular networks hinder dissolution in common solvents by facilitating strong associations between iodine and imino-nitrogen atoms from neighbouring molecules, enhancing their stability.

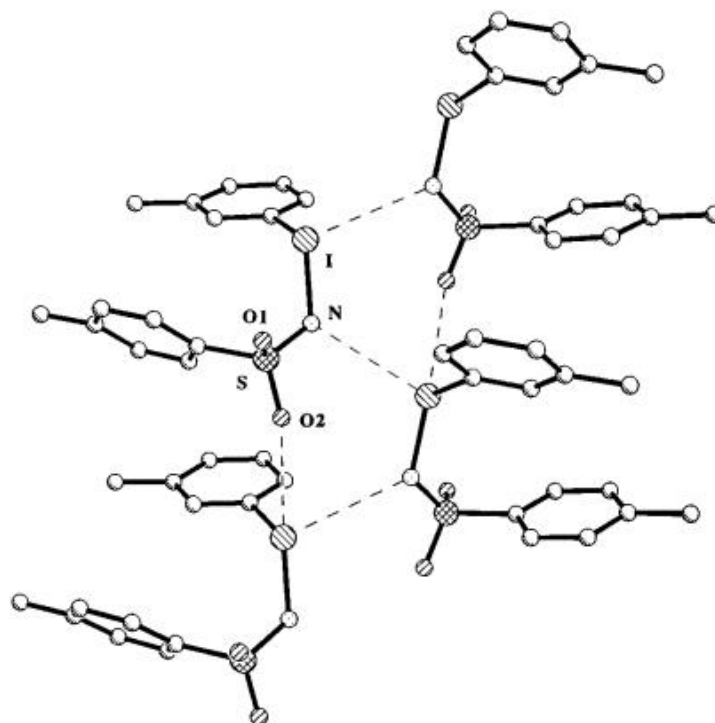


Figure 1-5: Intermolecular bonding in early PhINTs reagents. Reprinted (adapted) with permission from Boucher, M.; Macikenas, D.; Ren, T.; Protasiewicz, J. D., Secondary Bonding as a Force Dictating Structure and Solid-State Aggregation of the Primary Nitrene Sources (Arylsulfonylimino)iodoarenes (ArINSO₂Ar'). *J. Am. Chem. Soc.* **1997**, *119* (40), 9366-9376.. Copyright (1997) American Chemical Society.

More recent advances in ArINTs chemistry sought to overcome the strong intermolecular forces of these early studies and improve solubility and hence nitrene transfer yields. The greatest breakthrough in this regard was by Macikenas⁹, who studied the interactions of ArINTs derivatives with N-oxides with inconclusive results as to the mechanism of the enhancement of nitrene transfer in the presence of these additives. A year later, the same group introduced *ortho*-tosylate groups into the ArINTs

framework¹⁴ to provide competing intra-molecular forces and thus preclude the formation of insoluble polymeric networks, thus dramatically improving solubility (Figure 1-6).

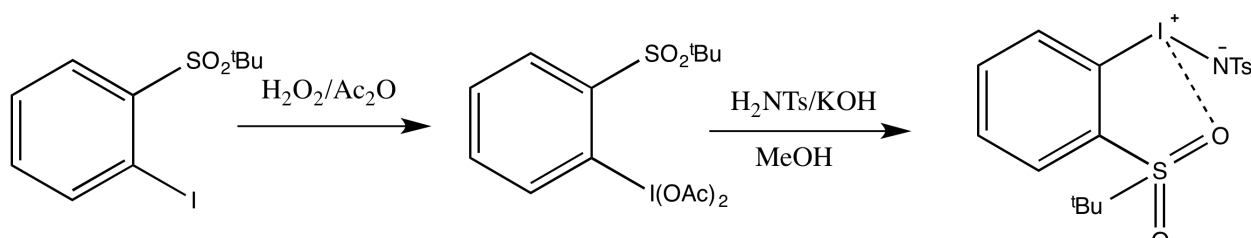


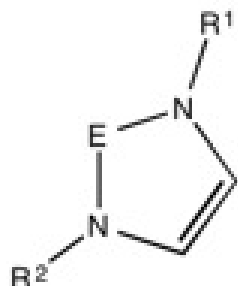
Figure 1-6: Synthesis of stabilized ArINTs derivatives.

While structural data on precursors to nitrenes has given insight into their intramolecular and intermolecular bonding interactions, allowing their efficient use in the generation of electron-deficient nitrogen for chemical reactions such as alkene insertion, the number of diffraction studies on single crystals of electron-deficient nitrogen species themselves is comparatively scarce. There are no reported crystal structures of free nitrenes. There are; however, numerous noble gas matrix isolation studies¹⁵, spectroscopic analyses¹⁶ and theoretical studies¹⁷ detailing these intermediates. Crystallographic characterization of carbenes is also limited to only one example of an alkyl carbene not stabilized by flanking π -donors¹⁸. The carbocations are also still sparsely studied, with studies mostly done on the trityl cations (Ph_3C^+) for which there are 252 structures reported¹⁹.

Cationic nitrogen analogues of the carbocations are also structurally relatively well known. Thanks to the coupling of the Copper-catalyzed 1,3-dipolar cycloaddition²⁰ and its later variants with N-alkylation using various alkylating reagents, there are 309 structurally characterized 1,2,3-triazolium cations (CCDC¹⁹). The ease of synthesis of these species has caused the number of them that have been structurally characterized to trounce that of their carbon analogues, with only 98 structures of free NHCs having

been described. The average bond lengths and angles relative to the 1,2,3-triazole/N-C-N framework in these important classes of compound have been tabulated (Table 1-2).

Table 1-2: Average parameters for structurally characterized NHCs and triazolium cations.



	E = C	E = N ⁺
MIN N - E (Å)	1.285	1.247
MAX N - E (Å)	1.394	1.448
AVERAGE N - E (Å)	1.365(2)	1.328(42)
MIN N-E-N (°)	99.633	100.929
MAX N-E-N (°)	113.775	110.492
AVERAGE N-E-N (°)	102(3)	103(3)

While the average N-X-N bond angles and distances ($X = C_{\text{carbene}}, N(2)$) in NHCs and triazolium cations appear to be similar, the minimum and maximum X-N bond lengths are rather telling. With the stabilizing inductive effects of the nitrogen lone-pair, the N(2) – N bond lengths are shorter. Is this due to an increase in N=N double bond character or greater sp^2/sp^2 overlap? This is one of the questions we seek to answer throughout this dissertation. As a result of these shortened bonds 1,2,3-triazolium cations and 1-substituted 1,2,3-triazole-3-oxides are stabilized in comparison to their analogous carbenes and are also more structurally rigid, lowering the range of the N(1) – N(2) – N(3) bond angle as compared to the NHCs.

Table 1-3: Geometric comparison of structurally characterized triazolium and benzotriazolium cations with analogous NHCs.

	1,2,3-Bt ⁺	NHC (benzimidazole)	1,2,3- Triazolium	NHC (imidazole)
MIN N-N(2) (Å)	1.296	1.355	1.254	1.351
MAX N - N(2) (Å)	1.408	1.387	1.408	1.381
AVERAGE N - N(2) (Å)	1.336(6)	1.371(3)	1.331(2)	1.365(3)
MIN N(1) - N(2) - N(3) (°)	102.1	103.2	100.929	100.4
MAX N(1) - N(2) - N(3) (°)	109.3	104.8	109.339	102.3
AVERAGE N(1) - N(2) - N(3) (°)	105.5(4)	104.1(3)	103.9(2)	101.3(3)

The data in Table 1-3 suggests there is no increase in stability of the N-X-N framework upon the introduction of a benzene ring into the triazole system, due to similar average X-N bond lengths. There is; however, a statistically significant difference in the bond angles at the carbene carbon or electron-deficient N(2). In both cases, the angles in the nitrogen analogues are larger.

1.3 Synthesis of Isolable Electron-Deficient Nitrogen Species

The synthetic methods to generate electron-deficient nitrogen in isolable form are not very diverse. While there has been successful isolation of one donor-stabilized carbene reported as mentioned earlier, the same for the simple nitrene has yet to transpire. Conversely, the triazolium salts have been isolated and the same holds true for their carbon analogs, the NHCs. This is due to a few established synthetic methods that are used to make either of these two classes of compounds. By far the most prevalent is the alkylation of 1-substituted benzotriazoles and triazoles with alkylating agents. Such a procedure has been known for nearly a century (Figure 1-7)²¹.

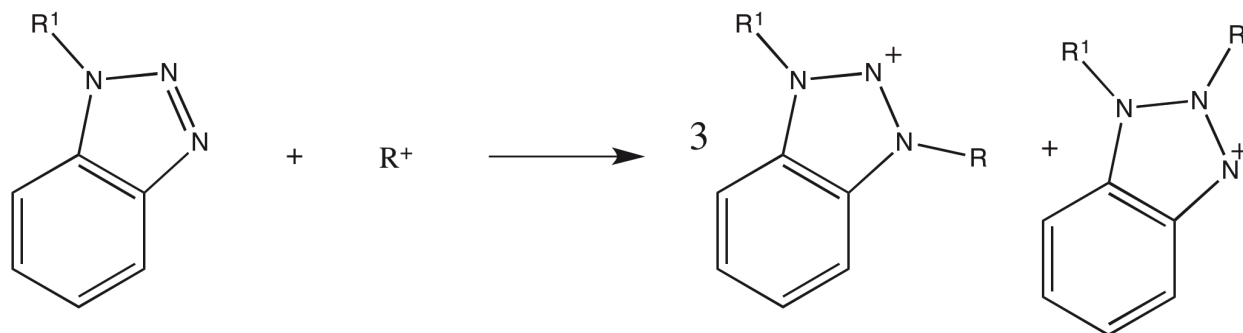


Figure 1-7: Generation of benzotriazolium cations by N-alkylation.

The drawbacks to this procedure are only electropositive ligands can be used since it involves attack of the un-substituted nitrogen atom of the benzotriazole on the alkyl cation. In addition, as seen in Figure 1-8, substitution by alkyl cations can occur on either of the un-substituted nitrogen atoms, resulting in a mixture of products. In either case, the alkyl groups added in this manner would then donate into the triazole ring, lessening the effective positive charge at the remaining nitrogen.

Electron-deficiency in the triazole framework can also be created using electronegative oxygen and nitrogen species, however, and there are 29 reliable reports of such methods. Much of the research in this area has gone into the creation of energetic ionic liquids derived from 1*H*-1,2,3-triazol-1-amine, which is commercially accessible²². While alkylation was one method of generating 3-substitution, Klapötke and co-workers reported the synthesis of some 1,3-diaminotriazoles from substitution using O-tosylhydroxylamine (Figure 1-8)^{22h, 23}.

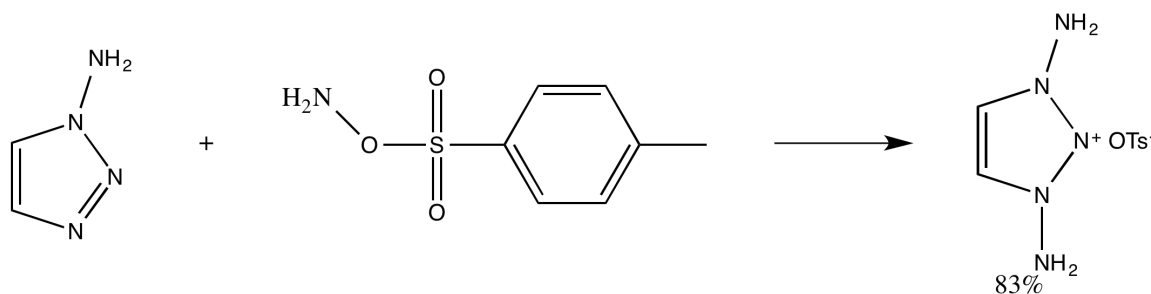
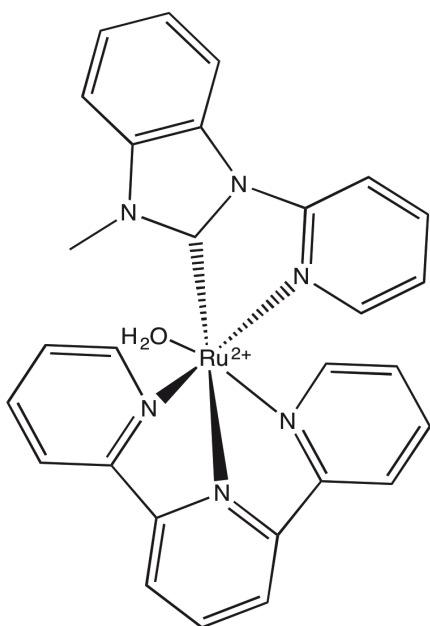


Figure 1-8: Synthesis of 1,3-diaminotriazolium tosylate. Reprinted (adapted) with permission from (Klapoetke, T. M.; Petermayer, C.; Piercey, D. G.; Stierstorfer, J., 1,3-Bis(nitroimido)-1,2,3-triazolate Anion, the N-Nitroimide Moiety, and the Strategy of Alternating Positive and Negative Charges in the Design of Energetic Materials. *J. Am. Chem. Soc.* 2012, 134 (51), 20827-20836.). Copyright (2012) American Chemical Society.

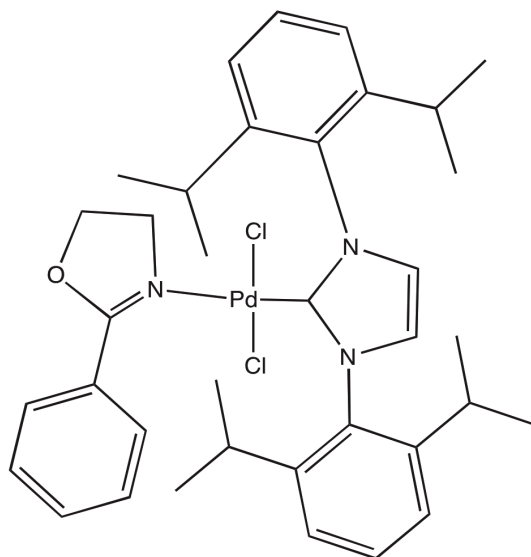
Similar modifications also included nitration with $\text{HNO}_3/\text{H}_2\text{SO}_4$ to give the corresponding nitroaminotriazoles reported by Huang²⁴. Despite the use of these methods for generation of exotic triazoles, apart from the formation of N-oxides using dimethyldioxirane²⁵, the analogous benzotriazolium systems are still seemingly unreported. The only comparable systems involving benzotriazoles was the di-imine reported by Shitov²⁶ using picrylhydroxylamine.

1.4 Coordination chemistry of triazolium cation

Having established ways to make triazolium cations, studies have begun on their complexes with transition metals. One comparison that can be made is of average structural parameters for known N-heterocyclic carbene (NHC) complexes with those of the newly discovered N-heterocyclic nitrenes of Tulchinsky²⁷ and Heims²⁸ to ascertain the effects of substitution of carbon for nitrogen in these systems, a few examples of which are shown in Figure 1-9.

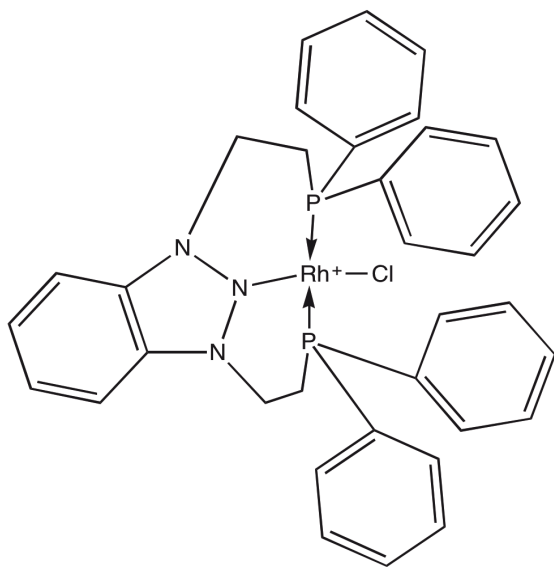


Concepcion *et al. Inorg. Chem.* **49** (2010), 1277

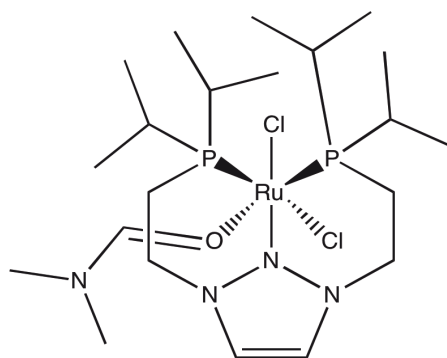


Huang *et al. Organometallics* **49** (2010), 1277

Coordinated NHCs



Tulchinsky *et. al. Nature Chem.* **3** (2011), 525



Coordinated triazolium and benzotriazolium cations

Figure 1-9: Selected examples of coordinated NHC and triazolium-based ligands^{27c, 29}.

Of interest is the comparison of N_{nitrene} - Metal and $P_{\text{phosphine}}$ - Metal bond lengths with those of known NHCs. These results for structurally characterized complexes with chelating phosphines are tabulated in Table 1-4.

Table 1-4: Tabulated M-C_{carbene} and M-N_{nitrene} for known phosphine chelate transition metal complexes.

Carbenes						
	Ru	Rh	Mo	Pd	Pt	Ni
MIN M - C _{carbene}	1.901	1.904	2.268	1.943	1.931	1.846
MAX M - C _{carbene}	2.205	2.124	2.321	2.123	2.062	1.986
AVERAGE M - C _{carbene}	2.061(6)	2.024(10)	2.303(18)	2.020(5)	2.019(6)	1.898(6)
MIN M - P	2.182	2.145	2.468	2.155	2.208	2.103
MAX M - P	2.505	2.396	2.506	2.382	2.369	2.295
AVERAGE M - P	2.348(6)	2.290	2.484(14)	2.291(6)	2.280(7)	2.205(9)
Nitrenes						
	Ru	Rh	Mo	Pd	Pt	Ni
MIN M - N _{nitrene}	2.041	1.991	2.257	N/A	2.064	1.986
MAX M - N _{nitrene}	2.059	2.360	2.266	N/A	2.124	2.021
AVERAGE M - N _{nitrene}	2.047(19)	2.128(76)	2.261(4)	2.075	2.103(62)	2.004(4)
MIN M - P	2.289	2.282	2.522	N/A	2.273	N/A
MAX M - P	2.323	2.391	2.548	N/A	2.371	N/A
AVERAGE M - P	2.305(31)	2.335(13)	2.531(16)	2.330	2.314(34)	N/A

From the limited data, it seems that short M - N_{Nitrene} bonds can result with Ru, Rh, Pd and Pt centres. Carbenes also form more stable late transition metal complexes. The nitrenes are better π -acceptors than the carbenes, which is evidenced by the generally longer M-phosphine bonds in their chelate complexes than in the carbenes examined in the table above. This is due to increased competition for π -backdonation from nitrenes than from carbenes.

1.5 Reactivity of 1,2,3-triazolium and -benzotriazolium cations

The triazolium cations exhibit very useful reactivity. Despite increased availability of triazole species thanks to the 1,3-dipolar cycloaddition under Sharpless conditions, a recent review shows that the chemistry of their derived cations is still in its infancy³⁰. Two major characteristics of note in these compounds are: 1) the increased acidity of the 4- and 5- positions that allow the generation of NHCs at these positions under basic conditions, which can then add to all manner of substrates and 2) the ability of the triazole network to assume excess electron density and return it, giving these compounds usefulness as catalysts in chemical reactions. Recent developments in this respect include the chemistry performed by Fall and co-workers³¹ demonstrating the usefulness of 1,2,3-triazolium cations over analogous imidazolium salts in the Morita–Baylis–Hillman reaction due to the absence of the acidic proton at the 2-position, which resulted in side-product formation (Figure 1-10).

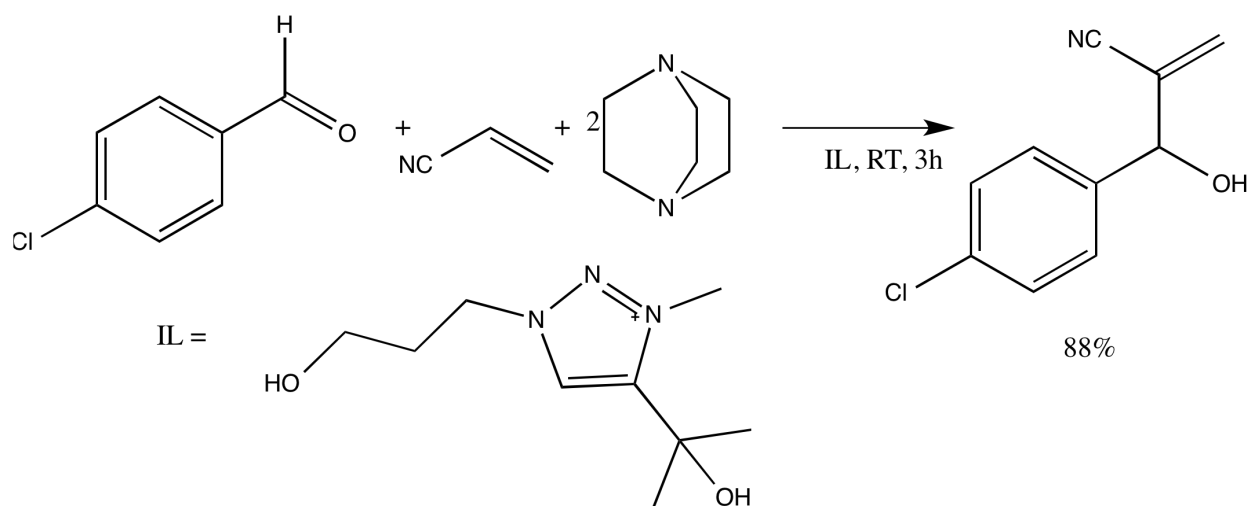


Figure 1-10: Use of triazolium cations in catalysis. Reprinted (adapted) with permission from Fall, A.; *et al.* Tetrahedron Lett. (2015), <http://dx.doi.org/10.1016/j.tetlet.2015.07.026>. Copyright (2015) Elsevier.

Klein has also reported the superior activity of triazolium salts over NHCs in iron-catalyzed aryloxy allylation of allylic carbonates since they promote higher regioselectivity³². It was reasoned that the increased regioselectivity was due to the enhanced redox ability of the triazolium salts over analogous NHCs. Also of note in this study is the fact that of all of the 1-aryl substituents on the triazolium salts, those that were particularly electron-poor tended to have the best reaction outcomes. Similar redox activity was demonstrated in benzotriazolium cations that were able to effectively act as a bridge between redox active metals³³ (Figure 1-11). The authors hypothesize that hole transfer from the benzotriazole is responsible for its activity in these experiments.

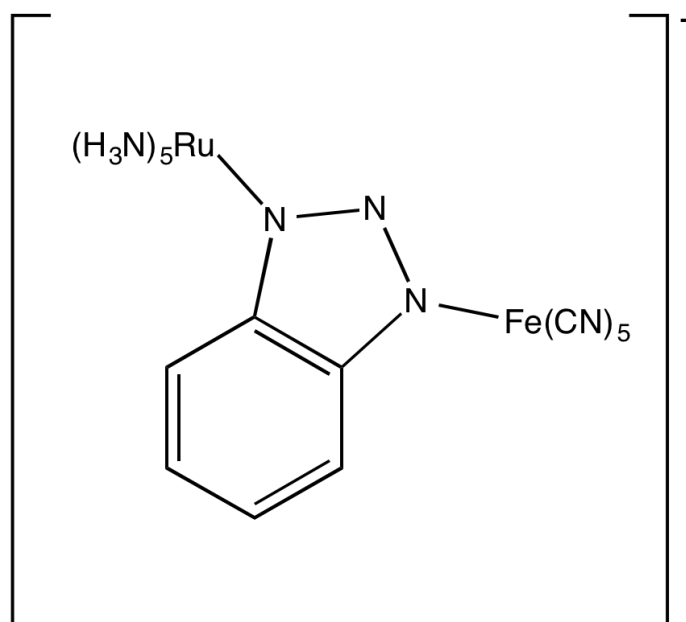


Figure 1-11: Representative benzotriazolium salt as a redox bridge.

1.6 Generation and reactivity of nitrene intermediates

1.6.1 From ArINTs systems

Much of the known chemistry of electron-deficient nitrogen is derived from its use as a reactive intermediate in the form of uncharged nitrenes. By uncovering methods to control the electronic state, namely singlet or triplet, in these species would allow

predictability of reactivity and provide a way to harness their synthetic potential. From the solid-state data, optimization of the structures of ArINTs-based systems to induce greatest nitrene transfer yields have made these precursor molecules some of the most widely used electron-deficient nitrogen sources. They function through fission of the long imido-iodine linkage to release ArI and “NTs” where the nitrogen has 6 valence electrons. This was first demonstrated by Breslow³⁴ and Mansuy³⁵ in their work based on the nitrene-containing organometallic complexes prepared by Groves³⁶ and Mahy³⁷ involving high-valent iron-porphyrin complexes. With structural data also indicating that iodo-arene substitution would affect the solubility of ArINTs and hence their nitrene transferring ability, additional modifications to further improve the desired nitrene generation process were examined. Meprathu³⁸ and co-workers introduced a bulky *tert*-butyl substituent at the *para* position. This modification did not affect the catalytic ability for nitrene-based aziridination reactions of alkenes, however, enough reagent could be dissolved in chloroform to reach molar concentrations. This modulated approach was also taken by Yoshimura and co-workers³⁹, who introduced various alkoxy-based *ortho*-substituents, which were more effective in Cu-catalyzed nitrene generation reactions than any of the ArINTs derivatives discussed previously, giving comparable yields and using only a fraction of the reaction time. While useful, the use of ArINTs-based nitrene generation process requires both the introduction of a tosylate group and, most often, a transition metal catalyst, such as the manganese-based systems studied by Zdilla⁴⁰. Useful methodologies, such as the protocol developed by Yang also used for the silver-catalyzed ArINTs-based production of heterocycles from appropriate linear amines through a nitrene-dependent mechanism, have resulted from their use in combination with transition metals (Figure 1-12)⁴¹.

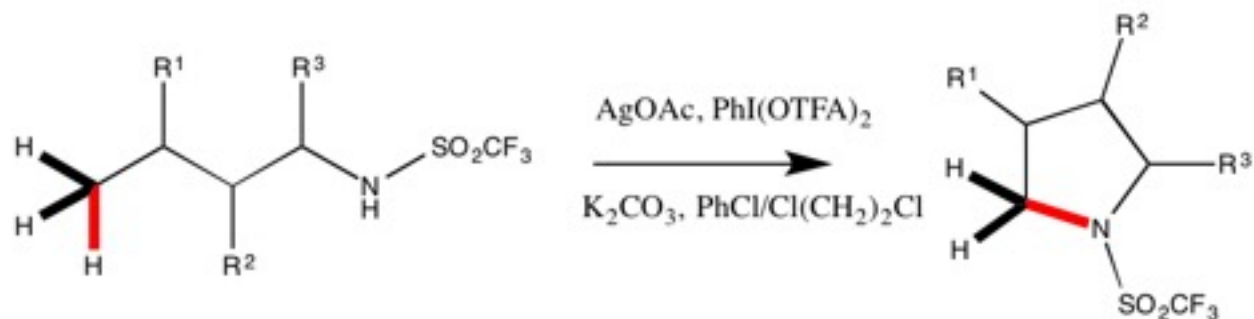


Figure 1-12: Silver-catalyzed nitrene generation and C-H bond insertion using linear amines. Reprinted (adapted) with permission from Yang, M.; Su, B.; Wang, Y.; Chen, K.; Jiang, X.; Zhang, Y.-F.; Zhang, X.-S.; Chen, G.; Cheng, Y.; Cao, Z.; Guo, Q.-Y.; Wang, L.; Shi, Z.-J., Silver-catalysed direct amination of unactivated C-H bonds of functionalized molecules. *Nat. Commun.* **2014**, *5*, 4707. Copyright (2014) Macmillan Publishers Ltd.

More recent advances as reported by Postle and Stephen⁴², however, show effective use of these reagents to form exotic nitrogen-containing boranes under metal-free conditions (Figure 1-13).

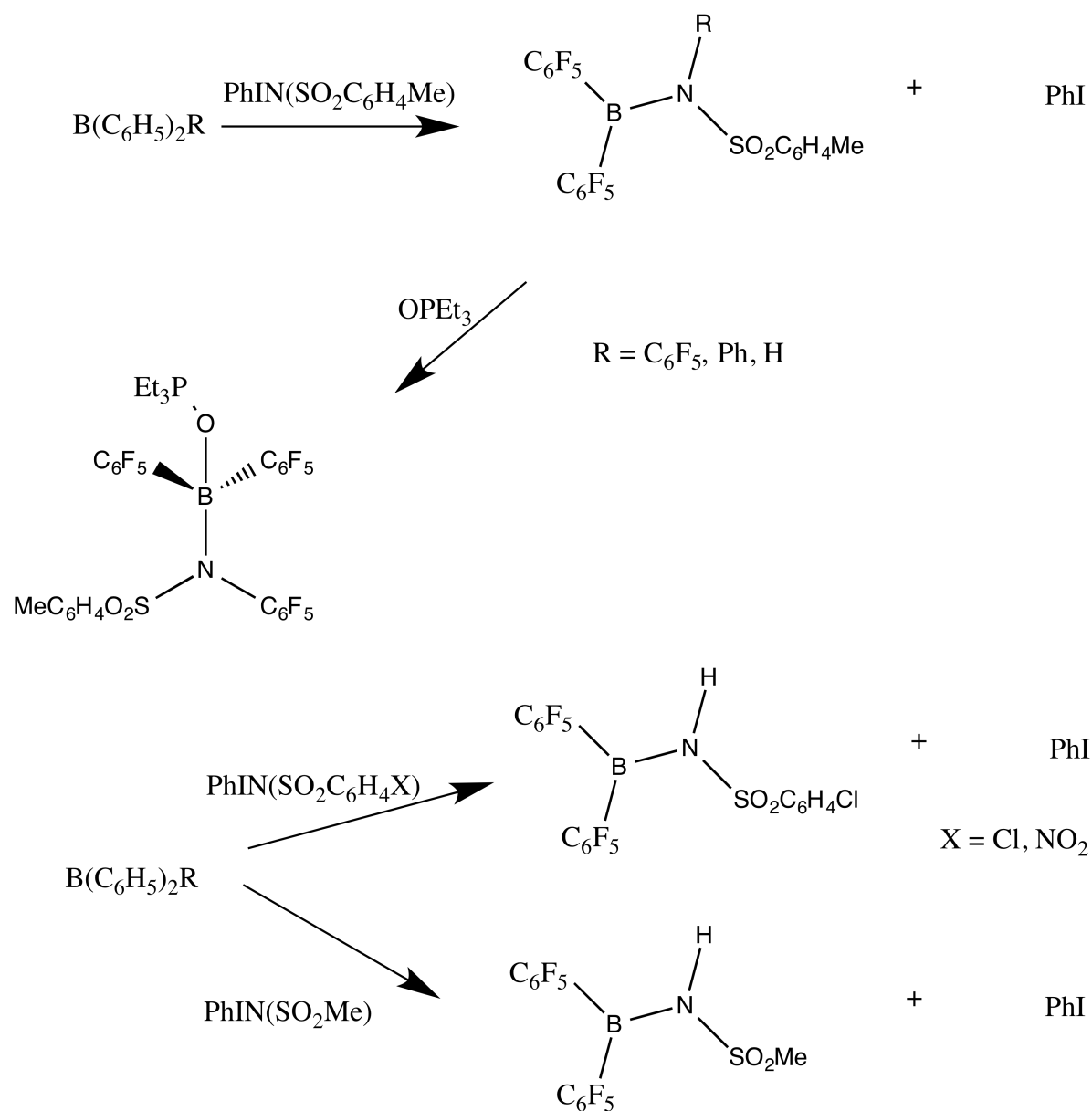


Figure 1-13: Use of ArINTs-based systems for the synthesis of novel boranes. Reprinted (adapted) with permission from Postle, S.; Stephan, D. W., Reactions of iodine-nitrene reagents with boranes. *Dalton Trans.* **2015**, 44 (10), 4436-4439. Copyright (2015) The Royal Society of Chemistry.

1.6.2 From azides

One method of carbene generation is to generate them by photolysis of azoalkanes⁴³ and diazirines⁴⁴ and infer their presence as intermediates on a phenomenological basis or study them in noble gas matrices. Likewise, the photolysis of azides results in the formation of nitrene intermediates. Early studies involved the photolysis of hydrazoic acid (HN_3) in noble gas matrices to produce singlet $^1\text{N-H}$, which was found to be able to undergo the three processes commonly associated with nitrenoid species: insertion, abstraction and relaxation upon reaction with ethane, which could be detected using spectroscopic methods⁴⁵. The same does not hold for alkyl azides, which did not yield nitrenes upon photolysis. Upon irradiation, they rearrange to form imines, and do not insert into chemical bonds (Figure 1-14)⁴⁶.

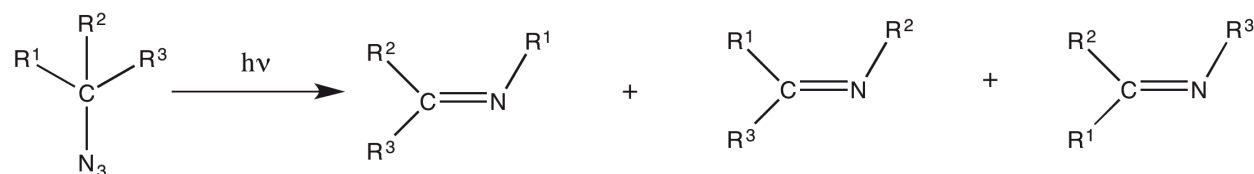


Figure 1-14: Rearrangement upon photolysis of alkyl azides.

Instead, the primary products of reaction were found to be the result of alkyl, aryl or hydrogen migration accompanied with the loss of molecular nitrogen. Later studies by Kyba and Abramovitch⁴⁷ demonstrated that there is no significant change in migratory potential upon changing alkyl substituents and that when alkyl azides bearing aromatic substituents were used, no aziridination products were formed (Figure 1-15).

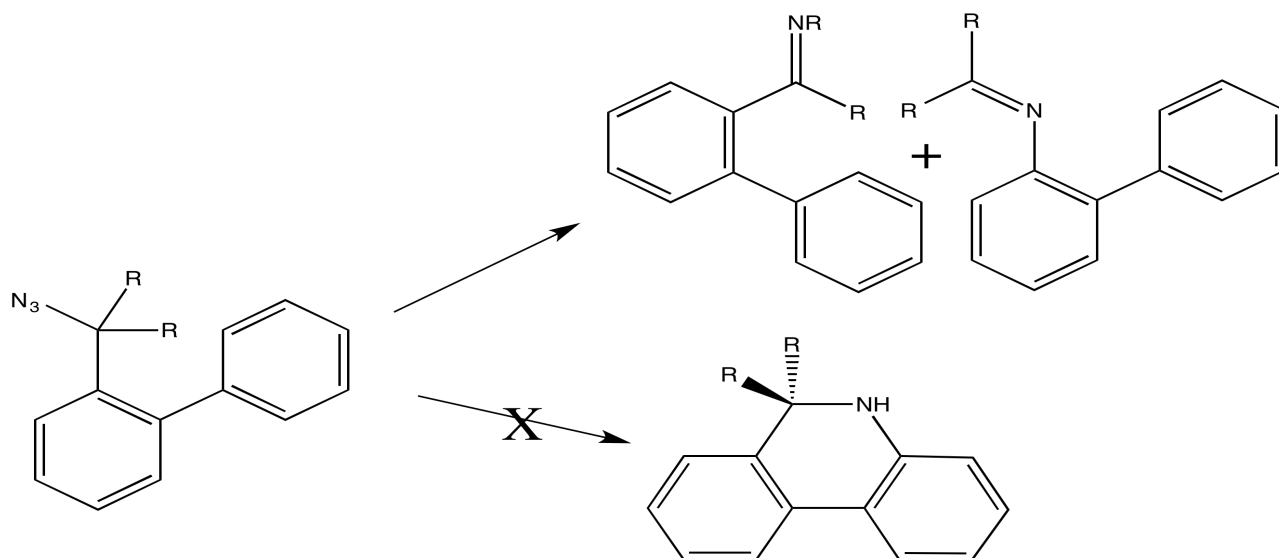


Figure 1-15: Photo-rearrangement of di-substituted derivatives of 2-biphenylmethyl azide.

There are only a few studies⁴⁸ on alkyl azides that have demonstrated possible involvement of nitrenes in their photochemistry. While Banks succeeded in obtaining small yields of insertion products, Pancrazi failed to prove his assertion of nitrene involvement and only succeeded in obtaining imines formed from rearrangement of the parent azide accompanied with loss of N_2 in his studies. Bicyclic systems derived from azidonorborane and adamantanes⁴⁹ also proved to be a disappointment, lacking specificity and producing only moderate yields of nitrene insertion products. These assertions were supported by ESR and measurements indicating the presence of triplet nitrenes as minor by-products from aminoadmantane in glassy mixtures at low temperature, with signals at 8210 G and a klystron frequency of 9.3 GHz in the X-band region.

A truly accessible source of alkyl nitrenes was only discovered upon photolysis experiments of carbonyl-containing alkyl azides. Lewis and Saunders first asserted that in the presence of a photosensitizer, energy transfer from a carbonyl to azide could occur, resulting in a “non-spectroscopic triplet” and a bending of the azide from its normal 180° geometry⁵⁰. Photosensitization of the triplet ketones in α -benzoyl- ω -azidoalkanes studied by Wagner⁵¹ allowed the discovery that two competing processes occurred in the photolysis. The first was γ -hydrogen abstraction giving mainly acetophenone through a radical decomposition process and the second was the production of a triplet nitrene due to energy transfer from the proximal carbonyl, resulting in N-heterocycles from nitrene insertion as major products (Figure 1-16).

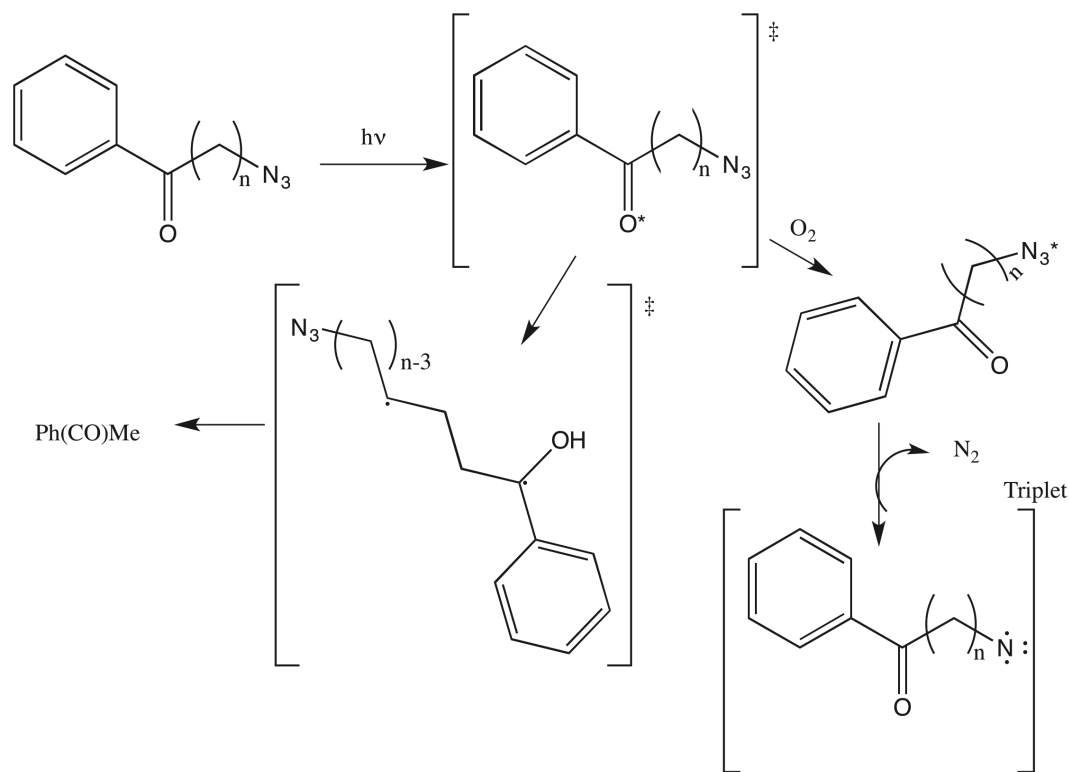


Figure 1-16: The primary processes in the photochemistry of α -benzoyl- ω -azidoalkenes. Reprinted (adapted) with permission from Wagner, P. J.; Scheve, B. J., Competing triplet reactions in azidoketones. *J. Am. Chem. Soc.* 1979, 101 (2), 378-83. Copyright (1979) American Chemical Society.

Demonstration of the presence of nitrenes in these sensitized carbonyl-based systems was confirmed by Muthukrishnan⁵² who also obtained mostly α -cleavage leading to benzaldehyde radical and only small yields of nitrene insertion products. In addition, it was shown that continued photolysis of the singlet nitrene also ended in α -cleavage, producing benzaldehyde radical as a thermodynamic minimum for the system (Figure 1-17).

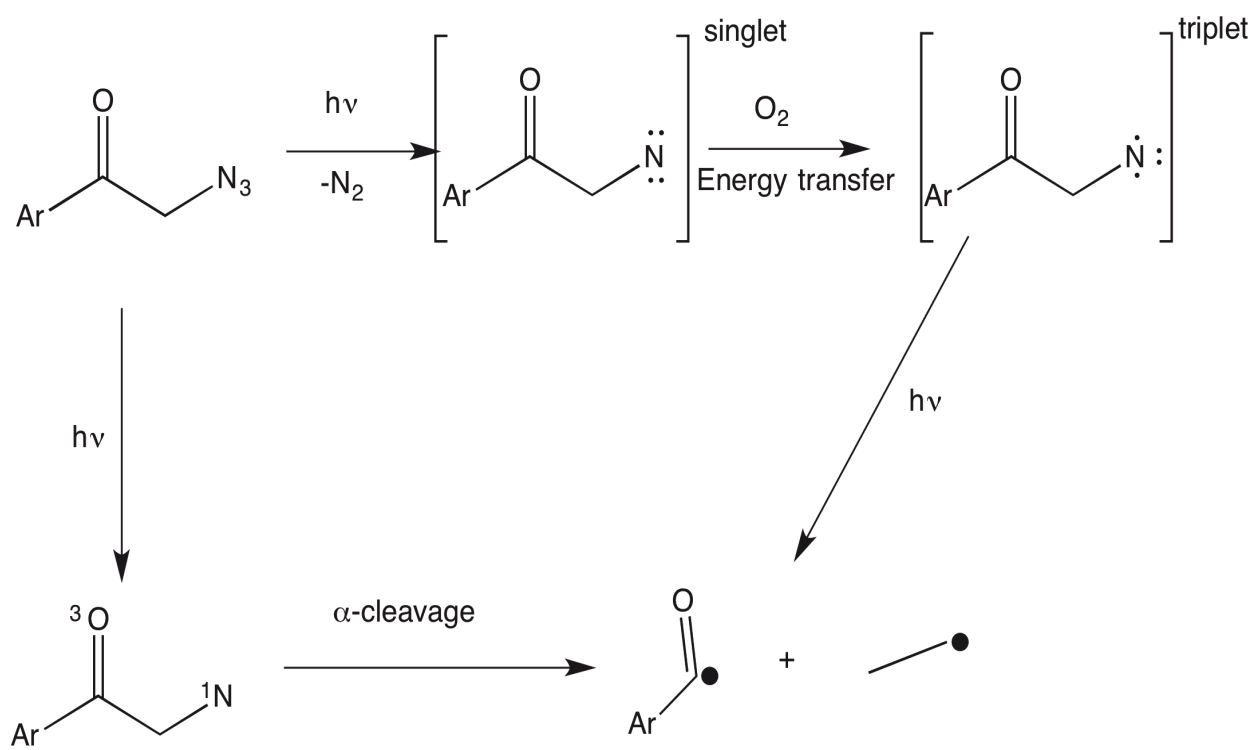


Figure 1-17: Competitive processes upon photolysis of carbonyl-containing azides⁵². Reprinted (adapted) with permission from (Muthukrishnan, S.; Mandel, S. M.; Hackett, J. C.; Singh, P. N. D.; Hadad, C. M.; Krause, J. A.; Gudmundsdottir, A. D., Competition between α -Cleavage and Energy Transfer in α -Azidoacetophenones. *J. Org. Chem.* 2007, 72 (8), 2757-2768. Copyright (2007) American Chemical Society.

Singh and co-workers⁵³ calculated the lifetimes of the nitrenes generated from carbonylazides to be on the millisecond timescale. These species are most likely triplet nitrenes, based on the direct observation of ³NMe from these systems using electronic absorption spectroscopy⁵⁴. The failure to detect the singlet-state by the same methods⁵⁵ supported by calculations that suggest conversion of ¹NMe to NH=CH₂ is a rather exothermic process ($\Delta H = -83 \text{ kcal/mol}$) and that the inter-conversion barrier from singlet to triplet lies in the range 0.5 – 3.8 kcal/mol from independent sources⁵⁶, suggests that these compounds are predominantly in the triplet state under normal conditions. To ascertain the effect, if any, of unsaturation in the photolysis of alkyl azides, similar experiments were performed⁵⁷ on vinyl azides. Similar conclusions, despite the formation of minute yields of aziridine-based products, were reached. Accordingly, simple alkyl azides, aside from highly fluorinated and photosensitized derivatives are not significant sources of alkyl nitrenes.

The photochemistry of phenyl azide has also been extensively studied⁵⁸ (Figure 1-18).

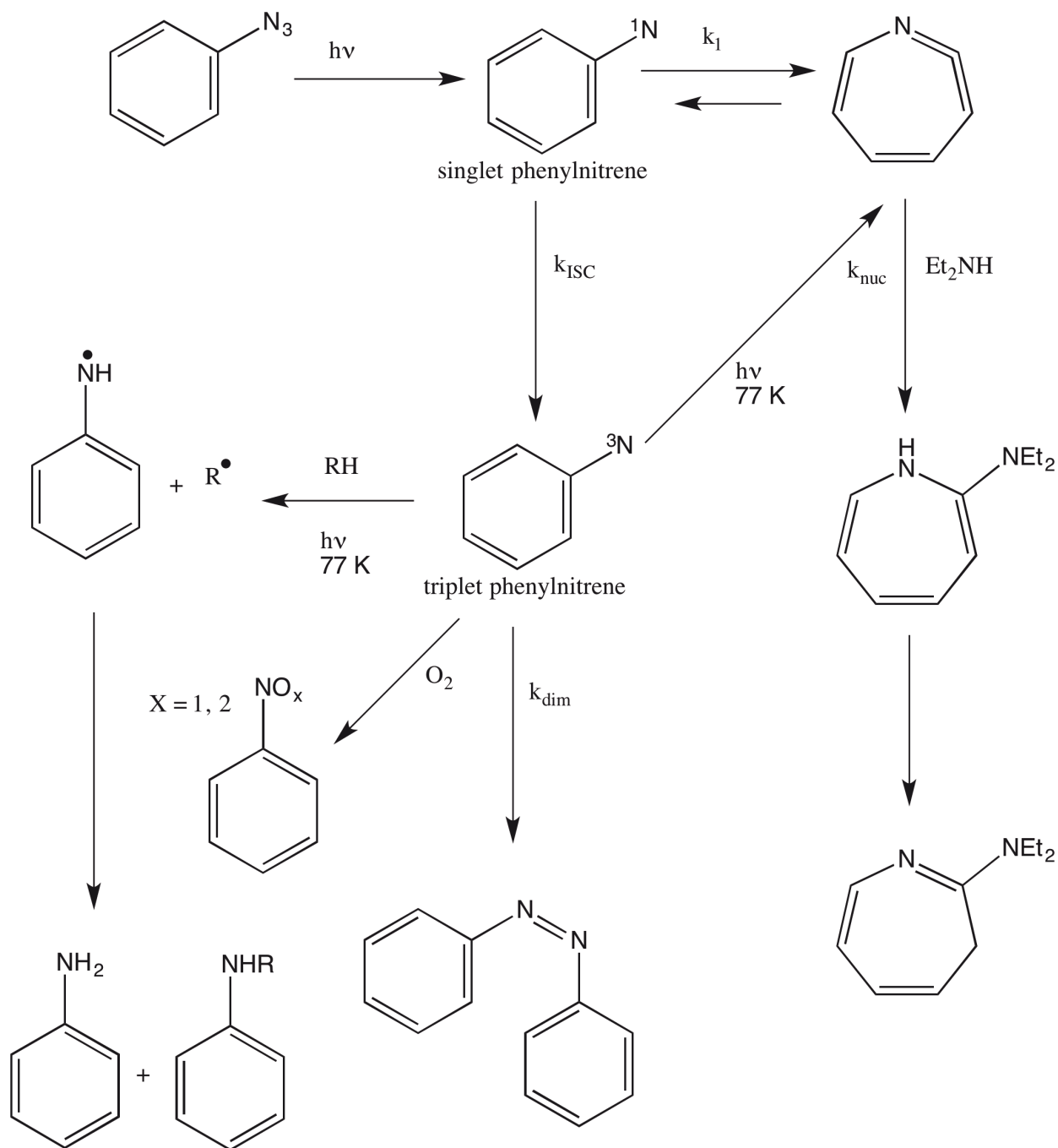


Figure 1-18: Photodecomposition pathways of phenyl azide.

It has been examined theoretically and using time-resolved spectroscopic techniques^{16b, 17a, 59}. Femtosecond-scale studies of arylazides and their photochemical and photophysical properties have been detailed⁶⁰ along the processes by which nitrenes derived from these azides decay and react. Consequently, the knowledge of the chemistry of

phenylnitrene has incredible breadth. Unfortunately, photolysis of most aryl azides leads to the formation of black tars and seldom yields diagnostic insertion products. Despite this setback, there are a few reports of useful photolysis reactions of aryl azides. Notably, studies⁶¹ by the Huisgen group and then later by Doering⁶² show azepines being made from the photolysis of phenyl azide to singlet phenylnitrene in the presence of primary amines. Other studies have shown dilution of phenylnitrene in non-nucleophilic solvents produces mainly azobenzene, due to suppression of polymerization to intractable tars⁶³. Interpretation of this behaviour is that, at lower concentrations, the rate of polymerization is slowed and thus conversion from singlet to triplet phenylnitrene can compete allowing subsequent dimerization. The reaction with oxygen has been shown to eventually produce the analogous -nitro and -nitroso compounds, even at high dilution⁶⁴. Irradiation has also been examined⁶⁵, with longer exposure times causing the formation of a ketamine from insertion. This unstable product is then able to react with nucleophiles to produce the corresponding 3H-azepine. The ketamine as well as triplet phenylnitrene were individually confirmed dependent on the wavelength of light used for the photolysis by low-temperature ¹³C-NMR⁶⁶. They exhibited extremely long lifetimes of 32 minutes and 75 days, respectively at 194 K. This result, coupled with work by Dunkin⁶⁷, confirm the photolysis of phenylazide can be made to generate triplet nitrenes exclusively, resulting in high yields of triplet-based products. The photo-dependence of the reaction pathway at low temperature is such that higher energy wavelengths result in predominantly singlet nitrene species while lower energy light promotes triplet species. At room temperature, the singlet state predominates and dimerization products are rare.

1.6.3 Rearrangements involving nitrene intermediates

A very useful method to control the reactive nature of nitrenes is to generate them in a specific molecular context and utilize their reactivity to generate specific reaction products. One widely used method to achieve this is through rearrangement reactions that ultimately result in nitrene generation. The following section describes the four main reactions of this type: the Curtius, Hofmann, Lossen and Schmidt rearrangements. These rearrangements all share a common isocyanate intermediate and are often discussed along with the Wolff rearrangement⁶⁸; however, the latter does not form an electron-deficient nitrogen intermediate and therefore will not be discussed in detail here. These important reactions collectively continue to be a major source of electron-deficient nitrogen in synthetic schemes and a recent review by Aubé summarizes recent developments in this rearrangement chemistry⁶⁹.

1.6.3.1 The Curtius rearrangement

The Curtius rearrangement is useful in the production of nitrenes from carbonyl-containing azides⁷⁰. The commonly accepted reaction is a release of nitrogen gas from a terminal carbonylazide, followed by rearrangement to an isocyanate and ultimately CO₂ release following hydrolysis to form a new N-N bond in appropriate substrates (Figure 1-19).

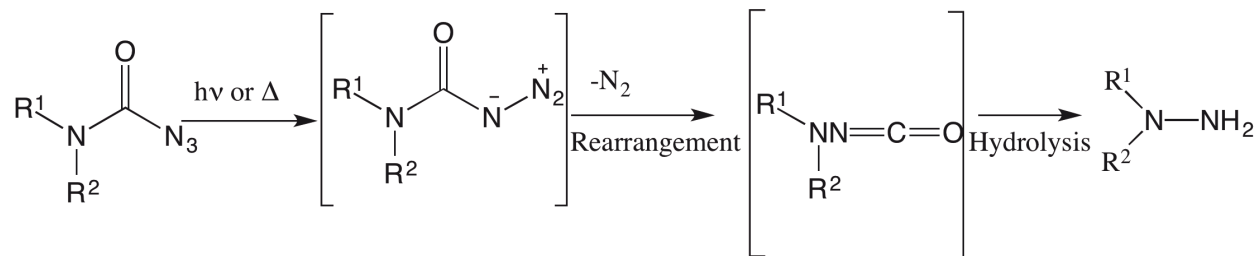


Figure 1-19: Curtius rearrangement of a suitable urea.

There has been much interest in uncovering the nature and stability of the precursors leading to the isocyanate intermediate⁷¹. The two hypothetical routes most widely used to explain the mechanism of the rearrangement are either the stepwise loss of nitrogen to form a nitrene, or the concerted loss of nitrogen and formation of the isocyanate, without the formation of an electron-deficient nitrogen species. When a nitrene-based mechanism is invoked, the singlet state is usually assumed to be the lower lying state for carbonyl-based nitrenes due to electron donation from the carbonyl oxygen^{71g, 72}. This contrasts the ground-state triplet seen in carbonyl compounds examined earlier that are separated from their adjacent azides by aliphatic carbon chains.

In recent studies by Zeng⁷³ and Sun⁷⁴, flash photolysis and pyrolysis, respectively, of carbonazidic fluoride in argon under vacuum gave mostly FC(O)N, which confirms stepwise nitrene formation to be more important in the conversion process. The high energy of these nitrenes, often termed “hot” singlets and triplets, is such that they are difficult to detect due to their rapid reaction *via* insertion into chemical bonds or intersystem-crossing and subsequent dimerization. Of importance in the study of carbonyl azides, however, was the proof that, by both photolysis and thermolysis, the ground state in these species is indeed a triplet state. This ground state configuration is relatively close in energy to the first excited singlet state with $\Delta_{ST} = 7.9$ kcal/mol, making the conversion rate to the singlet state extremely high and hence reactivity to produce diagnostic insertion products is maintained.

1.6.3.2 The Lossen Rearrangement

The Lossen rearrangement has been known since 1872. It involves the generation of an isocyanate from a hydroxamic acid in the presence of strong base and the chemistry of the hydroxamic acids has been known for many years⁷⁵ (Figure 1-20).

The reactive intermediate in this process that decomposes to give the rearrangement is an O-acyl, -sulfonyl or -phosphoryl derivative. The ambiguity in this rearrangement as with the case of the previous rearrangements arises once the O-acyl, -tosyl or – phosphoryl group departs, leaving an electron-deficient nitrogen atom.

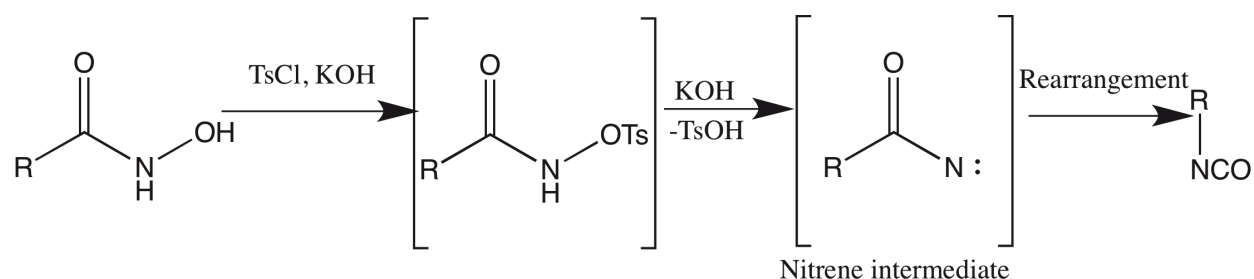


Figure 1-20: Schematic representation of the Lossen rearrangement.

The mechanism proposed for the Lossen rearrangement, as in the case of its analogous isocyanate-generating reactions has been a contentious subject. The intermediates of the reaction are proposed to result from one of two processes: nitrene generation or aziridinone formation. The ability of the reaction to produce insertion products and heterocycles has resulted in the general acceptance that a non-concerted rearrangement producing a nitrene intermediate, however brief, is the mechanism for the rearrangement.

Despite being known since the late 1800s, this reaction is far from dated and Lossen-type rearrangements of suitable hydroxamic acids are still in current use and thus new developments to improve the reaction efficiency are still being made. Recently, Vasantha and co-workers reported a novel Lossen-type reaction using *N*-methylmorpholine as an initiator⁷⁶. This rearrangement can also be initiated by various catalytic schemes. For instance, Hoshino was able to affect the transformation of aliphatic and aromatic hydroxamic acids to amines in moderately polar solvents under mild conditions using catalytic amounts of acetic anhydride as an initiator⁷⁷. Likewise,

Hafez and co-workers have also recently reported that the Lossen rearrangement can be initiated by conditions used during the Heck reaction⁷⁸ (Figure 1-21).

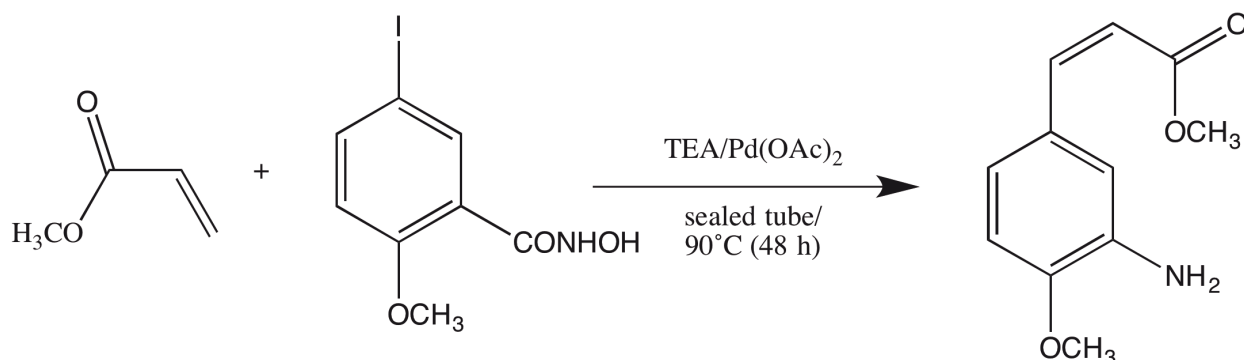


Figure 1-21: Heck reaction resulting in Lossen rearrangement.

This implies that nitrenes can be a source of side-product formation in these catalytic systems given the right substrate.

In addition to improving efficiency, fundamental studies of the Lossen rearrangement and its use in new reactions are still being researched. Shan⁷⁹ discovered that chlorinated benzoquinones could be used in Lossen rearrangement reactions and that the stability of the reaction intermediates depended on the position of the -chloro substituent. Pichette has shown that ring-contracted products derived from cyclic hydroxamic acids can be formed and that regioselectivity of the transformation was dependent on the nature of the base used⁸⁰. It is also used to make bio-active materials, including intermediates of antiviral drugs⁸¹ and antifungals⁸². One of the most important breakthroughs in this regard was made by Zhao⁸³ who not only demonstrated the effectiveness of carbonyldiimidazole as an initiator, but also that this reaction could be scaled to produce kilograms of glucosylceramide synthase (GCS) inhibitor, which is used in the treatment of Fabry disease (Figure 1-22). In addition, his route involving the Lossen rearrangement proved to be much more efficient than the analogous route to the product using a Curtius rearrangement.

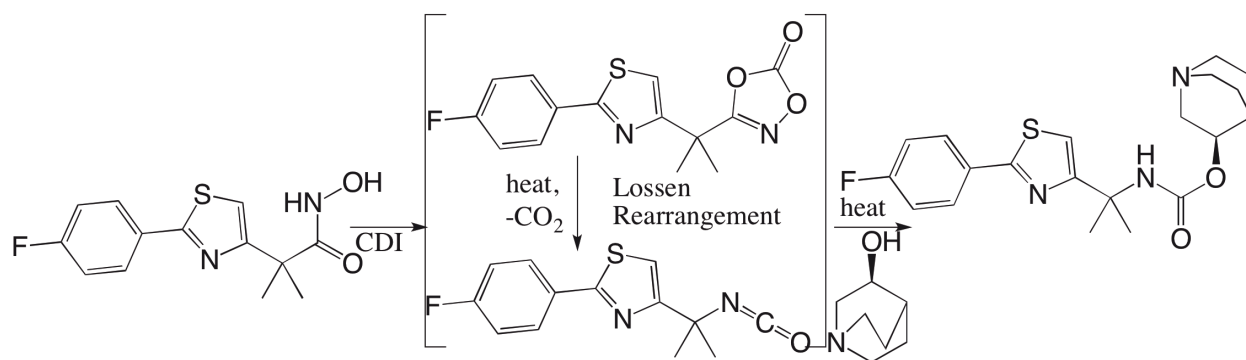


Figure 1-22: Preparation of a small-molecule GCS inhibitor by a scalable Lossen rearrangement. CDI = Carbonyldiimidazole⁸³.

With the functional group tolerance and breadth of reactions that can be accomplished using the Lossen rearrangement, it is no surprise that this reaction continues to be the subject of active study. Its utility surpasses the photo-induced Curtius rearrangement in many respects, including accessibility of suitable substrates, fewer degradation products and compatibility with other transition-metal catalyzed reaction schemes that do not function under photolytic conditions.

1.6.3.3 The Hofmann Rearrangement

The Hofmann rearrangement (Chapter 3) differs from the Curtius rearrangement in how its characteristic isocyanate intermediate is generated. This reaction was discovered by Hofmann in the early 1900s and is promoted by a hypohalite⁸⁴. Starting from urea derivatives, the rearrangement occurs following chlorination to form a chloramine and subsequent proton and chloride elimination in the presence of strong base (Figure 1-23).

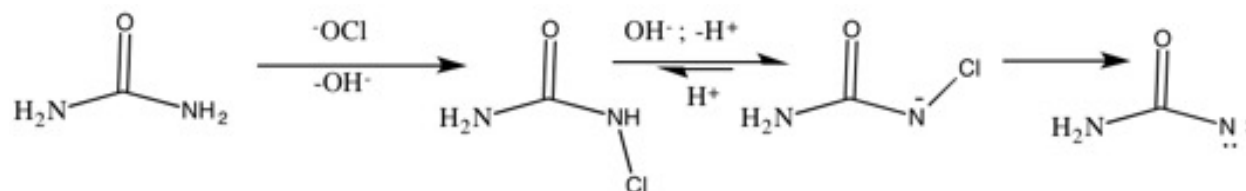
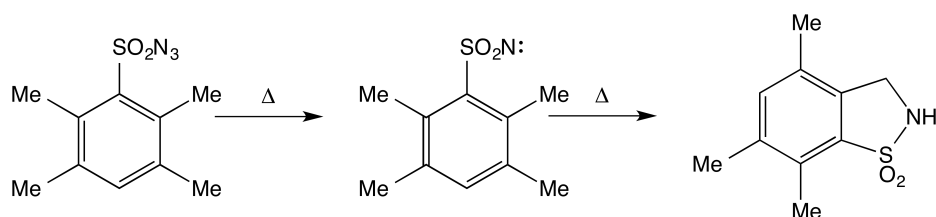


Figure 1-23: Nitrene generation from the Hofmann rearrangement of urea.

The versatility of chloramines like the ones seen in the above scheme was reviewed by Kovacic⁸⁵ and the Hofmann rearrangement remains an important method to generate electron-deficient nitrogen intermediates. The use of the Hofmann rearrangement as it was originally proposed is not practical on many substrates, since the basic and oxidative conditions required can be destructive to any pH-sensitive functional groups. Work by Ochiai on reactions using an ArINTs-based methodology, with a hypervalent bromine-containing reagent to effect a nitrene generation illustrates the prominence and also the ambiguity still present in the knowledge of Hofmann rearrangement chemistry (Figure 1-24)⁸⁶.

C-H Insertion



Hofmann Rearrangement

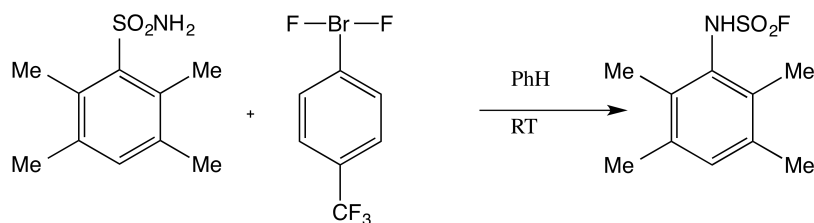


Figure 1-24: Hofmann rearrangement vs. intramolecular C-H insertion^{86b}.

Reprinted (adapted) with permission from Ochiai, M., *et. al.*, Difluoro- λ 3-bromane-Induced Hofmann Rearrangement of Sulfonamides: Synthesis of Sulfamoyl Fluorides. *J. Am. Chem. Soc.* **2009**, *131* (24), 8392-8393. Copyright (2010) The Royal Society of Chemistry.

While the Hofmann rearrangement in Figure 1-24 does not produce a C-H insertion product, this could be simply due to thermal barriers precluding the proper orientation to form it. The nature of the rearrangement process leading to nitrogen replacing sulfur on the aryl ring may indeed proceed via a nitrene-based route. The ambiguity of the intermediates notwithstanding, it is evident from these recent studies that the ability to generate halogenated amines as a possible nitrene source continues to be actively used in modern synthesis.

1.6.3.4 The Schmidt Reaction

Karl Friedrich Schmidt discovered the Schmidt reaction in 1924. It allows the formation of amines from carboxylic acids or carbonyl compounds *via* an isocyanate. While related to the Curtius reaction in that it involves azide precursors to the active nitrene intermediates, it proceeds through acid catalysis as opposed to a photolytic pathway. In fact, Curtius himself acknowledged the reactivity of his azides in the presence of acid catalysts and noted that similar decomposition to photolysis occurred. As with the other rearrangements of its type, the isocyanate is thought to originate from a nitrenoid species (Figure 1-25).

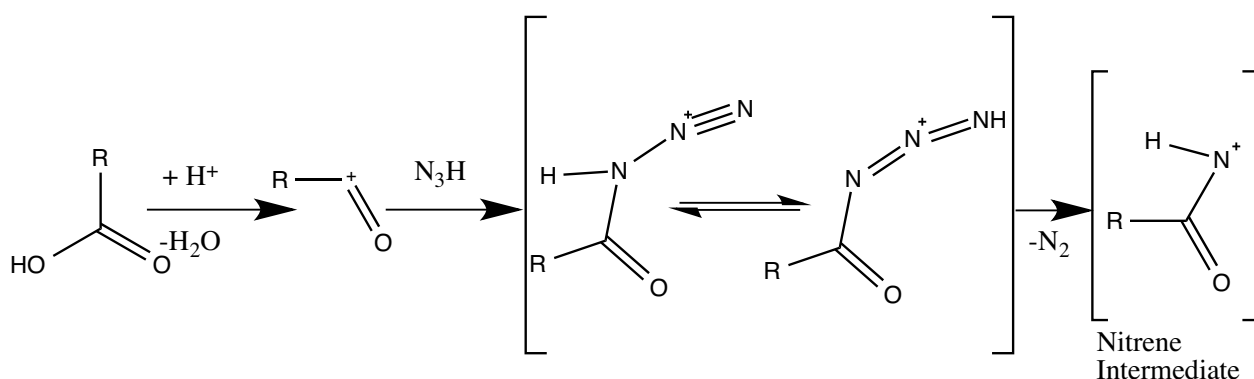


Figure 1-25: Nitrene generation during the Schmidt reaction.

The known chemistry stemming from a Schmidt reaction was also recently reviewed by Aubé, along with the Hofmann, Curtius and Lossen rearrangements⁶⁹. A more specific review of the reaction under zinc catalysis was done by González⁸⁷. The accessibility of the azide precursors and acid catalysts make this an attractive method of electron-deficient nitrogen generation, however; their toxicity makes avoiding the use of this method desirable. As in the case of the other rearrangement reactions examined here, the Schmidt reaction, when employed, is primarily used in modern synthetic schemes to produce amines and N-heterocycles. Specifically, developments in Schmidt reaction chemistry are concentrated in the biomaterials and pharmaceutical industries, with efforts to make medicinally important molecules accounting for most of its use. A recent example of such work includes the reactions by Wang to produce pyrrolizine by intramolecular capture of the isocyanate intermediate produced in the Schmidt reaction by alkenes or alkynes⁸⁸.

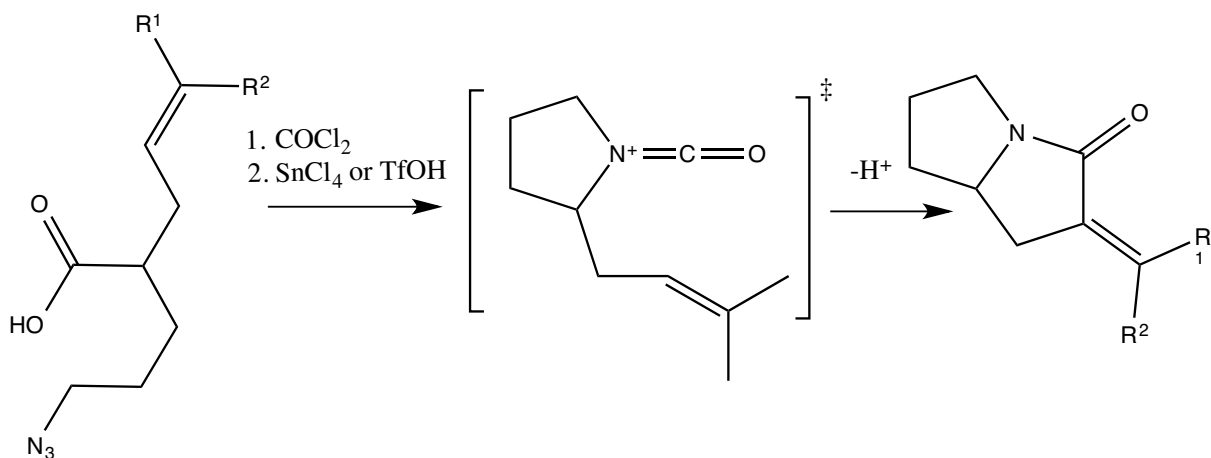


Figure 1-26: Intramolecular trapping of isocyanate generated via Schmidt reaction.

Tang and co-workers have examined the reaction in an aromatic context using 2-acetylbiphenyls in order to develop a method for facile synthesis of phenanthridines –

an important class of compounds due to their considerable presence at the core of many medicinally and biologically important molecules and alkaloids (Figure 1-27)⁸⁹.

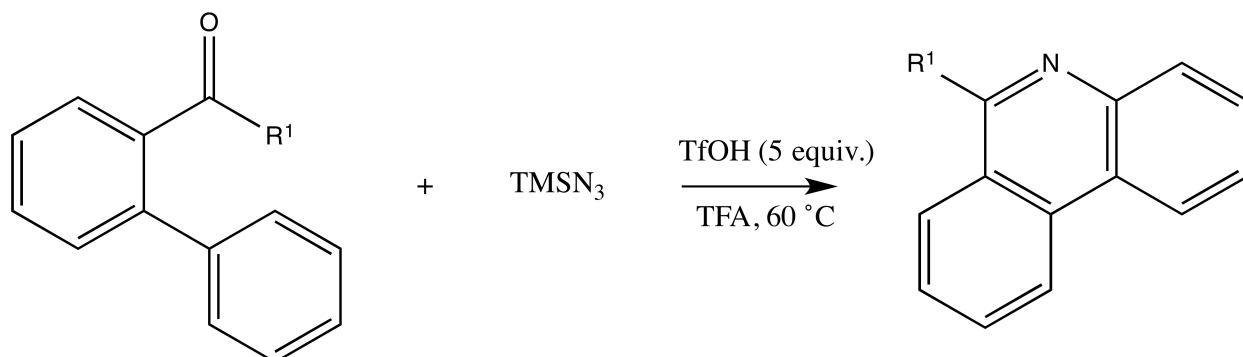


Figure 1-27: Synthesis of phenanthridines from biphenylazides.

While useful, the above reaction is still mechanistically ambiguous. It is thought to proceed by one of two possible routes. Ubiquitous to both is attack of the hydrazoic acid (N₃H) on the substrate to give an alcoholic intermediate. This intermediate is then thought to react by dehydration in one of two ways; either by losing nitrogen and reacting *via* a Friedel-Crafts process or, alternatively, by alkyl migration to form a cationic nitrile, which then condenses with the aryl ring by electrophilic cyclization (Figure 1-28). Given the absence of a Lewis acid catalyst, a more likely explanation for the first reaction pathway is the formation of a triplet nitrene, which undergoes C-H bond insertion, but further study of the Schmidt reaction will need to be done to conclusively identify all of its key intermediates.

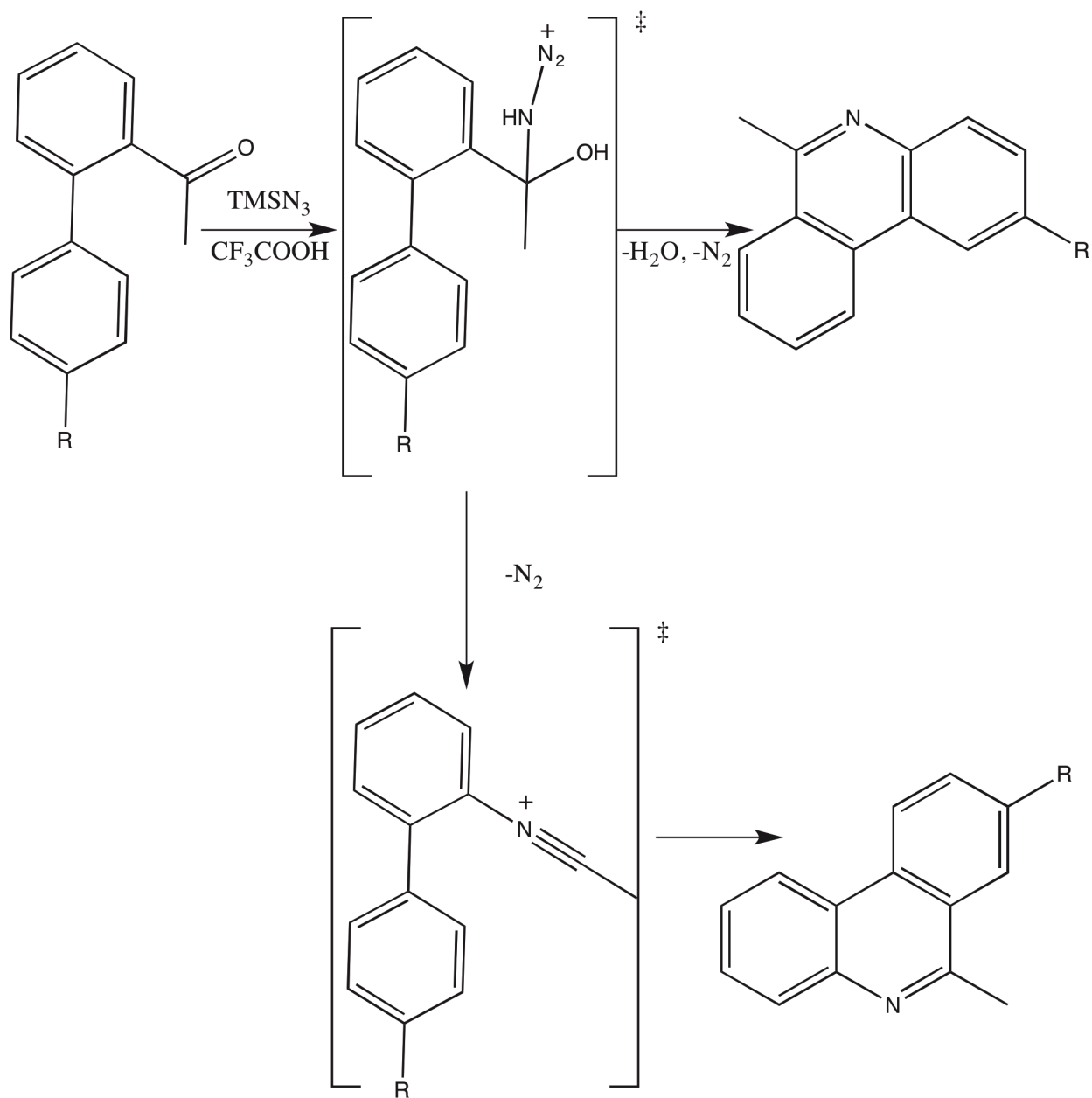


Figure 1-28: Possible decomposition routes for intermediates in the Schmidt reaction.

1.6.4 Reactivity of nitrene intermediates

Nitrogen has an electronegativity rating of 3.04 on the Pauling scale⁹⁰, making it one of the most electronegative elements surpassed only by oxygen, fluorine and chlorine.

Consequently, once it is made electron-deficient it becomes a potent electrophile. Like the carbenes, nitrenes react with even the most chemically inert sources of electrons. Their generation, therefore, must be carried out *in situ* in the presence of only the other reactants necessary to make use of them from a synthetic standpoint and their involvement in chemical reactions inferred on a phenomenological basis by the products obtained when ultrafast spectroscopic methods are unavailable. An overview of the main types of chemistry that these types of reactive intermediates engage in is therefore essential. The isoelectronic nitrogen analogues to the carbenes undergo analogous chemistry, that is, they tend to promote molecular rearrangements or are primarily used as a nitrogen source that is readily able to insert into all manner of chemical bonds. They are even reactive towards the deactivated C-H bonds of aromatic rings and their use in the de-functionalization of alkenes, cascade reactions for the formation of natural products and their use in the synthesis of simple N-heterocycles has recently been reviewed (Figure 1-29)⁹¹. As this chemistry is still in its infancy compared to that of the carbenes, new uses and novel reactions are continually emerging.

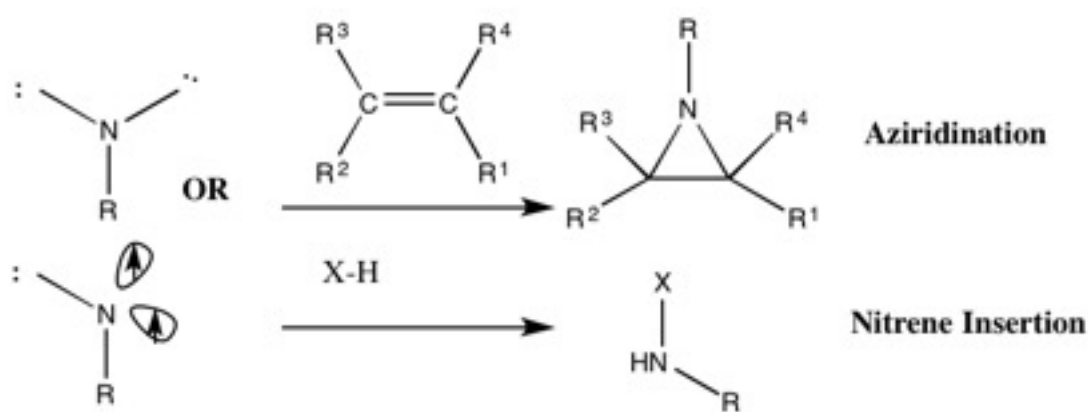


Figure 1-29: Typical reactions of nitrenes.

1.6.5 Catalyzed Aziridination Reactions

Relevant chemistry of nitrenes in aromatic frameworks includes aziridination of alkenes. These cyclizations have been well studied and their chemistry has been reviewed by Sweeney⁹². Nevertheless, multiple uses for nitrenes in aziridination chemistry have emerged since and computational methods are being employed to uncover even more exotic alkene-based substrates like the C(100) surface of diamond⁹³ for such reactions. The mechanism for nitrene insertion has also been studied computationally for both singlet and triplet states^{92, 94}. As in carbene chemistry, triplet and singlet nitrenes can be differentiated by the method with which they react with alkenes to form aziridines (Figure 1-30).

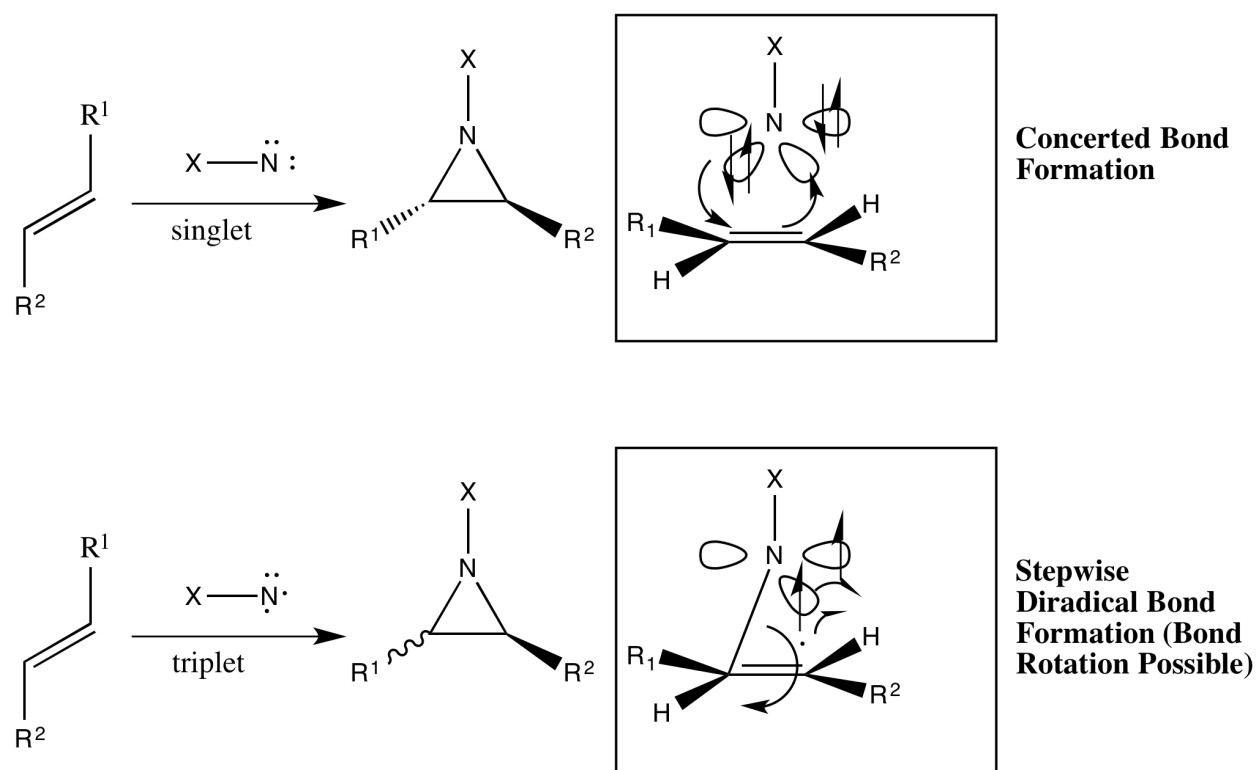


Figure 1-30: Mechanisms of reactions of singlet and triplet nitrenes with alkenes.

Triplet-state nitrenes undergo reaction through stepwise a di-radical mechanism, allowing for bond rotation in the transition state of the starting alkene. This can result in racemization and leads invariably to a mixture of products. Conversely, singlet nitrenes, while being more difficult to generate, are consumed in a concerted mechanism by alkenes, giving stereospecific reaction products. This mechanistic insight allows for the maintenance of stereo-control in these aziridinations, depending on the desired synthetic outcome.

Due to the lack of stereo-control that tends to result from the use of triplet nitrenes formed through the photolysis of azides, methods of enhancing stereo-control have gained impetus in the literature. One method to ensure stereo-selectivity is to use aromatic substrates. These comparatively rigid structures do not allow the bond rotation required to generate stereoisomers, allowing for the use of reagents that generate triplet nitrenes. Ramasumdaram and co-workers⁹⁵ have utilized fullerenes and terminal azido-based catechols for the synthesis of photo-catalysts. Use of nitrenes to introduce nitrogen into these aromatic frameworks imparted visible light absorption properties to the catalysts. Studies on the chemistry of such aziridination products of fullerenes are now starting to emerge⁹⁶ (Figure 1-31).

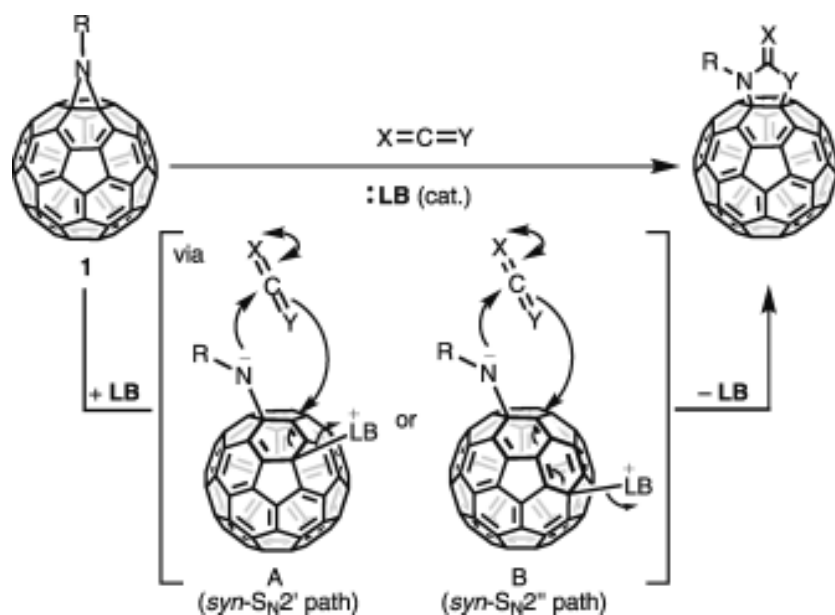


Figure 1-31: Lewis base-catalyzed ring expansion of aziridinofullerenes (1) with heterocumulenes⁹⁶. Reprinted (adapted) with permission from Takeda, Y.; Kawai, H.; Minakata, S., PCy₃-Catalyzed Ring Expansion of Aziridinofullerenes with CO₂ and Aryl Isocyanates: Evidence for a Two Consecutive Nucleophilic Substitution Pathway on the Fullerene Cage. *Chem. Eur. J.* **2013**, *19* (40), 13479-13483. Copyright (2013) Wiley-VCH Verlag GmbH & Co. KGaA, Weinheim.

In a similar surface modification, Servinis *et. al.*⁹⁷ used nitrenes derived from azides to functionalize carbon fibres, and demonstrated an increase in friction coefficient upon nitrene addition. Catalytic aziridinations on the surface of nanoparticles have also started to appear in the literature⁹⁸ with stereospecificity being maintained, indicative of a singlet nitrene transfer reaction, when zinc peroxide nanoparticles are used. Aziridines produced in this manner are already seeing applicability in large-scale materials chemistry⁹⁹ to introduce various properties onto surfaces *via* coatings of aziridine-containing groups made from nitrene-alkene coupling processes.

Another method of restricting stereo-variability is by developing metallic nitrene-transfer reagents with specific reactivity and hence increased stereospecificity.

Transition-metal catalysis for nitrene transfer from ArINTs has become an important part of modern chemistry for the incorporation of nitrogen into all manner of molecular architectures. Most of the catalysts currently being produced are based on the group XI or group VIII metals with copper, iron, ruthenium and silver being the metal centers of choice. Evans introduced organometallic catalysis through the use of low-valent copper-catalyzed aziridination using ArINTs (Figure 1-32)¹⁰⁰.

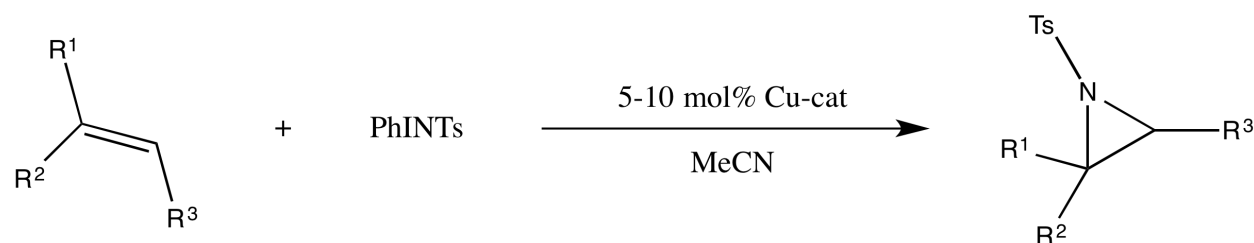


Figure 1-32: Copper-catalyzed aziridination of olefins.

The success of the catalytic copper-based ArINTs aziridation system prompted the study of its mechanism by Li and co-workers (Figure 1-33)¹⁰¹. They studied the question of a covalently attached nitrene transfer intermediate versus an analogous redox-based mechanism in the presence of copper catalyst. Owing to retention of stereochemistry based on the %ee of the di-imine supporting ligand, they obtained similar values for reactions of nitrenes derived from either ArINTs or azide-based systems. The authors admit, however, that this is anomalous and may be a result unique to the particular system studied.

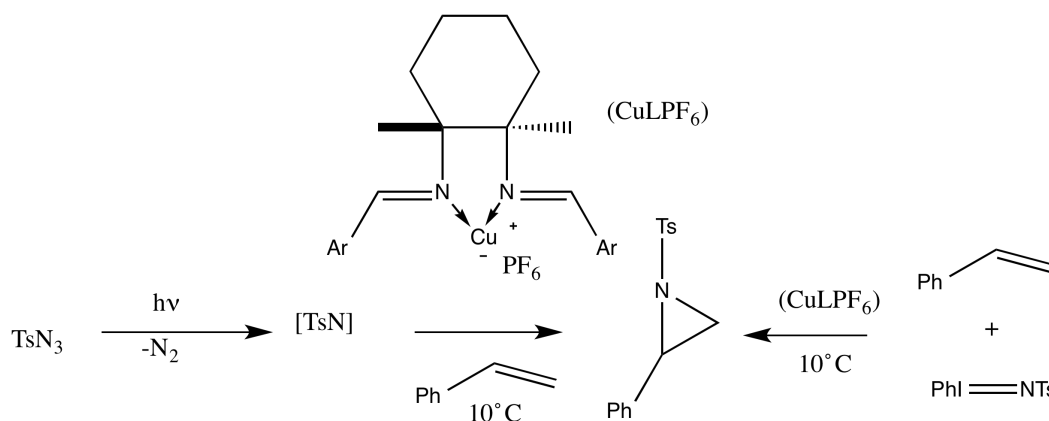


Figure 1-33: Equality of azide and PhINTs-derived nitrenes. Reprinted (adapted) with permission from Li, Z.; Quan, R. W.; Jacobsen, E. N., Mechanism of the (Diimine)copper-Catalyzed Asymmetric Aziridination of Alkenes. Nitrene Transfer via Ligand-Accelerated Catalysis. *J. Am. Chem. Soc.* 1995, 117 (21), 5889-90. Copyright (1995) American Chemical Society.

This was soon followed with selective N-insertion ortho- to doubly-bonded carbon atoms using iron and manganese tetraphenylporphyrin (TPP) derivatives in the mid-1990s¹⁰². This incited numerous experiments of Ru¹⁰³, Ag¹⁰⁴, Fe¹⁰⁵ and Cu-based TPP-like derivatives, each showing promise with a particular class of substrates. There is also one preparation¹⁰⁶ in the recent literature involving cobalt complexes of tetraphenylporphyrin (TPP) derived from azides, however; the use of azides results in considerably less stereospecificity in the reaction products than syntheses involving ArINTs-based systems – even where aromatic frameworks are concerned. Most of the TPP derivatives, unfortunately, are not as effective on aromatic substrates. To perform these aziridinations, Liang and co-workers discovered¹⁰⁷ a scorpionate-based complex that could act preferentially on aromatic substrates. Their approach, however, still needs optimization to achieve better chemoselectivity in the products to be competitive compared to other catalytic systems mentioned earlier.

1.6.6 Coordination Chemistry of Nitrenes

Basolo¹⁰⁸ first reviewed the chemistry of metal-imido species, which formally contain an $M=NR$ bond and there have been many studies on the electronic structure in these complexes^{37, 109}. Cundari¹¹⁰ predicted a triplet ground state in copper diketamate structures. This group later synthesized these Copper complexes and ascertained their crystal structures¹¹¹. Despite these efforts, however, no crystal structure of the free nitrene products was reported. Recent structurally characterized imido complexes include the coinage metal complexes reported by Dielmann¹¹², where the di-imido species were isolated along with mono-imido derivatives where the nitrene nitrogen is bridging two copper centres. The angles at nitrogen for the di-imido and bridging species are 175.72° and 94.58° , respectively (Figure 1-34). The mono-imido species were never isolated.

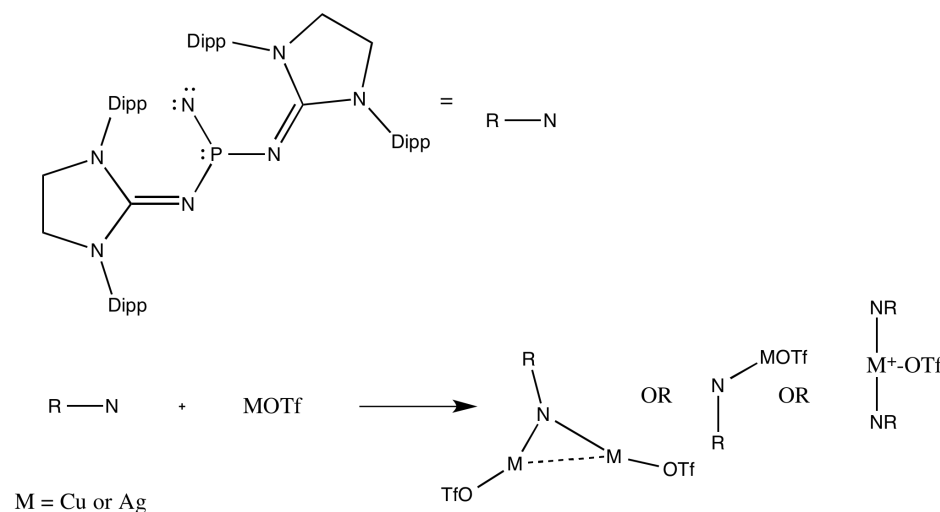


Figure 1-34: Isolation of bridging and di-imido complexes derived from nitrenes.

1.7 Conclusion

The chemistry of electron-deficient nitrogen has been vital in producing many new classes of materials and has proven useful in the enhancement of catalytic transformations. In addition, the use of these species as ligands in organometallic complexes to understand the extent of their physical, chemical and electronic properties is a newly emerging field with considerable potential. The nitrenium ions provide a redox non-innocence for which uses are constantly being developed. Particular stability of triazolium species has been shown in aromatic systems whose electron-deficiency has allowed the stabilization and subsequent use of these cationic nitrogen centres. The nitrenes, for their part, have also been of considerable interest in the synthesis of novel nitrogen-containing reagents, heterocycles and metal complexes.

1.8 Thesis Scope

Using methodologies to generate electron-deficient nitrogen in aromatic settings, we sought to study the synthesis of especially electron-deficient 1,1-diarylhydrazines that can be used in turn to generate N-heterocycles, ligands and organometallic complexes. The stability of these products will be investigated with particular focus on structural attributes and will provide insight into the effect of increased electron-deficiency on the geometric and chemical behaviour of these important cations and reactive intermediates for materials applications. Specifically: 1) the Hofmann rearrangement of 1,1-diaryllureas will be studied to produce analogous hydrazines containing electron-withdrawing substituents through a nitrene-based mechanism; 2) derivatives of these hydrazines will be made and the effects on nitrogen will be ascertained with particular attention being paid to hybridization state and bonding mode following substitution; 3) the characteristics of these new derivatives will be studied in reactions with metal complexes to ascertain their reactivity to form new routes to N-

heterocyclic ligands and to ascertain their properties as ligands in organometallic complexes.

1.9 References

1. (a) Smith, P. A. S.; Hall, J. H., Kinetic evidence for the formation of azene (electron-deficient nitrogen) intermediates from aryl azides. *J. Am. Chem. Soc.* **1962**, *84*, 480-5; (b) Smith, P. A. S.; Kalenda, N. W., Investigation of some dialkylamino isocyanides. *J. Org. Chem.* **1958**, *23*, 1599-1603; (c) Smith, P. A. S., Rearrangements involving migration to an electron-deficient nitrogen or oxygen. *Mol. Rearrange.* **1963**, *1*, 457-591.
2. Falvey, D. E., Nitrenium Ions. In *Reactive Intermediate Chemistry*, Moss, R. A.; Platz, M. S.; Jones, M., Eds. Wiley: Hoboken, NJ, 2004; pp 593-650.
3. Falvey, D. E., Singlet and triplet states in the reactions of nitrenium ions. *J. Phys. Org. Chem.* **1999**, *12* (8), 589-596.
4. Miessler, G. L.; Tarr, D. A., In *Inorg. Chem.*, 2nd Ed. ed.; Prentice-Hall: 1999; pp 358-360.
5. (a) Falvey, D. E.; Cramer, C. J., Aryl- and alkyl nitrenium ions: singlet-triplet gaps via ab initio and semiempirical methods. *Tetrahedron Lett.* **1992**, *33* (13), 1705-8; (b) Gonzalez, C.; Restrepo-Cossiot, A.; Marquez, M.; Wiberg, K. B.; De Rosa, M., Ab Initio Study of the Solvent Effects on the Singlet-Triplet Gap of Nitrenium Ions and Carbenes. *J. Phys. Chem. A* **1998**, *102* (16), 2732-2738; (c) Gobbi, A.; Frenking, G., The singlet-triplet gap of the halonitrenium ions NHX^+ , NX_2^+ and the halocarbenes CHX , CX_2 ($\text{X} = \text{F}, \text{Cl}, \text{Br}, \text{I}$). *J. Chem. Soc., Chem. Commun.* **1993**, (14), 1162-4; (d) Gobbi, A.; Frenking, G., Theoretical studies of inorganic compounds. Part III. The lowest lying singlet and triplet states of the halonitrenium ions NX_2^+ and NHX^+ and a comparison with the carbon analogs CX_2 and CHX ($\text{X} = \text{F}, \text{Cl}, \text{Br}, \text{I}$). A theoretical study. *Bull. Chem.*

- Soc. Jpn.* **1993**, *66* (11), 3153-65; (e) Borocci, S.; Bronzolino, N.; Grandinetti, F., FN+Cl ions from ionized F₂NCl: A computational investigation on the structure and reactivity toward H₂O. *Helv. Chim. Acta* **2004**, *87* (6), 1467-1482; (f) Glover, S. A.; Scott, A. P., MNDO properties of heteroatom and phenyl substituted nitrenium ions. *Tetrahedron* **1989**, *45* (6), 1763-76; (g) Sullivan, M. B.; Brown, K.; Cramer, C. J.; Truhlar, D. G., Quantum Chemical Analysis of para-Substitution Effects on the Electronic Structure of Phenylnitrenium Ions in the Gas Phase and Aqueous Solution. *J. Am. Chem. Soc.* **1998**, *120* (45), 11778-11783; (h) Cramer, C. J.; Dulles, F. J.; Falvey, D. E., Ab Initio Characterization of Phenylnitrenium and Phenylcarbene: Remarkably Different Properties for Isoelectronic Species. *J. Am. Chem. Soc.* **1994**, *116* (21), 9787-8; (i) Ford, G. P.; Herman, P. S., Alkyl and acyl substituent effects on nitrenium ion stabilities: ab initio molecular orbital calculations. *J. Mol. Struct.: THEOCHEM* **1990**, *63*, 121-30; (j) Cramer, C. J.; Falvey, D. E., Computational prediction of a ground-state triplet arylnitrenium ion and a possible ground-state triplet silylene. *Tetrahedron Lett.* **1997**, *38* (9), 1515-1518; (k) Winter, A. H.; Falvey, D. E.; Cramer, C. J., Effect of meta Electron-Donating Groups on the Electronic Structure of Substituted Phenyl Nitrenium Ions. *J. Am. Chem. Soc.* **2004**, *126* (31), 9661-9668.
6. Boche, G.; Andrews, P.; Harms, K.; Marsch, M.; Rangappa, K. S.; Schimeczek, M.; Willeke, C., Crystal and Electronic Structure of Stable Nitrenium Ions. A Comparison with Structurally Related Carbenes. *J. Am. Chem. Soc.* **1996**, *118* (21), 4925-4930.
 7. McIlroy, S.; Cramer, C. J.; Falvey, D. E., Singlet-Triplet Energy Gaps in Highly Stabilized Nitrenium Ions: Experimental and Theoretical Study of 1,3-Dimethylbenzotriazolium Ion. *Org. Lett.* **2000**, *2* (16), 2451-2454.
 8. Poater, A.; Ragone, F.; Giudice, S.; Costabile, C.; Dorta, R.; Nolan, S. P.; Cavallo, L., Thermodynamics of N-Heterocyclic Carbene Dimerization: The Balance of Sterics and Electronics. *Organometallics* **2008**, *27* (12), 2679-2681.

9. Macikenas, D.; Meprathu, B. V.; Protasiewicz, J. D., Solubilization of the primary nitrene sources (tosyliminoiodo)arenes (ArINTs). *Tetrahedron Lett.* **1998**, *39* (3/4), 191-194.
10. Abramovitch, R. A.; Bailey, T. D.; Takaya, T.; Uma, V., Reaction of methanesulfonyl nitrene with benzene. Attempts to generate sulfonyl nitrenes from sources other than the azides. *J. Org. Chem.* **1974**, *39* (3), 340-5.
11. Cicero, R. L.; Zhao, D.; Protasiewicz, J. D., Polymorphism of ((Tosylimino)iodo)-o-toluene: Two New Modes of Polymeric Association for ArINTs. *Inorg. Chem.* **1996**, *35* (2), 275-6.
12. White, R. E., Methanolysis of ((tosylimino)iodo)benzene. *Inorg. Chem.* **1987**, *26* (23), 3916-19.
13. Boucher, M.; Macikenas, D.; Ren, T.; Protasiewicz, J. D., Secondary Bonding as a Force Dictating Structure and Solid-State Aggregation of the Primary Nitrene Sources (Arylsulfonylimino)iodoarenes (ArINSO₂Ar'). *J. Am. Chem. Soc.* **1997**, *119* (40), 9366-9376.
14. Macikenas, D.; Skrzypczak-Jankun, E.; Protasiewicz, J. D., A New Class of Iodonium Ylides Engineered as Soluble Primary Oxo and Nitrene Sources. *J. Am. Chem. Soc.* **1999**, *121* (30), 7164-7165.
15. (a) Zeng, X.; Beckers, H.; Willner, H., Thermally Persistent Fluorosulfonyl Nitrene and Unexpected Formation of the Fluorosulfonyl Radical. *J. Am. Chem. Soc.* **2013**, *135* (6), 2096-2099; (b) Upul Ranaweera, R. A. A.; Sankaranarayanan, J.; Casey, L.; Ault, B. S.; Gudmundsdottir, A. D., Triplet-Sensitized Photoreactivity of a Geminal Diazidoalkane. *J. Org. Chem.* **2011**, *76* (20), 8177-8188; (c) Hoej, M.; Kvaskoff, D.; Wentrup, C., Nitrene-Carbene-Carbene Rearrangement. Photolysis and Thermolysis of Tetrazolo[5,1-a]phthalazine with Formation of 1-Phthalazinylnitrene, o-Cyanophenylcarbene, and Phenylcyanocarbene. *J. Org. Chem.* **2014**, *79* (1), 307-313; (d) Li, D.; Li, H.; Zhu, B.; Zeng, X.; Willner, H.; Beckers, H.; Neuhaus, P.; Grote, D.;

- Sander, W., Decomposition of fluorophosphoryl diazide: a joint experimental and theoretical study. *Phys. Chem. Chem. Phys.* **2015**, *17* (9), 6433-6439; (e) Ranaweera, R. A.; Krause, J. A.; Ault, B. S.; Gudmundsdottir, A. D. In *Reactivity of vinyl azides in solution and matrix isolation studies*, American Chemical Society: 2012; pp ORGN-198; (f) Wentrup, C. In *Gas-phase and matrix studies*, Academic: 1984; pp 395-432.
16. (a) Platz, M. S. In *Physical and spectroscopic methods*, Academic: 1984; pp 359-93; (b) Gritsan, N. P.; Platz, M. S., Kinetics, Spectroscopy, and Computational Chemistry of Arylnitrenes. *Chem. Rev. (Washington, DC, United States)* **2006**, *106* (9), 3844-3867; (c) Coombe, R. D. *Reactions and spectroscopy of excited nitrenes*; Colorado Seminary: 1992; p 29/
17. (a) Borden, W. T.; Gritsan, N. P.; Hadad, C. M.; Karney, W. L.; Kemnitz, C. R.; Platz, M. S., The Interplay of Theory and Experiment in the Study of Phenylnitrene. *Acc. Chem. Res.* **2000**, *33* (11), 765-771; (b) Gritsan, N. P.; Platz, M. S.; Borden, W. T., The study of nitrenes by theoretical methods. *Mol. Supramol. Photochem.* **2005**, *13* (Computational Methods in Photochemistry), 235-356.
18. Lavallo, V.; Mafhouz, J.; Canac, Y.; Donnadieu, B.; Schoeller, W. W.; Bertrand, G., Synthesis, Reactivity, and Ligand Properties of a Stable Alkyl Carbene. *J. Am. Chem. Soc.* **2004**, *126* (28), 8670-8671.
19. Cambridge Crystallographic Database. CCDC: Cambridge, 2015.
20. Huisgen, R., Proceedings of the Chemical Society. October 1961. *Proc. Chem. Soc.* **1961**, (October), 357-396.
21. (a) Krollpfeiffer, F.; Wolf, G.; Walbrecht, H., Action of acid chlorides on aryl- β -naphthylamine azo compounds. *Ber. Dtsch. Chem. Ges. B* **1934**, *67B*, 908-16; (b) Tome, A. C., Product class 13: 1,2,3-triazoles. *Sci. Synth.* **2004**, *13*, 415-601.
22. (a) Zhao, X.-H.; Ye, Z.-W., A facile synthesis of a novel energetic surfactant 1-amino-3-dodecyl-1,2,3-triazolium nitrate. *Chin. Chem. Lett.* **2014**, *25* (2), 209-211; (b) Ye, Z.; Lu, D. Method for synthesis of 1-amino-3-alkyl-1,2,3-triazole nitrate.

CN103382186A, 2013; (c) Ye, Z.; Hua, W. Method for preparing 1-amino-3-methyl-1,2,3-triazole nitrate. CN103508966A, 2014; (d) Shackelford, S. A.; Belletire, J. L.; Boatz, J. A.; Schneider, S.; Wheaton, A. K.; Wight, B. A.; Hudgens, L. M.; Ammon, H. L.; Strauss, S. H., Pairing Heterocyclic Cations with closo-Icosahedral Borane and Carborane Anions. I. Benchtop Aqueous Synthesis of Binary Triazolium and Imidazolium Salts with Limited Water Solubility. *Org. Lett.* **2009**, *11* (12), 2623-2626; (e) Shackelford, S. A.; Belletire, J. L.; Boatz, J. A.; Schneider, S.; Wheaton, A. K.; Wight, B. A.; Ammon, H. L.; Peryshkov, D. V.; Strauss, S. H., Bridged Heterocyclium Dicationic closo-Icosahedral Perfluoroborane, Borane, and Carborane Salts via Aqueous, Open-Air Benchtop Synthesis. *Org. Lett.* **2010**, *12* (12), 2714-2717; (f) Lin, Q.-H.; Li, Y.-C.; Li, Y.-Y.; Wang, Z.; Liu, W.; Qi, C.; Pang, S.-P., Energetic salts based on 1-amino-1,2,3-triazole and 3-methyl-1-amino-1,2,3-triazole. *J. Mater. Chem.* **2012**, *22* (2), 666-674; (g) Li, L.; Ye, Z.-w.; Lu, C.-x., Synthesis and characterization of 1-amino-3-methyl-1,2,3-triazolium nitrate. *Hanneng Cailiao* **2012**, *20* (1), 9-12; (h) Klapoetke, T. M.; Piercey, D. G.; Stierstorfer, J., The 1,3-Diamino-1,2,3-triazolium Cation: A Highly Energetic Moiety. *Eur. J. Inorg. Chem.* **2013**, *2013* (9), 1509-1517; (i) Kaplan, G.; Drake, G.; Tollison, K.; Hall, L.; Hawkins, T., Synthesis, characterization, and structural investigations of 1-amino-3-substituted-1,2,3-triazolium salts, and a new route to 1-substituted-1,2,3-triazoles. *J. Heterocycl. Chem.* **2005**, *42* (1), 19-29; (j) Drake, G. W.; Kaplan, G. M.; Hawkins, T. W. Preparation of substituted-1,2,3-triazoles. US7550601B1, 2009; (k) Drake, G.; Kaplan, G.; Hall, L.; Hawkins, T.; Larue, J., A new family of energetic ionic liquids 1-amino-3-alkyl-1,2,3-triazolium nitrates. *J. Chem. Crystallogr.* **2007**, *37* (1), 15-23.

23. Klapoetke, T. M.; Petermayer, C.; Piercey, D. G.; Stierstorfer, J., 1,3-Bis(nitroimido)-1,2,3-triazolate Anion, the N-Nitroimide Moiety, and the Strategy of Alternating Positive and Negative Charges in the Design of Energetic Materials. *J. Am. Chem. Soc.* **2012**, *134* (51), 20827-20836.

24. Huang, Y.; Gao, H.; Twamley, B.; Shreeve, J. n. M., Nitroamino triazoles: nitrogen-rich precursors of stable energetic salts. *Eur. J. Inorg. Chem.* **2008**, (16), 2560-2568.
25. Katritzky, A. R.; Maimait, R.; Denisenko, S. N.; Steel, P. J.; Akhmedov, N. G., Conversions by Dimethyldioxirane of 1-Alkylbenzotriazoles into Their N-Oxides and of 2-Alkylbenzotriazoles into 2-Alkyl-trans-4,5,6,7-diepoxy-4,5,6,7-tetrahydrobenzotriazoles. *J. Org. Chem.* **2001**, 66 (16), 5585-5589.
26. Shitov, O. P.; Vyazkov, V. A.; Tartakovskii, V. A., Synthesis of a new nitrogen-oxygen system - 1-nitramino-3-nitrimido-1,2,3-triazole salts. *Izvestiya Akademii Nauk SSSR, Seriya Khimicheskaya* **1989**, (11), 2654-5.
27. (a) Tulchinsky, Y.; Kozuch, S.; Saha, P.; Mauda, A.; Nisnevich, G.; Botoshansky, M.; Shimon, L. J. W.; Gandelman, M., Coordination Chemistry of N-Heterocyclic Nitrenium-Based Ligands. *Chemistry - A European Journal* **2015**, 21 (19), 7099-7110; (b) Tulchinsky, Y.; Kozuch, S.; Saha, P.; Botoshansky, M.; Shimon, L. J. W.; Gandelman, M., Cation-cation bonding in nitrenium metal complexes. *Chem. Sci.* **2014**, 5 (4), 1305-1311; (c) Tulchinsky, Y.; Iron, M. A.; Botoshansky, M.; Gandelman, M., Nitrenium ions as ligands for transition metals. *Nature Chemistry* **2011**, 3 (7), 525-531.
28. Heims, F.; Pfaff, F. F.; Abram, S.-L.; Farquhar, E. R.; Bruschi, M.; Greco, C.; Ray, K., Redox Non-Innocence of a N-Heterocyclic Nitrenium Cation Bound to a Nickel-Cyclam Core. *J. Am. Chem. Soc.* **2014**, 136 (2), 582-585.
29. (a) Concepcion, J. J.; Jurss, J. W.; Norris, M. R.; Chen, Z.; Templeton, J. L.; Meyer, T. J., Catalytic Water Oxidation by Single-Site Ruthenium Catalysts. *Inorganic Chemistry* **2010**, 49 (4), 1277-1279; (b) Huang, P.; Wang, Y.-X.; Yu, H.-F.; Lu, J.-M., N-Heterocyclic Carbene-Palladium(II)-4,5-Dihydrooxazole Complexes: Synthesis and Catalytic Activity toward Amination of Aryl Chlorides. *Organometallics* **2014**, 33 (7), 1587-1593.

30. Aizpurua, J. M.; Fratila, R. M.; Monasterio, Z.; Perez-Esnaola, N.; Andreieff, E.; Irastorza, A.; Sagartzazu-Aizpurua, M., Triazolium cations: from the "click" pool to multipurpose applications. *New J. Chem.* **2014**, *38* (2), 474-480.
31. Fall, A.; Seck, I.; Diouf, O.; Gaye, M.; Seck, M.; Gómez, G.; Fall, Y., Synthesis of new triazolium-based ionic liquids and their use in the Morita–Baylis–Hillman reaction. *Tetrahedron Letters*.
32. Klein, J. E. M. N.; Holzwarth, M. S.; Hohloch, S.; Sarkar, B.; Plietker, B., Redox-Active Triazolium-Derived Ligands in Nucleophilic Fe-Catalysis – Reactivity Profile and Development of a Regioselective O-Allylation. *European J. Org. Chem.* **2013**, *2013* (28), 6310-6316.
33. Rocha, R. C.; Toma, H. E., Intervalence transfer in a new benzotriazolate bridged ruthenium-iron complex. *Canadian Journal of Chemistry* **2001**, *79* (2), 145-156.
34. Breslow, R.; Gellman, S. H., Tolylsulfonylamidation of cyclohexane by a cytochrome P-450 model. *J. Chem. Soc., Chem. Commun.* **1982**, (24), 1400-1.
35. Mansuy, D.; Mahy, J.-P.; Dureault, A.; Bedi, G.; Battioni, P., Iron- and manganese-porphyrin catalysed aziridination of alkenes by tosyl- and acyl-iminoiodobenzene. *Journal of the Chemical Society, Chemical Communications* **1984**, (17), 1161-1163.
36. Groves, J. T.; Haushalter, R. C.; Nakamura, M.; Nemo, T. E.; Evans, B. J., High-valent iron-porphyrin complexes related to peroxidase and cytochrome P-450. *J. Am. Chem. Soc.* **1981**, *103* (10), 2884-6.
37. Mahy, J. P.; Battioni, P.; Mansuy, D.; Fisher, J.; Weiss, R.; Mispelter, J.; Morgenstern-Badarau, I.; Gans, P., Iron porphyrin-nitrene complexes: preparation from 1,1-dialkylhydrazines. Electronic structure from NMR, Moessbauer, and magnetic susceptibility studies and crystal structure of the [tetrakis(p-chlorophenyl)porphyrinato][(2,2,6,6-tetramethyl-1-piperidyl)nitrene]iron complex. *J. Am. Chem. Soc.* **1984**, *106* (6), 1699-706.

38. Meprathu, B. V.; Protasiewicz, J. D., Enhancing the solubility for hypervalent ortho-sulfonyl iodine compounds. *Tetrahedron* **2010**, *66* (31), 5768-5774.
39. Yoshimura, A.; Nemykin, V. N.; Zhdankin, V. V., o-Alkoxyphenyliminoiodanes: Highly Efficient Reagents for the Catalytic Aziridination of Alkenes and the Metal-Free Amination of Organic Substrates. *Chemistry – A European Journal* **2011**, *17* (38), 10538-10541.
40. Zdilla, M. J.; Abu-Omar, M. M., Mechanism of catalytic aziridination with manganese corrole: the often postulated high-valent Mn(V) imido is not the group transfer reagent. *J Am Chem Soc* **2006**, *128* (51), 16971-9.
41. Yang, M.; Su, B.; Wang, Y.; Chen, K.; Jiang, X.; Zhang, Y.-F.; Zhang, X.-S.; Chen, G.; Cheng, Y.; Cao, Z.; Guo, Q.-Y.; Wang, L.; Shi, Z.-J., Silver-catalysed direct amination of unactivated C-H bonds of functionalized molecules. *Nat. Commun.* **2014**, *5*, 4707.
42. Postle, S.; Stephan, D. W., Reactions of iodine-nitrene reagents with boranes. *Dalton Transactions* **2015**, *44* (10), 4436-4439.
43. Adam, W.; Doerr, M.; Hill, K.; Peters, E. M.; Peters, K.; Von Schnering, H. G., Synthesis, photolysis, and thermolysis of azoalkanes derived from spirocyclopropane-substituted norbornenes: competitive nitrogen loss and diazoalkane formation. *J. Org. Chem.* **1985**, *50* (5), 587-95.
44. Figuera, J. M.; Perez, J. M.; Tobar, A., A systematic study of the energy partitioning in the photolysis of diazoalkanes and alkyl diazirines. *An. Quim.* **1976**, *72* (9-10), 737-42.
45. (a) McDonald, J. R.; Miller, R. G.; Baronavski, A. P., Laser induced photodissociation of HN₃ at 266 nm. II. Reactions of imidogen(¹Δ) with HN₃, hydrogen chloride and hydrocarbon species. *Chem. Phys.* **1978**, *30* (2), 133-45; (b) Kajimoto, O.; Fueno, T., Reactions of electronically excited imidogen radical (a¹Δ) with ethane. *Chem. Phys. Lett.* **1981**, *80* (3), 484-7.

46. (a) Moriarty, R. M.; Reardon, R. C., Direct and photosensitized decomposition of alkyl azides. *Tetrahedron* **1970**, *26* (6), 1379-92; (b) Montgomery, F. C.; Saunders, W. H., Jr., Migration aptitudes in the photolysis of some tertiary alkyl azides. *J. Org. Chem.* **1976**, *41* (14), 2368-72.
47. Kyba, E. P.; Abramovitch, R. A., Photolysis of alkyl azides. Evidence for a nonnitrene mechanism. *J. Am. Chem. Soc.* **1980**, *102* (2), 735-40.
48. (a) Banks, R. E.; Berry, D.; McGlinchey, M. J.; Moore, G. J., Azide chemistry. II. Photolysis of 2H-hexafluoropropyl and 2-chloro-1,1,2-trifluoroethyl azide. *J. Chem. Soc., C* **1970**, (8), 1017-23; (b) Pancrazi, A.; Khuong, H. Q., Steroidal alkaloids. CLXXIII. Thermolysis and acid-catalyzed decomposition of 6-azido steroids. Comparison with photolytic reactions. *Tetrahedron* **1975**, *31* (17), 2049-56.
49. (a) Sheridan, R. S.; Ganzer, G. A., Observation of 2-azabicyclo[3.2.1]oct-1-ene, highly reactive bridgehead imine. *J. Am. Chem. Soc.* **1983**, *105* (19), 6158-60; (b) Michl, J.; Radziszewski, G. J.; Downing, J. W.; Wiberg, K. B.; Walker, F. H.; Miller, R. D.; Kovacic, P.; Jawdosiuk, M.; Bonacic-Koutecky, V., Highly strained single and double bonds. *Pure Appl. Chem.* **1983**, *55* (2), 315-21; (c) Radziszewski, J. G.; Downing, J. W.; Jawdosiuk, M.; Kovacic, P.; Michl, J., 4-Azahomoadamant-3-ene: spectroscopic characterization and photoresolution of a highly reactive strained bridgehead imine. *J. Am. Chem. Soc.* **1985**, *107* (3), 594-603; (d) Dunkin, I. R.; Shields, C. J.; Quast, H.; Seiferling, B., The photolysis of 1-azido-4-methylbicyclo[2.2.2]octane and 1-azidoadamantane in low-temperature matrixes. *Tetrahedron Lett.* **1983**, *24* (36), 3887-90.
50. Lewis, F. D.; Saunders, W. H., Jr., Sensitized photolysis of organic azides. Possible case of nonclassical energy transfer. *J. Amer. Chem. Soc.* **1968**, *90* (25), 7033-8.
51. Wagner, P. J.; Scheve, B. J., Competing triplet reactions in azidoketones. *J. Am. Chem. Soc.* **1979**, *101* (2), 378-83.

52. Muthukrishnan, S.; Mandel, S. M.; Hackett, J. C.; Singh, P. N. D.; Hadad, C. M.; Krause, J. A.; Gudmundsdottir, A. D., Competition between α -Cleavage and Energy Transfer in α -Azidoacetophenones. *J. Org. Chem.* **2007**, *72* (8), 2757-2768.
53. Singh, P. N. D.; Mandel, S. M.; Sankaranarayanan, J.; Muthukrishnan, S.; Chang, M.; Robinson, R. M.; Lahti, P. M.; Ault, B. S.; Gudmundsdottir, A. D., Selective Formation of Triplet Alkyl Nitrenes from Photolysis of β -Azido-Propiophenone and Their Reactivity. *J. Am. Chem. Soc.* **2007**, *129* (51), 16263-16272.
54. (a) Shang, H.; Yu, C.; Ying, L.; Zhao, X., Investigation of the $\sim A3E \leftrightarrow \sim X3A2$ system of methylnitrene radical by laser spectroscopy. *J. Chem. Phys.* **1995**, *103* (11), 4418-26; (b) Ferrante, R. F., Vibrational frequencies in the $\sim A3E$ state of methylnitrene. *J. Chem. Phys.* **1991**, *94* (6), 4678-9.
55. Travers, M. J.; Cowles, D. C.; Clifford, E. P.; Ellison, G. B.; Engelking, P. C., Photoelectron spectroscopy of the CH_3N^- ion. *J. Chem. Phys.* **1999**, *111* (12), 5349-5360.
56. (a) Arenas, J. F.; Marcos, J. I.; Otero, J. C.; Sanchez-Galvez, A.; Soto, J., A multiconfigurational self-consistent field study of the thermal decomposition of methyl azide. *J. Chem. Phys.* **1999**, *111* (2), 551-561; (b) Kemnitz, C. R.; Ellison, G. B.; Karney, W. L.; Borden, W. T., CASSCF and CASPT2 Ab Initio Electronic Structure Calculations Find Singlet Methylnitrene Is an Energy Minimum. *J. Am. Chem. Soc.* **2000**, *122* (6), 1098-1101.
57. (a) Smolinsky, G.; Pryde, C. A., Vinyl azide chemistry. Thermally induced reactions. *J. Org. Chem.* **1968**, *33* (6), 2411-16; (b) Smolinsky, G., Formation of azacyclopropenes by pyrolysis of vinyl azides. *J. Org. Chem.* **1962**, *27*, 3557-9; (c) Hassner, A.; Fowler, F. W., Stereochemistry. XXXII. Synthesis and reactions of 1-azirines. *J. Amer. Chem. Soc.* **1968**, *90* (11), 2869-75; (d) Isomura, K.; Okada, M.; Taniguchi, H., Azirine formation by decomposition of terminal vinyl azides. *Tetrahedron Lett.* **1969**, (46), 4073-6; (e) Hassner, A.; Fowler, F. W., Stereochemistry. XXVIII.

General synthesis of 2H-azirines from olefins. Fused azirines. *Tetrahedron Lett.* **1967**, (16), 1545-8; (f) Bauer, W.; Hafner, K., Synthesis and reactions of a 2H-azirine unsubstituted on C-3. *Angew. Chem., Int. Ed. Engl.* **1969**, *8* (10), 772-3; (g) Boyer, J. H.; Krueger, W. E.; Modler, R., Acid-catalyzed reactions of α - and β -styryl azides. *J. Org. Chem.* **1969**, *34* (6), 1987-9; (h) Boyer, J. H.; Krueger, W. E.; Mikol, G. J., β -Styrylnitrene. *J. Am. Chem. Soc.* **1967**, *89* (21), 5504-5; (i) Chapman, O. L.; Le Roux, J. P., 1-Aza-1,2,4,6-cycloheptatetraene. *J. Am. Chem. Soc.* **1978**, *100* (1), 282-5; (j) Fowler, F. W.; Hassner, A.; Levy, L. A., Stereospecific introduction of azide functions into organic molecules. *J. Am. Chem. Soc.* **1967**, *89* (9), 2077-82; (k) Bock, H.; Dammel, R.; Aygen, S., Gas-phase reactions. 36. Pyrolysis of vinyl azide. *J. Am. Chem. Soc.* **1983**, *105* (26), 7681-5; (l) Lohr, L. L., Jr.; Hanamura, M.; Morokuma, K., The 1,2 hydrogen shift as an accompaniment to ring closure and opening: ab initio MO study of thermal rearrangements on the C₂H₃N potential energy hypersurface. *J. Am. Chem. Soc.* **1983**, *105* (17), 5541-7; (m) Yamabe, T.; Kaminoyama, M.; Minato, T.; Hori, K.; Isomura, K.; Taniguchi, H., Electronic structures of vinyl azide, vinylnitrene and 2H-azirine. Mechanism of the conversion of vinyl azide to 2H-azirine. *Tetrahedron* **1984**, *40* (11), 2095-9; (n) Parasuk, V.; Cramer, C. J., Multireference configuration interaction and second-order perturbation theory calculations for the 13A'', 11A'', and 11A' electronic states of vinylnitrene and vinylphosphinidene. *Chem. Phys. Lett.* **1996**, *260* (1,2), 7-14.

58. Schuster, G. B.; Platz, M. S., Photochemistry of phenyl azide. *Adv. Photochem.* **1992**, *17*, 69-143.

59. (a) Gritsan, N. P.; Platz, M. S., Kinetics and spectroscopy of substituted phenylnitrenes. *Adv. Phys. Org. Chem.* **2001**, *36*, 255-304; (b) Karney, W. L.; Borden, W. T., Differences between phenylcarbene and phenylnitrene and the ring expansion reactions they undergo. *Adv. Carbene Chem.* **2001**, *3*, 205-251.

60. (a) Gritsan, N. P.; Polshakov, D. A.; Tsao, M.-L.; Platz, M. S., A study of 2-azido-3,5-dichlorobiphenyl by nano- and picosecond laser flash photolysis and computational methods. *Photochem. Photobiol. Sci.* **2005**, *4* (1), 23-32; (b) Burdzinski, G. T.; Gustafson, T. L.; Hackett, J. C.; Hadad, C. M.; Platz, M. S., The Direct Detection of an Aryl Azide Excited State: An Ultrafast Study of the Photochemistry of para- and ortho-Biphenyl Azide. *J. Am. Chem. Soc.* **2005**, *127* (40), 13764-13765; (c) Burdzinski, G.; Hackett, J. C.; Wang, J.; Gustafson, T. L.; Hadad, C. M.; Platz, M. S., Early Events in the Photochemistry of Aryl Azides from Femtosecond UV/Vis Spectroscopy and Quantum Chemical Calculations. *J. Am. Chem. Soc.* **2006**, *128* (41), 13402-13411; (d) McCulla, R. D.; Burdzinski, G.; Platz, M. S., Ultrafast Study of the Photochemistry of 2-Azidonitrobenzene. *Org. Lett.* **2006**, *8* (8), 1637-1640; (e) Burdzinski, G. T.; Middleton, C. T.; Gustafson, T. L.; Platz, M. S., Solution Phase Isomerization of Vibrationally Excited Singlet Nitrenes to Vibrationally Excited 1,2-Didehydroazepine. *J. Am. Chem. Soc.* **2006**, *128* (46), 14804-14805; (f) Wang, J.; Kubicki, J.; Platz, M. S., An Ultrafast Study of Phenyl Azide: The Direct Observation of Phenylnitrenium Ion. *Org. Lett.* **2007**, *9* (20), 3973-3976; (g) Wang, J.; Burdzinski, G.; Zhu, Z.; Platz, M. S.; Carra, C.; Bally, T., Ultrafast Spectroscopic and Matrix Isolation Studies of p-Biphenylyl, o-Biphenylyl, and 1-Naphthylnitrenium Cations. *J. Am. Chem. Soc.* **2007**, *129* (26), 8380-8388; (h) Wang, J.; Burdzinski, G.; Platz, M. S., Solvent Effects on Intermolecular Proton Transfer: The Rates of Nitrene Protonation and Their Correlation with Swain Acity. *Org. Lett.* **2007**, *9* (25), 5211-5214.
61. Huisgen, R.; Vossius, D.; Appl, M., Thermolysis of phenyl azide in primary amines; the constitution of dibenzamil. *Chem. Ber.* **1958**, *91*, 1-12.
62. Doering, W. v. E.; Odum, R. A., Ring enlargement in the photolysis of phenyl azide. *Tetrahedron* **1966**, *22* (1), 81-93.
63. (a) Schrock, A. K.; Schuster, G. B., Photochemistry of phenyl azide: chemical properties of the transient intermediates. *J. Am. Chem. Soc.* **1984**, *106* (18), 5228-34;

- (b) Liang, T. Y.; Schuster, G. B., Photochemistry of p-nitrophenyl azide: single-electron-transfer reaction of the triplet nitrene. *J. Am. Chem. Soc.* **1986**, *108* (3), 546-8.
64. (a) Pritchina, E. A.; Gritsan, N. P., Mechanism of p-azidoaniline photolysis in the presence of oxygen. *J. Photochem. Photobiol., A* **1988**, *43* (2), 165-82; (b) Gritsan, N. P.; Pritchina, E. S., Mechanism of photochemical transformations of aromatic azides. *J. Inf. Rec. Mater.* **1989**, *17* (5-6), 391-404; (c) Brinen, J. S.; Singh, B., Electron spin resonance and luminescence studies of the reaction of photochemically generated nitrenes with oxygen. Phosphorescence of nitrobenzenes. *J. Amer. Chem. Soc.* **1971**, *93* (24), 6623-9; (d) Pritchina, E. A.; Gritsan, N. P.; Bally, T., Matrix isolation and computational study of the photochemistry of p-azidoaniline. *Phys. Chem. Chem. Phys.* **2006**, *8* (6), 719-727.
65. Leyva, E.; Platz, M. S.; Persy, G.; Wirz, J., Photochemistry of phenyl azide: the role of singlet and triplet phenylnitrene as transient intermediates. *J. Am. Chem. Soc.* **1986**, *108* (13), 3783-90.
66. (a) Warmuth, R.; Makowiec, S., The Phenylnitrene Rearrangement in the Inner Phase of a Hemicarcerand. *J. Am. Chem. Soc.* **2005**, *127* (4), 1084-1085; (b) Warmuth, R.; Makowiec, S., Photochemical and Thermal Reactions of Intermediates in the Phenylnitrene Rearrangement Inside a Hemicarcerand. *J. Am. Chem. Soc.* **2007**, *129* (5), 1233-1241.
67. Dunkin, I. R.; Lynch, M. A.; McAlpine, F.; Sweeney, D., A medium effect in the photolysis of phenyl azide in low-temperature matrixes. *J. Photochem. Photobiol., A* **1997**, *102* (2-3), 207-212.
68. Wolff, L., Diazo Anhydrides (1,2,3-Oxydiazoles or Diazo Oxides) and Diazo Ketones. *Justus Liebigs Ann. Chem.* **1913**, *394*, 23-59.
69. Aube, J.; Fehl, C.; Liu, R.; McLeod, M. C.; Motiwala, H. F., Hofmann, Curtius, Schmidt, Lossen, and related reactions. In *Comprehensive Organic Synthesis*, 2 ed.; Elsevier B.V.: 2014; Vol. 6, pp 598-635.

70. Curtius, T., On hydrazoic acid (azoimide). *Ber. Dtsch. Chem. Ges.* **23**, 3023.
71. (a) Vyas, S.; Kubicki, J.; Luk, H. L.; Zhang, Y.; Gritsan, N. P.; Hadad, C. M.; Platz, M. S., An ultrafast time-resolved infrared and UV-vis spectroscopic and computational study of the photochemistry of acyl azides. *J. Phys. Org. Chem.* **2012**, *25* (8), 693-703; (b) Tarwade, V.; Dmitrenko, O.; Bach, R. D.; Fox, J. M., The Curtius Rearrangement of Cyclopropyl and Cyclopropenoyl Azides. A Combined Theoretical and Experimental Mechanistic Study. *The J. Org. Chem.* **2008**, *73* (21), 8189-8197; (c) Wentrup, C.; Bornemann, H., The Curtius Rearrangement of Acyl Azides Revisited – Formation of Cyanate (R–O–CN). *European J. Org. Chem.* **2005**, *2005* (21), 4521-4524; (d) Kubicki, J.; Zhang, Y.; Xue, J.; Luk, H. L.; Platz, M., Ultrafast time resolved studies of the photochemistry of acyl and sulfonyl azides. *Phys. Chem. Chem. Phys.* **2012**, *14* (30), 10377-10390; (e) Kubicki, J.; Zhang, Y.; Wang, J.; Luk, H. L.; Peng, H.-L.; Vyas, S.; Platz, M. S., Direct Observation of Acyl Azide Excited States and Their Decay Processes by Ultrafast Time Resolved Infrared Spectroscopy. *J. Am. Chem. Soc.* **2009**, *131* (12), 4212-4213; (f) Kubicki, J.; Zhang, Y.; Vyas, S.; Burdzinski, G.; Luk, H. L.; Wang, J.; Xue, J.; Peng, H.-L.; Pritchina, E. A.; Sliwa, M.; Buntinx, G.; Gritsan, N. P.; Hadad, C. M.; Platz, M. S., Photochemistry of 2-Naphthoyl Azide. An Ultrafast Time-Resolved UV-Vis and IR Spectroscopic and Computational Study. *J. Am. Chem. Soc.* **2011**, *133* (25), 9751-9761; (g) Liu, J.; Mandel, S.; Hadad, C. M.; Platz, M. S., A Comparison of Acetyl- and Methoxycarbonylnitrenes by Computational Methods and a Laser Flash Photolysis Study of Benzoylnitrene. *J. Org. Chem.* **2004**, *69* (25), 8583-8593; (h) Sigman, M. E.; Autrey, T.; Schuster, G. B., Aroylnitrenes with singlet ground states: photochemistry of acetyl-substituted aroyl and aryloxycarbonyl azides. *J. Am. Chem. Soc.* **1988**, *110* (13), 4297-305; (i) McConaghy, J. S., Jr.; Lwowski, W., Singlet and triplet nitrenes. II. Carbethoxynitrene generated from ethyl azidoformate. *J. Am. Chem. Soc.* **1967**, *89* (17), 4450-6.

72. Pritchina, E. A.; Gritsan, N. P.; Maltsev, A.; Bally, T.; Autrey, T.; Liu, Y.; Wang, Y.; Toscano, J. P., Matrix isolation, time-resolved IR, and computational study of the photochemistry of benzoyl azide. *Phys. Chem. Chem. Phys.* **2003**, *5* (6), 1010-1018.
73. Zeng, X.; Beckers, H.; Willner, H.; Grote, D.; Sander, W., The Missing Link: Triplet Fluorocarbonyl Nitrene FC(O)N. *Chem. Eur. J.* **2011**, *17* (14), 3977-3984, S3977/1-S3977/8.
74. Sun, H.; Zhu, B.; Wu, Z.; Zeng, X.; Beckers, H.; Jenks, W. S., Thermally Persistent Carbonyl Nitrene: FC(O)N. *J. Org. Chem.* **2015**, *80* (3), 2006-2009.
75. Yale, H. L., The Hydroxamic Acids. *Chem. Rev.* **1943**, *33* (3), 209-256.
76. Vasantha, B.; Hemantha, H. P.; Sureshbabu, V. V., 1-Propanephosphonic acid cyclic anhydride (T3P) as an efficient promoter for the Lossen rearrangement: application to the synthesis of urea and carbamate derivatives. *Synthesis* **2010**, (17), 2990-2996.
77. Hoshino, Y.; Shimbo, Y.; Ohtsuka, N.; Honda, K., Self-propagated Lossen rearrangement induced by a catalytic amount of activating agents under mild conditions. *Tetrahedron Lett.* **2015**, *56* (5), 710-712.
78. Abdel Hafez, E.-S. M. N.; Aly, O. M.; Abuo-Rahma, G. E.-D. A. A.; King, S. B., Lossen Rearrangements under Heck Reaction Conditions. *Adv. Synth. Catal.* **2014**, *356* (16), 3456-3464.
79. Shan, G.-Q.; Yu, A.; Zhao, C.-F.; Huang, C.-H.; Zhu, L.-Y.; Zhu, B.-Z., A Combined Experimental and Computational Investigation on the Unusual Molecular Mechanism of the Lossen Rearrangement Reaction Activated by Carcinogenic Halogenated Quinones. *J. Org. Chem.* **2015**, *80* (1), 180-189.
80. Pichette, S.; Aubert-Nicol, S.; Lessard, J.; Spino, C., Photochemical and Thermal Ring-Contraction of Cyclic Hydroxamic Acid Derivatives. *J. Org. Chem.* **2012**, *77* (24), 11216-11226.

81. Rajeev, K. S.; Li, Y. A new method for preparation of Oseltamivir intermediate. CN104447451A, 2015.
82. Sulzer-Mosse, S.; Cederbaum, F.; Lamberth, C.; Berthon, G.; Umarye, J.; Grasso, V.; Schlereth, A.; Blum, M.; Waldmeier, R., Synthesis and fungicidal activity of N-thiazol-4-yl-salicylamides, a new family of anti-oomycete compounds. *Bioorg. Med. Chem.* **2015**, *23* (9), 2129-2138.
83. Zhao, J.; Gimi, R.; Katti, S.; Reardon, M.; Nivorozhkin, V.; Konowicz, P.; Lee, E.; Sole, L.; Green, J.; Siegel, C. S., Process Development of a GCS Inhibitor Including Demonstration of Lossen Rearrangement on Kilogram Scale. *Org. Process Res. Dev.* **2015**, *19* (5), 576-581.
84. Hofmann, A. W., Ueber die Einwirkung des Broms in alkalischer Lösung auf die Amine. *Ber. Dtsch. Chem. Ges.* **1883**, *16* (1), 558-560.
85. Kovacic, P.; Lowery, M. K.; Field, K. W., Chemistry of N-bromamines and N-chloramines. *Chem. Rev.* **1970**, *70* (6), 639-65.
86. (a) Ochiai, M.; Miyamoto, K.; Hayashi, S.; Nakanishi, W., Hypervalent N-sulfonylimino- λ^3 -bromane: active nitrenoid species at ambient temperature under metal-free conditions. *Chem. Commun. (Cambridge, U. K.)* **2010**, *46* (4), 511-521; (b) Ochiai, M.; Okada, T.; Tada, N.; Yoshimura, A.; Miyamoto, K.; Shiro, M., Difluoro- λ^3 -bromane-Induced Hofmann Rearrangement of Sulfonamides: Synthesis of Sulfamoyl Fluorides. *J. Am. Chem. Soc.* **2009**, *131* (24), 8392-8393.
87. Gonzalez, M. J.; Lopez, L. A.; Vicente, R., Zinc reagents as non-noble catalysts for alkyne activation. *Tetrahedron Lett.* **2015**, *56* (13), 1600-1608.
88. Wang, B.-J.; Xue, P.; Gu, P., Intramolecular Schmidt reaction of acyl chlorides with alkyl azides: preparation of pyrrolizine by intramolecular capture of intermediates with alkenes or alkynes. *Chem. Commun. (Camb)* **2015**, *51* (12), 2277-9.

89. Tang, C.; Yuan, Y.; Jiao, N.; Jiao, N., Metal-free nitrogenation of 2-acetylbiphenyls: expeditious synthesis of phenanthridines. *Org. Lett.* **2015**, *17* (9), 2206-9.
90. McNaught, A. D.; Wilkinson, A., IUPAC. In *Compendium of Chemical Terminology*, 2nd Ed. ed.; Blackwell Scientific Publications: Oxford, 1997.
91. Dequierez, G.; Pons, V.; Dauban, P., Nitrene Chemistry in Organic Synthesis: Still in Its Infancy? *Angew. Chem. Int. Ed.* **2012**, *51* (30), 7384-7395.
92. Sweeney, J. B. In *Synthesis of aziridines*, Wiley-VCH Verlag GmbH & Co. KGaA: 2006; pp 117-144.
93. Xu, Y.-J.; Zhang, Y.-F.; Li, J.-Q., Functionalization of Diamond (100) by Organic Cycloaddition Reactions of Nitrenes: A Theoretical Prediction. *J. Org. Chem.* **2005**, *70* (19), 7773-7775.
94. Lin, X.; Xi, Y.; Sun, J., A computational study on the competing intramolecular amidation and aziridination reactions catalyzed by dirhodium tetracarboxylate. *Comput. Theor. Chem.* **2012**, *999*, 74-82.
95. Ramasundaram, S.; Hwang, S. W.; Lee, J.; Jung, J.; Choi, K. J.; Hong, S. W., Facile synthesis of catechol functionalized aziridinofullerenes for visible light photocatalysis applications. *Mater. Lett.* **2013**, *106*, 213-217.
96. Takeda, Y.; Kawai, H.; Minakata, S., PCy₃-Catalyzed Ring Expansion of Aziridinofullerenes with CO₂ and Aryl Isocyanates: Evidence for a Two Consecutive Nucleophilic Substitution Pathway on the Fullerene Cage. *Chem. Eur. J.* **2013**, *19* (40), 13479-13483.
97. Servinis, L.; Henderson, L. C.; Gengenbach, T. R.; Kafi, A. A.; Huson, M. G.; Fox, B. L., Surface functionalization of unsized carbon fiber using nitrenes derived from organic azides. *Carbon* **2013**, *54*, 378-388.

98. Verma, S.; Jain, S. L., Nanocrystalline zinc peroxide mediated unprecedented nitrene transfer: an expeditious access to N-tosylaziridines. *RSC Adv.* **2013**, *3* (43), 19830-19833.
99. McVerry, B. T.; Wong, M. C. Y.; Marsh, K. L.; Temple, J. A. T.; Marambio-Jones, C.; Hoek, E. M. V.; Kaner, R. B., Scalable Antifouling Reverse Osmosis Membranes Utilizing Perfluorophenyl Azide Photochemistry. *Macromol. Rapid Commun.* **2014**, *35* (17), 1528-1533.
100. Evans, D. A.; Faul, M. M.; Bilodeau, M. T., Copper-catalyzed aziridination of olefins by (N-(p-toluenesulfonyl)imino)phenyliodinane. *J. Org. Chem.* **1991**, *56* (24), 6744-6.
101. Li, Z.; Quan, R. W.; Jacobsen, E. N., Mechanism of the (Diimine)copper-Catalyzed Asymmetric Aziridination of Alkenes. Nitrene Transfer via Ligand-Accelerated Catalysis. *J. Am. Chem. Soc.* **1995**, *117* (21), 5889-90.
102. Evans, D. A.; Bilodeau, M. T.; Faul, M. M., Development of the Copper-Catalyzed Olefin Aziridination Reaction. *J. Am. Chem. Soc.* **1994**, *116* (7), 2742-53.
103. Chang, J. W. W.; Chan, P. W. H., Highly efficient ruthenium(II) porphyrin catalyzed amidation of aldehydes. *Angew. Chem., Int. Ed.* **2008**, *47* (6), 1138-1140.
104. Maestre, L.; Sameera, W. M. C.; Diaz-Requejo, M. M.; Maseras, F.; Perez, P. J., A General Mechanism for the Copper- and Silver-Catalyzed Olefin Aziridination Reactions: Concomitant Involvement of the Singlet and Triplet Pathways. *J. Am. Chem. Soc.* **2013**, *135* (4), 1338-1348.
105. (a) Liu, Y.; Guan, X.; Wong, E. L.-M.; Liu, P.; Huang, J.-S.; Che, C.-M., Nonheme Iron-Mediated Amination of C(sp³)-H Bonds. Quinquepyridine-Supported Iron-Imide/Nitrene Intermediates by Experimental Studies and DFT Calculations. *J. Am. Chem. Soc.* **2013**, *135* (19), 7194-7204; (b) Liu, Y.; Che, C.-M., [Fe(III)(F(20)-tpp)Cl] is an effective catalyst for nitrene transfer reactions and amination of saturated hydrocarbons with sulfonyl and aryl azides as nitrogen source under thermal and

microwave-assisted conditions. *Chem. Eur. J.* **2010**, *16* (34), 10494-501; (c) Liu, G.-S.; Zhang, Y.-Q.; Yuan, Y.-A.; Xu, H., Iron(II)-Catalyzed Intramolecular Aminohydroxylation of Olefins with Functionalized Hydroxylamines. *J. Am. Chem. Soc.* **2013**, *135* (9), 3343-3346; (d) Hennessy, E. T.; Liu, R. Y.; Iovan, D. A.; Duncan, R. A.; Betley, T. A., Iron-mediated intermolecular N-group transfer chemistry with olefinic substrates. *Chem. Sci.* **2014**, *5* (4), 1526-1532.

106. Tao, J.; Jin, L.-M.; Zhang, X. P., Synthesis of chiral N-phosphoryl aziridines through enantioselective aziridination of alkenes with phosphoryl azide via Co(II)-based metalloradical catalysis. *Beilstein J. Org. Chem.* **2014**, *10*, 1282-1289, 8 pp.

107. Liang, S.; Jensen, M. P., Half-sandwich scorpionates as nitrene transfer catalysts. *Organometallics* **2012**, *31* (23), 8055-8058.

108. Basolo, F., Metal nitrene chemistry. *J. Indian. Chem. Soc.* **1977**, *54* (1-3), 7-12.

109. (a) Berry, J. F., The role of three-center/four-electron bonds in superelectrophilic dirhodium carbene and nitrene catalytic intermediates. *Dalton Trans.* **2012**, *41* (3), 700-13; (b) Conradie, J.; Ghosh, A., Electronic structure of an iron-porphyrin-nitrene complex. *Inorg. Chem.* **2010**, *49* (1), 243-8; (c) Duarte, D. J. R.; Miranda, M. S.; Esteves da Silva, J. C. G., Theoretical characterization of molecular complexes formed between triplet vinyl nitrene and Lewis acids. *Struct. Chem.* **2015**, *26* (2), 565-571.

110. Cundari, T. R.; Dinescu, A.; Kazi, A. B., Bonding and Structure of Copper Nitrenes. *Inorg. Chem.* **2008**, *47* (21), 10067-10072.

111. Badiei, Y. M.; Dinescu, A.; Dai, X.; Palomino, R. M.; Heinemann, F. W.; Cundari, T. R.; Warren, T. H., Copper-Nitrene Complexes in Catalytic C-H Amination. *Angew. Chem. Int. Ed.* **2008**, *47* (51), 9961-9964.

112. Dielmann, F.; Andrada, D. M.; Frenking, G.; Bertrand, G., Isolation of Bridging and Terminal Coinage Metal-Nitrene Complexes. *J. Am. Chem. Soc.* **2014**, *136* (10), 3800-3802.

2

Synthesis, Characterization and Comparison of Group 14 Pyrrolides and Indolides Ph_3MX ($\text{M} = \text{Si}, \text{Ge}, \text{Sn}$; $\text{X} = \text{C}_4\text{H}_4\text{N}, \text{C}_8\text{H}_6\text{N}$)

2.1 Preamble

The study of nitrogen in states of electron-deficiency would not be complete without a reference to its normal behaviour and chemical reactivity. For the current thesis, this involves its behaviour as an electron-rich nucleophile set in an aromatic framework. Using the heterocycles pyrrole and indole, not only can this be illustrated, but also the reactivity of N-heterocyclic systems containing a single nitrogen atom can be highlighted. This reactivity can then be juxtaposed with that of hydrazine-derived species containing two directly bonded nitrogen atoms, which comprises the subsequent chapters in this thesis. A striking feature exhibited by the single-nitrogen heterocycles of this present chapter is their increased nucleophilicity and hence ability to self-polymerize, which are characteristics not common to the higher heterocycles containing N-N bonds.

The work in this chapter was originally published in the *Journal of Organometallic Chemistry* and is adapted from:

Joël Poisson, Ivor Wharf, D. Scott Bohle, Mirela M. Barsan, Yuxuan Gu and Ian S. Butler, "Synthesis, Characterization and Comparison of Group 14 Pyrrolides and Indolides Ph_3MX ($\text{M} = \text{Si}, \text{Ge}, \text{Sn}$; $\text{X} = \text{C}_4\text{H}_4\text{N}, \text{C}_8\text{H}_6\text{N}$)", *Journal of Organometallic Chemistry*, **2010**, 695 (23), 2557-2561, Copyright (2010) with permission from Elsevier.

2.2 Introduction

The chemistry of transition metals coupled to organic moieties has been explored for many years. This major research area is still continuing to develop today, as evidenced by the ever-increasing number of journals dedicated solely to transition metal-organic chemistry¹. One class of main group compounds, which is of considerable practical interest, is that of organotins². These compounds have many important uses, most notably as biocides and in the development of novel treatments for various diseases³. There are only a few compounds known in which a tin atom is bonded to the hetero-atom of a heterocycle. Two heterocycles of particular biological significance are pyrrole, C_4H_4N , and indole, C_8H_6N , the synthetic organic chemistry of which has been studied since the early 20th century⁴. These heterocycles play important roles in nature, e.g., in chlorophyll, the green pigment of plant leaves and algae, and in tryptophan, $(C_8H_6N)CH_2CH(NH_2)(COOH)$, the essential amino acid that is released from proteins by the enzyme trypsin during digestion. Linkage of a metal centre to the heterocycles can be achieved exclusively at the nitrogen atoms in both cases by using an alkyl-lithium or -sodium reagent, and it has already proven possible to attach various metal atoms to them, usually with the formation of only one major product⁵.

There are several instances of syntheses of pyrrolides and indolides using the group 14 elements in the literature⁶. These studies have usually focused on the reactivity of only one particular group 14 metal with pyrrole and indole. The number of comparative experiments employing several of the group 14 elements is, however, limited⁷. There is also no instance of a comparative study contrasting the unsubstituted group 14 pyrrolides with the corresponding indolides. The group 14 triphenylchlorides, Ph_3MCl ($M = Si, Ge, Sn$), are ideal precursors for the controlled coupling of pyrrole and indole to main group metal centres to facilitate such a comparison. While the synthesis of triphenylgermanium(IV) pyrrolide⁸, and triphenyltin(IV) pyrrolide⁹, and the use of

triphenyllead(IV) pyrrole and indole derivatives¹⁰ in mass spectrometric studies have been reported previously, the synthesis of the analogous pyrrolides and indolides of the other group 14 elements have apparently not been attempted. It is possible that the best synthetic conditions for these compounds had not been found previously because of the facile self-polymerization of the heterocyclic reagents, which would hinder this type of product formation¹¹ by competing with chloride substitution on the metal centre. We report here the first successful synthesis and characterization of the complete series of group 14 triphenylmetal(IV) pyrrolides and indolides (Figure 2-1), Ph_3MX ($\text{M} = \text{Si}, \text{Ge}, \text{Sn}$; $\text{X} = \text{C}_4\text{H}_4\text{N}, \text{C}_8\text{H}_6\text{N}$).

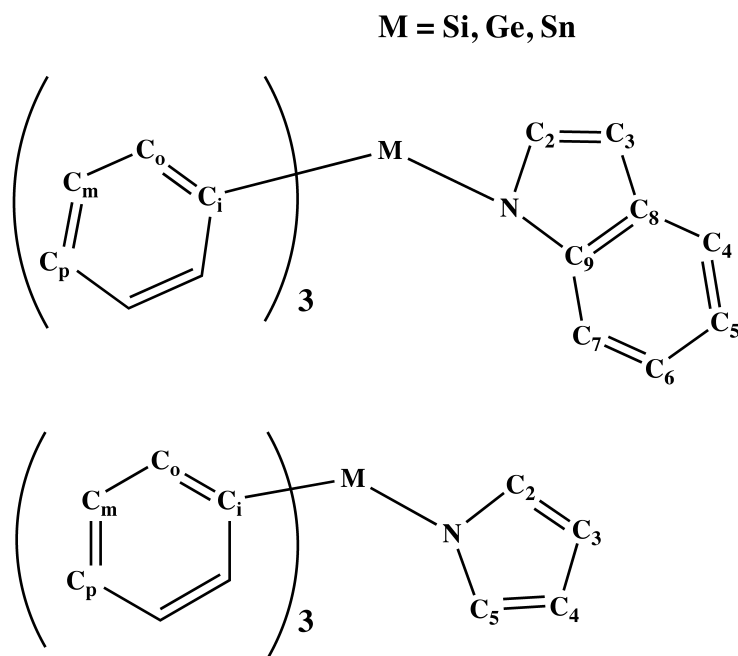


Figure 2-1: General structure of pyrrolides and indolides.

2.3 Results and Discussion

The reactions of the group 14 triphenylchlorides, Ph_3MCl ($\text{M} = \text{Si}, \text{Ge}, \text{Sn}$), with lithiated pyrrole and indole were all successful and resulted in the formation of a single product in each case. Most products gave the appropriate microanalyses but for 5 carbon results were consistently low (~77%) for several samples, even after drying.

These data are consistent with **5** being a monohydrate at room temperature. In contrast, $^1\text{H-NMR}$ (CDCl_3) suggests that **5** has about $\frac{1}{2}\text{H}_2\text{O}$ per pyrrolyl unit. This presumed hydrate is now under further investigation. All white crystalline solids obtained are stable over a period of several days in air and light but eventually darken due to hydrolysis of the heterocyclic moiety. Relatively low temperatures had to be used in the syntheses in order to minimize the possibility of self-polymerization of the heterocycles and, presumably for this reason, the product yields were quite low (<55%), with the best yields being obtained for the germanium compounds in both cases: $\text{Ph}_3\text{M}(\text{pyrrole})$ [Sn (8.2%); Si (13.6%); Ge (20.9%)]; $\text{Ph}_3\text{M}(\text{indole})$: [Si (37.5%); Sn (38.0%); Ge (54.7%)]. The melting points for the pyrrole compounds (**4-6**) range between 202-205 °C and are significantly higher than are those for the corresponding indole compounds (**1-3**) (144.7-153.6 °C). This trend parallels that observed earlier for the related tetraphenyl derivatives, Ph_4M , which upon replacement of one of the phenyl groups with another substituent results in a lowering of the overall spherical geometry of the molecules. For example, tetraphenyltin(IV) (m.p. = 225 °C) melts at a much higher temperature than does triphenyltin(IV) acetate (m.p. = 122-124 °C). The similarity in the shapes of the pyrrole and phenyl groups allows an energetically favourable arrangement of substituents around the metal centre. The more bulky nature of the indole group, however, hinders the packing in the crystal lattices and, consequently, the indolides melt at lower temperatures than do the analogous pyrrolides. The sizes of the central atoms can also be correlated with the stabilities in this series of complexes. Upon going from Si to Ge and then to Sn, the melting points of the triphenylmetal(IV) pyrrolides increase. Conversely, the melting points decrease for the same central atom replacement in the indolides. This difference can be attributed to lengthening of the N-metal linkage as the main group element becomes larger.

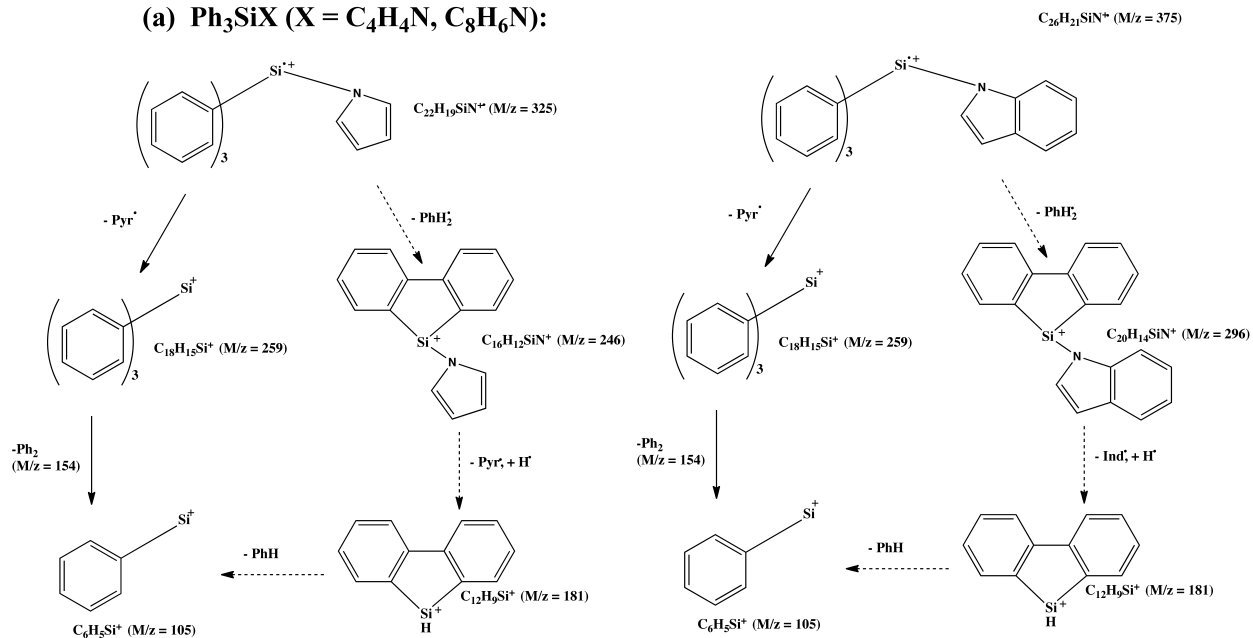
2.3.1 NMR Spectra

The ^{13}C -NMR chemical shifts for the four new group 14 metal compounds (**1**, **2**, **3** and **5**) are consistent with the literature values for the trimethyltin(IV) indolide and triphenyltin(IV) pyrrolide (**4**), and the observed chemical shifts are similar. The deshielding effect on the *ortho*, *para* and *ipso* aromatic carbons in both the pyrrolides and indolides follows the order $\text{Ge} < \text{Si} < \text{Sn}$. This inversion of Ge and Si from the expected periodic trend may be one more example of the tendency of germanium to resemble carbon more than silicon¹². NMR data are not available for $\text{Ph}_3\text{C}(\text{Pyr})$ ¹³ or $\text{Ph}_3\text{C}(\text{Ind})$ ¹⁴.

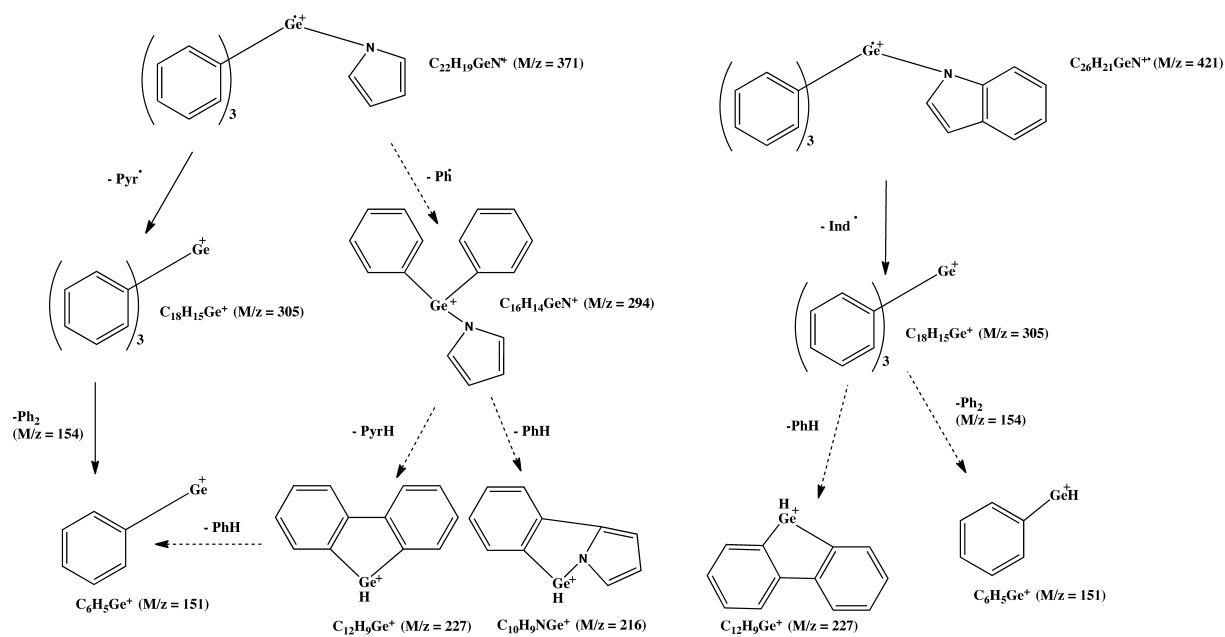
2.3.2 Mass Spectra

From the mass spectral data, it was evident that the parent molecular ions were present in each case and several reasonable fragmentation pathways can be postulated (Figure 2-2). The fragments containing group 14 elements were readily identified from their isotope abundance patterns¹⁵. Mass peaks corresponding to the formation of biphenyl-silicon fragments, for which there is precedent in the literature¹⁶, were observed. Similar behaviour was noted for the germanium species, but not for the tin compounds. This is contrary to what has been observed previously for triphenylgermanium(IV) pyrrolide. The isotopic patterns obtained experimentally for the molecular ions were in excellent agreement with the theoretically calculated values (see Table S1, Appendix A).

(a) Ph_3SiX ($\text{X} = \text{C}_4\text{H}_4\text{N}, \text{C}_8\text{H}_6\text{N}$):



(b) Ph_3GeX ($\text{X} = \text{C}_4\text{H}_4\text{N}, \text{C}_8\text{H}_6\text{N}$):



(c) Ph_3SnX ($\text{X} = \text{C}_4\text{H}_4\text{N}, \text{C}_8\text{H}_6\text{N}$):

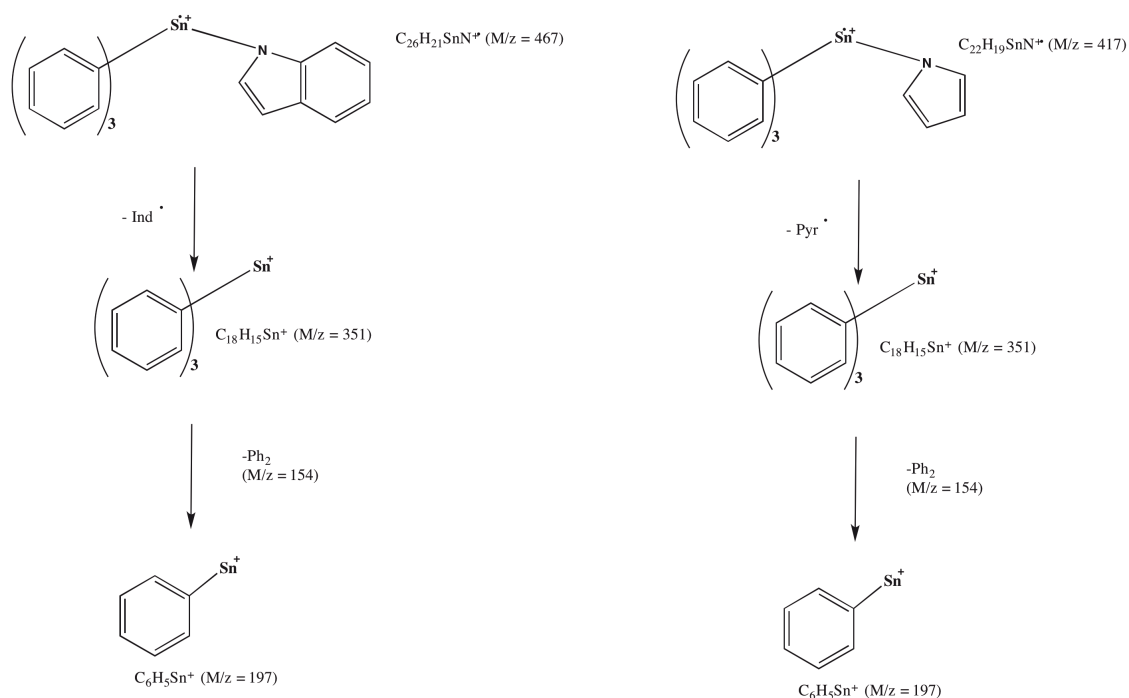


Figure 2-2: Mass spectrum decomposition of group 14 pyrrolides and indolides.

2.3.3 Raman Spectra

Raman spectroscopy provided key information in support of the formation of the metal indolides and pyrrolides. Two linkages of interest, which are broken and formed, respectively, are the N-H bond of the free heterocycle and the N-metal bond of the resulting complex. There are a number of weak vibrational modes, associated with the M-indole and M-pyrrole motions, observed in the 500-100 cm^{-1} region. In addition, a peak at $\sim 3480 \text{ cm}^{-1}$, which is attributed to the N-H stretching motion in free indole and pyrrole, disappears upon reaction with the triphenylmetal(IV) chlorides. These observations provide further evidence that the heterocycles are attached to the metal centres *via* the N atom in these reactions. Moreover, the Raman spectra of the indolides and pyrrolides reveal the presence of both the triphenylmetal(IV) and the heterocycles, and are quite similar to those of the tetraphenylmetal(IV) derivatives,

Ph₄M (M = Si, Ge, Sn). There are characteristic stretching and bending modes appearing at low wavenumbers accompanied by the well-known N-C aromatic stretch in the 1290-1390 cm⁻¹ region.

2.3.4 Single-crystal X-ray Diffraction Study of (5)

In addition to the spectroscopic measurements for **5**, single crystal X-ray diffraction data were obtained. While a satisfactory solution at ambient temperature was not possible, the 100 K low temperature data set allowed for a good, albeit disordered, model for the structure. Figure 2-3 depicts the asymmetric unit for compound **5**, which is otherwise isostructural with both tetraphenylsilane¹⁷ and tetrapyrrol-1-ylsilane^{6a, 6b} and all three crystallize in the same $P\bar{4}2_1/c$ space group.

The pyrrole ring is disordered among the four coordination sites of the central Si atom

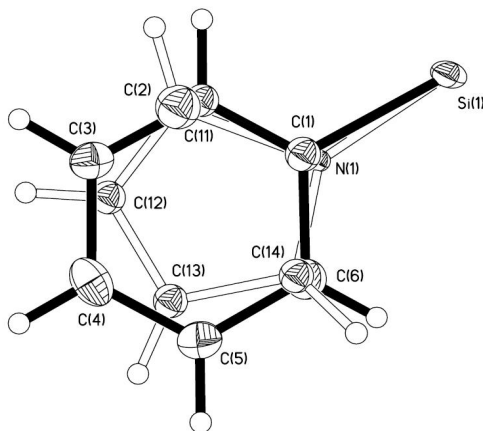


Figure 2-3: ORTEP representation of the asymmetric unit of Ph₃Si(Pyr) showing the disordered arrangement of the pyrrolyl and phenyl ligands in the crystal lattice.

with the other sites being occupied by phenyl rings. The disorder increases the uncertainty of specific molecular dimensions and the geometry. Consequently, we will not discuss specific metric parameters. However, the values for the crystal unit cell of **5** can be reliably compared with those of tetraphenylsilane and tetrapyrrol-1-

ylsilane (Table 2-1). Systematic differences in unit cell dimensions, and densities, correlate with a single phenyl/Pyr substitution. Moreover, the experimental density determined for **5** mirrors the calculated density and independently confirms the structure as having only one phenyl/Pyr substitution.

Table 2-1: Comparison of arylsilane unit cell dimensions.

Compound	T (K)	a, b (Å)	c (Å)	V (Å ³)	d _{calc} (g/mL)	d _{exp} (g/mL)	Reference
SiPh ₄	-	-	-	-	-	-	-
5	100(2)	11.331(2)	6.561(2)	842.3(4)	1.283	-	This work.
Si(Pyr) ₄	153	10.918(2)	6.046(1)	720.7(2)	1.348	-	13
SiPh ₄	293(10)	11.440(2)	7.060(4)	924(1)	1.207	-	25
5	295(1)	11.334(6)	6.882(8)	883(1)	1.223(2)	1.23(2)	This work.
Si(Pyr) ₄	293(10)	10.924(6)	6.238(4)	744.4(7)	1.30	-	7

2.4 Conclusions

The coupling of lithiated N-heterocycles to the group 14 elements (Si, Ge, Sn) under inert atmosphere conditions is an efficient method for the synthesis of novel compounds. While the yields are relatively low, the reactions work best when completed over long periods under moderate reaction conditions. These conditions provide adequate samples to perform spectroscopic studies and are a convenient way to expand the knowledge base in this relatively unexplored field of chemistry. Gentle heating may be useful in obtaining even better yields, however, great care must be taken to avoid any self-polymerization of the heterocycles. In future work, it is planned to examine the possibility of coupling the triphenylmetal(IV) pyrrolides and indolides to a Cr(CO)₃ fragment. These reactions could lead to new heterocyclic organometallic complexes and these bimetallic compounds may well have some interesting biocidal properties. The thermal lability of the N-metal bond might also be worth investigating, leading to novel catalytic agents.

2.5 Experimental

2.5.1 General methods

Triphenyltin(IV) chloride, pyrrole and *n*-butyllithium were obtained from Aldrich Chemical Co., while triphenylsilicon(IV) chloride and indole were purchased from Alfa Aesar. Triphenylgermanium(IV) chloride was provided by Strem Chemical Co. All solvents were dried over sodium ribbon prior to use. Solid reagents were used as received and pyrrole was distilled under vacuum and stored under N₂ prior to use.

Raman spectra (band position accuracy, ± 1 cm⁻¹) were measured on a Renishaw InVia spectrometer using an argon-ion (514.5-nm) laser. The propriety Renishaw WiRE 2.0 software was used for data acquisition and processing. NMR spectra (CDCl₃) were obtained using JEOL 270-MHz or Varian 300-MHz [¹³C (SiMe₄, int.), ¹H (SiMe₄, int.)] and Unity 500-MHz [¹¹⁹Sn (SnMe₄, ext.), ²⁹Si, (SiMe₄, int.)] spectrometers. Electron impact (70 eV) spectra were recorded on a Kratos MS25RFA instrument. Elemental analyses were performed at the Laboratoire d'analyse élémentaire de l'Université de Montréal.

The single crystal X-ray diffraction study of Ph₃Si(C₄H₄N) was undertaken at 100 K on a BRUKER SMART CCD diffractometer, using graphite-monochromated Mo K_α radiation ($\lambda=0.71073$ Å). The structure was solved by direct methods (using SHELX 97 software) on an absorption-corrected model generated by SADABS (SAINT-V7 software). Refinement was achieved by a full-matrix least-squares procedure based on F^2 . The phenyl ring was modeled with a site occupancy factor of 0.75 with the *meta* and *para* carbon atoms being modeled anisotropically, whilst the *ipso* and *ortho* carbons could only be modelled isotropically because of the overlap of electron density with the pyrrole ring. The pyrrole ring was modeled with a site occupancy of 0.25 with isotropic carbons. The hydrogen atoms were located at calculated positions.

The x-ray data for compound **5** are: C₂₂H₁₉NSi, colourless, plates, tetragonal, space group $P\bar{4}_2/c$, $a = b = 11.331(2)$, $c = 6.561(2)\text{\AA}$, $\alpha = \beta = \gamma = 90.00^\circ$, $U = 842.3(4)\text{\AA}^3$, $T = 100\text{K}$, $Z = 2$, 963 reflections measured, 753 observed ($I > 2\sigma(I)$), parameters = 62, $R(\text{obs}) = 0.0822$, $R(\text{total}) = 0.1098$

2.5.2 Syntheses

Ph₃Ge(C₈H₆N) (**1**)

Dropwise addition of *n*-butyllithium (36 mmol, 1.6 M solution in hexane) to indole (33 mmol) in dried hexane (100 mL) under inert conditions followed by stirring for 24 h afforded the lithiated indole as a white precipitate. Triphenylgermanium(IV) chloride (31 mmol) in toluene (50 mL) was added dropwise to the solution and a pink colour was observed to develop. The mixture was stirred overnight at room temperature. Filtering over silica yielded the crude reaction product, which was then crystallized from toluene. Yield: 6.32 g, 54.7% (based on Ph₃GeCl). M.p. 145-147 °C. *Anal.* Calcd for C₂₆H₂₁NGe: C, 74.34%; H, 5.04%; N, 3.01%. Found: C, 74.35%; H, 4.99%; N, 3.26%. ¹³C-NMR (ppm): 141.3 (C-9), 134.8 (C-*o*), 133.2 (C-*l*), 131.8 (C-2), 131.2 (C-*p*), 130.4 (C-*m*), 128.8 (C-8), 121.0 (C-5), 120.5 (C-4), 119.4 (C-6), 113.8 (C-7), 103.9 (C-3). Raman (cm⁻¹): 130w, $\nu(\text{Ge-Ind})$; 171w, $\nu[\text{Ge-Ph}(x)]$; 203vw, $\delta[\text{Ge-Ph}(\mu)]$; 226mw, $\nu[\delta\text{Ge-Ph}(t')]$; 1337m, $\nu(\text{C-N})$.

Ph₃Si(C₈H₆N) (**2**)

Compound **2** was prepared as a white crystalline solid using the same procedure as for compound **1**: C₈H₇N (21.6 mmol), *n*-C₄H₉Li (24.0 mmol) and Ph₃SiCl (22.3 mmol). Yield: 3.04 g, 37.5%, based on Ph₃SiCl. M.p. 153.3-153.6°C. *Anal.* Calcd for C₂₆H₂₁NSi: C, 83.15%; H, 5.64%; N, 3.73%. Found: C, 82.76%; H, 5.57%; N, 3.58%. ²⁹Si-NMR (ppm): -14.6. ¹³C-NMR (ppm), [$^nJ(^{29}\text{Si}-^{13}\text{C})$, Hz]: 141.0 (C-9), 135.9 (C-*o*), [2J ,

11], 132.2 (C-*l*), 131.8 (C-2), 131.7 (C-*p*), 130.6 (C-*m*), 128.2 (C-8), 121.5 (C-5), 120.6 (C-4), 120.3 (C-6), 114.7 (C-7), 105.5 (C-3). Raman (cm⁻¹): 146w, ν (Si-Ind); 172vw, ν [Si-Ph(*x*)]; 212vw, ν [δ Si-Ph(μ)]; 237w, ν [δ Si-Ph(*t'*)]; 1334m, ν (C-N).

Ph₃Sn(C₈H₆N) (3)

Compound **3** was prepared using the same method as for compound **1**, using C₈H₇N (24 mmol), *n*-C₄H₉Li (24 mmol) and Ph₃SnCl (25 mmol) to give white crystals (yield: 4.22g, 62.4%, based on C₄H₉Li). M.p. 144.7-145.1°C. ¹¹⁹Sn-NMR (ppm): -109.9. ¹³C-NMR (ppm), [$^nJ(^{119}\text{Sn}-^{13}\text{C})$, Hz]: 143.0 (C-9), 137.0 (C-*o*), [²J, 45], 135.9 (C-*l*), [¹J, 627], 133.2 (C-2), 130.6 (C-*p*), [⁴J, 13], 129.5 (C-*m*), [³J, 60], 121.0 (C-5), 120.6 (C-4), 119.3 (C-6), 113.6 (C-7), 104.2 (C-3), [³J, 18]. Raman (cm⁻¹): 124vw, ν (Sn-Ind); 152vw, ν [Sn-Ph(*x*)]; 206mw, δ [Sn-Ph(μ)]; 215 δ [Sn-Ph(*t'*)]; 263vw, ν [Sn-Ph(*t*)]; 277vw, ν [Sn-Ph(*t*)]; 1294m, ν (C-N).

Ph₃Ge(C₄H₄N) (4)

Compound **4** was prepared using the same method as for compound **1**, using 33 mmol C₄H₅N, 36.0 mmol *n*-C₄H₉Li and 31.0 mmol Ph₃GeCl to give white crystals (yield: 3.40g, 20.9%, based on (C₆H₅)₃GeCl). M.p. 203-204°C. *Anal.* Calcd for C₂₂H₁₉NGe: C, 71.42%; H, 5.18%; N, 3.79% Found: C, 71.0%; H, 5.16%; N, 3.67%. ¹H-NMR (ppm): 6.7 (H-2, H-5), 6.3 (H-3, H-4). ¹³C-NMR (ppm): 134.7 (C-*o*), 133.0 (C-*l*), 130.4 (C-*p*), 128.6 (C-*m*), 124.9 (C-2, C-5), 110.1 (C-3, C-4). Raman (cm⁻¹): 162sh, ν (Ge-Pyr); 174mw, δ [GePh(*x*)]; 215vw, δ [GePh(*x*)]; 234m, ν [Ge-Ph(*t'*)]; 247vw, Ge-Ph(*t*); 263vw, ν (Ge-N); 1385m, ν (C-N),

Ph₃Si(C₄H₄N) (5)

Compound **5** was prepared using the same method as for compound **1**, using 29.0 mmol C₄H₅N, 32.0 mmol *n*-C₄H₉Li and 26.0 mmol Ph₃SiCl to give white crystals (yield: 1.15g, 13.62% based on (C₆H₅)₃SiCl). M.p. 202-203°C. *Anal* Calcd for C₂₂H₁₉NSi•*n*H₂O; *n* = 0: C, 81.18%; H, 5.88%; N, 4.30%; *n* = 1: C, 76.93%; H, 6.16%; N, 4.08%. Found: C, 77.02%; H, 5.64%; N, 4.05%. ²⁹Si-NMR (ppm): -21.6. ¹H-NMR (ppm): 6.7 (H-2, H-5), 6.3 (H-3, H-4). ¹³C NMR (ppm): 135.9 (C-*o*), 132.1 (C-*l*), 130.6 (C-*p*), 128.2 (C-*m*), 125.8 (C-2, C-5), 111.5 (C-3, C-4). Raman (cm⁻¹): 176mw, δ[Si-Ph(*μ*)]; 227vw, ν[SiPh(*t*)]; 244m, ν[Si-Ph(*t*)]; 247w, ν[SiPh(*t*)]; 263vw, ν(Si-N), 1385 ν(C-N),

Ph₃Sn(C₄H₄N) (**6**)

Compound **6** was prepared using the same method as for compound **1**, using 38 mmol C₄H₅N, 36.0 mmol *n*-C₄H₉Li and 33.0 mmol Ph₃SnCl to give white crystals (yield: 1.15g, 8.2% based on (C₆H₅)₃SnCl). M.p. 204-205°C. *Anal*. Calcd for C₂₂H₁₉NSn: C, 63.51%; H, 4.60%; N, 3.37% Found: C, 63.18%; H, 4.68%; N, 3.08%. ¹¹⁹Sn-NMR (ppm): -104.8. ¹H-NMR (ppm): 6.7 (H-2, H-5), 6.3 (H-3, H-4). ¹³C-NMR (ppm), [*n*J(¹¹⁹Sn-¹³C), Hz]: 136.9 (C-*o*), [²J, 44], 135.9 (C-*l*), 130.6 (C-*p*), [⁴J, 13], 129.3 (C-*m*), [³J, 60] 126.1 (C-2, C-5), [²J, 15] 110.1 (C-3, C-4), [³J, 21]. Raman (cm⁻¹): 158mw, δ[SnPh(*x*)]; 188vw, δ[SnPh(*x*)]; 218s, ν[Sn-Ph(*t*)]; 270w, ν[SnPh(*t*)]; 295w, ν(Sn-N); 1383mw, ν(C-N).

2.6 Acknowledgements

The research was generously supported by a Discovery grant from the NSERC (Canada).

2.7 References

1. Douthwaite, R. E., Catalysis and organometallic chemistry of monometallic species. *Annu. Rep. Prog. Chem., Sect. A: Inorg. Chem.* **2004**, *100*, 385-406.
2. Mitchell, T. N., Some new organotin synthons. *Main Group Met. Chem.* **1989**, *12* (5-6), 425-36.
3. Hoeti, N.; Ma, J.; Tabassum, S.; Wang, Y.; Wu, M., Triphenyl tin benzimidazolethiol, a novel antitumor agent, induces mitochondrial-mediated apoptosis in human cervical cancer cells via suppression of HPV-18 encoded E6. *J. Biochem.* **2003**, *134* (4), 521-528.
4. (a) Reynolds, J. E., Silicon Researches. XI. Silicotetrapyrrole. *J. Chem. Soc., Trans.* **1909**, *95*, 505-8; (b) Vorlaender, D.; Apelt, O., Preparation of indole from indoxyl. *Ber. Dtsch. Chem. Ges.* **1904**, *37*, 1134-1135.
5. Reinecke, M. G.; Sebastian, J. F.; Johnson, H. W., Jr.; Pyun, C., NMR spectral study of some organometallic derivatives of indoles. *J. Org. Chem.* **1971**, *36* (21), 3091-5.
6. (a) Atwood, J. L.; Cowley, A. H.; Hunter, W. E.; Sena, S. F., *Gov. Rep. Announce. Index (U.S.)* **1982**, *82*; (b) Atwood, J. L.; Cowley, A. H.; Hunter, W. E.; Sena, S. F., *Chem. Abstr.* **1983**, *98*; (c) Fessendon, R.; Crowe, D. F., Synthesis and cleavage of N-trimethylsilylpyrrole. *J. Org. Chem.* **1960**, *25*, 598-603; (d) Schwarz, R.; Reinhardt, W., Chemistry of germanium. XI. Further organic germanium compounds. *Ber. Dtsch. Chem. Ges. B* **1932**, *65B*, 1743-6; (e) Hillmann, J.; Hausen, H. D.; Schwarz, W.; Weidlein, J., Trimethylstannyl- and dimethylstannyl-substituted pyrroles - synthesis, spectra, and structures. *Z. Anorg. Allg. Chem.* **1995**, *621* (10), 1785-96; (f) Klingebiel, U.; Luettker, W.; Noltemeyer, M., Mono-, bis-, tris- and tetrakis(indol-1-yl)silane. *J. Organomet. Chem.* **1993**, *455* (1-2), 51-5.
7. (a) Wrackmeyer, B., Multinuclear magnetic resonance study (boron-11, carbon-13, nitrogen-14, nitrogen-15, silicon-29, phosphorus-31, tin-119, lead-207 NMR) of

some N-pyrrolyl derivatives. *J. Organomet. Chem.* **1985**, 297 (3), 265-72; (b) Frenzel, A.; Herbst-Irmer, R.; Klingebiel, U.; Noltemeyer, M.; Schaefer, M., Indolyl- and pyrrolylsilanes. Syntheses and crystal structures. *Z. Naturforsch., B: Chem. Sci.* **1995**, 50 (11), 1658-64.

8. (a) Quane, D.; Roberts, S. D., Synthesis and reactivity of some N-triphenylgermyl heterocyclic amines. *J. Organomet. Chem.* **1976**, 108 (1), 27-33; (b) Rijkens, F.; Janssen, M. J.; van der Kerk, G. J. M., Investigations on organogermanium compounds. III. N-Tributylgermyl-substituted aliphatic and heterocyclic amines. *Recl. Trav. Chim. Pays-Bas* **1965**, 84 (11), 1597-1609.

9. (a) Wrackmeyer, B.; Kehr, G.; Maisel, H. E.; Zhou, H., N-triorganostannyl-substituted pyrroles and indoles and N-trimethylstannylcarbazole: determination of signs of coupling constants and isotope-induced chemical shifts $1\Delta^{14/15}\text{N}(^{119}\text{Sn})$. *Magn. Reson. Chem.* **1998**, 36 (1), 39-45; (b) Luijten, J. G. A.; van der Kerk, G. J. M., Organotin compounds. XIX. Preparation of some organotin compounds. with heterocyclic nitrogen tin bonds. *Recl. Trav. Chim. Pays-Bas* **1963**, 82 (11), 1181-8.

10. Bazinet, M. L.; Merritt, C., Jr.; Sacher, R. E., IKE [ion kinetic energy] and metastable ion evidence for fragmentation pathways in the mass spectra of organolead-substituted nitrogen heterocycles. *Int. J. Mass Spectrom. Ion Phys.* **1975**, 17 (1), 9-16.

11. Katritzky, A. R.; Lagowski, J. M., *The Principles of Heterocyclic Chemistry*. Academic Press: New York, 1968.

12. Allred, A. L.; Rochow, E. G., Electronegativities of carbon, silicon, germanium, tin, and lead. *J. Inorg. Nucl. Chem.* **1958**, 5, 269-88.

13. Mandell, L.; Piper, J. U.; Pesterfield, C. E., Diels-Alder additions to pyrroles. *J. Org. Chem.* **1963**, 28, 574-5.

14. Funakubo, E.; Hirotsu, T., Introduction of the triphenylmethyl group. I. *Ber. Dtsch. Chem. Ges. B* **1936**, 69B, 2123-30.

15. Weast, R. C., *CRC Handbook of Chemistry and Physics*. 52 ed.; The Chemical Rubber Co.: USA, 1972.
16. Bowie, J. H.; Nussey, B., Electron-impact studies. LV. Skeletal rearrangement and hydrogen scrambling processes in the positive and negative-ion mass spectra of phenyl derivatives of elements of Group IV and V. *Org. Mass Spectrom.* **1970**, 3 (7), 933-40.
17. Chieh, P. C., Crystal chemistry of tetraphenyl derivatives of Group IVA elements. *J. Chem. Soc., Dalton Trans.* **1972**, (12), 1207-8.

3

Synthesis of Reduction-Sensitive 1,1-Diarylhydrazines from 1,1-Diarylamines

3.1 Preamble

The nitrogen atom in the single-nitrogen heterocycles can act as a nucleophile and is inherently electron-rich. Chemistry of similar nitrogen atoms that are electron-poor is more rare. One system that has been only very sparsely examined in terms of electron-deficient nitrogen chemistry is 2-nitrodiphenylamine. With the nitrogen lone pair conjugated into the aromatic rings, this compound has seen very little use in synthetic schemes due to its rather poor nucleophilicity. Formation of the hydrazine of 2-nitrodiphenylamine, however, was an attractive target for exploring nitrogen-based electronics in such a system.

Until recently, the best method of synthesizing a 1,1-diarylhydrazine containing an electron withdrawing substituent was using the Hofmann rearrangement of a suitable urea. Surprisingly, despite having been used for decades in the formation of hydrazines as well as many other products, no structural elucidation of this important chemical transformation was available. Chapter 3 provides such a structural elucidation of the transformation of non-nucleophilic, conjugated amines into their urea analogues as well as provides a convincing argument for the involvement a nitrene along the reaction pathway of the Hofmann rearrangement in going from a 1,1-diaryl urea to a 1,1-diaryl hydrazine. Gas-phase density functional theory is used to support the experimental data by providing a model for geometric changes that occur during the rearrangement to support the involvement of an electron-deficient nitrogen intermediate. The choice of basis set and level of DFT theory employed here is based on past experience with

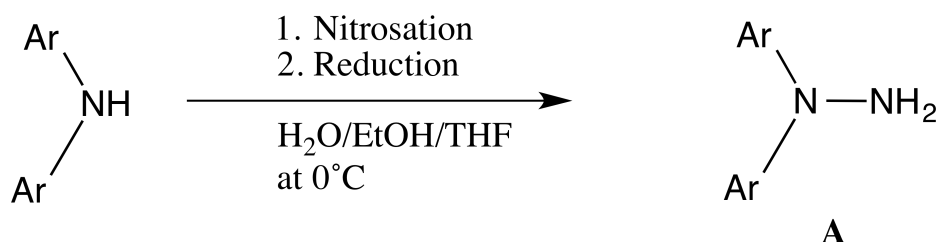
calculations for related nitrogen species with numerous lone pairs. In general this theoretical model has excellent predicts of ground state configurations and vibrational energy levels for related compounds. Although the specific metric parameters may very well be dependent on basis set, and the functionals employed, the contrasts made with experimental data are intended to reconfirm their utility for the predictions made for this class of compounds as well. With these features confirmed for the ground states we have established their utility for predicting intermediates, transition states, and reaction pathways.

The work in this chapter was originally published in the *Canadian Journal of Chemistry* and is reproduced from:

Cheryl D. Bain, Julia M. Bayne, D. Scott Bohle, Ian S. Butler and Joël Poisson,
“Synthesis of Reduction-Sensitive 1,1-Diarylhydrazines from 1,1-Diarylamines” *Can. J. Chem.*, **92** (2014), 904.

3.2 Introduction

Although 1,1-diarylhydrazines have proven useful in medicinal chemistry¹ and in the catalysis of hydrohydrazination reactions,² their syntheses³ often require a two-step nitrosation/reduction of a diarylamine (Scheme 3-1).



Scheme 3-1: Amination by the reductive nitration sequence of 1,1-diarylamines.

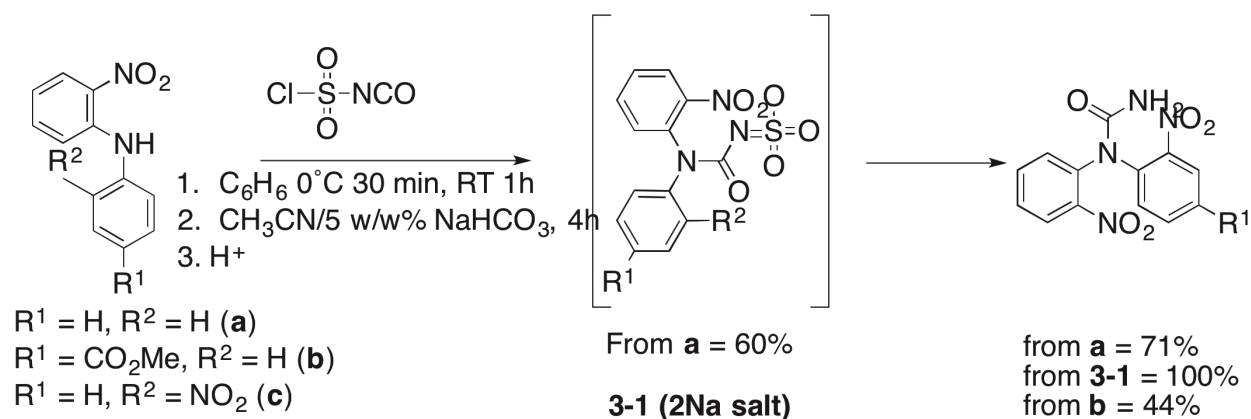
Many possible amines, for example those containing nitro or carboxyl substituents, are not compatible with these reductive conditions and the intermediary nitrosamines are often potent carcinogens. In addition to these limitations, 1,1-diarylamines often cannot be transformed to hydrazines by this method due to the cleavage of the weak N–NO bonds in the product under reducing conditions.⁴ One method for circumventing these obstacles is to use copper⁵ or patented palladium complexes for the amination of diarylamines⁶; however, the ligand selection process to obtain useful results is often cumbersome and somewhat unpredictable.

A rather less-developed method for the synthesis of **A** is via a mild base-catalyzed Hofmann rearrangement⁷ of 1,1-diarylureas. This methodology offers selectivity and moderate to good yields and utilizes inexpensive and commercially available materials. However, the sole preliminary report on this reaction only succeeded in isolating derivatives of the initial hydrazine and inferred the presence and intermediacy of the parent hydrazines. We report here the production of novel redox-

sensitive 1,1-diarylureas and the first complete structural characterization of the key species in the stepwise conversion of diarylamines to substituted 1,1-diarylhydrazines via the Hofmann rearrangement of suitable urea derivatives. Among the structurally characterized intermediates is the di-anionic sulfimidate of the urea, $[R'RNC(O)NSO_3]^{2-}$, with $R = Ph$ and $R' = 2-C_6H_4NO_2$. This novel disodium salt is sufficiently stable for isolation and characterization by X-ray diffraction. To understand the unusual stability and reactivity of these species, density functional theory is used to theoretically characterize these intermediates and to determine the key intermediates and transition states in their Hofmann rearrangements.

3.3 Results and Discussion

The substituted ureas were produced by the action of chlorosulfonyl isocyanate, $OCNSO_2Cl$, on 1,1-diarylamines (Scheme 3-2).



Scheme 3-2: Synthetic route to 1,1-diarylureas.

While 1-(2-nitrophenyl)-1-phenylamine (**a** in the above Scheme) is commercially available, bis(2-nitrophenyl)amine (**c**) and methyl 4-((2-nitrophenyl)amino)benzoate (**b**) were synthesized using the methods of Ren⁸ and Tietze,⁹ respectively. The latter

compound has a high melting point (145–146 °C), suggesting strong crystalline packing. Coupled with this observation is the fact that despite varying reaction temperatures and reaction times, the bis(2-nitrophenyl)amine failed to react with chlorosulfonyl isocyanate. A trend operating here is that there is diminished availability of the nitrogen lone pair, which is necessary for this reaction to occur. Hence, by increasing the number and strength of electron-withdrawing groups on the flanking phenyl rings, it is easy to reduce the nucleophilicity of the diphenylamine to the point of no reaction.

It was expected, based on literature precedent,¹⁰ that following the reaction of such amines with chlorosulfonyl isocyanate, and subsequent hydrolysis, the reactions would furnish the desired urea derivatives directly (Scheme 3-2). In the two examples reported here, the desired urea can be generated reliably if an extraction with aqueous dilute hydrochloric acid is performed. In the presence of excess sodium bicarbonate, the desired urea was formed only as a small by-product in the case of 1-(2-nitrophenyl)-1-phenylamine with the main product being the frequently proposed intermediate 1-(2-nitrophenyl)-1-phenylcarbamoysulfimidate (**1**), which crystallized as a disodium pentahydrate. An ORTEP representation of the structure of the di-anion is shown in Figure 3-1, with images of the salt and its hydration sphere being shown in Appendix B.

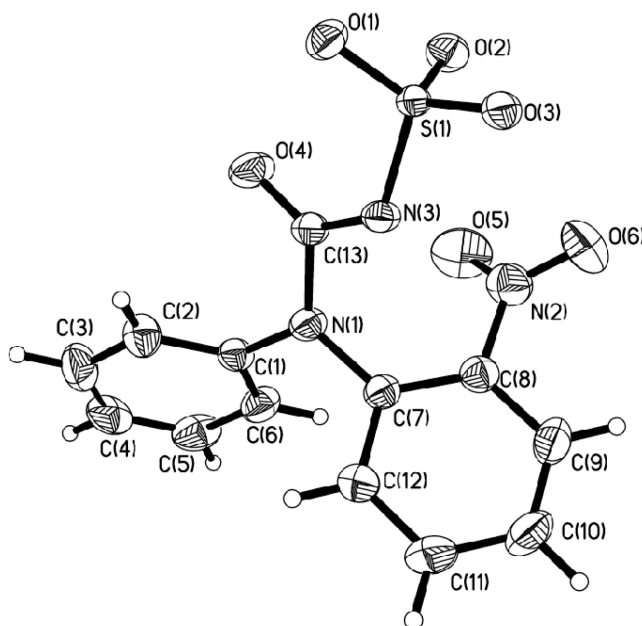


Figure 3-1: ORTEP representation of the solid structure of the di-anion in sodium 1-(2-nitrophenyl)-1-phenylcarbamoylsulfimide pentahydrate (1). Key metric parameters: N(1)–C(13) 1.411(2) Å, C(13)–N(3) 1.344(2) Å, N(3)–S(1) 1.598(1) Å, N(1)–C(1) 1.430(2) Å, N(1)–C(7) 1.420(2) Å, N(3)–S(1) 1.598(1) Å, and C(7)–N(1)–C(13)–N(3) 171.4(1)°.

A comparison of the sulfimide, urea, and hydrazine for the 1-(2-nitrophenyl)-1-phenylamine-derived products also reveals bond angles as well as a near planar geometry at N(1) (Table 1), consistent with partial sp^2 hybridization and delocalization of its lone pair. The C(13)–N(3)–S(1) bond angle of $118.1(1)^\circ$ indicates an sp^2 hybridization about N(3). Such an arrangement results in an increased S–N bond order, N(3)–S(1) = 1.598(1) Å, which helps stabilize the sulfimide. The increased Lewis basicity of the sulfoxyl oxygens enhances the ability to coordinate sodium leading to unusually robust and isolable salts.

Table 3-1: Comparison of geometry around N(1) in 1-(2-nitrophenyl)-1-phenyl derivatives.

Parameter	Sulfimide (1)	Urea (2a)	Hydrazine (3)
Out-of-plane distance of N(1) (Å) ^a	0.0031	0.0184	0.1158
C(7)-N(1)-C(1) (°)	117.4(1)	117.8(1)	123.7(1)
C(7)-N(1)-C(13) (°)	120.5(1)	118.7(1)	N/A
C(13)-N(1)-C(1) (°)	122.1(1)	123.4(1)	N/A
C(7)-N(1)-N(3) (°)			113.7(1)
C(1)-N(1)-N(3) (°)			120.6(1)
Addition of angles around N(1)	360.0(1)	359.9(1)	358.0(1)

^a Separation of N(1) from the plane defined by the three carbon atoms to which it is bound.

The isolation of this intermediate is unexpected, since the sulfonyl chlorides generated upon reaction with chlorosulfonyl isocyanate are typically unstable and undergo decomposition in aqueous media to give the desired substituted ureas. There are only a few reports of the isolation of these types of products¹¹ and only a single remotely related structure has been described.¹² Terminal sulfimic acid moieties and their carbamoylsulfimide derivatives similar to **1** have not been reported. In the cases where sulfimides have been isolated, they are engineered such that the sulfur atom is annealed into a relatively inert organic ring¹³ or is part of a tosylate group,¹⁴ which abates their inherent instability. Although the urea carbamoyl sulfimide framework in **1** is unusual, the related carbamoyl sulfinate esters $\text{-O}_3\text{SNHC(O)OR}$ include the natural product saxitoxin and allied neurotoxins isolated from dinoflagellates.¹⁵

The addition of acid at room temperature in a final acid workup step leads to sulfimide decomposition to give the corresponding 1,1-substituted urea quantitatively. The acid addition could be made following the isolation of the sulfimide or as an additive to the mother liquor. Analysis of the urea by single-crystal X-ray diffraction

(Figure 3-2) shows that it crystallizes in the centro-symmetric space group $P\bar{1}$ with a planar 1,1-diarylurea.

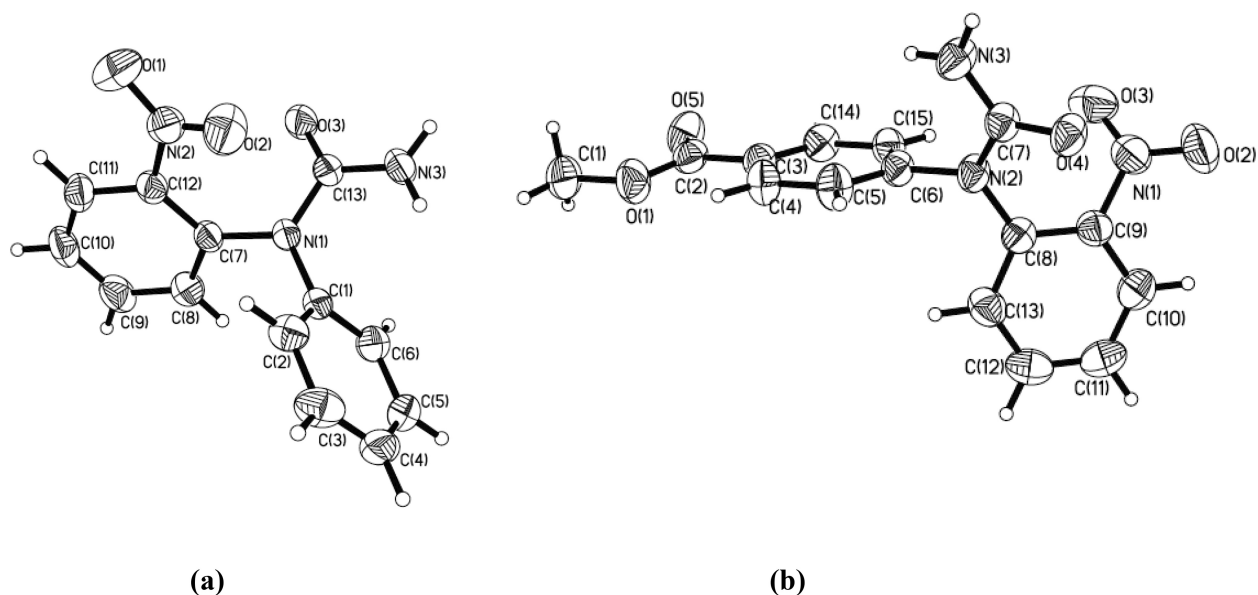
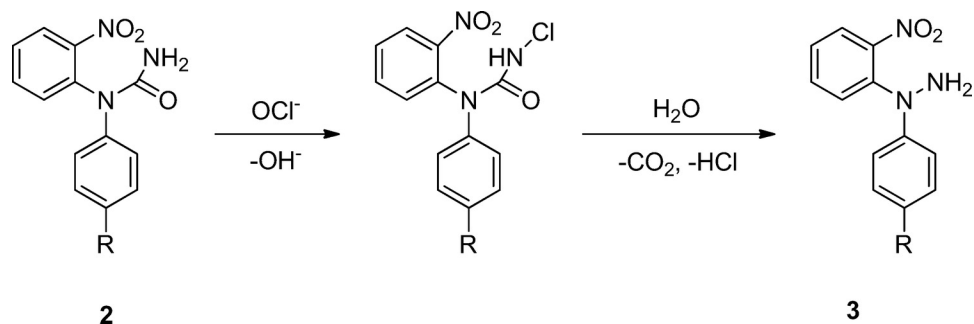


Figure 3-2: ORTEP representations of the solid-state structures of (a) 1-(2-nitrophenyl)-1-phenylurea (2a) and (b) methyl 4-(1-(2-nitrophenyl)ureido)benzoate (2b). Key metric parameters for 2a: N(1)–C(13) 1.387(1) Å, C(13)–N(3) 1.342(2) Å, N(1)–C(1) 1.438(1) Å, N(1)–C(7) 1.426(1) Å, and C(7)–N(1)–C(13)–N(3) 169.9(1)°. Key metric parameters for 2b: N(2)–C(7) 1.394(2) Å, C(7)–N(3) 1.332(2) Å, N(2)–C(6) 1.438(2) Å, N(2)–C(8) 1.421(2) Å, and C(6)–N(2)–C(7)–N(3) –11.2(2)°.

To illustrate the compatibility of this urea formation with amines containing other functional groups sensitive to reduction, the synthesis of the analogous urea derivative starting from methyl 4-((2-nitrophenyl)amino)benzoate was also demonstrated following a similar procedure (Figure 3-2b). This second derivative also crystallizes in the space group $P\bar{1}$ and has a coplanar diarylamine and urea groups with very small out-of-plane geometries for the diarylamine nitrogen N(1) Table 3-1. Hydrogen bonding organizes

efficient packing in **2a** and **2b** with there being extensive intermolecular hydrogen bonds between adjacent urea carbonyls and amino groups.



Scheme 3-3: Reaction sequence in the hypochlorite-promoted Hofmann rearrangement of ureas.

While 1-(2-nitrophenyl)-1-phenylhydrazine has recently been synthesized in high yield¹⁶, the number of steps and exotic nature of the starting materials make this published method disadvantageous. As such, to obtain the hydrazine, a modified Hofmann rearrangement was performed (Scheme 3-3). Extensive kinetics by Judd¹⁷ of the hypohalite-promoted Hofmann rearrangement indicates that the reaction is first order in hypochlorite and urea. Since the stoichiometric amounts of hypochlorite have been shown to be of consequence in producing the desired hydrazine and commercially available sodium hypochlorite is variable in its composition, degrading over time, the more stable solid calcium salt, $\text{Ca}(\text{OCl})_2$, was used. As such, the stoichiometry of hypochlorite used could be more tightly controlled so as to minimize the degradation of the desired hydrazine product.

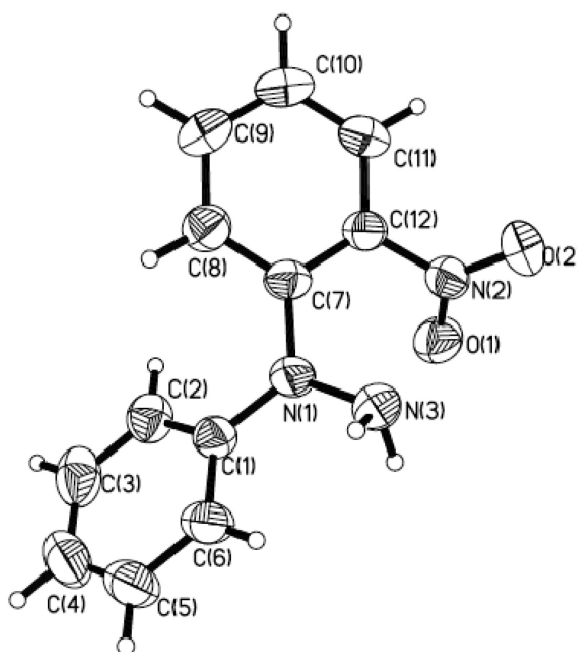


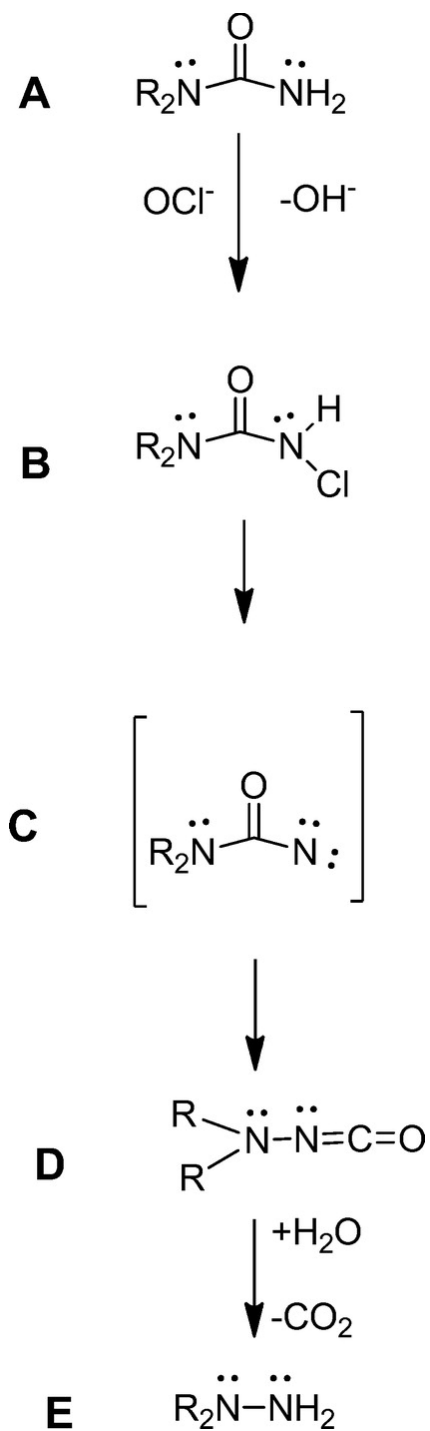
Figure 3-3: ORTEP representation of the solid-state structure of 1-(2-nitrophenyl)-1-phenylhydrazine (3). Key metric parameters: N(1)–N(3) 4.416(3) Å, N(1)–C(1) 1.413(2) Å, N(1)–C(7) 1.401(2) Å, C(2)–C(1)–N(1)–N(3) –163.5(1)°, and C(8)–C(7)–N(1)–N(3) –134.1(1)°.

Although the crude yields obtained were comparable with those of the prior report, this modified preparation allowed the isolation of the desired hydrazine **3** (Scheme 3-3) in crystalline form (Figure 3-3) without requiring derivatization as was reported previously.⁷ The crystals of **3** were of outstanding quality for single-crystal X-ray diffraction and sufficiently high-resolution data were collected to allow for the location of all hydrogen atoms, including those of the terminal nitrogen, being located in the penultimate electron density maps. These hydrogen atoms were included in the final refinement, which led to the geometry shown in Figure 3-3. Thus, it is possible to have a meaningful interpretation of the terminal amino group geometry in **3**, which orients the dipoles of the amine and nitro groups.

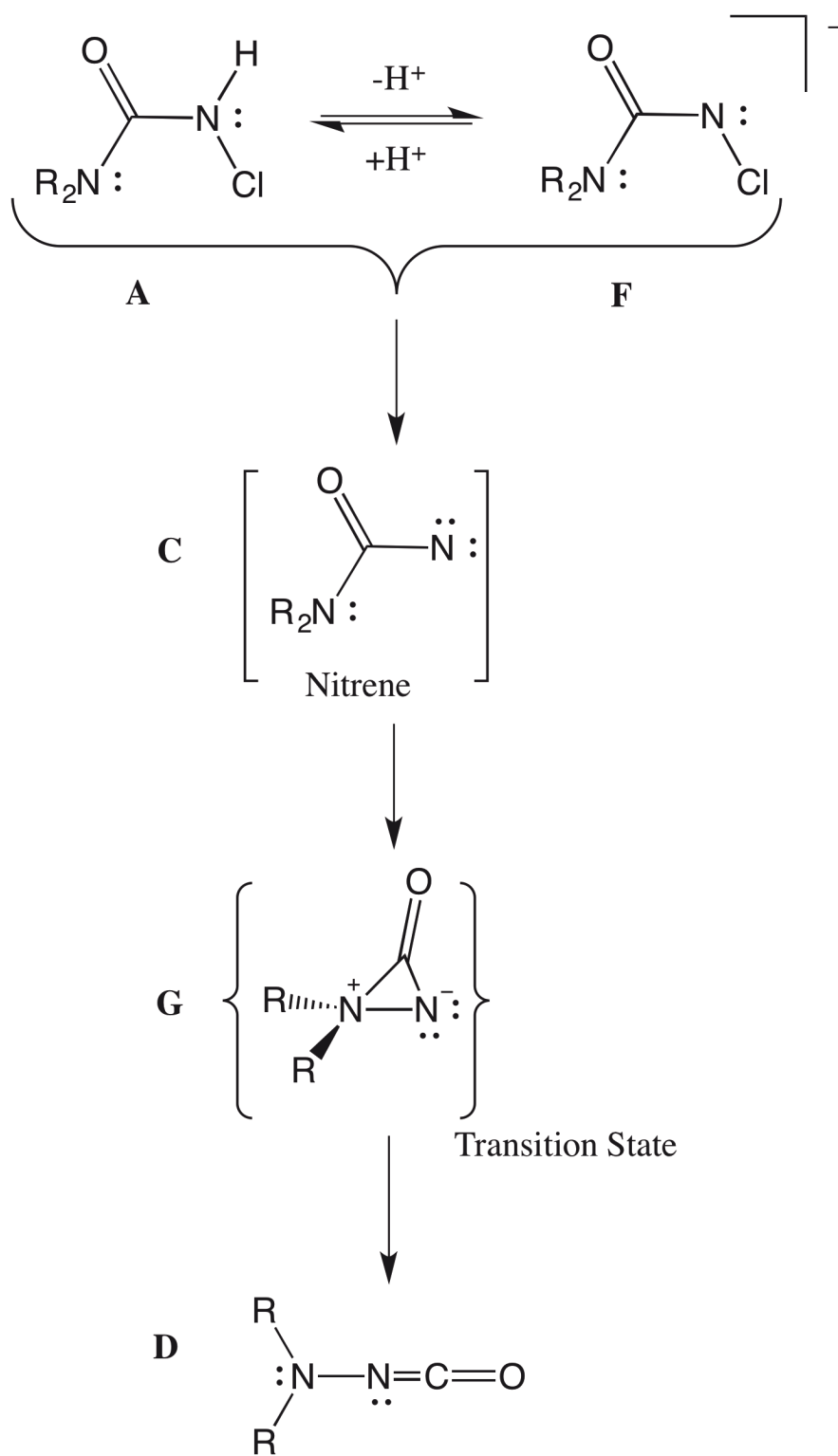
This geometry is not compatible with an intramolecular hydrogen bond, although there are numerous intermolecular hydrogen-bonding interactions. Even though hydrazine conformational dynamics are surprisingly complicated,¹⁸ this crystalline conformation is noteworthy by the absence of an intramolecular hydrogen bond. Examination of this hydrazine and its urea and its sulfimide shows global delocalization of the N(1) lone pair electrons into their aromatic systems (Table 3-1). In addition, delocalization is seen in the sulfimide and carbonyl groups, resulting in near planar geometry at N(3) in the sulfimide and the urea. Despite a slightly larger distortion of N(1) out of its plane in the hydrazine, the N–N bond length, angular geometry, and planar positioning are also consistent with sp^2 -hybridization. All of these observations are consistent with those made by Carrillo,¹⁹ supporting the assertion that the π NN interactions lead to minor bonding effects in diarylhydrazines, as the nitrogen lone pair is strongly conjugated with the π -system of the aromatic rings.

The generalization of the hypochlorite-promoted urea decarboxylations to include diarylhydrazines, and the stability of some of the key intermediates, has important implications for the Hofmann rearrangement. Mechanistically, the Hofmann rearrangement is often discussed along with the Curtius, Wolff, Schmidt, and Lossen reactions, which share a common substituent nitrogen bond forming step, and an initial isocyanate product, but which are distinguished in the approach to generating the leaving group at the nitrogen.²⁰ Key characteristics of these rearrangements are the retention of the stereointegrity of the R= group of the amides, $R=C(O)NH_2$,²¹ the lack of scrambling of its isotopically labelled R' and NH_2 fragments,^{20b, 22} their overall first-order kinetics,^{20a, 23} and the interception of the isocyanate intermediate with methanol.²⁴ Although the mechanistic discussion of the Hofmann rearrangement was extensive in the heyday of physical organic chemistry, and based on a variety of sound experimental studies,^{20a, 22a, 25} more recent density functional theoretical approaches^{20c, 26} have largely concerned the Curtius rearrangement. In outline, the Hofmann rearrangement

(Schemes 3-4 and 3-5) is a variant of the Shestakov reaction,²⁷ with the key step being the formation of the new N–N bond. Given the poor nucleophilicity of the diarylamine groups used here, we sought to clarify some of these mechanistic questions with density functional theory.²⁸ In prior publications, we have found that B3LYP/6-311++G** is an excellent combination of method and model for the ground-state geometries and vibrational modes for electron-rich nitrogen species with multiple lone pairs such as these.²⁹ Here, the inclusion of diffuse functions is an important factor.³⁰ This is the case for these urea starting materials and hydrazine products, which have theoretically calculated ground-state structures and vibrational modes (Appendix B) that match well the expected intensities and positions of the experimental data.



Scheme 3-4: Reaction mechanism for formation of hydrazines from ureas (R = alkyl or aryl). All structures shown in square brackets are proposed species.



Scheme 3-5: Proposed nitrene intermediate and transition state in the Hofmann rearrangement.

To theoretically screen the possible intermediates, simple diphenylamino-systems were initially employed in these calculations, with the ground and transition states located therein being used to aid in the location of those for the 2-fluoro and 2-nitro derivatives. Chlorination of **A** to give **B** followed by its deprotonation would lead to **F** as either *Z* or *E* *N*-chloroanions (Figure 3-4).

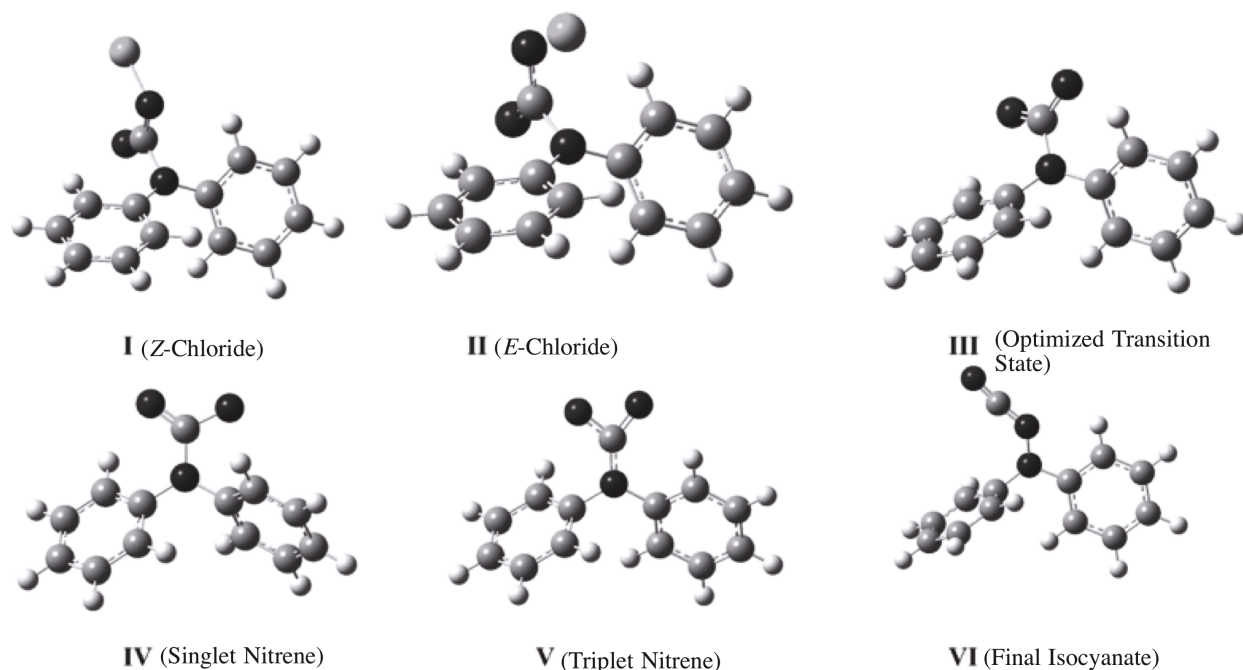





Figure 3-4: Optimized structures for the intermediates for the Hofmann rearrangement of 1,1-diphenylurea. The urea anions with *Z* and *E* chloride geometries are shown in **I** and **II**, respectively, and **III** depicts the optimized transition state between the singlet nitrene in **IV** and the isocyanate product. **VI** shows the isocyanate. Note the coplanarity of the NC(O)N unit and the compact O–C–N bond angle in the nitrene **IV** as compared with the more expanded orthogonal orientation for the transition state in **III**. The singlet and triplet nitrenes are shown in **IV** and **V**, respectively.

N-haloamides such **F** are strong acids that are known to form well-characterized but unstable sodium salts.³¹ Theoretically, either conformation corresponds to a local minimum with the *Z*-isomer being more stable by approximately 6 kcal/mol in the gas phase. Although the NC(O)NCl atoms are all co-planar, this plane is almost orthogonal to that defined by the diphenylamine. From Scheme 3-5, the chlorinated anions would lose chloride to go to a singlet nitrene intermediate, **C**, Ph₂NC(O)N, by heterolysis of the weak N–Cl bond. In analogy to carbenes, nitrene intermediates such as **C** form either stable singlet or triplet states, both of which correspond to local minima with the triplet state being ~8.48 kcal/mol more stable (Table 3-2).

Table 3-2: Theoretical results for the Hofmann intermediates and transition states (G).

Structure RR=N and species	Absolute energy (au) ^a	Relative energy (kcal/mol) ^b	CNCN torsion angle (°) ^c
Diphenylamine			
Singlet nitrene	-686.39252451	0	-0.83
Transition state	-686.39252451 	+6.88	129.61
Isocyanate	-686.46054470	-42.7	-8.87
Triplet nitrene	-686.4060394	-8.48	-175.08
2-Nitrophenyl			
Singlet nitrene	-890.944689	0	178.72
Transition state	-890.7314099 	+7.80	129.65
Isocyanate	-891.0124295	-42.5	-44.08
Triplet nitrene	-890.960301	-9.80	-177.78
2-Fluorophenyl			
Singlet nitrene	-785.6488335	0	-179.74
Transition state	-785.441599 	+10.53	-115.06
Isocyanate	-785.716939	-42.7	-41.88
Triplet nitrene	-785.6617371	-8.10	-171.50

^aAll calculations performed with restricted B3LYP density functionals and 6-311++G** basis sets except for the triplet nitrenes where unrestricted methods were employed. All ground-state energies are zero-point corrected.

^bRelative energies from singlet nitrenes for ground states include zero-point energy; the relative energies for the transition states are for the electronic components only.

^cTorsion angle is from the ipso carbon of one of the two aryl rings to the diaryl nitrogen and then to the carbonyl carbon and the terminal (nitrene) nitrogen.

These intermediates are predicted to have completely planar NC(O)N groups that, in their ground states, are co-planar with the diarylamine, which is also planar (Figure 3-4). The singlet nitrene has an unusual geometry for the modified urea group with angles for the terminal nitrogen of 89.61° and 140.09° for O–C–N and N–C–N, respectively. Both C–N bond lengths are short with C–N to the terminal nitrogen being 1.27575 Å, which is 0.0722 Å shorter than to the diphenylamine. Significantly, in these ground states, the migration to give the new N–N bond is not well poised for a Hofmann rearrangement.

The transition states for the Hofmann rearrangement were located and then demonstrated to connect the singlet nitrene intermediate **C** to the isocyanate **D** by reaction pathway following intrinsic reaction coordinate (IRC) calculations. The nitrene side of these potential energy surfaces corresponds to a rotational conformer of the nitrene arising from rotation of the C(O)N group out of the plane of the diarylamine. Rotation of the nitrene around the Ph₂N–C(O)N bond so that it is orthogonal leads to a state only 6.88 kcal/mol below the actual transition state, which is reactant-like in geometry with a significantly lengthened Ph₂N–C bond of 1.44992 Å (Figure 3-5). The gas-phase energy change for the rearrangement is –42.7 kcal/mol, and hydrolysis to the product hydrazine would render the rearrangement irreversible.

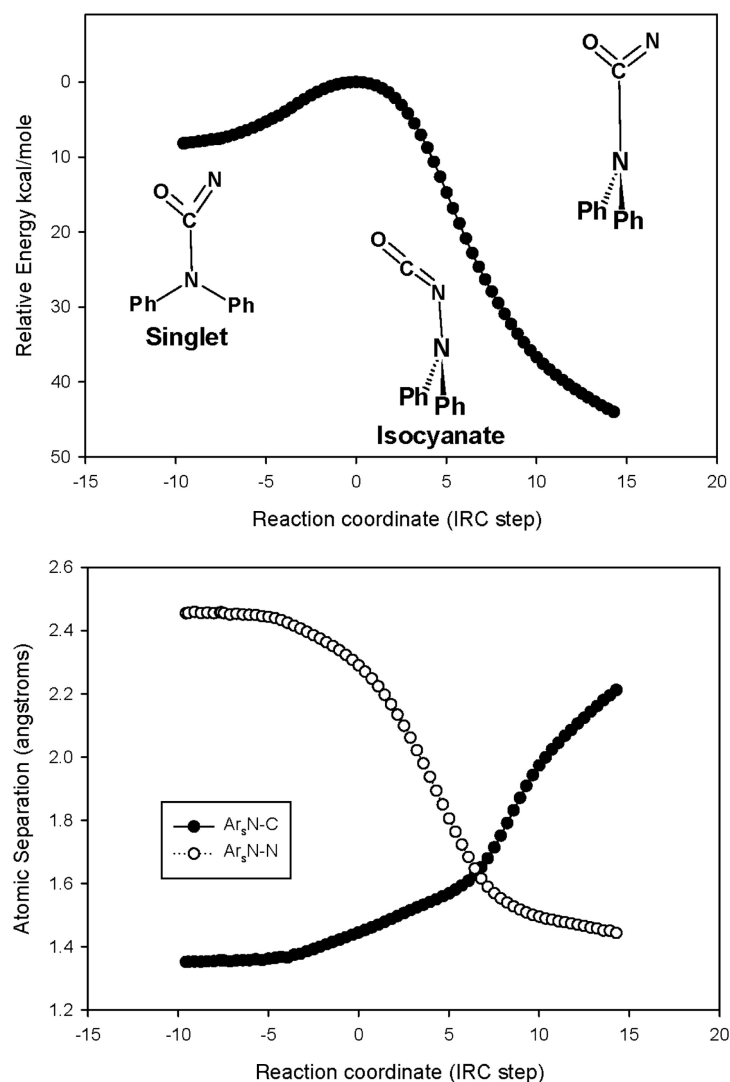
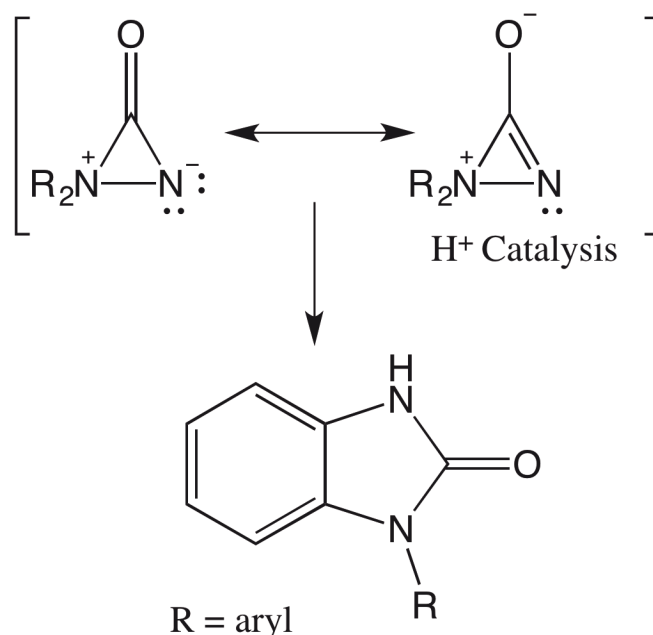


Figure 3-5: Density functional theory results. Shown is the isomerization of the singlet nitrene from $\text{Ph}(2\text{-O}_2\text{NC}_6\text{H}_4)\text{N}(\text{CO})\text{N}$ with a reaction coordinate step (IRC) of approximately -10, to the corresponding isocyanate with an IRC of approximately 15. In the top panel, the transition state with an IRC = 0 is shown to separate the two minima and in the bottom panel, the C-N bond that breaks (solid circles) is contrasted with the N-N bond that forms (open circles). At an IRC of approximately 7, the two bond lengths are equal, and the C-N-N ring is an isosceles triangle. Note that in the top panel, the nitro group is not shown in the structures.

These values are only slightly smaller than those found for the 2-nitro derivative (Figure 3-5). The transition states in these transformations are reactant-like (Figure 3-5, bottom) where at the transition state, with a reaction following step IRC = 0, the N–C bonds are only marginally lengthened. Given the magnitude of the energy change alone (Figure 3-5), this reaction is irreversible, and to go back to the urea precursor would be even farther uphill. While solvation is expected to have some influence on these energetics, when the calculations are transferred to a polar aqueous media by using an Onsager model for the reaction field for the optimized structures, the only notable difference from the gas-phase data in Table 3-2 is a stabilization of the singlet nitrene intermediate (Appendix B, Supplementary Table 1). Thus, the key feature of the profiles in Figure 3-5 and for the diphenyl and the fluorine analogs is that the only instance for the presence of a $R_2NC(O)N$ cyclic species is in the transition state structure **G**. It is not an intermediate.

Earlier researchers have proposed that the Hofmann rearrangement for disubstituted hydrazines goes through a cyclic aziridinone-type intermediate, **H** (Scheme 3-6).^{20b} A proposed species such as **H** was described in these same studies as “undoubtedly of high energy” but that it “should exist as a discrete entity, occupying a small minimum on the potential energy profile.” Related cations are thought to be formed³² in the reactions for 1,2-dialkylureas. Density functional theory predicts that intermediates such as **H** would not lead to a protonated isocyanate **D**. The prediction of a high-energy minor local minimum has not been borne out with density functional theory calculations where the aziridones consistently appear only as transition states. Indeed, species such as **H** are likely to have basic nitrogen, and their generation and protonation consistently led to net aromatic ring addition to give *N*-arylbenzimidazolone **I** following ring addition and deprotonation. It is significant that *N*-arylbenzimidazolones

have not been seen as products in our reactions. Thus, for the diarylureas used in our studies, the presence of cyclic aziridionone intermediates is unlikely.



Scheme 3-6: Related mechanisms for the Hofmann rearrangement (R = aryl).

3.4 Conclusions

We report here the first crystallization of a functionalized 1,1- diarylhydrazine in its basic form produced via a Hofmann rearrangement. Generation of the required precursors to the hydrazine involves a rare intermediate sulfimidate species, which can be isolated in aqueous medium with enhanced ionic strength and subsequently decomposed by inhibiting its hydrogen-bonding ability. This decomposition leads the corresponding urea, which can be transformed using an easily controlled Hofmann rearrangement employing $\text{Ca}(\text{OCl})_2$ into the corresponding hydrazine, which bears potentially useful reactivity in its un-substituted form that has yet to be explored. Density functional theory suggests that the rearrangement involves a single nitrene species where the transition state for N–N bond formation is reached by rotation of the $\text{C}(\text{O})\text{N}$ fragment out of the plane of the diarylamine fragment. The methodology communicated

here is suitable for forming ureas from amines, which contain reduction-sensitive functionalities such as methyl esters and nitro groups.

3.5 Experimental

3.5.1 General Methods

Benzene was dried over potassium/benzophenone and toluene was dried over molecular sieves and stored under nitrogen before use. All other reagents were obtained from commercial sources and used as received. Melting points were recorded with a micromelting apparatus and were calibration corrected. ^1H and ^{13}C NMR spectra were recorded on a 300 MHz spectrometer. High-resolution mass spectroscopy was measured by electrospray techniques with a time of flight detector (ESI/TOF).

3.5.2 Syntheses

Sodium 1-(2-nitrophenyl)-1-phenylcarbamoylsulfimidate pentahydrate (**1**)

A 500 mL three-necked flask equipped with a reflux condenser and purged with nitrogen was charged with benzene (70 mL). Solid 1-(2-nitrophenyl)-1-phenylamine (6.43 g, 30 mmol) was added and the dark red solution was cooled in an ice bath for 30 min. Chlorosulfonyl isocyanate (2.61 mL, 1 equiv.) was then added over a period of 20 min. The mixture was left to stir cold for 30 min and then warmed to room temperature and stirred for an additional 2 h. The resulting solid green intermediate was collected by filtration and dissolved in acetonitrile (300 mL). An aqueous solution of sodium bicarbonate (200 mL, 5% *w/w*) was added and the mixture was allowed to stir at room temperature for 4 h. Distilled water was added to dissolve the precipitate produced and the biphasic solution was left to crystallize at 4 °C. The resulting yellow crystals were collected in 8.52 g (60%) yield; mp 180–182 °C. ^1H NMR (300 MHz, D_2O) δ (ppm):

7.03 (t, 2H, $J = 8.10$ Hz), 7.15 (m, 5H), 7.35 (t, 1H, $J = 7.3$ Hz), 7.76 (dd, 1H, $J = 9$ Hz). ^{13}C NMR (300 MHz, D_2O) δ (ppm): 124.9, 125.6, 125.8, 127.6, 128.8, 130.2, 133.9, 138.2, 143.5, 145.7, 161.2. IR (KBr, cm^{-1}): 507 (w), 599 (w), 643 (w), 699 (w), 776 (w), 848 (w), 858 (w), 1018 (vs), 1116 (m), 1146 (m), 1237 (vw), 1277 (w), 1307 (m), 1362 (s), 1394 (w), 1496 (w), 1530 (vs), 1603 (vs), 1660 (vw), 3501 (br, vs), 3584 (m). Elemental anal. calcd. for $\text{C}_{13}\text{H}_{20}\text{N}_3\text{Na}_2\text{O}_{11}\text{S}$: C, 33.13%, H, 4.06%, N, 8.91%, S, 6.80%; found: C, 33.22%, H, 4.12%, N, 8.80%, S, 6.51%.

1-(2-Nitrophenyl)-1-phenylurea (**2a**)

A 500 mL three-necked flask equipped with a reflux condenser and purged with nitrogen was charged with benzene (70 mL). 1-(2-Nitrophenyl)-1-phenylamine (12.85 g, 60 mmol) was added and dissolved. The dark red solution was cooled in an ice bath and chlorosulfonyl isocyanate (6.5 mL, 1.2 equiv.) was added over a period of 20 min. The mixture was left to stir cold for 30 min and then warmed to room temperature and stirred for an additional 2 h. The resulting solid green intermediate was collected by filtration and dissolved in acetonitrile (300 mL). An aqueous solution of sodium bicarbonate (200 mL, 5% w/w) was added and the mixture was allowed to stir at room temperature for 4 h. The resulting mixture was evaporated under reduced pressure to remove the volatile solvent. The crude product that resulted was stirred in 200 mL of benzene for 4 h and the insoluble portion was collected and dissolved in 150 mL of ethyl acetate. The mixture was extracted three times with a 5% v/v solution of hydrochloric acid. The organic phase was then washed three times with saturated sodium chloride (60 mL), dried over magnesium sulfate, and evaporated to give the crude urea. Recrystallization from ethanol yielded the yellow-green crystalline product in 10.925 g (71%) yield; mp 186–186.6 °C. ^1H NMR (300 MHz, DMSO-d_6) δ (ppm): 6.23 (s br, 2H), 7.14 (d, 1H, $J = 8.10$ Hz), 7.26–7.44 (m, 6H), 7.92 (dd, 1H, $J = 8.40$ Hz). ^{13}C NMR (300 MHz, DMSO-d_6) δ (ppm): 125.2, 126.8, 127.4, 128.2, 130.1, 130.2, 134.2, 137.1, 142.4,

146.6, 156.3. IR (KBr, cm^{-1}): 704 (m), 1146 (w), 1345 (m), 1392 (m), 1486 (w), 1523 (vs), 1594 (s), 1679 (vs), 3200 (w), 3293 (vw), 3351 (vw), 3478 (m). Elemental anal. calcd. for $\text{C}_{13}\text{H}_{11}\text{N}_3\text{O}_3$: C, 60.70, H, 4.31, N, 16.33; found: C, 60.44, H, 4.28, N, 16.21.

1-(2-Nitrophenyl)-1-phenylhydrazine (**3**)

To 100 mL of distilled water was added 1-(2-nitrophenyl)-1-phenylurea (0.69 g, 2.6 mmol) and the solution was cooled in ice for 30 min. Calcium hypochlorite (0.2648 g, 0.65 equiv.) was added along with sodium hydroxide (0.5369 g, 5 equiv.). The suspension was placed in an oil bath and refluxed for 1 h. The resulting red solution was cooled and extracted (3×75 mL) with ethyl acetate to remove the amine by-product. The aqueous phase was then acidified, neutralized with sodium bicarbonate, and extracted (3×50 mL) with dichloromethane. The organic washings were combined, washed with saturated sodium chloride (3×50 mL), dried over magnesium sulfate, and evaporated to yield a crude hydrazine in 0.498 g (80%) yield as a red oil. This red oil was then heated under vacuum at 140°C for 12 h and the residue combined with ethanol, which, upon refrigeration, furnished the red crystalline product in 0.243 g (55%) yield; mp $85.3\text{--}87.0^\circ\text{C}$. ^1H NMR (300 MHz, DMSO-d_6) δ (ppm): 5.16 (s, 2H), 6.86 (t, 1H, $J = 7.50$ Hz), 7.03 (d, 2H, $J = 8.7$ Hz), 7.52 (m, 2H), 7.79 (d, 1H, $J = 6.60$ Hz). ^{13}C NMR (300 MHz, DMSO-d_6) δ (ppm): 116.6, 121.2, 123.7, 125.7, 125.8, 129.3, 133.7, 142.3, 143.7, 148.7. IR (KBr, cm^{-1}): 476 (w), 510 (s), 613 (w), 658 (w), 697 (s), 748 (vs), 764 (s), 781 (m), 849 (s), 880 (s), 949 (s), 1037 (w), 1163 (w), 1191 (vw), 1247 (m), 1299 (m), 1367 (s), 1442 (m), 1488 (vs), 1518 (vs), 1590 (vs), 1621 (s), 3343 (w). HRMS calcd. for $\text{C}_{12}\text{H}_{11}\text{N}_3\text{O}_2\text{Na}$: 252.0743; found: 252.0756. Elemental anal. calcd. for $\text{C}_{12}\text{H}_{11}\text{N}_3\text{O}_2$: C, 62.87, H, 4.84, N, 18.33; found: C, 62.94, H, 4.80, N, 18.52.

Methyl 4-((2-nitrophenyl)amino)benzoate (**4**)

To a 250 mL three-necked flask equipped with a reflux condenser and flushed with nitrogen was added 2-nitroaniline (2.000 g, 14.47 mmol), cesium carbonate (9.429 g, 2 equiv.), methyl 4-bromobenzoate (4.667 g, 1.5 equiv.), tris(dibenzylideneacetone)-dipalladium(0) (0.416 g, 5 mol%), 2,2'-bis(diphenylphosphino)-1,1'-binaphthyl (0.676 g, 7.5 mol%), and 50 mL of freshly dried toluene. The contents were heated to 110 °C for 20 h. The mixture was then cooled, filtered through a pad of celite, and the filtrate reduced to small volume. The crude product was obtained by column chromatography on silica gel with dichloromethane as eluent and rinsed with ethanol to furnish the pure product in 3.522 g (89%) yield; mp 145–146 °C. ¹H NMR (300 MHz, CDCl₃) δ (ppm): 3.92 (s, 3H), 6.90 (dt, 1H, *J* = 8.40 Hz), 7.30 (d, 2H, *J* = 8.70 Hz), 7.45 (d, 2H), 8.04 (d, 2H, *J* = 8.70), 8.21 (d, 1H, *J* = 8.70 Hz), 9.48 (s, 1H). ¹³C NMR (300 MHz, CDCl₃) δ (ppm): 52.1, 117.0, 119.2, 121.2, 125.8, 126.8, 131.3, 131.4, 131.5, 134.8, 135.6, 140.6, 143.6, 166.4. IR (KBr, cm⁻¹): 736 (s), 764 (m), 1076 (w), 1106 (m), 1119 (w), 1149 (m), 1166 (m), 1175 (m), 1194 (vw), 1219 (sh), 1232 (m), 1268 (s), 1285 (s), 1308 (w), 1354 (m), 1403 (vw), 1428 (m), 1446 (vw), 1499 (m), 1515 (vs), 1574 (m), 1587 (m), 1604 (s), 1619 (w), 1724 (vs), 2958 (vw), 3067 (vw), 3326 (m). HRMS calcd. for C₁₄H₁₂N₂O₄Na: 295.0689; found: 295.0684. Elemental anal. calcd. for C₁₄H₁₂N₂O₄: C, 61.76, H, 4.44, N, 10.29; found: C, 61.62, H, 4.38, N, 10.38.

Methyl 4-(1-(2-nitrophenyl)ureido)benzoate (**2b**)

A 500 mL three-necked flask equipped with a reflux condenser and purged with nitrogen was charged with benzene (70 mL). Methyl 4-((2-nitrophenyl)amino)benzoate (1.20 g, 4.4 mmol) was added and dissolved. The orange solution was cooled in an ice bath and chlorosulfonyl isocyanate (0.46 mL, 1.2 equiv.) was added over a period of 20 min. The mixture was left to stir cold for 30 min and then warmed to room temperature and stirred for an additional 2 h. The resulting solid yellow–orange intermediate was collected by filtration and dissolved in acetonitrile (300 mL). An aqueous solution of

sodium bicarbonate (200 mL, 5% w/w) was added and the mixture was allowed to stir at room temperature for 4 h. The resulting mixture was evaporated under reduced pressure to remove the volatile solvent. The crude product that resulted was stirred in 200 mL of benzene for 4 h and the insoluble portion was collected and dissolved in 150 mL of ethyl acetate. The mixture was extracted three times with a 5% v/v aqueous solution of hydrochloric acid. The organic phase was then washed three times with saturated sodium chloride (60 mL), dried over magnesium sulfate, and evaporated to give the crude urea. Recrystallization from ethanol gave the pale yellow crystalline product in 0.602 g (44%) yield; mp 219–220 °C. ¹H NMR (300 MHz, DMSO-d) δ (ppm): 3.82 (s, 3H), 6.50 (s, br, 2H), 7.24 (d, 1H, J = 6.60 Hz), 7.33 (d, 2H, 8.70 Hz), 7.48 (t, 1H, J = 7.80 Hz), 7.66 (t, 1H, J = 7.80 Hz), 7.93 (t, 2H, 8.70 Hz), 8.00 (d, 1H, 9.00 Hz). ¹³C NMR (300 MHz, DMSO-d) δ (ppm): 52.6, 125.7, 126.8, 126.9, 128.0, 130.8, 131.1, 134.8, 136.4, 146.7, 146.9, 155.7, 166.2. IR (KBr, cm⁻¹): 704 (s), 745 (m), 774 (m), 783 (s), 829 (vw), 849 (s), 1016 (w), 1027 (vw), 1054 (vw), 1110 (m), 1117 (s), 1171 (w), 1194 (w), 1281 (s), 1305 (m), 1358 (m), 1392 (s), 1436 (m), 1448 (w), 1509 (m), 1528 (vs), 1581 (w), 1601 (s), 1621 (m), 1693 (vs), 1726 (vs), 2953 (w), 3168 (s), 3307 (w), 3403 (vs). HRMS calcd. for C₁₅H₁₃N₃O₅Na: 338.0747; found: 338.0751. HRMS calcd. for C₁₅H₁₃N₃O₅K: 354.0487; found: 354.0490. Elemental anal. calcd. for C₁₅H₁₃N₃O₅: C, 57.04, H, 4.16, N, 13.33; found: C, 57.08, H, 3.91, N, 13.30.

3.5.3 X-Ray Crystallography

The X-ray diffraction data were measured with graphite mono-chromated Mo K α radiation (λ = 0.71073 Å) on crystals that were attached to a glass fiber with viscous paratone N oil. The structures were solved by direct methods on an absorption-corrected model generated by SADABS. Refinement was achieved by a full-matrix least-squares procedure based on F^2 . The hydrogen atoms were located at calculated

positions. The structures have been deposited with the Cambridge Crystallographic Data Center under deposition Nos. 964267, 964268, 964269, and 964271.

3.5.4 Theoretical Methods

All of the calculations described were performed using Gaussian 03.³³ Computations were carried out at the restricted Hartree–Fock³⁴ and density functional theory (DFT) levels. Density functional theory calculations used the hybrid B3LYP functional and triple zeta 6-311++G** basis sets.³⁵ The calculated molecular geometries were fully optimized and correspond to minima on the potential energy surface as confirmed by the absence of imaginary vibrational frequencies. All transition states were confirmed by reaction path (IRC) following calculations.

3.6 Acknowledgements

This research was supported by NSERC discovery grants to D.S.B. and I.S.B. The authors are grateful to Dr. Alexander Wahba and Nadim Saade for mass spectrometry analysis.

3.7 References

1. Sasikumar, T. K.; Burnett, D. A.; Zhang, H.; Smith-Torhan, A.; Fawzi, A.; Lachowicz, J. E., Hydrazides of clozapine: a new class of D1 dopamine receptor subtype selective antagonists. *Bioorg. Med. Chem. Lett.* **2006**, *16* (17), 4543-7.
2. (a) Schwarz, A. D.; Onn, C. S.; Mountford, P., A remarkable switch from a diamination to a hydrohydrazination catalyst and observation of an unprecedented catalyst resting state. *Angew. Chem. Int. Ed.* **2012**, *51* (49), 12298-302; (b) Weitershaus, K.; Wadepohl, H.; Gade, L. H., Titanium Hydrazinediido Half-Sandwich Complexes: Highly Active Catalysts for the Hydrohydrazination of Terminal Alkynes at Ambient Temperature. *Organometallics* **2009**, (13), 3381-3389.

3. Ramsden, C. A., Product Class 34: Arylhydrazines. *Science of Synthesis* **2007**, 31b, 1773-1773.
4. Smith, P. A. S., *Derivatives of Hydrazine and other Hydronitrogens Having N-N Bonds*. Benjamin/Cummings: New York, 1983.
5. (a) Hong, S.-S.; Bavadekar, S. a.; Lee, S.-I.; Patil, P. N.; Lalchandani, S. G.; Feller, D. R.; Miller, D. D., Bioisosteric phentolamine analogs as potent alpha-adrenergic antagonists. *Bioorg. Med. Chem. Lett.* **2005**, 15 (21), 4691-5; (b) Ishii, H.; Sugura, T.; Akiyama, Y.; Ichikawa, Y.; Watanabe, T.; Murakami, Y., Fischer indolization of Ethyl Pyruvate 2-(2,6-Dimethoxyphenyl)phenylhydrazone. *Chem. Pharm. Bull.* **1990**, 38, 2118-2126; (c) Rao, H.; Jin, Y.; Fu, H.; Jiang, Y.; Zhao, Y., A versatile and efficient ligand for copper-catalyzed formation of C-N, C-O, and P-C bonds: pyrrolidine-2-phosphonic acid phenyl monoester. *Chemistry (Weinheim an der Bergstrasse, Germany)* **2006**, 12 (13), 3636-46.
6. (a) Blumenfeld, M.; Compere, D.; Gauthier, J. M. Preparation of substituted 4-[[[N-[2-(piperidin-1-yl)phenyl]hydrazino]carbonyl]methyl]benzoic acids and related derivatives inhibitors of human papilloma virus and their pharmaceutical compositions. FR2901273A1, 2007; (b) Blumenfeld, M.; Compere, D.; Gauthier, J.-M. Preparation of substituted 4-[[[N-[2-(piperidin-1-yl)phenyl]hydrazino]carbonyl]methyl]benzoic acids and related derivatives inhibitors of human papilloma virus and their pharmaceutical compositions. WO2007135106A1, 2007.
7. Murakami, Y.; Yokoyama, Y.; Sasakura, C.; Tamagawa, M., An Efficient Synthesis of 1,1-Disubstituted Hydrazines. *Chem. Pharm. Bull.* **1983**, 31 (2), 423-423.
8. Ren, P.; Vechorkin, O.; von Allmen, K.; Scopelliti, R.; Hu, X., A structure-activity study of Ni-catalyzed alkyl-alkyl Kumada coupling. Improved catalysts for coupling of secondary alkyl halides. *J. Am. Chem. Soc.* **2011**, 133 (18), 7084-95.
9. Tietze, M.; Iglesias, A.; Merisor, E.; Conrad, J.; Klaiber, I.; Beifuss, U., Efficient methods for the synthesis of 2-hydroxyphenazine based on the Pd-catalyzed N-arylation of aryl bromides. *Org. Lett.* **2005**, 7 (8), 1549-52.
10. (a) Dhar, D. N.; Murthy, K. S. K., Recent Advances in the Chemistry of Chlorosulfonyl Isocyanate. *Synthesis* **1986**, 6, 437-449; (b) Graf, R., Reactions with N-Carbonylsulfamoyl Chloride. *Angew. Chem. Int. Ed.* **1968**, 7 (3), 172-182; (c) Rasmussen, J. K.; Hassner, A., Recent developments in the synthetic uses of chlorosulfonyl isocyanate. *Chem. Rev.* **1976**, 76 (3), 389-408.
11. (a) Backer, H. J.; Groot, J., The properties of the sulfonyl group. XIII. Intramolecular rearrangement of (nitrophenylsulfonyl)ureas. *Recl. Trav. Chim. Pay. B.* **1950**, 69, 1323-1347; (b) Ceric, H.; Kovacevic, M.; Sindler-Kulyk, M., Regioselective Epimerisation of cis-3-Amino-4-oxo-azetidine-2-sulphonic acid and Synthesis of Monocyclic b-Lactams q. *Tetrahedron Lett.* **2000**, 56, 3985-3993; (c) Sircar, I.; Gudmundsson, K. S.; Martin, R.; Liang, J.; Nomura, S.; Jayakumar, H.; Teegarden, B. R.; Nowlin, D. M.; Cardarelli, P. M.; Mah, J. R.; Connell, S.; Griffith, R. C.; Lazarides, E.,

Synthesis and SAR of N-benzoyl-L-biphenylalanine derivatives: discovery of TR-14035, a dual $\alpha(4)\beta(7)/\alpha(4)\beta(1)$ integrin antagonist. *Bioorg. Med. Chem.* **2002**, *10* (6), 2051-66.

12. Schaumann, E.; Kausch, E.; Imbert, J.-P.; Adiwidjaja, G., Cycloadditionsreaktionen von Heterocumulenen, XII: Umsetzung von persubstituierten Isothioharnstoffen mit Isocyanaten. *Chem. Ber.* **1978**, *111* (4), 1475-1485.

13. Elsegood, M. R. J.; Kelly, P. F.; Reid, G.; Slawin, A. M. Z.; Staniland, P. M., Sulfimideation of thioether groups--a versatile method for modifying and linking thia/oxa crowns. *Dalton Trans.* **2008**, (37), 5076-82.

14. (a) Chow, T. W.-S.; Chen, G.-Q.; Liu, Y.; Zhou, C.-Y.; Che, C.-M., Practical iron-catalyzed atom/group transfer and insertion reactions. *Pure Appl. Chem.* **2012**, *84* (8), 1685-1704; (b) Giribabu, L.; Singh, S. P.; Patil, N. M.; Kantam, M. L.; Gupte, S. P.; Chaudhari, R. V., Highly Efficient Sulfimideation of 1,3 - Dithianes by Cu(I) Complexes. *Synth. Commun.* **2008**, *38* (4), 619-625; (c) Liu, Y.; Che, C.-M., [Fe(III)(F(20)-tpp)Cl] is an effective catalyst for nitrene transfer reactions and amination of saturated hydrocarbons with sulfonyl and aryl azides as nitrogen source under thermal and microwave-assisted conditions. *Chem. Eur. J.* **2010**, *16* (34), 10494-501.

15. (a) Wichmann, C. F.; Niemczura, W. P.; Schnoes, H. K.; Hall, S.; Reichardt, P. B.; Darling, S. D., Structures of two novel toxins from *Protogonyaulax*. *J. Am. Chem. Soc.* **1981**, *103* (23), 6977-6978; (b) Hall, S.; Darling, S. D.; Boyer, G. L.; Reichardt, P. B.; Liu, H. W., Dinoflagellate neurotoxins related to saxitoxin: Structures of toxins C3 and C4, and confirmation of the structure of neosaxitoxin. *Tetrahedron Lett.* **1984**, *25* (33), 3537-3538.

16. Berezin, A. A.; Zissimou, G.; Constantinides, C. P.; Beldjoudi, Y.; Rawson, J. M.; Koutentis, P. A., Route to Benzo- and Pyrido-Fused 1,2,4-Triazinyl Radicals via N'-(Het)aryl-N'-[2-nitro(het)aryl]hydrazides. *J. Org. Chem.* **2014**, *79* (1), 314-327.

17. Judd, W. P. Rearrangements of N-Halogenoamides. 1967.

18. (a) Shvo, Y.; Nahlieli, A., Detection of thermal isomerization of hydrazones by NMR spectroscopy. *Tetrahedron Lett.* **1970**, (49), 4273-4; (b) van Alsenoy, C.; Williams, J. O.; Scarsdale, J. N.; Geise, H. J.; Smits, G.; Schäfer, L., Ab initio studies of structural features not easily amenable to experiment: 9. molecular structure and conformational analysis of hydrazine and methyl-hydrazine. *Bull. Soc. Chim. Belges* **1980**, *89* (9), 737-742; (c) Nelsen, S. F.; Gannett, P. M., Conformational interconversions in pentaalkylhydrazine cation tetrafluoroborates. *J. Am. Chem. Soc.* **1981**, *103* (12), 3300-3304.

19. Carrillo, D., [MoO₂ (acac)₂], a versatile precursor for diazenido- and hydrazido-complexes. *C. R. Acad. Sci. Sér. IIC* **2000**, *3*, 175-181.

20. (a) Hauser, C. R.; Kantor, S. W., Some Observations on the Hofmann, Lossen and Curtius Rearrangements. *J. Am. Chem. Soc.* **1950**, *72* (9), 4284-4285; (b) Smith, P. A. S., Rearrangements involving migration to an electron-deficient nitrogen or

oxygen. *Mol. Rearrange.* **1963**, *1*, 457-591; (c) Tarwade, V.; Dmitrenko, O.; Bach, R. D.; Fox, J. M., The Curtius Rearrangement of Cyclopropyl and Cyclopropenoyl Azides. A Combined Theoretical and Experimental Mechanistic Study. *J. Org. Chem.* **2008**, *73* (21), 8189-8197.

21. Campbell, A.; Kenyon, J., 9. Retention of asymmetry during the Beckmann, Lossen, and Curtius changes. *J. Chem. Soc. (Resumed)* **1946**, (0), 25-27.

22. (a) Brower, K. R., The Volume Change of Activation in the Claisen and Curtius Rearrangements. *J. Am. Chem. Soc.* **1961**, *83* (21), 4370-4372; (b) Prosser, T. J.; Eliel, E. L., Confirmation of the Intramolecular Nature of the Hofmann "Haloamide" Reaction by Double Labeling. *J. Am. Chem. Soc.* **1957**, *79* (10), 2544-2546; (c) Wentrup, C.; Bornemann, H., The Curtius Rearrangement of Acyl Azides Revisited – Formation of Cyanate (R–O–CN). *European J. Org. Chem.* **2005**, *2005* (21), 4521-4524.

23. (a) Renfrow, W. B.; Hauser, C. R., The Relative Rates of Decomposition of the Potassium Salts of Certain Meta and Para Substituted Dibenzhydroxamic Acids. A Study of the Lossen Rearrangement^{1,2}. *J. Am. Chem. Soc.* **1937**, *59* (11), 2308-2314; (b) Bright, R. D.; Hauser, C. R., The Influence of Substituents on the Rates of Decomposition of the Potassium Salts of Dihydroxamic Acids. The Lossen Rearrangement. *J. Am. Chem. Soc.* **1939**, *61* (3), 618-629; (c) Hauser, C. R.; Renfrow, W. B., The Removal of HX from Organic Compounds by Means of Bases. III. The Rates of Removal of Hydrogen Bromide from Substituted N-Bromobenzamides and their Relative Ease of Rearrangement in the Presence of Alkali. The Hofmann Rearrangement. *J. Am. Chem. Soc.* **1937**, *59* (1), 121-125.

24. Lwowski, W.; Scheiffele, E., Curtius and Lossen Rearrangements. I. The Benzenesulfonyl System. *J. Am. Chem. Soc.* **1965**, *87* (19), 4359-4365.

25. Horner, L.; Bauer, G.; Döriges, J., Über Lichtreaktionen, XVIII: Photolyse von Benzazid in verschiedenen Reaktionsmedien und ihre Sensibilisierung. *Chem. Ber.* **1965**, *98* (8), 2631-2642.

26. (a) Abu-Eittah, R. H.; Mohamed, A. A.; Al-Omar, A. M., Theoretical investigation of the decomposition of acyl azides: Molecular orbital treatment. *International J. Quantum Chem.* **2006**, *106* (4), 863-875; (b) Zabalov, M. V.; Tiger, R. P., Mechanism and structural aspects of thermal Curtius rearrangement. Quantum chemical study. *Russ. Chem. Bull.* **2005**, *54* (10), 2270-2280.

27. Shestakov, P. German Patent 164,755; Chem. Zentr. 1905II, 1703.

28. Bohle, D. S.; Chua, Z.; Perepichka, I.; Rosadiuk, K., E/Z Oxime Isomerism in PhC(NO₂)CN. *Chem. Eur. J.* **2013**, *19* (13), 4223-4229.

29. (a) Bohle, D. S.; Rosadiuk, K. A., *Inorg. Chem.* **2014**, In Press; (b) Bohle, D. S.; Chua, Z.; Johnstone, T.; Moiseev, A. G.; Perepichka, I.; Rosadiuk, K. A., Permethylated Salts and Radicals Derived from Azo peri-Naphthalenes. *ChemPlusChem* **2012**, *77* (5), 387-395.

30. (a) Petersson, G. A.; Al - Laham, M. A., A complete basis set model chemistry. II. Open - shell systems and the total energies of the first - row atoms. *J. Chem. Phys.* **1991**, *94* (9), 6081-6090; (b) Petersson, G. A.; Bennett, A.; Tensfeldt, T. G.; Al - Laham, M. A.; Shirley, W. A.; Mantzaris, J., A complete basis set model chemistry. I. The total energies of closed - shell atoms and hydrides of the first - row elements. *The J. Chem. Phys.* **1988**, *89* (4), 2193-2218.
31. Mauguin, C., Bromo-Sodio Amides and their Role in the Hofmann Transposition. *Ann. Chim. Phys.* **1911**, *22*, 297-369.
32. Greene, F. D.; Stowell, J. C.; Bergmark, W. R., Diaziridinones (2,3-diazacyclopropanones). II. Synthesis, properties, and reactions. *The J. Org. Chem.* **1969**, *34* (8), 2254-2262.
33. Frisch, M. J.; Trucks, G. W.; Schlegel, H. B.; Scuseria, G. E.; Robb, M. A.; Cheeseman, J. R.; Zakrzewski, V. G.; Montgomery, J. A.; Stratmann, R. E.; Burant, J. C.; Dapprich, S.; Millam, J. M.; Daniels, A. D.; Kudin, K. N.; Strain, M. C.; Farkas, O.; Tomasi, J.; Barone, V.; Cossi, M.; Cammi, R.; Mennucci, B.; Pomelli, C.; Adamo, C.; Clifford, S.; Ochterski, J.; Petersson, J. A.; Ayala, P. Y.; Cui, Q.; Morokuma, K.; Malick, D. K.; Rabuck, A. D.; Raghavachari, K.; Foresman, J. B.; Cioslowski, J.; Ortiz, J. V.; Stefanov, B. B.; Liu, G.; Liashenko, A.; Piskorz, P.; Kamaromi, L.; Gomperts, R.; Martin, R. L.; Fox, D. J.; Keith, T.; Al-Laham, M. A.; Peng, C. Y.; Nanayakkara, A.; Gonzalez, C.; Challacombe, M.; Gill, P. M. W.; Johnson, B. G.; Chen, W.; Wong, M. W.; Andres, J. L.; Head-Gordon, M.; Replogle, E. S.; Pople, J. A. *Gaussian 98*, Gaussian Inc.: Pittsburgh, PA, 1998.
34. Roothaan, C., New Developments in Molecular Orbital Theory. *Rev. Mod. Phys.* **1951**, *23* (2), 69-89.
35. (a) Becke, A. D., Density - functional thermochemistry. III. The role of exact exchange. *J. Chem. Phys.* **1993**, *98* (7), 5648-5652; (b) Lee, C.; Yang, W.; Parr, R., Development of the Colle-Salvetti correlation-energy formula into a functional of the electron density. *Phys. Rev. B* **1988**, *37* (2), 785-789.

π - Delocalization in the Vicinal Lone Pairs of Hydrazines

Electronic Effects in Derivatives of 1-(2-Nitrophenyl)-1-phenylhydrazine

4.1 Preamble

Having synthesized 1-(2-nitrophenyl)-1-phenylhydrazine (NDPH) in high yield and purity, we proposed to examine its reactivity by preparing several derivatives and characterizing them in the solid-state. By substituting the free hydrazine with various substituents, the effects of variation of electron density and sterics on the hydrazine framework can be evaluated. Gas-phase DFT calculations also provide an energetic basis for extrapolation to what is observed experimentally in the solution and solid phases. Gas-phase density functional theory is used to support the experimental data by providing a model for geometric changes observed. The choice of basis set and level of DFT theory employed here is based on past experience with calculations for related nitrogen species with numerous lone pairs. In general this theoretical model has excellent predicts of ground state configurations and vibrational energy levels for related compounds. Although the specific metric parameters may very well be dependent on basis set, and the functionals employed, the contrasts made with experimental data are intended to reconfirm their utility for the predictions made for this class of compounds as well. With these features confirmed for the ground states we have established their utility for predicting intermediates, transition states, and reaction pathways.

From the results of this study, the electronic, steric and sensitivities of these new compounds can be ascertained and provide useful knowledge about the reactivity of the electron-deficient 1,1-diarylhydrazines. Reactivity of these compounds has not yet been

explored in the literature and these experiments provide insight into the possible metals with which these ligands might best form coordination compounds for further applications of these compounds, for example in heterocycle synthesis.

4.2 Introduction

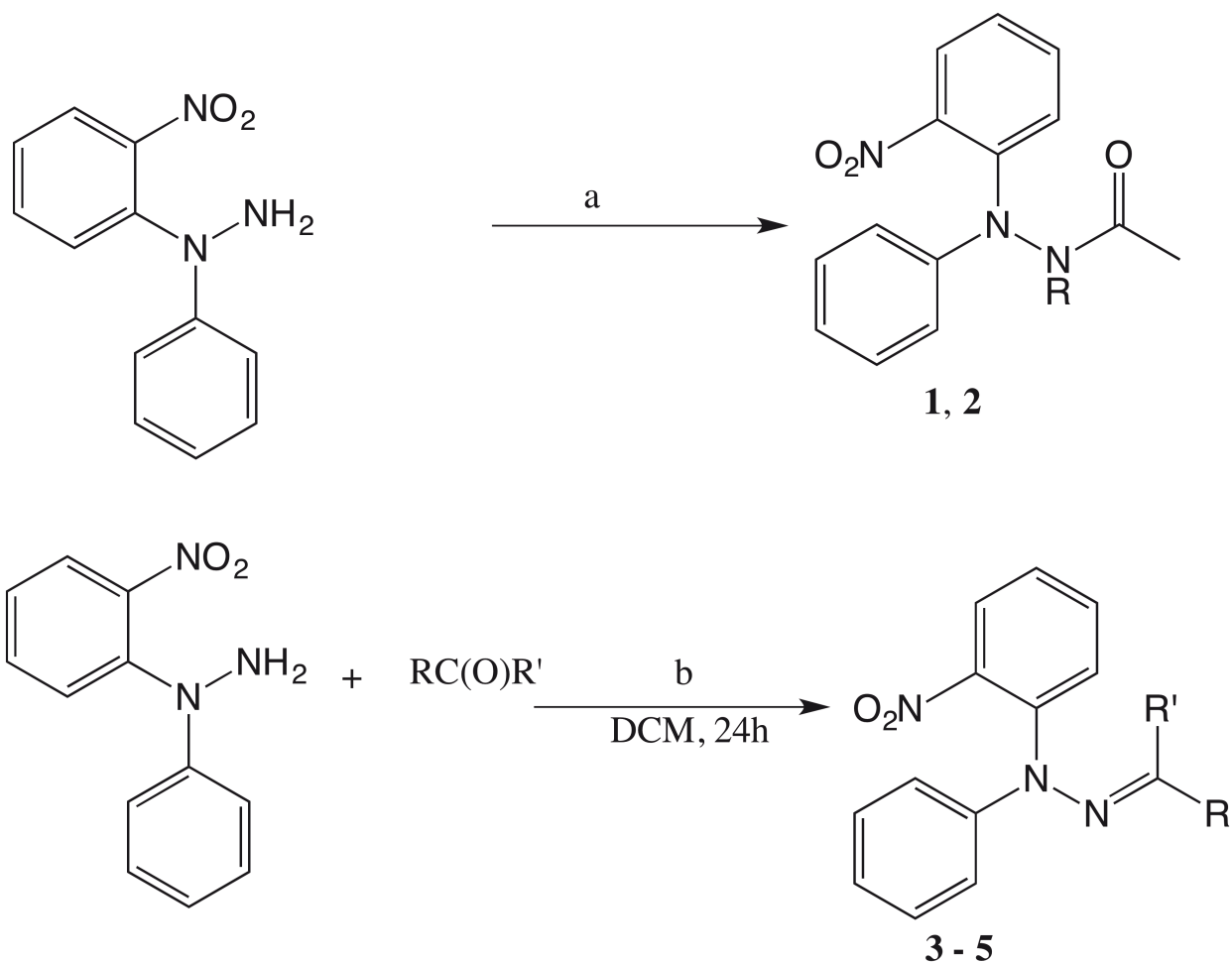
One of the stronger contrasts in the chemistry of carbon and nitrogen are the ranges of their single bond lengths. While crystallographically determined C-C single bonds span a relatively narrow range with a median value of 1.5595(70)Å, single N-N bonds vary markedly with a mean value of 1.3845(34)Å and may range up to 2.1Å.¹ Not too surprisingly, the bond enthalpies for these bonds reflect these trends. For example, N-N single bonds that are found in remarkably stable heterocycles stand in contrast with the weak Van der Waals adducts such as [NO]₂ or in the hydrazines. Related trends are also behind the outstanding synthetic utility of hydrazine derivatives which stems in part from the presence of a responsive N-N bond and the nucleophilicity of the lone pairs of electrons on the nitrogen atoms, which are alpha to one another. While hydrazine has a long N-N bond that readily undergoes homolysis, upon derivatization, the N-N bond is often retained as a strong, short bond in its products. The conformational consequences of these vicinal lone pairs have been studied extensively and the increased nucleophilicity of these nitrogen atoms is recognized in the alpha kinetic effect.² A particularly striking feature of hydrazine derivatives, however, is the tuneable nature of these vicinal lone-pair interactions, where not only is the reactivity modified, but the N-N bonding can be converted to double or even robust, strong N-N single bonds. This variability offers considerable scope for applications of these compounds in analytical,³ electronic,⁴ optical,⁵ and material science.⁶ N,N-diaryl hydrazines, Ar₂NNH₂, generally contain planar and formally sp²-hybridized Ar₂N units where the nitrogen lone pair is conjugated with the aromatic rings.

Recently, we reported a method for the facile preparation of N,N-diaryl hydrazines containing electron-withdrawing substituents,⁷ which allowed us to prepare a series of related derivatives in order to tune the electronic structure of the N-N bonded framework. Such substitutions illustrate the competition of intramolecular π -bonding to

form either an N=N double bond, or, by conjugation through a proximal electron-withdrawing group such as *o*-C₆H₄(NO₂), a C=N bond. In addition, the possibility of intermolecular interactions, such as London forces and donor-acceptor pairings, may further split or modulate these interactions which give rise to varying N-N bond strengths. Herein, we describe (1) the effect of substitution with electron donating or withdrawing organic functional groups on bond order throughout the diaryl and -amino domains of N,N-diarylhydrazines; (2) the effect on molecular geometry and hence electron mobility across the N-N bond and consequently, the type of N-N bond; (3) the electronic spectroscopy of the new compounds; and (4) the overall implications of these results in terms of molecular stabilities of the hydrazine derivatives.

4.3 Results and Discussion

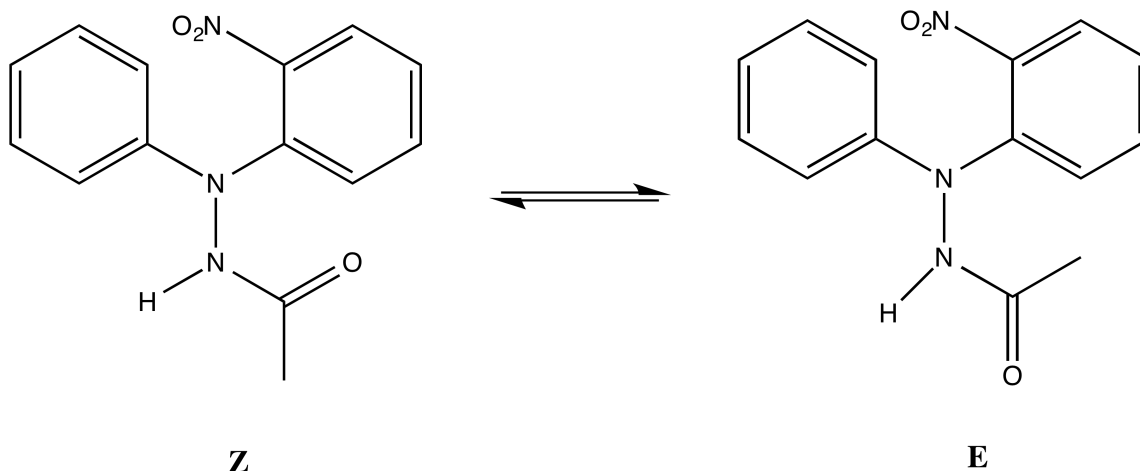
To explore the electronic effects of various substituents in 1,1-diarylhydrazines, 1-(2-nitrophenyl)-1-phenyl hydrazine (NDPH) was derivatized with five different functional groups (Scheme 4-1). With the exception of its mono-acetyl **1** and Schiff base **5**⁸ all of these compounds are described here for the first time as single well-defined stereoisomers.



	1	2	3	4	5
R	H	Ac	Me	H	H
R'			Me	o-(C ₆ H ₄)OH	Ph
a	CH ₃ COOH reflux / 24h	3 eq. Ac ₂ O reflux / 24h			
b			H ₂ SO ₄ (cat.)	HCl (cat.)	HCl (cat.)

Scheme 4-1: Synthesis of 1,1-diarylhydrazine derivatives.

The mono-acetylation of NDPH with acetic anhydride results in an equilibrium mixture of atropisomers for 1. These correspond to the E and Z isomers around the amide bond (Scheme 4-2).



Scheme 4-2: Isomerism in N'-(2-nitrophenyl)-N'-phenylacetohydrazide.

By ^1H NMR in DMSO there is an 10:1 mixture of Z:E and in chloroform this reaches a more closely balanced 2:1 mixture. Although prior studies⁸ have reported similar isomeric ratios in DMSO, we have employed 2D-NOESY NMR to definitively show that in either solution, the Z isomer is the major species due to the NOE correlation between the more abundant amide proton with the signal for the corresponding acetyl methyl protons (See Appendix C). Given the sharpness of the acetyl peaks in the room temperature ^1H NMR spectrum, there is little indication of exchange on the NMR timescale, but this isomerism in amides has been studied mechanistically,⁹ theoretically using MO theory,¹⁰ and has been a subject of considerable biological interest.¹¹ The studies show the Z/E equilibrium to be directly affected by the molecular environment. In the solid state the single crystal X-ray diffraction structure corresponds solely to the Z isomer (Figure 4-1) but when these single crystals are re-dissolved, and this equilibrium is monitored by NMR, we find that within mixing/dissolution the same ratio of Z:E isomers in solution is rapidly formed from the single isomer present in the crystal. For comparison, gas-phase DFT calculations, B3LYP/6-311++g**, indicate that the Z isomer has a larger electronic stabilization,

some 1.62 kcal/mole more stable than the E isomer, and thus under the conditions of our NMR measurements this would correspond to a 15.3:1 ratio. Solvent polarity and hydrogen bonding ability will clearly alter the position of this equilibrium, and we note that the solid-state structure has intermolecular H-bonding between the amides of neighbouring molecules.

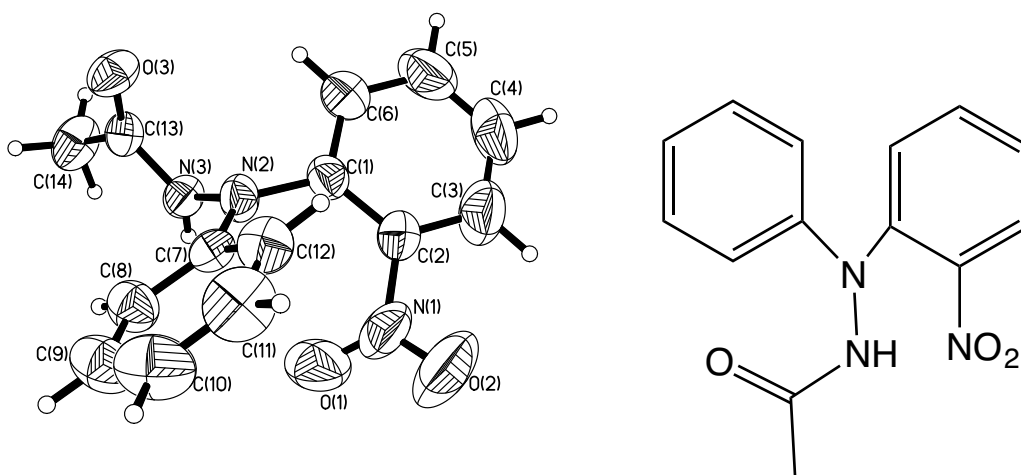


Figure 4-1. ORTEP representation of one molecule in the asymmetric unit of compound 1. Selected structural parameters are: N(2)-N(3) 1.386(3) Å, N(2)-C(1)-C(2)-N(1) 5.2(5)°, N(2)-N(3)-C(13)-C(14) -179.9(2)°.

Each derivative **1-5** has been characterized by single crystal X-ray diffraction, Figures 4-1 to 4-5, and the key metric parameters are collected in Table 4-1. The compounds provide for a different degree of possible electron delocalization and hence deactivation of the remaining nitrogen lone pair from the hydrazine framework. The electronic modulation by the hydrazine substitution has direct consequences on the solid-state structures. Specifically, there are three structural aspects of interest which

are directly affected by the electronic properties of the substituent on N(3): (1) the N-N bond length; (2) the orientation of the N-substituents relative to one another; and (3) the degree of planarity of the diaryl nitrogen as assessed by the sum of the angles about these atoms or a measure of their distance out of the plane of their substituents. For the final consideration, the five derivatives **1** to **5** were selected because they all share a formally sp^2 hybridized N atom bound to an Ar_2N nitrogen atom. In spite of this similarity, they have different N-CR₂ orientations with **1**, **2** and **3** having an orthogonal N-CR₂ group to the Ar_2N plane and **4** and **5** having all N substituents coplanar. Although **1**, **2**, **4** and **5** all have short N-N bonds, there is a significant increase in the N-N bond length upon substitution with an electron-rich 2-propenyl group, =CMe₂, from 1.4159(18) Å in the parent hydrazine to 1.4400(16) Å in **3**. Clearly, there is subtle electronic control of this bonding.

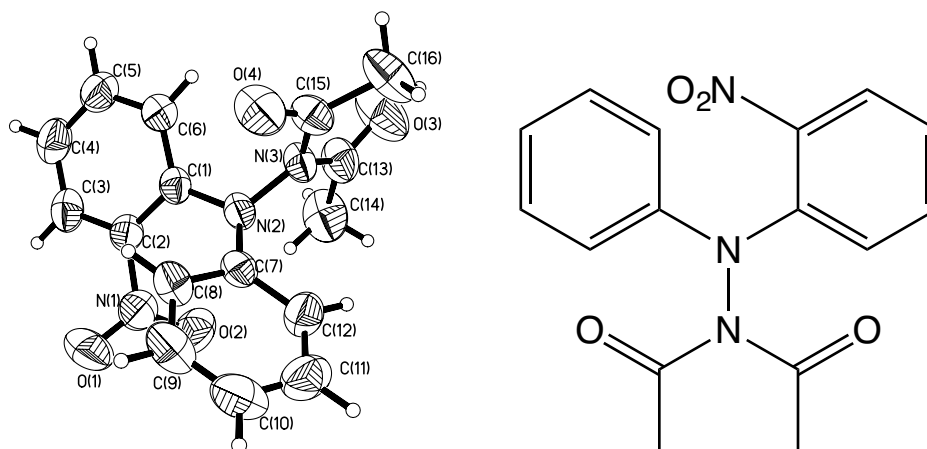


Figure 4-2. ORTEP representation of compound **2**. Selected structural parameters are: N(2)-N(3) 1.402(2) Å, N(2)-C(1)-C(2)-N(1) -0.8(3)°, O(3)-C(13)-N(3)-N(2) 167.2(2), O(4)-C(15)-N(3)-N(2) -12.8(3), out-of-plane distance of N(3) 0.02(3)Å.

Table 4-1: X-ray Diffraction Structural Parameters for Derivatives of NDPH.

Parameter	NDPH ³	1	2	3	4	5
N(2)-N(3) (Å)	1.4159(18)	1.386(3)	1.402(2)	1.4400(16)	1.3748(13)	1.369(2)
N(2)-C(1) (Å)	1.4012(17)	1.409(4)	1.411(2)	1.3994(18)	1.4246(14)	1.391(2)
N(2)-C(7) (Å)	1.4134(18)	1.409(4)	1.423(2)	1.4362(19)	1.4064(15)	1.424(2)
N(3)-C(13) (Å)	N/A	1.343(3)	1.406(3)	1.273(2)	1.2845(14)	1.272(2)
C(1)-C(2) (Å)	1.3981(19)	1.381(4)	1.395(3)	1.399(2)	1.3862(18)	1.382(2)
C(2)-N(1) (Å)	1.4624(19)	1.469(4)	1.468(3)	1.4703(18)	1.4590(18)	1.461(2)
C(13)-N(3)-N(2)-C(1) (°)	N/A	110.03(30)	-83.0(2)	-151.09(11)	-6.88(16)	-178.0(1)
C(13)-N(3)-N(2)-C(7) (°)	N/A	191.68(30)	121.7(2)	70.17(12)	176.39(10)	4.3(2)
N(3)-N(2)-C(1)-C(2) (°)	-41.63	-115.97(30)	154.8(2)	36.68(12)	-72.07(15)	24.2(2)
N(3)-N(2)-C(7)-C(8) (°)	-163.49	-6.7(3)	130.4(2)	-146.23(12)	-179.24(11)	-99.7(2)
N(2)-N(3)-C(13)-C(14) (°)	N/A	-179.9(2)	-11.7(3)	-178.44(12)	-177.55(10)	178.3(1)
C(1)-N(2)-N(3) (°)	113.69(11)	114.0(2)	116.76(15)	111.33(11)	120.72(9)	115.7(1)
C(7)-N(2)-N(3) (°)	120.64(11)	117.6(2)	116.09(14)	115.36(11)	117.89(9)	122.6(1)
C(7)-N(2)-C(1) (°)	123.66(12)	124.4(2)	122.02(14)	118.49(11)	121.31(9)	121.7(1)
Sum of angles about N(2) (°)	357.99(20)	356.0(3)	354.87(25)	345.18(19)	359.92(16)	360.0(2)
Distance of N(2) from its plane (Å)	0.1158	0.164 or 0.051 ^a	0.186	0.321	0.023	0.016 or 0.018 ^a

^a Two independent molecules per asymmetric unit.

Given that substitution with one acetyl group causes such a structural alteration in both the Ar₂N and NH₂ moieties of NDPH, we prepared the diacetyl derivative **2** for comparison. As found for **1** the N(C(O)Me)₂ group in **2** is planar and orthogonal to the Ar₂N group. However the N-N bond in **2** is slightly longer than for that found in **1**. Structural studies on di-acetylated hydrazine derivatives are sparse with only 8 structures having been described (Table S1, Appendix C).¹² As can be seen from Table S1, most of the structurally characterized N,N-diacetylhydrazines contain a short N-N bond and a roughly planar sp²-hybridized N(C(O)Me)₂ nitrogen. Substitution of the adjacent nitrogen with bulky electron-withdrawing phenyl rings as in **2** (Figure 4-2) produces an unusual structural effect that is present in only a couple entries in Table S1. It contains a rather long N-N bond, similar to that seen in the structures of 2,3,4-tri-O-acetyl-N-(diacetylamino)-[beta]-d-glucopyranurono-1,6-lactam^{12c} and N,N'-Diacetyl-N'-[(4-nitrophenoxy)acetyl]acetohydrazide, which was reported by Hu.^{12d} A common feature of both structures is their electron-withdrawing carbonyl functionalities flanking both sides of the N-N bond. As with **2**, these structures also have both nitrogen atoms in sp²-hybridization states.

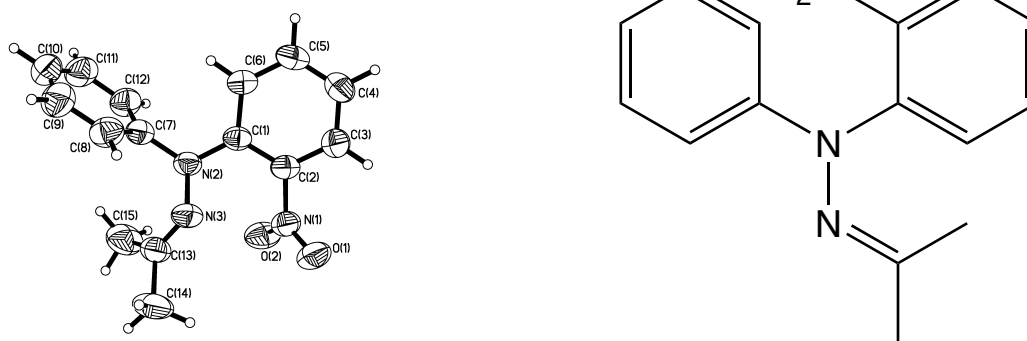
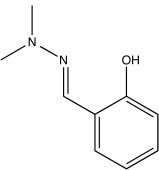


Figure 4-3. ORTEP Representation of compound **3**. Selected structural parameters are: N(2)-N(3) 1.4400(16) Å, N(2)-C(1)-C(2)-N(1) 8.7(2)°, N(2)-N(3)-C(13)-C(14) -178.4(1)°.

Condensation of NDPH with acetone leads to **3** with an electron-rich 2-propanylimine group (Figure 4-3) which has the longest N-N s-bond of all the derivatives examined here. With a torsion angle around N(2)-C(1) of $36.68(12)^\circ$, very little π -delocalization of the added electron density on N(3) is possible, but there is nevertheless a shorter N(2)-C(1) bond than in NDPH. The other phenyl ring, in contrast, is orthogonal to the N-N bond as well as the C₆H₄NO₂ ring and has a longer N(2)-C(7) bond. As a result of these geometric considerations, the diarylamine nitrogen N(2) is forced out of the plane of its surrounding functional groups by a distance of 0.321 Å, further hindering π -based delocalization.

Schiff base formation by condensation of NDPH with salicylaldehyde or benzaldehyde gives **4** and **5** respectively. By single crystal X-ray diffraction they have the shortest N-N bonds of the derivatives studied here. This observation is interestingly in line with pre-quantum mechanical assertions made in 1913 by Graziani¹³. The experimental values obtained here can also be compared with the semi-empirical SCF-MO calculations performed by Bren and co-workers for (*E*)-2-((2,2-dimethylhydrazono)methyl)phenol (Table 4-2),¹⁴ which illustrate the added stability of **4** over its dimethyl analogue.

Table 4-2: Comparison of Bond Lengths in Dimethyl- and (Diarylhydrazono)methyl)phenol Derivatives^a

Bond	Bond Length in compound 4 (Å)	Analogous Calculated Bond Lengths in  (MINDO) ¹⁴ B3LYP/6-311++g**	
O(3)-C(15)	1.359(2)	1.372	1.35022
C(15)-C(14)	1.401(1)	1.400	1.41761
C(14)-C(13)	1.452(2)	1.464	1.45833
C(13)-N(3)	1.284(2)	1.289	1.29236
N(3)-N(2)	1.375(1)	1.385	1.36289
N(3)----O(3)	2.650(1)		2.66002

^a Numbering is based on atom labels in the structure of **4**

In addition, a small increase in planarity as compared to compound **1** is seen in the solid state (Figure 4-4) with N(2) being only 0.023Å out of the plane of its substituents. The phenol of the salicylaldehyde group forms an internal hydrogen bonding (O(3) – N(3) = 2.650(1) Å) and hence only the *E*-isomer is observed in the solid state and in solution. This is seen as a broadening and downfield shift of the O-H signal in the NMR, from that of salicylaldehyde¹⁵, as well as in the considerable broadening of the ν(OH) in the IR spectrum.

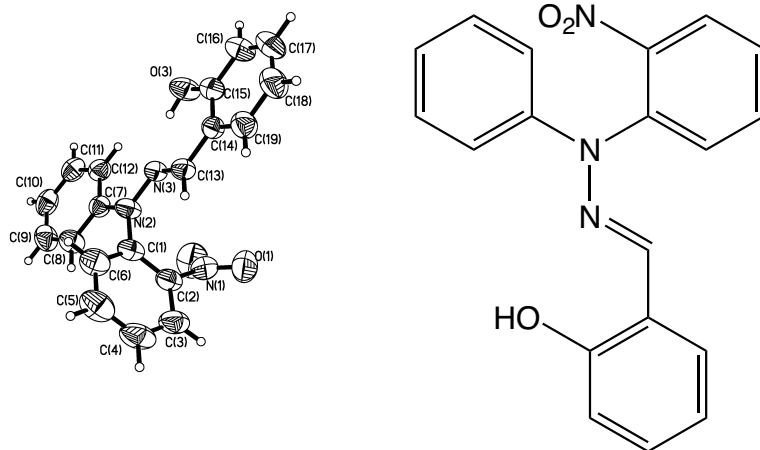


Figure 4-4. ORTEP Representation of 4. Selected structural parameters are: N(2)-N(3) 1.386(3) Å, N(2)-C(1)-C(2)-N(1) 5.2(5)°, N(2)-N(3)-C(13)-C(14) -179.9(2)°.

The bond lengths for **4** are commensurate with or even shorter than those predicted theoretically¹⁴ by semi-empirical MINDO methods for the –dimethyl analog. Allowing for decreased steric hindrance and increased planarity, this particular derivative is perfectly engineered to efficiently delocalize electron density throughout the entire molecule and form a stable sp^2 - sp^2 N-N bond. In addition, the salicylaldehyde adducts are stabilized by intramolecular hydrogen bonding (Figure 4-5), with an O(3) – N(3) distance of 2.650(1).

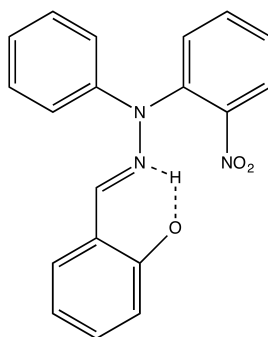


Figure 4-5: Intramolecular hydrogen bonding in 4.

To definitively examine the role of hydrogen bonding in the decreased N-N bond length in **4** and in 1,1-diaryl hydrazines, the adduct of NDPH and benzaldehyde (**5**) was synthesized from NDPH and structurally characterized (Figure 4-6). The reverse reaction, the hydrolysis of **5** to give NDPH, is known in the literature prior to our work⁸ but it has not been structurally characterized.

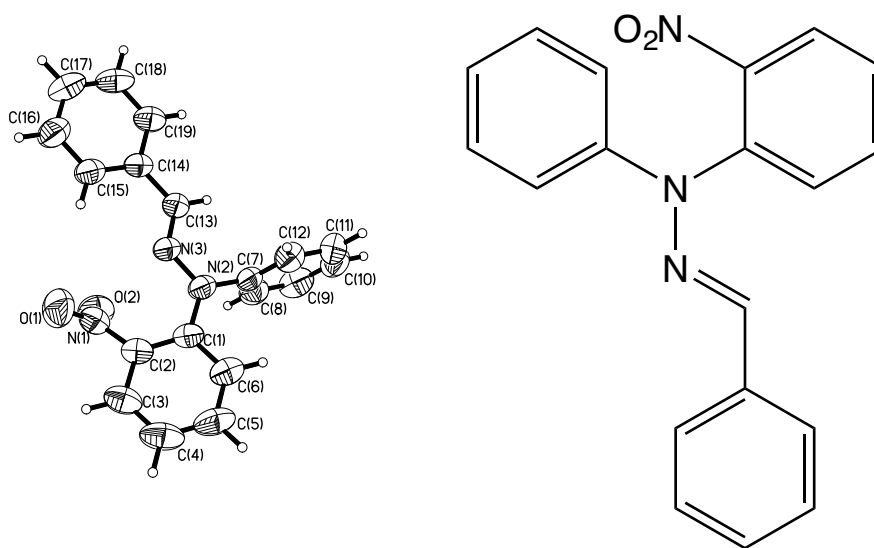


Figure 4-6. ORTEP Representation of 5. Selected structural parameters are: N(2)-N(3) 1.369(2) Å, N(2)-C(1)-C(2)-N(1) 5.2(5)°, N(2)-N(3)-C(13)-C(14) -179.9(2)°

Although **5** cannot form a stabilizing hydrogen bond, its hydrazine/Schiff's base geometry is isostructural with **4**. Given a distance of 0.016 Å separating N(2) from the plane formed by its substituents, this derivative is the most planar at nitrogen N(2), suggesting pronounced sp²-hybridization at its diaryl nitrogen. In addition, the N-N bond and the C₆H₄NO₂ ring are co-planar, with the latter feature being unique amongst the five structures **1 -5**.

In order to interpret any of the structural data for the Ar₂N moiety we sought to establish the presence and/or absence of significant intermolecular π -stacking interactions. In Figure 4-7 the variation of N-N bond lengths is plotted against the N(2) - C(1) and N(2) - C(7) bond lengths, as well as the sum of their lengths. In addition, the closest intermolecular approaches in the solid state are listed in Table 4-3. Critically in none of these structures do the aromatic rings orient and pack in ways that would lead to significant π - π stacking interactions. Packing in these structures is dominated by herringbone side-on interactions.

Table 4-3: Closest Intermolecular Interactions in NDPH Derivatives

Compound	Ph	Ph(NO ₁)	R _{N(3)}
1	3.666 Å (C(20) - C(6))	3.213 Å (C(4) - O(5))	3.527 Å (C(14B) - O(3))
2	3.701(3) Å (C(10) - C(16))	3.761(3) Å (C(3) - C(12))	3.199(3) Å (C(4) - O(4))
3	3.767(3) Å (C(9) - C(5))	3.878(2) Å (O(2) - C(14))	3.878(2) Å (O(2) - C(14))
4	3.8311(2) Å (C(3) - C(10))	3.539(2) Å (C(4) - O(1))	3.562(1) Å (C(13) - O(3))
5	3.068 Å (O(1) - C(14B))	3.068 Å (O(1) - C(14B))	3.570(3) Å (C(18) - C(7B))

To assess any significant donor-acceptor interactions of each compound with solvents and neighbouring molecules in solution, the UV-visible spectra of the compounds in chloroform were acquired and the lowest energy transitions were tabulated (Table 4-4).

Table 4-4: Lowest Energy UV-Visible Absorption Bands for NDPH Derivatives.

Compound	λ_{max} (nm)	Molar Absorptivity (ϵ) (M ⁻¹ cm ⁻¹)
1	418	1541
2	377	2952
3	410	3681
4	338	20471
5	324	1341

Two aspects of molar absorptivity and absorption maxima for **1** – **5**, warrant discussion. First is the apparent spread of the peak absorption values. There is a red shift of the $n \rightarrow \pi^*$ transition in the order $5 < 4 < 2 < 3 < 1$ with the position of **4** relying on the presence of its phenolic proton. This trend is in line with structural aspects of these derivatives. With the exception of **4** the extinction coefficients are all similar and consistent with $n \rightarrow \pi^*$ transitions. In compound **4** this band is overlapped by an intense $\pi \rightarrow \pi^*$ transition, which possibly owes its lower energy to the stabilizing effects of the internal hydrogen bonding and extensive conjugation in that derivative.

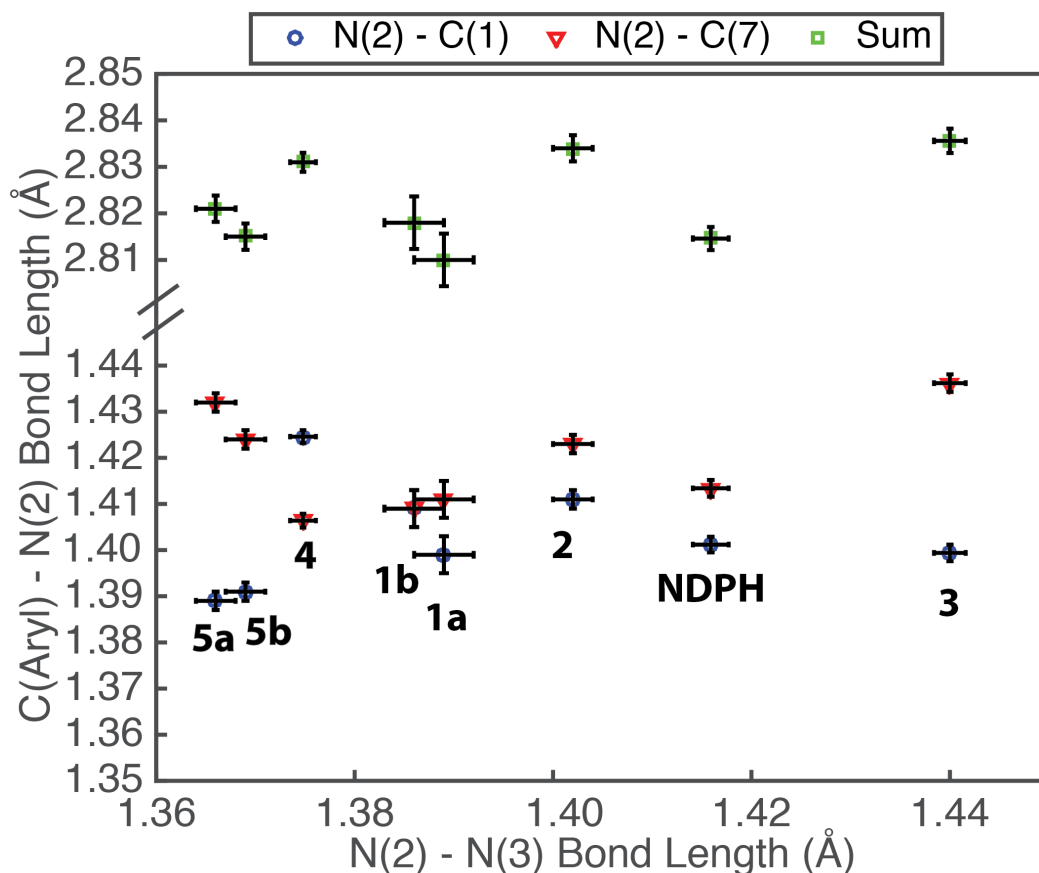


Figure 4-7. Variation in C-N bond length with N-N separation. Suffixes (a, b) denote independent molecules in the unit cells of **1** and **5**.

A general trend operating in these systems is between the longer C(7)-N(2) bond lengths and the C(1)-N(2) bond lengths. Moreover, this difference is accentuated for the longest and shortest N(2) – N(3) bond lengths. These bond lengths reflect aryl competition for N(2) π -bonding, but their sum remains fairly constant, 2.83(0.01) Å.

One of the most interesting aspects of the bonding in **1** – **5** is the possibility of N-N bond contraction from either π - bond formation or from valence re-hybridization as sp^2 - sp^2 single bonds. Both would be expected to lead to N-N bond shortening and planar nitrogen. Based on this evidence, we propose that strong N-N bonds can result from two different types of N-N interactions (Table 4-5). Types **2a** and **2b** will differ, however, in that π - bond formation requires co-planarity of the Ar₂N and NR₂ fragments to ensure π - π overlap at the nitrogen atoms. Table 4-5 describes aspects of this formal view, with **1-5** falling under categories **2a** and **b** and ranking **5** < **4** < **1** < **2** < **NDPH** << **3** in terms of N-N bond length. Significantly the imine **3** not only has the longest N-N bond, but it is also the only species with pyramidalized nitrogen (Table 4-1) albeit only modestly to give the sum of bond angles at N(2) of 345.18(19). In each of **1-3** the orthogonality of the nitrogen atoms, which are formal sp^2 centers, rules out strong N-N π -bond character.

Table 4-5: Formal Description of Bonding in Ar₂NNR₂

Type	N Hybridization States	Geometry	Relative Bond Strength	Contributing Bonding Interactions
1	sp ³ -sp ³		Weak	σ only
2a	sp ² -sp ² (available lone pairs)	orthogonal	Strong	σ only
2b	sp ² -sp ² (delocalized lone pairs)	Co-planar	Strong	σ and π
3	sp ² -sp ² (no available lone pairs)		Strong	σ only

Although **5** and **4** share co-planar Ar₂N-N=CH(Ar) frameworks, the conformation in **4** allows for an internal H-bond while the simple Schiff Base **5** cannot form this bond. Is there thus strong π-character to the N-N bond? To shed light on this, we have used density functional theory to examine the highest two occupied MOs in **5**, which are shown in Figure 4-8. The HOMO in particular has strong C=N π-character and in both cases the simple phenyl rings are occupied in these orbitals. Examination of the lower energy filled orbitals does not suggest contribution to a strong N-N bond from a delocalized π-bond. Thus the sp²-sp² hybridization results in strong σ-bonding of type 2a.

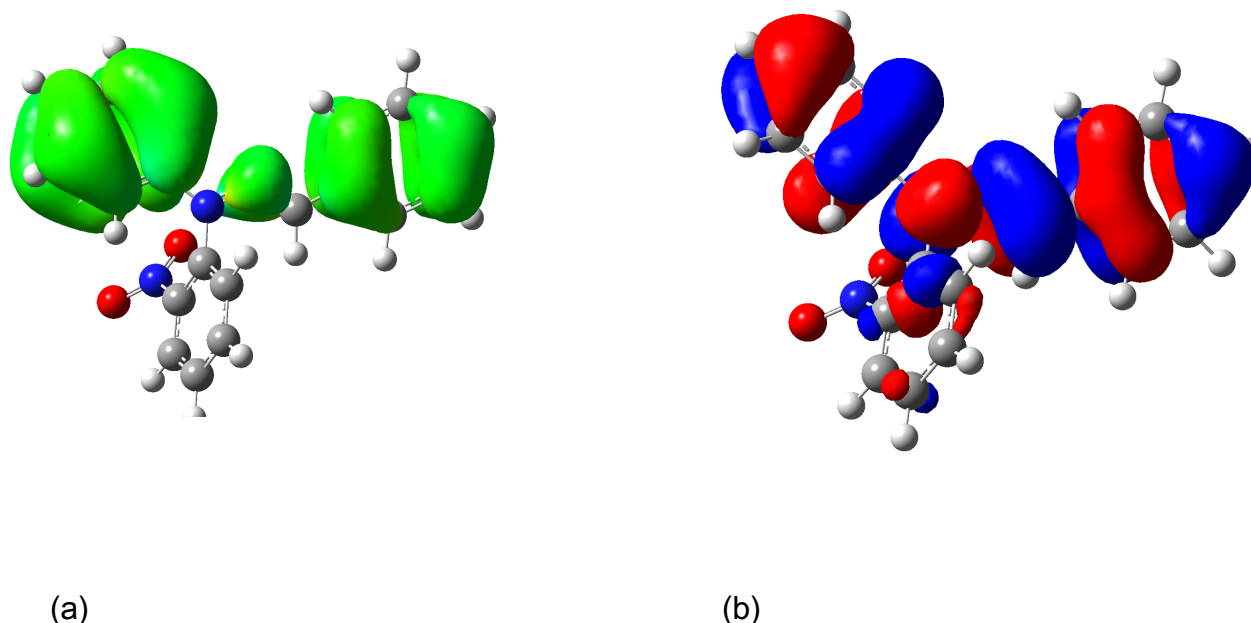


Figure 4-8. (a) Calculated orbital compositions in the HOMO-1 orbital of 5. (b) Calculated orbital composition in the HOMO of 5.

4.4 Conclusions

From 1-(2-nitrophenyl-1-phenyl hydrazine), synthesized under oxidative conditions, several derivatives can be made in good yield and of high purity. These derivatives illustrate the electronic interplay between the diaryl system and any substituents on the terminal NH_2 group of the parent hydrazine, which are nearly unaffected by intermolecular interactions as demonstrated by UV-visible data. The effects of these two environments can work synergistically by reducing the N-N repulsion between the nitrogen lone pairs, providing an even more stable N-N bond; or antagonistically, should the electronic environments of the N-N nitrogen atoms become congruent and lone pair repulsion be increased.

The balance of the electronic environments in these hydrazines can be quantified in the solid-state by measuring the N-N bond length. This bond length can vary from a long N-

N bond typical of hydrazine itself, which is rather reactive, to a length reminiscent of an N=N double bond. Surprisingly, the structural orientations reported here, supported by DFT calculations, suggest that the π -contribution to the short bond distances is minimal. This suggests overwhelming σ -bonding, which is strengthened in systems where the nitrogen atoms are made electronically dissimilar, whereas similar electronic environments for both nitrogen atoms, even equivalent π -delocalization of the N-lone pairs, results in repulsion, decreased σ -overlap and a longer N-N bond. This knowledge is useful for the production of stable hydrazine derivatives as potential reagents in organic synthesis and spectroscopic studies.

4.5 Experimental

4.5.1 General methods

Dichloromethane was continuously dried over a column of SiO₂. All other reagents and solvents were obtained from commercial sources and were used as received. ¹H- and ¹³C-NMR spectra were recorded on 300 and 500 MHz Varian spectrometers. High-resolution mass spectra (HRMS) was measured by electrospray techniques with a time-of-flight detector (ESI/TOF). UV/Vis spectra of all the compounds were acquired on a Carey 100 Bio spectrophotometer. Melting and decomposition points were determined by differential scanning calorimetry by sealing samples in aluminum pans under a nitrogen atmosphere with heating rates of 2 °C/min to within 10 °C of the melting temperature determined by a micromelting apparatus and then slowing the rate to 0.5 °C/min.

4.5.2 Syntheses

N-(2-nitrophenyl)-*N*-phenylacetohydrazide (**1**)

1-(2-nitrophenyl)-1-phenylhydrazine (0.3000g, 1.31mmol) was dissolved in concentrated acetic acid (15 mL) under N₂(g) and the solution was refluxed overnight. After cooling to room temperature, the solution was neutralized with aqueous sodium bicarbonate (5% w/w) and then extracted (3 x 20 mL) with ether. The organic washings were dried (MgSO₄) and left to crystallize at 0°C, giving the dark red crystalline product (0.2506 g, 70% yield); m.p. (DSC) onset 141.56 °C (lit. 140.9 °C), peak max 143.30 °C (lit.⁸ 141.7°C); ¹H-NMR (300 MHz, DMSO-d₆) δ (ppm) mixture of *E*- and *Z*-isomers, *Z*-isomer: 1.89 (3H, s), 6.76 (d, 2H, J = 7.80Hz), 6.90 (1H, t, J = 7.50 Hz), 7.21 (t, 2H, J = 7.80 Hz), 7.35 (1H, t, J = 8.10Hz), 7.53 (d, 1H, J = 8.10Hz), 7.67 (t, 1H, J = 8.40Hz), 7.85 (d, 1H, J = 8.10Hz), 10.49 (s, 1H); *E*-isomer: 1.94 (3H, s), 6.81 (d, 2H, J = 7.80Hz), 7.02 (1H, t, J = 7.50 Hz), 7.27 (t, 2H, J = 7.80 Hz), 7.40 (1H, t, J = 8.10Hz), 7.57 (d, 1H, J = 8.10Hz), 7.78 (t, 1H, J = 8.40Hz), 7.92 (d, 1H, J = 8.10Hz), 10.09 (s, 1H); ¹³C-NMR (300 MHz, DMSO-d₆) δ (ppm), only *Z*-isomer detectable: 20.7, 116.0, 121.9, 125.6, 125.9, 126.9, 129.4, 134.5, 138.6, 146.1, 157.8, 169.5; UV-Vis (CHCl₃): λ_{max} = 418 nm, ε = 1541 M⁻¹cm⁻¹; HRMS calcd for C₁₄H₁₂N₃O₃: 270.0884, Found: 270.0873; Anal. Calcd for C₁₄H₁₃N₃O₃: C, 61.99%; H, 4.83%; N, 15.49%; Found: C, 61.91%; H, 4.78%; N, 15.59%.

N-acetyl-*N*-(2-nitrophenyl)-*N*-phenylacetohydrazide (**2**)

1-(2-nitrophenyl)-1-phenylhydrazine (150 mg, 0.65 mmol) was dissolved in chloroform (50 mL) along 5 mL of acetic anhydride. The reactants were heated at 60°C for 2 days, at which point TLC (dichloromethane) indicated consumption of the starting material. The solution was reduced *in vacuo* and the residue was dissolved in ethanol (15 mL). After cooling for 24 h at -10°C, the solution was exposed to air upon which crystals of **2** began to form. Yield 0.173 g (0.55 mmol, 84% yield). A sample was

recrystallized from dichloromethane to yield red prisms. m.p. (DSC) onset 172.05 °C, peak max 173.75 °C; ¹H-NMR (300 MHz, CDCl₃) δ (ppm): 2.52 (6H, s), 6.97 (d, 2H, J = 8.40Hz), 7.09 (1H, t, J = 7.50 Hz), 7.12 (d, 1H, J = 4.50 Hz), 7.19 (1H, t, H = 7.50Hz), 7.27 (m, 2H), 7.54 (t, 1H, J = 7.50Hz), 7.77 (d, 1H, J = 8.10Hz); ¹³C-NMR (300 MHz, CDCl₃) δ (ppm): 25.6, 118.6, 121.0, 123.7, 125.1, 125.9, 129.5, 129.6, 134.0, 136.9, 144.0, 172.8; IR (KBr, cm⁻¹): 477 (vw), 525 (w), 587 (w), 596 (vw), 631 (m), 665 (vw), 701 (m), 744 (m), 758 (m), 776 (m), 828 (w) 857 (w), 903 (vw), 919 (vw), 938 (vw), 950 (vw), 991 (m), 1028 (vw), 1042 (vw), 1137 (sh), 1165 (w), 1203 (vs), 1234(s), 1261 (w), 1287 (w), 1301 (w), 1321 (vw), 1365 (s), 1415 (w), 1456 (w), 1482 (s), 1491 (s), 1530 (vs), 1597 (m), 1718 (vs), 1734 (vs), 3044 (vw); UV-Vis (CHCl₃): λ_{max} = 445 nm, ε = 1095 M⁻¹cm⁻¹, λ_{max} = 377 nm, ε = 2952 M⁻¹cm⁻¹ λ_{max} = 259 nm, ε = 17130 M⁻¹cm⁻¹; HRMS calcd for C₁₆H₁₅N₃O₄Na: 336.0955, Found: 336.0944; Anal. Calcd for C₁₆H₁₅N₃O₄: C, 61.34; H, 4.83; N, 13.41; Found: C, 61.69; H, 4.80; N, 13.48.

1-(2-nitrophenyl)-1-phenyl-2-(propan-2-ylidene)hydrazine (**3**)

1-(2-nitrophenyl)-1-phenylhydrazine (0.0853 g, 0.373 mmol) was dissolved in dry dichloromethane (50 mL). HPLC-grade acetone (10 mL) was added, along with a catalytic amount of concentrated sulfuric acid. A static vacuum was applied to the system and the reaction was stirred 15 h at room temperature. Evaporation of the solvents and acid under high vacuum yielded the crude product, which was recrystallized by slow evaporation from dichloromethane to give 0.055 g of an orange crystalline product (0.20 mmol, 54%); m.p. 81.2–82.0 °C; ¹H-NMR (300 MHz, CDCl₃) δ (ppm): 1.80 (s, 3H), 2.10 (s, 3H), 7.09 (m, 5H) 7.31 (tt, 3H), 7.74 (dd, 1H); ¹³C-NMR (300 MHz, CDCl₃) δ (ppm): 21.1, 24.6, 122.3, 122.6, 122.8, 124.3, 125.5, 129.5, 132.5, 142.5, 143.8, 146.1, 173.1; IR (KBr, cm⁻¹): 419 (vw), 428 (vw), 437 (vw), 466 (vw), 497 (vw), 520 (w), 533 (w), 614 (vw), 640 (vw), 678 (vw), 705 (s), 713 (w), 741 (s), 751 (w), 770 (m), 776 (m), 841 (m), 850 (m), 906 (vw), 923 (vw), 942 (vw), 993 (vw), 1004 (vw),

1026 (vw), 1050 (vw), 1072 (w), 1093 (sh), 1156 (w), 1173 (w), 1205 (w), 1255 (m), 1272 (m), 1292 (m), 1309 (sh), 1324 (vw), 1363 (s), 1426 (vw), 1447 (w), 1486 (s), 1524 (vs), 1573 (w), 1591 (m), 1602 (m), 1630 (vw), 1644 (vw), 1955 (vw), 1972 (vw), 2915 (vw), 2951 (vw), 2991 (vw), 3034 (vw), 3064 (vw); UV-Vis (CHCl₃): λ_{max} = 410 nm, ϵ = 3681 M⁻¹ cm⁻¹; HRMS calcd for C₁₅H₁₅N₃O₂Na: 292.1056, Found: 292.1052; Anal. Calcd for C₁₅H₁₅N₃O₂: C, 66.90%; H, 5.61%; N, 15.60%; Found: C, 66.62%; H, 5.48%; N, 15.63%.

(E)-2-((2-(2-nitrophenyl)-2-phenylhydrazono)methyl)phenol (**4**)

To a 250 mL round-bottomed flask under N₂ (g) was added a solution of 1-(2-nitrophenyl)-1-phenylhydrazine (0.1700 g, 0.44 mmol) in dry dichloromethane (20 mL) along with 2 drops each of salicylaldehyde and hydrochloric acid. The red reaction mixture was stirred 12 h at room temperature, during which, the solution adopted a lighter orange colour. The product was obtained as a crude solid by simple evaporation of the solvent under reduced pressure and recrystallized from dichloromethane:ethanol (1:2) to give red crystals in 0.2004 g (0.60 mmol, 81%) yield. m.p. (DSC) onset 125.53 °C, peak max 127.06 °C; ¹H-NMR (300 MHz, CDCl₃) δ (ppm): 6.83 (t, 1H, J = 8 Hz), 6.96(t, 2H, J = 8 Hz), 7.03 (d, 2H, J = 8 Hz), 7.11 (t, 1H, J = 7 Hz), 7.22 (t, 1H, J = 8 Hz), 7.35 (t, 2H, J = 8 Hz), 7.39 (s, 1H), 7.40 (d, 1H, 8 Hz) 7.56 (t, 1H, J = 8 Hz), 7.76 (t, 1H, J = 10 Hz), 8.04 (d, 1H, J = 8 Hz), 10.90 (s, 1H); ¹³C-NMR (300 MHz, CDCl₃) δ (ppm): 116.8, 118.4, 118.8, 119.4, 123.9, 126.1, 128.6, 129.7, 130.2, 130.4, 130.5, 134.5, 134.7, 142.3, 143.7, 147.2, 157.1; IR (KBr, cm⁻¹): 472 (w), 553 (w), 588 (w), 624 (vw), 657 (w), 667 (w), 688 (s), 712 (w), 746 (vs), 759 (s), 776 (w), 795 (w), 810 (vw), 848 (m), 1033 (w), 1071 (w), 1098 (vw), 1153 (w), 1220 (s), 1271 (s), 1296 (m), 1363 (s), 1387 (vw), 1413 (vw), 1496 (vs), 1527 (vs), 1594 (vs), 1620 (w), 2875 (vw), 3042 (vw); UV-Vis (CHCl₃): λ_{max} = 338 nm, ϵ = 20471 M⁻¹ cm⁻¹; λ_{max} = 241 nm, ϵ = 17000 M⁻¹ cm⁻¹ HRMS calcd for C₁₉H₁₅N₃O₃Na: 356.1002, Found: 356.1006; Anal. Calcd for

C₁₉H₁₅N₃O₃: C, 68.46%; H, 4.54%; N, 12.61%; Found: C, 68.26%; H, 4.31%; N, 12.43%.

(*E*)-2-benzylidene-1-(2-nitrophenyl)-1-phenylhydrazine (**5**)

1-(2-nitrophenyl)-1-phenylhydrazine (145 mg, 0.63 mmol) was dissolved in dichloromethane (50 mL) along with benzaldehyde (120 μ L, 1.17 mmol) was added along with anhydrous magnesium sulfate (0.23 g, 1.91 mmol). The yellow solution was stirred 12 h at room temperature. The solvent was removed under reduced pressure and the residue loaded onto a silica gel column with dichloromethane as eluent. The first yellow band was collected and the solvent evaporated to yield the pure product directly as a yellow solid in 0.115 g (0.36 mmol, 57% yield). A sample was recrystallized from dichloromethane to yield yellow prisms. m.p. (DSC) onset 109.22 °C (lit. 102.6 °C), peak max 109.64 °C (lit.⁸ 104.8°C); ¹H-NMR (500 MHz, CDCl₃) δ (ppm): 7.11 (1H, d, J = 8.50 Hz), 7.17 (t, 4H, J = 6.0 Hz), 7.25 (d, 1H, J = 7.50 Hz), 7.29-7.34 (m, 3H), 7.38 (t, 2H, J = 8Hz), 7.51 (d, 2H, J = 7.50 Hz), 7.55 (d, 1H, J = 7.50 Hz), 7.86 (d, 1H, J = 9 Hz); ¹³C-NMR (500-MHz, CDCl₃) δ (ppm): 122.0, 125.0, 125.6, 125.9, 126.6, 127.3, 128.6, 128.7, 129.7, 133.4, 135.1, 136.9, 137.8, 142.8, 145.6; UV-Vis (CHCl₃): λ_{max} = 324 nm, ϵ = 1341 M⁻¹ cm⁻¹; HRMS calcd for C₁₉H₁₅N₃O₂Na: 340.1056, Found: 340.1068; Anal. Calcd for C₁₉H₁₅N₃O₂: C, 71.91; H, 4.76; N, 13.24; Found: C, 71.63; H, 4.66; N, 13.29.

4.5.3 X-ray crystallography

The X-ray diffraction data were measured with graphite monochromated Mo Ka radiation (λ =0.71073 Å) on crystals that were attached to a glass fiber with viscous paratone N oil. The structures were solved by direct methods on an absorption-corrected model generated by SADABS. Refinement was achieved by a full- matrix

least-squares procedure based on F_2 . The hydrogen atoms were located at calculated positions.

4.5.4 Theoretical Methods

All of the calculations were performed using Gaussian 03.¹⁶ Computations were carried out at the restricted Hartree-Fock (RHF),¹⁷ and Density Functional Theory (DFT) levels. DFT calculations used the hybrid B3LYP functional and triple zeta 6-311++G** basis sets.^{18,19} The calculated molecular geometries were fully optimized and correspond to minima on the potential energy surface as confirmed by the absence of imaginary vibrational frequencies.

4.6 Acknowledgements

This research was supported by NSERC discovery grants to DSB and ISB. The authors are grateful to Dr. Alexander Wahba and Nadim Saade for mass spectrometry analysis.

4.7 References

1. CCSD, Cambridge Crystallographic Database. CCSD: Cambridge, 2015; Vol. 1.17.
2. Fina, N. J.; Edwards, J. O., Alpha effect. Review. *Int. J. Chem. Kinet.* **1973**, *5* (1), 1-26.
3. Kedare, S. B.; Singh, R. P., Genesis and development of DPPH method of antioxidant assay. *J. Food. Sci. Technol.* **2011**, *48* (4), 412-22.

4. Koller, J.; Ajmera, H. M.; Abboud, K. A.; Anderson, T. J.; McElwee-White, L., Synthesis and Characterization of Diorganohydrazido(2-) Tungsten Complexes. *Inorg. Chem.* **2008**, *47* (11), 4457-4462.
5. (a) Davies, M. J.; Gilbert, B. C.; McLauchlan, K. A., Electron Paramagnetic Resonance. In *Electron Paramagnetic Resonance*, The Royal Society of Chemistry: Cambridge, UK, 2000; Vol. 17, pp 178-79; (b) Romanov, N.; Anastasi, C.; Liu, X. Cyanine dyes for labeling molecular ligands with improved fluorescence intensity and photostability. WO2013041117A1, 2013; (c) Shen, P.; Liu, X.; Jiang, S.; Wang, L.; Yi, L.; Ye, D.; Zhao, B.; Tan, S., Synthesis of new N,N-diphenylhydrazone dyes for solar cells: Effects of thiophene-derived π -conjugated bridge. *Dyes Pigm.* **2012**, *92* (3), 1042-1051.
6. (a) Demeter, D.; Mohamed, S.; Diac, A.; Grosu, I.; Roncali, J., Small Molecular Donors for Organic Solar Cells Obtained by Simple and Clean Synthesis. *ChemSusChem* **2014**, *7* (4), 1046-1050; (b) Yanase, M.; Hara, Y. Formation of dense conductive films without use of dangerous gases in firing, their compositions, and preparation thereof. JP2010176976A, 2010; (c) Tonks, I. A.; Durrell, A. C.; Gray, H. B.; Bercaw, J. E., Groups 5 and 6 Terminal Hydrazido(2-) Complexes: N β Substituent Effects on Ligand-to-Metal Charge-Transfer Energies and Oxidation States. *J. Am. Chem. Soc.* **2012**, *134* (17), 7301-7304.
7. Bain, C. D.; Bayne, J. M.; Bohle, D. S.; Butler, I. S.; Poisson, J., Synthesis of reduction-sensitive 1,1-diarylhydrazines from 1,1-diarylamines. *Can. J. Chem.* **2014**, *92* (9), 904-912.
8. Berezin, A. A.; Zissimou, G.; Constantinides, C. P.; Beldjoudi, Y.; Rawson, J. M.; Koutentis, P. A., Route to Benzo- and Pyrido-Fused 1,2,4-Triazinyl Radicals via N'-(Het)aryl-N'-[2-nitro(het)aryl]hydrazides. *J. Org. Chem.* **2014**, *79* (1), 314-327.

9. Dugave, C., General mechanisms of cis-trans isomerization: a rapid survey. In *cis-trans Isomerization in Biochemistry*, Wiley-VCH Verlag GmbH & Co. KGaA: 2006; pp 7-13.
10. Andrews, P. R., Cis-trans isomerism of the peptide bond. *Biopolymers* **1971**, *10* (11), 2253-67.
11. (a) Micheau, J.-C.; Zhao, J., Cis/trans configurations of the peptide C-N bonds: isomerization and photoswitching. *J. Phys. Org. Chem.* **2007**, *20* (11), 810-820; (b) Schiene-Fischer, C.; Luecke, C., Secondary amide peptide bond cis/trans isomerization in polypeptide backbone restructuring: Implications for catalysis. In *Protein Folding Handbook*, Wiley-VCH Verlag GmbH & Co. KGaA: 2005; Vol. 3, pp 415-428; (c) Dugave, C.; Demange, L., Cis-Trans Isomerization of Organic Molecules and Biomolecules: Implications and Applications. *Chem. Rev. (Washington, DC, US)* **2003**, *103* (7), 2475-2532.
12. (a) Derieg, M. E.; Blount, J. F.; Fryer, R. I.; Hillery, S. S., 3-Aminoquinazolines: Structural assignments. *Tetrahedron. Lett.* **1970**, *11* (44), 3869-3872; (b) He, C.-L.; Du, Z.-M.; Tang, Z.-Q.; Cong, X.-M.; Meng, L.-Q., N-(1-Diacetylamino-1H-tetrazol-5-yl)acetamide. *Acta Crystallogr. Sect. E* **2009**, *65* (8), o1902; (c) Akimoto, T.; Takeda, Y.; Nawata, Y.; Iitaka, Y., Structure of 2,3,4-tri-O-acetyl-N-(diacetylamino)-[beta]-D-glucopyranurono-1,6-lactam. *Acta Crystallogr. Sect. C* **1988**, *44* (4), 760-762; (d) Hu, X.; Wang, Z.; Xu, W.; Zhao, G.; Wang, R., N,N'-Diacetyl-N'-[(4-nitrophenoxy)acetyl]acetohydrazide. *Acta Crystallogr. Sect. E* **2009**, *65* (2), o372; (e) Wolska, I.; Hejchman, E., 2-(N,N-Diacetamido)-3a,4,9,9a-tetrahydro-4,9-[1',2']benzeno-1H-benzo[f]isoindole-1,3(2H)-dione. *Acta Cryst. E* **2003**, *59* (12), o2007-o2009; (f) Sun, D.; Krawiec, M.; Campana, C. F.; Watson, W. H., 2-amino-1,2,3-triazole derivatives from vicinal diazides. *J. Chem. Crystallogr.* **1997**, *27* (10), 577-588; (g) Nakahara, R.; Doi, M.; Kitani, Y.; Yamaguchi, T.; Fujita, Y., Crystal Structure of Tetraacetyl Fluorescein Hydrazide. *X-ray Structure Analysis Online* **2009**, *25*, 21-22; (h) Struga,

M.; Kossakowski, J.; Mirosław, B.; Koziol, A. E., Synthesis of N-acetyl-N-(3,5-dioxo-10-oxa-4-aza-tricyclo[5.2.1.0^{2,6}]dec-4-yl)-acetamide. *Molbank* **2007**, M533.

13. Graziani, F.; Bovini, F., Study of Phototropy. *Atti Accad. Naz. Lincei, Cl. Sci. Fis., Mat. Nat., Rend.* **1913**, 22 (I), 793-7.

14. Bren, V. A.; Stul'neva, T. M.; Simkin, B. Y.; Minkin, V. I., Benzoid-quinoid tautomerism of azomethines and their structural analogs. XXIV. Structure of N,N-disubstituted hydrazones of o-hydroxy aromatic aldehydes. *Zh. Org. Khim.* **1976**, 12 (3), 633-40.

15. Abraham, R. J.; Mobli, M.; Smith, R. J., ¹H chemical shifts in NMR: part 19. Carbonyl anisotropies and steric effects in aromatic aldehydes and ketones. *Magn. Reson. Chem.* **2003**, 41 (1), 26-36.

16. Frisch, M. J.; Trucks, G. W.; Schlegel, H. B.; Scuseria, G. E.; Robb, M. A.; Cheeseman, J. R.; Zakrzewski, V. G.; Montgomery, J. A.; Stratmann, R. E.; Burant, J. C.; Dapprich, S.; Millam, J. M.; Daniels, A. D.; Kudin, K. N.; Strain, M. C.; Farkas, O.; Tomasi, J.; Barone, V.; Cossi, M.; Cammi, R.; Mennucci, B.; Pomelli, C.; Adamo, C.; Clifford, S.; Ochterski, J.; Petersson, J. A.; Ayala, P. Y.; Cui, Q.; Morokuma, K.; Malick, D. K.; Rabuck, A. D.; Raghavachari, K.; Foresman, J. B.; Cioslowski, J.; Ortiz, J. V.; Stefanov, B. B.; Liu, G.; Liashenko, A.; Piskorz, P.; Kamaromi, I.; Gomperts, R.; Martin, R. L.; Fox, D. J.; Keith, T.; Al-Laham, M. A.; Peng, C. Y.; Nanayakkara, A.; Gonzalez, C.; Challacombe, M.; Gill, P. M. W.; Johnson, B. G.; Chen, W.; Wong, M. W.; Andres, J. L.; Head-Gordon, M.; Replogle, E. S.; Pople, J. A. *Gaussian 98*, Gaussian Inc.: Pittsburgh, PA, 1998.

17. Roothaan, C. C., New Developments in Molecular Orbital Theory. *J. Rev. Mod. Phys.* **1951**, 23, 69-89.

18. Lee, C.; Yang, W.; Parr, R. G., Local softness and chemical reactivity in the molecules carbon monoxide, thiocyanate, and formaldehyde. *J. Mol. Struct.: THEOCHEM* **1988**, 40, 305-13.

19. Becke, A. D., A new mixing of Hartree-Fock and local-density-functional theories.
J. Chem. Phys. **1993**, *98* (2), 1372-7.

5

π -Delocalization in the Vicinal Lone Pairs of Hydrazines:

Electronic Effects in Derivatives of 9-Aminocarbazole

5.1 Preamble

Following the conclusion from structural data on derivatives of 1-(2-nitrophenyl)-1-phenylhydrazine (NDPH) that the N-N bonds in these systems are governed by σ -interactions, several of the functional groups used in Chapter 4 were treated with 9-aminocarbazole (AC). The fusion of the phenyl rings in the carbazole system precludes their ability to change orientation in response to various electronic changes to the hydrazine N-N framework and will introduce the possibility of π -overlap in these systems. The contrast of the results of the structural and electronic analysis for the carbazoles with those obtained for NDPH derivatives will provide insight into the effect of phenyl ring orientation on the bonding in 1,1-diarylhydrazines. Gas-phase density functional theory is used to support the experimental data by providing a model for geometric changes that occur during the rearrangement to support the involvement of an electron-deficient nitrogen intermediate. The choice of basis set and level of DFT theory employed here is based on past experience with calculations for related nitrogen species with numerous lone pairs. In general this theoretical model has excellent predicts of ground state configurations and vibrational energy levels for related compounds. Although the specific metric parameters may very well be dependent on basis set, and the functionals employed, the contrasts made with experimental data are intended to reconfirm their utility for the predictions made for this class of compounds as well. With these features confirmed for the ground states we have established their utility for predicting intermediates, transition states, and reaction pathways.

5.2 Introduction

1,1-diarylhydrazines are useful reagents in organic synthesis and the methodologies for making them have recently been reviewed¹. These compounds have interesting properties due to the absence of the so-called alpha kinetic effect², which decreases their nucleophilicity in comparison to 1-alkyl, 1,1-dialkyl and even 1-arylhydrazines. Still, they are able to add slowly to electrophilic centres to form useful products. The usefulness of the adducts of 1,1-diarylhydrazines has prompted the study of potential catalytic agents that might increase their reactivity to form condensation products³. These condensation products have found uses ranging from N-heterocycle formation⁴ to anti-allergy agents⁵, analgesics⁶ and to treat illnesses such as cancer⁷ and Alzheimer's disease⁸.

AC is a particularly stable 1,1-diarylhydrazine. Its reactivity can be understood by looking at its parent compound, *9H*-carbazole and its lower heterocyclic analogues, pyrrole and indole (Figure 5-1).

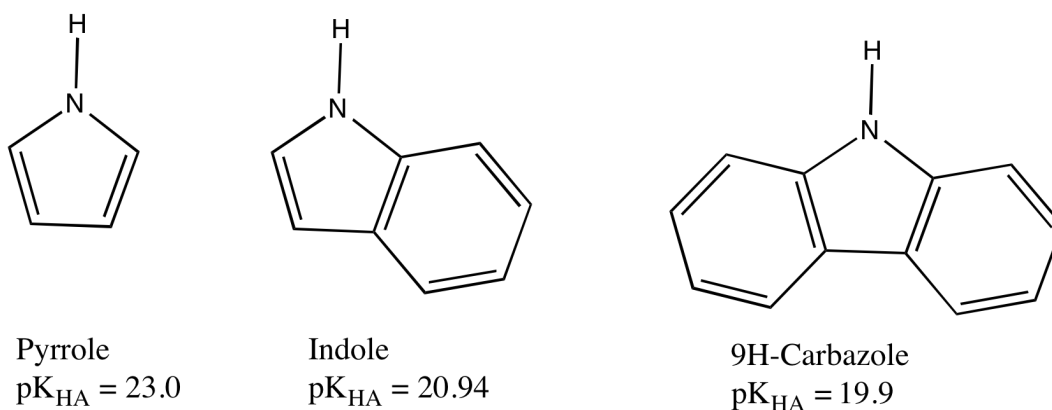


Figure 5-1: Structures and acidity constants of N-heterocycles.

Balón has determined the pK_a values of the above nitrogen acids to be -3.57(10), -2.43(30) and -4.87(15) in acidic solution⁹. In contrast, diphenylamine (Ph_2NH) was

found to be the weakest acid of all, with a pK_a of 0.765(2). This trend was rationalized in terms of the degree of aromaticity present in these compounds increasing with additional conjugation. The disruption of aromaticity upon deprotonation is in the order diphenylamine < pyrrole < indole < 9H-carbazole, with pyramidalization of the amine nitrogen following the opposite trend. The linkage between the *ortho*-positions of N,N-diphenylamine to form carbazole results in a significant decrease in its acidity and a gain in bond dissociation energy of ~5 kcal/mol due to a combination of aromaticity enhancement and the elimination of steric interactions that would hinder planarity. Such an increase in N-H bond strength would explain the reluctance of 9H-carbazole to act as a substrate in indole formation reactions¹⁰. Its stability also permits useful transformations such as decomposition processes including nitrenium ion formation¹¹ through condensation with appropriate keto-esters and its use in polymers for photovoltaic applications¹² when condensed with 8-hydroxyquinoline-5-carbaldehyde. In chapter 4, we reported a structural study on 1-(2-nitrophenyl)-1-phenylhydrazine (NDPH) derivatives. That study prompted us to propose three types of bonding possible in Ar_2NNH_2 systems (Table 5-1).

Table 5-1: Possible Bonding Interactions in 1,1-Diarylhydrazines

Type	N States	Hybridization	Geometry	Relative Bond Strength	Contributing Bonding Interactions
1		sp^3-sp^3		Weak	σ only
2a		sp^2-sp^2 (available lone pairs)	orthogonal	Strong	σ only
2b		sp^2-sp^2 (delocalized lone pairs)	Co-planar	Strong	σ and π
3		sp^2-sp^2 (no available lone pairs)		Strong	σ only

Although the NAr_2 electrons of NDPH are conjugated with the adjacent phenyl system, its adducts with carbonyl compounds exhibited strong, short type 3 N-N bonds with little π -character. To verify the contribution of phenyl ring dynamics to this stability, we have made several analogous derivatives of AC. Will the fusion of the Ar_2N rings result in increased aromaticity and a stronger N-N bond? How will electronic stress of various NR_2 substituents be manifested? To explore these questions, the structural data for AC and its derivatives will be compared with that previously found for their NDPH analogues. Herein we examine: 1) The effect on bond order throughout the diaryl and -amino domains; 2) the disposition of substituents about the N-atoms and

consequently the type of N-N bond; 3) the electronic spectroscopy of these derivatives in relation to NDPH analogues and 4) the effect on the bond joining the carbazole aryl rings and their relative orientations on overall molecular stability.

5.3 Results and Discussion

Despite its many uses, the structure of AC has never been reported. Possible reasons for this include difficulty to separate the pure compound from carbazole in reaction mixtures. It also tends to crystallize as long feathers that are difficult to analyze by diffraction. Despite these setbacks, we have managed to obtain the first reported structural data for AC. It crystallizes in the space group *Pca21* with 4 molecules per unit cell. Due to the weakly diffracting nature of the crystals, only isotropic refinement was achieved. While the N-N bond lengths of NDPH and AC of 1.4159(18) and 1.416(7) Å, respectively, are similar, there are drastically different angular environments for the NAr₂ nitrogen atoms. In NDPH, the dihedral angles about the N-C(Aryl) bonds are of -41.63 and -163.49°, respectively. As a result, planarity is disrupted and π -electron delocalization is rendered less probable. In AC, however, the same dihedral angles are -1(2) and 1(1)°, respectively. Despite the large error in these parameters, they still represent a significant difference in orientations between the two species. Linkage of the C(6) and C(12) carbons in 1,1-diarylhydrazines enforces planarity on the system. As a result, π -contributions to bonding become important and allow a study of the difference in stability granted between bonding of types 2a and 2b. Also of note is the orientation of the -NH₂ group, which was stable to refinement and supported by gas-phase DFT calculations (B3LYP/6-311++g**, Appendix D Figure S1). This orientation is not compatible with π -based delocalization since the lone pair of N(2) is orthogonal to the carbazole plane. Therefore, as in the case of NDPH, the shortness of the N-N bond in AC must depend primarily on σ interactions. Exchange is also fast in

dimethylsulfoxide-*d* on the NMR timescale as evidenced by the sharpness of the signal in the proton NMR spectrum.

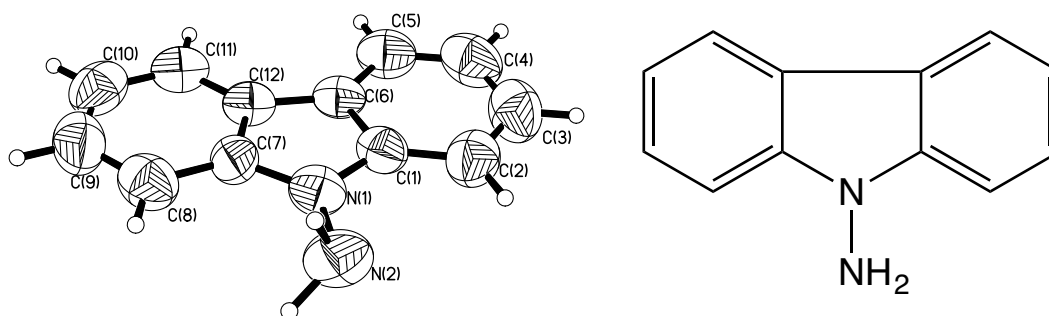
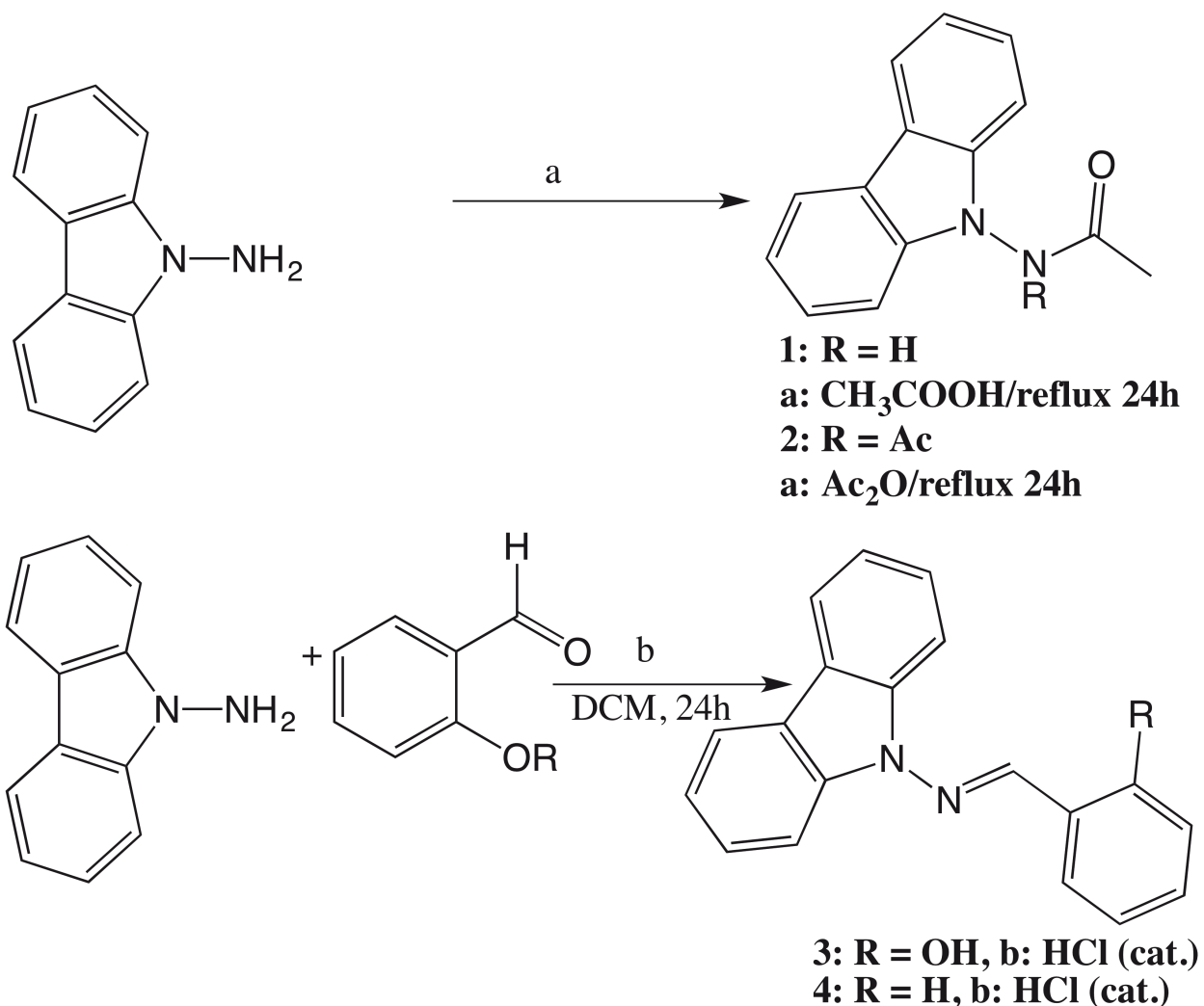


Figure 5-2: ORTEP representation of the structure of AC showing planar orientation of the carbazole framework. Selected angular parameters include C(1)-C(6)-C(12)-C(7) 1.6(9)°,

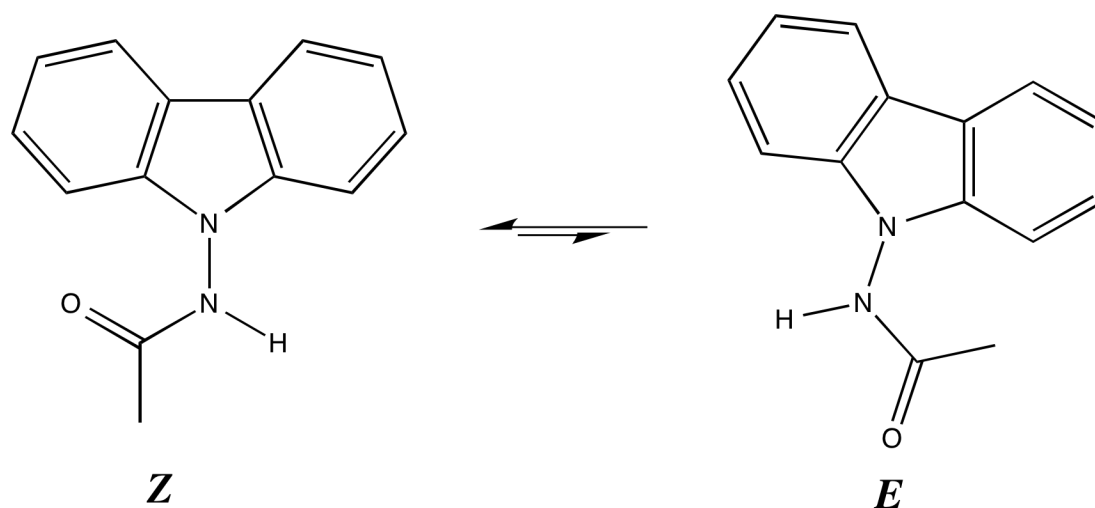
To ascertain the effect of phenyl ring mobility and π -overlap on the bonding in 1,1-diarylhydrazines, AC was coupled to several of the functional groups used previously to make derivatives of NDPH (Scheme 5-1). While the syntheses of the mono-acetyl¹³, salicylaldehyde^{13c, 14} and benzaldehyde^{13b, 14d, 15} adducts have appeared previously in the literature, the di-acetyl adduct as well as structural data for AC and compounds **1** – **3** are described here for the first time.



Scheme 5-1: Synthesis of 9-aminocarbazole derivatives.

As seen in Chapter 4 for NDPH, the mono-acetylation of AC results in an equilibrium mixture of isomers of *E* and *Z* conformation around the amide bond (Scheme 5-2). The isomeric composition of **1** has apparently not yet been studied in detail. From ¹H NMR data in DMSO, there is a 10:1 mixture of *Z* : *E* isomers with a slight decrease in isomeric preference in CDCl₃ of 5:1 *Z* : *E*. Two-dimensional NOESY NMR spectroscopy showed no NOE correlation of the amide proton with the acetyl group protons, however, the positioning of the signals for the amide protons in the two isomers was similar to NDPH, which facilitated assignment. Indeed, these results are supported by the solid-state single-crystal diffraction data obtained for **1** (Figure 5-1),

where only the *Z*-configuration was observed. Upon dissolution of these crystals, the equilibrium mixture of *Z* and *E* isomers was restored.



Scheme 5-2: Isomerism in *N*-(9*H*-carbazol-9-yl)acetamide.

This isomeric preference mirrors what was seen for NDPH in the solid state. In the case of **1**, however, gas-phase DFT calculations (B3LYP/6-311++g**, Appendix D Figure S2) indicate that the *E* isomer is lower in energy than the *Z*-isomer. The calculated HOMO (Appendix D, Figure S3) shows an anti-bonding interaction between the nitrogen atoms and a strong π -delocalization of N(1) into the carbazole. This is similar to what was seen in the NDPH derivative and is consistent with enhanced type 2a bonding between the nitrogen atoms.

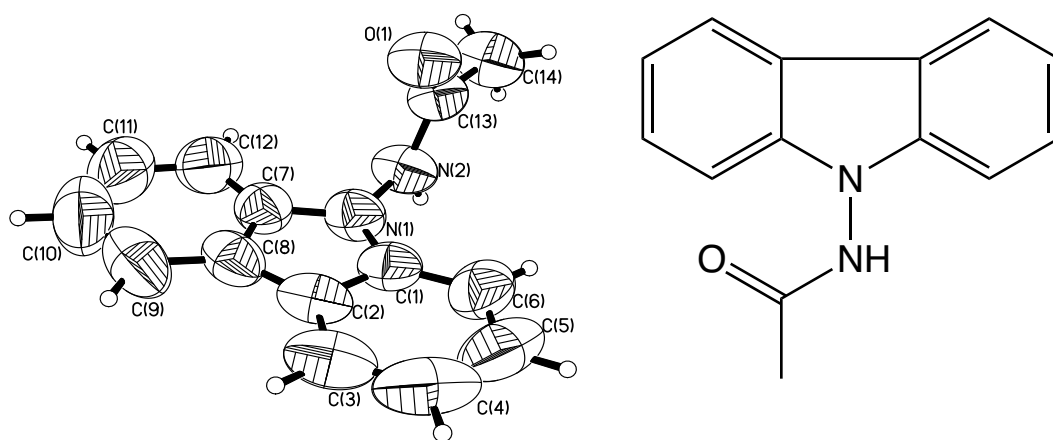


Figure 5-3: ORTEP representation of one molecule in the asymmetric unit of compound 1. Selected structural parameters are: N(2)-N(3) 1.379(3) Å, C(1)-C(6)-C(12)-C(7) 0.9(3)°, N(1)-N(2)-C(13)-C(14) - 177.3(3)°.

The key metric parameters for the solid-state orientations (Figures 5-2 to 5-5) obtained for AC and compounds 1- 3 are summarized in Table 5-2. Given the electronic modulation seen in NDPH derivatives bearing the same functional groups, absence of both possible conjugation through a proximal electron-withdrawing group and mobility of the Ar₂ system should have an effect on the solid-state structures. Important structural features for comparison include 1) the N-N bond lengths; 2) the torsion angles between the carbazole phenyl rings; 3) the orientations of the substituents in relation to the carbazole moiety and 4) the hybridization states of the nitrogen atoms. The derivatives 1-3 were chosen based on the contrasting orientations of the substituents in their NDPH-derived analogues, namely orthogonal (1, 2) and planar (3) CR₂ group arrangements. Crystals of 4, unfortunately, did not lead to a satisfactory solution.

Table 5-2: X-ray Diffraction Structural Parameters for Derivatives 9-Aminocarbazole

Parameter	AC	1	2 ^a	2 ^b	3
N(1)-N(2) Å	1.428(10)	1.375(3)	1.401(5)	1.384(5)	1.3699(16)
N(1)-C(1) Å	1.399(10)	1.387(4)	1.396(6)	1.404(6)	1.4070(18)
N(1)-C(7) Å	1.350(9)	1.385(4)	1.377(6)	1.374(6)	1.3980(18)
C(1)-C(2) Å	1.380(11)	1.384(5)	1.373(6)	1.369(6)	1.391(2)
N(2)-C(13) Å	N/A	1.339(3)	1.411(6)	1.432(6)	1.2740(18)
C(6)-C(12) Å	1.418(10)	1.438(5)	1.435(6)	1.443(6)	1.441(6)
C(13)-N(2)-N(1)-C(1) °	N/A	-79.3(4)	103.0(5)	80.5(5)	13.0(2)
C(13)-N(2)-N(1)-C(7) °	N/A	88.1(4)	-95.0(5)	-83.9(5)	-168.9(1)
N(1)-N(2)-C(13)-C(14) °	N/A	177.6(2)	-3.5(5)	-175.6(4)	-179.8(1)
N(2)-N(1)-C(7)-C(8) °	-1(2)	9.4(5)	13.4(7)	-13.2(7)	2.7(2)
N(2)-N(1)-C(1)-C(2) °	1(1)	-9.2(5)	-16.3(7)	13.7(7)	-0.4(3)
C(1)-N(1)-N(2) °	121.5(7)	124.5(3)	121.8(3)	122.5(3)	132.9(1)
C(7)-N(1)-N(2) °	128.2(7)	124.9(3)	124.7(3)	125.2(4)	109.1(1)
C(7)-N(1)-C(1) °	110.3(7)	109.6(3)	111.4(4)	110.7(4)	117.9(1)
Sum of angles about N(1) °	360(1)	359.0(5)	357.9(8)	358.4(6)	359.9(2)
Distance of N(1) from its plane (Å)	0.004	0.079	0.117	0.100	0.012

^{a, b} Independent molecules in the asymmetric unit.

Reaction of AC with acetic anhydride under basic conditions gave the diacetyl analogue (Figure 5-4).

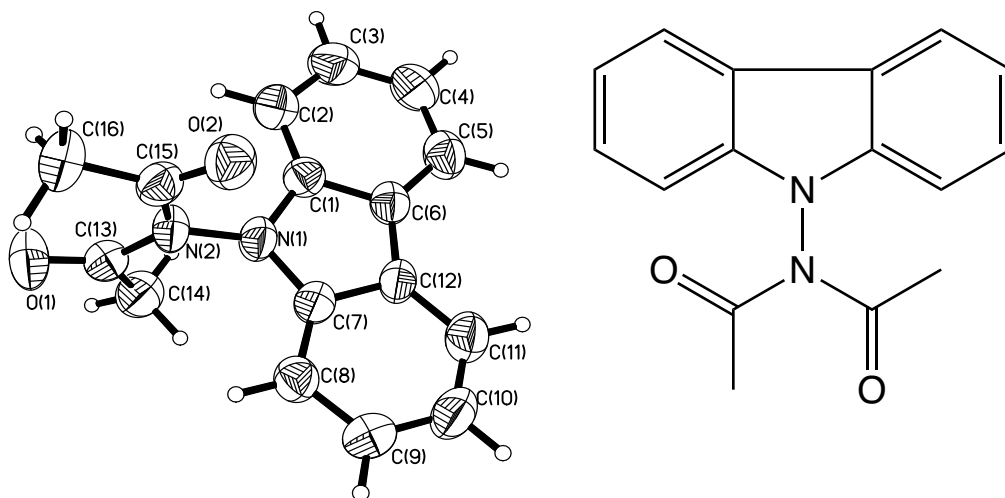


Figure 5-4: ORTEP representation of compound 2. Selected structural parameters are: N(1)-N(2) 1.384(5), 1.401(5) Å, C(1)-C(6)-C(12)-C(7) 1.0(5)°, -0.3(5)°, N(1)-N(2)-C(13)-C(14) -174.5(4), 2.5(6)°.

As in the case of NDPH, the acetyl groups are planar and orthogonal to the NAr_2 plane. The N-N bond lengths in the two independent molecules of the asymmetric unit are minimally shorter than in **1** or **AC** with values reminiscent of other structurally characterized N,N-diacetylhydrazines and both nitrogen atoms in either molecule are sp^2 -hybridized. Despite these similarities between **2** and NDPH, the N-N bond length in this derivative is the shorter of the two, even bearing in mind the high standard deviations in the bond length measurements, namely 1.401(5)Å and 1.384(5)Å, respectively. With dihedral angles of C(1)-C(6)-C(12)-C(7) of -0.30° and

C(1B)-C(6B)-C(12B)-C(7B) of 0.99° , the carbazole groups maintain their planarity. This observation coupled with the small dihedral angles about the N(1)-C(1) and N(2)-C(7) bonds, means that there is a possibility for π -delocalisation of electron density from N(1) to a greater extent than in NDPH, where these angles are larger. As a result of this increased planarity, delocalisation of the electron-pair from N(1) into the aromatic system would increase, strengthening its sp^2 -hybridization in this di-acetyl derivative. The out-of-plane distances of N(1) in the two molecules of the asymmetric unit of only 0.117\AA and 0.100\AA , respectively, are smaller than is the deviation of 0.186 in the NDPH-derived analogue.

Schiff base formation by condensation with salicylaldehyde yielded compound **3** (Figure 5-5), which exhibits the shortest N-N bond lengths of all of the carbazole derivatives studied of $1.3699(16)\text{\AA}$.

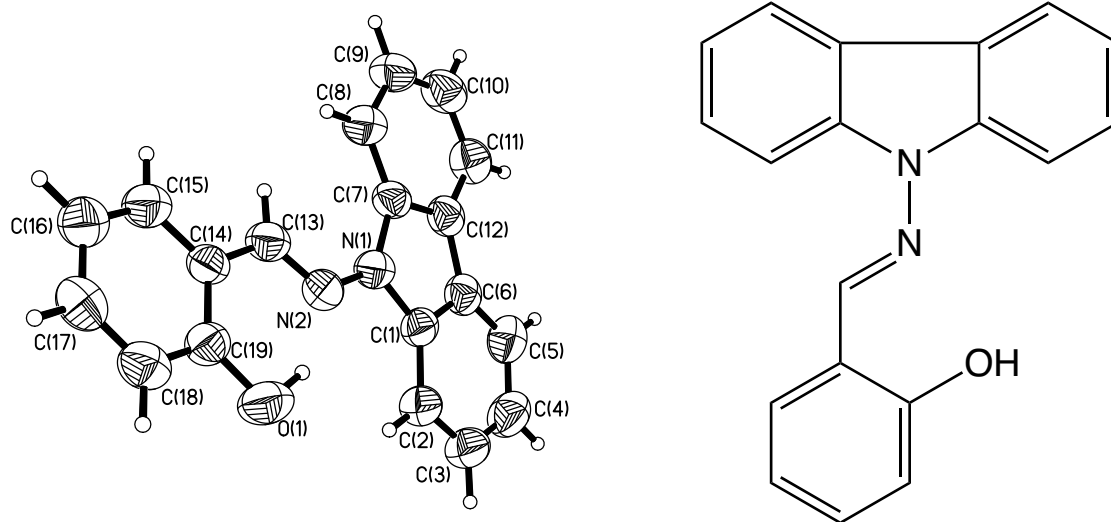


Figure 5-5: ORTEP Representation of 3. Selected structural parameters are: N(1)-N(2) $1.3699(16)\text{\AA}$, C(1)-C(6)-C(12)-C(7) $0.2(4)^\circ$

As with the analogue formed from NDPH, the *E* conformation is the only detectable contributor, both in the solid-state and in solution due to stabilization by an intramolecular hydrogen bond [N(2) – O(1) = 2.637(3)] Å. This observation is supported by the broadened OH signal in the IR. Interestingly, the alcoholic OH signal in the ¹H-NMR is very sharp in CDCl₃, indicative of a disruption of this hydrogen bond in solution; however, there is no evidence of the *Z* isomer. Comparison of these measurements with those of the NDPH-derivative of 1.3743(18) and 2.650(1) Å, respectively, demonstrate the even greater diffusion of electron density in **3** due to the forced planarity of the carbazole ring. Still, there is a slight twisting of the carbazole, precluding complete planarity of the structure, resulting of an angle of 12.07° between the plane of the salicylaldehyde group and that of the carbazole. The distance of N(1) from the plane of the carbazole ring also increases, albeit minimally, due to this strain (0.012Å). Given the imperfect planarity across the N-N bond, it can be predicted that the enhanced stability of this derivative over its NDPH analogue is due to enhanced sp²-hybridization of the nitrogen atoms due to increased π-contribution from their respective substituents with no π-delocalization over the N-N bond itself.

With the increased planarity of these carbazole derivatives compared to those derived from NDPH, it is important to verify that the measured metric parameters do not include significant intermolecular interactions. To that end the variation in N-N bond length was plotted against the N(1)-C(1) and N(1)-C(7) bond lengths, as well as their sum (Figure 5-6). The closest intermolecular approaches were also tabulated (Table 5-3).

Table 5-3: Closest Intermolecular Interactions in AC Derivatives

Compound	Carbazole plane	R_N 2)
AC	3.70 1) C 10) - C 11))	3.88 1) N 2) - C 6))
1	3.720 6) C 14) - C 3))	3.720 6) C 14) - C 3))
2	3.5- 7 6) C -) - O 1))	3.57- 6) C 14B) - O 1))
3	3.476 5) C 7) - C 1))	3.540 5) N 2) - C 18))

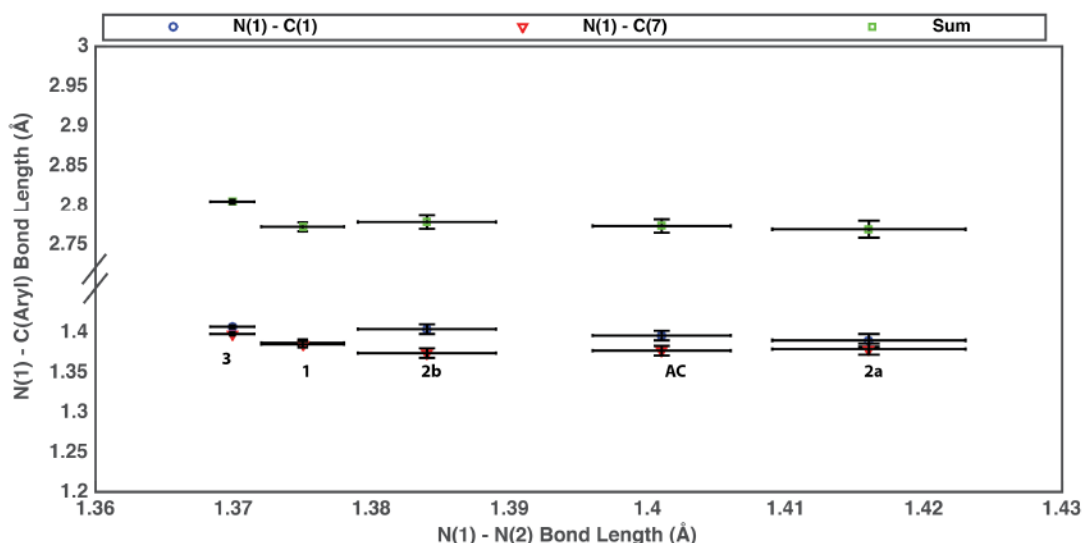


Figure 5 6: Variation in C-N bond length with N-N separation. Suffixes (a, b) denote independent molecules in the unit cells of 1 and 5.

In the majority of these structures, packing is dominated by herringbone side-on interactions. The only structure that exhibits possible π - π stacking type interactions is **3** where the salicylaldehyde groups are in the appropriate range (3 to 4 Å) from the carbazole rings of neighbouring molecules. A result of π - π stacking in this species is a slight lengthening of the N(1)-C(Aryl) bonds because of the increased competition for π -electron density. The remaining compounds do not have the correct orientations for these types of interactions.

By analogy to the study of NDPH, possible donor-acceptor interactions in these derivatives of AC were examined by UV-visible spectroscopy in chloroform (Table 5-4).

Table 5-4: Lowest Energy Absorption Bands for AC Derivatives.

Compound	λ_{max} (nm)	Molar absorptivity ($\text{M}^{-1}\text{cm}^{-1}$)
AC	343	3679
1	330	4838
2	328	5216
3	369	3073
4	360	19668

The molar absorptivities of the AC derivatives studied here are unique compared to the NDPH analogues in two respects. Firstly, the molar absorptivities decrease in the order **3 < AC < 1 < 2 << 4**. This trend is in line with the structural data obtained for AC and derivatives **1** to **3**. With the exception of **4**, all of the molar absorptivities are consistent with $n\text{-}\pi^*$ transitions. The large increase in molar absorptivity in compound **4** is clearly the result of a $\pi\text{-}\pi^*$ transition and reflects the planarity of the benzaldehyde derivative, with conjugation being greatly enhanced over the others. Unfortunately, data obtained for single crystals of **4** did not lead to a satisfactory solution; however, the delocalization in this derivative can also be inferred from the ^1H NMR spectrum. Whereas the analogous compound derived from NDPH (Chapter 4) shows the signal for the methine proton at a chemical shift of δ 7.3 ppm, the same proton is shifted to 9.074 ppm in the carbazole derivative. This is more reminiscent of the reported¹⁶ shift for the parent benzaldehyde methine proton shift of δ 10 ppm indicative of a restoration of aromaticity over the entire molecular structure in **4**, which was not present in the NDPH analogue.

5.4 Conclusions

From purified crystalline AC, several derivatives analogous to those previously derived from NDPH can be made in high yield and purity. The first structural elucidation of AC shows it to be a planar molecule with only a small torsion angle of $2(2)^\circ$ between the planes of the fused phenyl rings. This planarity has the effect of strengthening the sp^2 -hybridization state of its adjacent nitrogen through additional π -based electron delocalization. As a result, the N-N repulsion is lowered to an even greater extent, allowing greater orbital overlap and hence bonds in AC derivatives gain type 2b character and become shorter.

These studies have shown that the σ - and π -based contributions can be made to work synergistically in 1,1-diarylhydrazines to promote even stronger N-N bonds. We have also demonstrated the effect of sterics through comparison with analogous NDPH derivatives, where π -delocalization is hindered and bonding interactions are limited to having mostly σ -character only. Fusion of the aryl network produces an increase in aromaticity, just as in going from pyrrole to indole and finally to carbazole and this aromatic enhancement can be propagated to enhance overall molecular stability. Given the wide array of uses for AC and its conjugates in materials and medicinal chemistry, this knowledge will be useful for controlling the stability of these hydrazine-based products for various applications.

5.5 Experimental

5.5.1 General methods

Dichloromethane was continuously dried over a column of SiO_2 . All other reagents and solvents were obtained from commercial sources and were used as received. 9-nitrosocarbazole was synthesized following the method of Parakka¹⁷ and

was used without further purification. ^1H - and ^{13}C -NMR spectra were recorded on 300 and 500 MHz Varian spectrometers. High-resolution mass spectra (HRMS) were measured by electrospray techniques with a time-of-flight detector (ESI/TOF). UV/Vis spectra of all the compounds were acquired on a Carey 100 Bio spectrophotometer. Melting points were determined using a micro-melting apparatus and are calibration-corrected.

5.5.2 Syntheses

9-aminocarbazole (AC)

Following the method of Entwistle^{15e}, a solution of low-valent titanium reagent was made with 6.6 mL titanium(IV) chloride in 4:1 dichloromethane:diethyl ether (250 mL) by addition of magnesium turnings (1.5 g) and stirring at room temperature for 3 h. 9-nitrosocarbazole (1.38 g, 7.03 mmol) in diethyl ether (50 mL) was added and stirred at room temperature for 30 min. A solution of concentrated hydrochloric acid (1 mL) in water (40 mL) was carefully added (CAUTION: Gas evolution) and stirring continued for 1 h. The reaction mixture was made alkaline by the addition of a solution of sodium hydroxide (6 g, 0.15 mol) in water (40 mL) upon which it adopted a royal blue colour. The mixture was extracted (3 x 100 mL) with diethyl ether and the organic extracts were combined, washed with saturated sodium chloride (3 X 100 mL), dried over anhydrous magnesium sulfate and reduced *in vacuo* to give a crude solid containing the product and some carbazole. This solid was dissolved in ether and concentrated hydrochloric acid was added dropwise. The hydrochloride salt that precipitated was filtered, washed with ether and dissolved in water (250 mL). The solution was made very alkaline by the addition of solid sodium hydroxide (12 g, 0.3 mol) and extracted with diethyl ether (3 X 50 mL). Evaporation of the solvent and recrystallization from dichloromethane-doped ethanol yielded off-white needles. Yield 1.02 g (5.62 mmol, 80% yield). m.p. 154- 155

°C (lit^{15e}. 150 – 152 °C) ; ¹H-NMR (300 MHz, DMSO-d₆) δ (ppm): 5.82 (2H, s), 7.16 (t, 2H, J = 7.20 Hz), 7.44 (2H, t, J = 7.50 Hz), 7.59 (d, 2H, J = 8.10 Hz), 8.10 (2H, d, H = 7.80 Hz); ¹³C-NMR (300 MHz, DMSO-d₆) δ (ppm): 111.3, 118.9, 120.6, 122.8, 125.9, 140.1; IR (KBr, cm⁻¹): 420 (vw), 428 (w), 450 (vw), 526 (vw), 557 (vw), 566 (vw), 610 (vw), 622 (w), 722 (s), 749 (vs), 844 (m), 855 (m), 871 (vw), 932 (w), 961 (vw), 996 (vw), 1007 (vw), 1112 (vw), 1152 (m), 1234 (s), 1318 (s), 1334 (w), 1354 (vw), 1450 (m), 1479 (m), 1570 (w), 1586 (w), 1602 (m), 1628 (w), 1771 (vw), 1889 (vw), 1928 (vw), 3052 (w), 3264 (w), 3336 (m); UV-Vis (CHCl₃): λ_{max} = 329 nm, ε = 3716 M⁻¹cm⁻¹, λ_{max} = 343 nm, ε = 3679 M⁻¹cm⁻¹.

N-(9*H*-carbazol-9-yl)acetamide (**1**)

To an ice-cooled solution of AC (0.060 g, 0.329 mmol) in diethyl ether (50 mL) was added acetic anhydride (1 mL, excess). The solution was stirred at room temperature overnight. Addition of hexanes (50 mL) and removal of the ether under reduced pressure yielded the product as a white precipitate. Recrystallization from dichloromethane-doped methanol by slow evaporation yielded x-ray quality crystals. Yield 0.052 g (0.232 mmol, 70% yield). m.p. 256 – 257 °C (lit^{14a}. 256 – 257 °C); ¹H-NMR (300 MHz, DMSO-d₆) δ (ppm) mixture of *E*- and *Z*-isomers, *E*-isomer: 2.17 (3H, s), 7.23 (t, 2H, J = 7.80 Hz), 7.34 (2H, d, J = 8.10 Hz), 7.43 (t, 2H, J = 6.90 Hz), 8.14 (2H, t, J = 8.10 Hz), 11.12 (s, 1H) 7.67 (t, 1H, J = 8.40 Hz), 7.85 (d, 1H, J = 8.10 Hz), 10.49 (s, 1H); *Z*-isomer: 1.59 (3H, s), 7.23 (t, hidden), 7.28 (2H, d, J = 8.10 Hz), 7.51 (t, 2H, J = 7.20 Hz), 8.19 (2H, d, J = 7.80), 10.48 (s, 1H); IR (KBr, cm⁻¹): 422 (m), 548 (m), 577 (vw), 638 (w), 721 (s), 742 (vs), 751 (vs), 806 (vw), 932 (vw), 958 (vw), 1006 (w), 1114 (vw), 1152 (m), 1234 (s), 1268 (s), 1318 (s), 1333 (m), 1369 (m), 1383 (w), 1452 (s), 1484 (m), 1529 (br, m), 1580 (vw), 1606 (w), 1624 (w), 1682 (br, vs), 3023 (m), 3231 (s); UV-Vis (CHCl₃): λ_{max} = 330 nm, ε = 4838 M⁻¹cm⁻¹; HRMS calcd. for

C₁₄H₁₂N₂ONa: 247.0842, Found: 247.0852; Anal. Calcd. for C₁₄H₁₂N₂O: C, 74.98%; H, 5.39%; N, 12.49%; Found: C, 75.00%; H, 5.44%; N, 12.63%.

N-acetyl-*N*-(9*H*-carbazol-9-yl)acetamide (**2**)

To a solution of AC (0.100 g, 0.548 mmol) in dichloromethane (10 mL) was added acetic anhydride (1 mL, excess) and triethylamine (1 mL, excess) and the mixture stirred overnight at room temperature. The solvents were removed under reduced pressure and the residue combined with methanol (15 mL) and left at 4 °C for 24 h. Clear, colourless block crystals resulted which were filtered and suction dried. Yield 0.113 g (0.422 mmol, 77%). m.p. 147 – 148 °C; ¹H-NMR (300 MHz, CDCl₃) δ (ppm): 2.39 (s, 6H), 7.19 (d, 2H, J = 7.80 Hz), 7.36 (t, 2H, J = 7.50 Hz), 7.49 (t, 2H, J = 8.10 Hz), 8.11 (d, 2H, J = 7.80 Hz); ¹³C-NMR (300 MHz, CDCl₃) δ (ppm): 24.7, 107.6, 121.0, 121.5, 122.2, 126.9, 139.1, 171.3; IR (KBr, cm⁻¹): 563 (vw), 586 (vw), 595 (w), 635 (vw), 646 (vw), 725 (w), 754 (m), 852 (vw), 932 (vw), 996 (m), 1028 (vw), 1042 (vw), 1090 (vw), 1116 (vw), 1156 (w), 1203 (s), 1219 (m), 1233 (m), 1264 (m), 1317 (w), 1334 (w), 1365 (m), 1414 (w), 1451 (m), 1484 (w), 1583 (vw), 1602 (w), 1623 (vw), 1729 (vs), 1790 (vw), 2943 (vw), 3016 (vw), 3050 (vw), 3420 (vw); UV-Vis (CHCl₃): λ_{max} = 316 nm, ε = 5782 M⁻¹cm⁻¹, λ_{max} = 328 nm, ε = 5216 M⁻¹cm⁻¹; HRMS calcd. for C₁₆H₁₄N₂O₂Na: 289.0947, Found: 289.0947; Anal. Calcd. for C₁₆H₁₄N₂O₂: C, 72.17%; H, 5.30%; N, 10.52%; Found: C, 72.17%; H, 5.31%; N, 10.53%.

(*E*)-2-(((9*H*-carbazol-9-yl)imino)methyl)phenol (**3**)

To a solution of AC (0.055 g, 0.301 mmol) in dichloromethane (10 mL) was added 5 drops of salicylaldehyde and 4 drops of concentrated HCl. The white precipitate of the hydrochloride was seen to form immediately and the reaction flask was stoppered and stirred at room temperature for 2 days. The clear, yellow solution that resulted was evaporated under reduced pressure and recrystallization from DCM-doped methanol

(1:9) by slow evaporation gave yellow needles in two crops. Yield: 70 mg (0.24 mmol, 81%). m.p. 146 – 147 °C; ¹H-NMR (300 MHz, CDCl₃) δ (ppm): 7.02 (t, 1H, J = 7.50 Hz), 7.12 (d, 1H, J = 8.10 Hz), 7.34 (t, 2H, J = 7.50 Hz), 7.39 (d, 2H, J = 7.80 Hz), 7.51 (t, 2H, J = 7.20 Hz), 7.72 (d, 2H, J = 8.10 Hz), 8.10 (d, 2H, J = 7.80 Hz), 9.11 (s, 1H), 11.32 (s, 1H); ¹³C-NMR (300 MHz, CDCl₃) δ (ppm): 109.9, 117.4, 117.7, 119.7, 120.5, 121.3, 122.6, 126.6, 131.4, 132.3, 137.7, 155, 158; IR (KBr, cm⁻¹): 415 (vw), 479 (w), 542 (vw), 581 (vw), 695 (m), 716 (s), 740 (vs), 752 (vs), 799 (w), 883 (vw), 940 (vw), 1032 (vw), 1072 (vw), 1156 (w), 1202 (w), 1214 (w), 1266 (m), 1301 (s), 1313 (s), 1444 (vs), 1483 (vs), 1594 (m), 1623 (m), 3044 (vw); UV-Vis (CHCl₃): λ_{max} = 369 nm, ε = 3073 M⁻¹cm⁻¹; HRMS calcd. for C₁₉H₁₃N₂O: 285.10334, Found: 285.10328; Anal. Calcd. for C₁₉H₁₄N₂O: C, 79.70%; H, 4.93%; N, 9.78%; Found: C, 79.40%; H, 4.92%; N, 9.75%.

(E)-N-(9*H*-carbazol-9-yl)-1-phenylmethanimine (**4**)

To a solution of AC (0.060 g, 0.33 mmol) in dichloromethane (10mL) was added 5 drops of benzaldehyde and 3 drops of concentrated HCl. The white precipitate of the hydrochloride was seen to form immediately and the reaction flask was stoppered and stirred at room temperature for 1 h. The clear, amber solution that resulted was evaporated under reduced pressure and recrystallization from DCM-hexanes (1:25) by slow evaporation gave yellow prisms. Yield: 50 mg (0.19 mmol, 58%). m.p. 145 – 146 °C; ¹H-NMR (300 MHz, CDCl₃) δ (ppm): 7.32 (t, 2H, J = 7.20 Hz), 7.49 – 7.54 (m, 9H), 7.89 (d, 2H, J = 8.40 Hz), 7.96 (d, 2H, J = 7.80 Hz), 8.10 (d, 2H, J = 7.80 Hz), 9.08 (s, 1H, J = 8.10 Hz), 8.10 (d, 2H, J = 7.80 Hz), 9.11 (s, 1H), 11.32 (s, 1H); ¹³C-NMR (300 MHz, CDCl₃) δ (ppm): 122.1, 125.0, 125.6, 125.8, 126.6, 127.3, 128.6, 128.8, 129.8, 133.4, 135.1, 137.0; IR (KBr, cm⁻¹): 550 (m), 670 (w), 689 (s), 717 (s), 740 (s), 751 (vs), 892 (vw), 925 (w), 937 (vw), 965 (vw), 1058 (w), 1114 (vw), 1127 (vw), 1148 (w), 1162 (vw), 1286 (m), 1304 (s), 1208 (m), 1444 (vs), 1480 (m), 1486 (m), 1574 (w), 1588 (w),

1596 (w), 1614 (w), 3040 (vw); UV-Vis (CHCl₃): λ_{max} = 360 nm, ϵ = 19668 M⁻¹cm⁻¹; HRMS calcd. for C₁₉H₁₅N₂: 271.12298, Found: 271.12289; Anal. Calcd. for C₁₉H₁₄N₂: C, 84.42%; H, 5.22%; N, 10.36%; Found: C, 84.24%; H, 5.26%; N, 10.52%.

5.5.3 X-ray Crystallography

The X-ray diffraction data were measured with graphite monochromated Mo K α radiation (λ = 0.71073 Å) on crystals that were attached to a mitogen mount with viscous paratone N oil. The structures were solved by direct methods on an absorption-corrected model generated by SADABS. Refinement was achieved by a full-matrix least-squares procedure based on F^2 . The hydrogen atoms were located at calculated positions except for in AC, where they were refined from residual electron density peaks. For AC and 3, the carbon atoms comprising the carbazole rings were refined isotropically. For 1 and 2, all atoms other than hydrogen were refined anisotropically.

5.5.4 Theoretical Methods

All of the calculations described were performed using Gaussian 03.¹⁸ Computations were carried out at the restricted Hartree–Fock¹⁹ and density functional theory (DFT) levels. Density functional theory calculations used the hybrid B3LYP functional and triple zeta 6-311++G** basis sets.²⁰ The calculated molecular geometries were fully optimized and correspond to minima on the potential energy surface as confirmed by the absence of imaginary vibrational frequencies.

5.6 Acknowledgements

This research was supported by NSERC discovery grants to D.S.B. and I.S.B. The authors are grateful to Dr. Alexander Wahba and Nadim Saade for mass spectrometry analysis.

5.7 References

1. Begtrup, M.; Rasmussen, L. K., Arylhydrazines. *Sci. Synth.* **2007**, *31b*, 1773-1826.
2. Fina, N. J.; Edwards, J. O., Alpha effect. Review. *Int. J. Chem. Kinet.* **1973**, *5* (1), 1-26.
3. Kool, E. T.; Crisalli, P.; Chan, K. M., Fast Alpha Nucleophiles: Structures that Undergo Rapid Hydrazone/Oxime Formation at Neutral pH. *Org. Lett.* **2014**, *16* (5), 1454-1457.
4. Nguyen, R.; Huc, I., Optimizing the reversibility of hydrazone formation for dynamic combinatorial chemistry. *Chem. Commun. (Cambridge, U. K.)* **2003**, (8), 942-943.
5. (a) Unangst, P. C.; Carethers, M. E.; Webster, K.; Janik, G. M.; Robichaud, L. J., Acidic furo[3,2-b]indoles. A new series of potent antiallergy agents. *J. Med. Chem.* **1984**, *27* (12), 1629-33; (b) Unangst, P. C.; Connor, D. T.; Stabler, S. R.; Weikert, R. J.; Carethers, M. E.; Kennedy, J. A.; Thueson, D. O.; Chestnut, J. C.; Adolphson, R. L.; Conroy, M. C., Novel indolecarboxamidotetrazoles as potential antiallergy agents. *J. Med. Chem.* **1989**, *32* (6), 1360-6.
6. Glamkowski, E. J.; Fortunato, J. M.; Spaulding, T. C.; Wilker, J. C.; Ellis, D. B., 3-(1-Indoliny)benzylamines: a new class of analgesic agents. *J. Med. Chem.* **1985**, *28* (1), 66-73.

7. von, A. E.; Strohmeier, J., 2-Phenylindoles. Effect of N-benylation on estrogen receptor affinity, estrogenic properties, and mammary tumor inhibiting activity. *J. Med. Chem.* **1987**, *30* (1), 131-6.
8. Klein, J. T.; Davis, L.; Olsen, G. E.; Wong, G. S.; Huger, F. P.; Smith, C. P.; Petko, W. W.; Cornfeldt, M.; Wilker, J. C.; et, a., Synthesis and Structure-Activity Relationships of N-Propyl-N-(4-pyridinyl)-1H-indol-1-amine (Besipirdine) and Related Analogs as Potential Therapeutic Agents for Alzheimer's Disease. *J. Med. Chem.* **1996**, *39* (2), 570-81.
9. Balon, M.; Carmona, M. C.; Munoz, M. A.; Hidalgo, J., The acid-base properties of pyrrole and its benzologs indole and carbazole. A reexamination from the excess acidity method. *Tetrahedron* **1989**, *45* (23), 7501-4.
10. Barger, G.; Dyer, E., Synthesis of polycyclic indoles. *J. Am. Chem. Soc.* **1938**, *60*, 2414-16.
11. (a) Katritzky, A. R.; Suwinski, J. W., N-Oxides and related compounds. LI. Synthesis of N,N'-linked bi(heteroaryls). *Tetrahedron* **1975**, *31* (13-14), 1549-56; (b) Katritzky, A. R.; Suwinski, J. W., N,N'-linked bi(heteroaryls). Neutral species, cations, and dications. *Tetrahedron Lett.* **1974**, (47), 4123-4.
12. Deng, J.; Guo, L.; Xiu, Q.; Zhang, L.; Wen, G.; Zhong, C., Two polymeric metal complexes based on polycarbazole containing complexes of 8-hydroxyquinoline with Zn(II) and Ni(II) in the backbone: Synthesis, characterization and photovoltaic applications. *Mater. Chem. Phys.* **2012**, *133* (1), 452-458.
13. (a) Barba, N. A.; Vlad, L. A. In *Some hydrazones based on 9-aminocarbazole*, Shtiintsa: 1985; pp 82-7; (b) Kyziol, J.; Tarnawski, J., Synthesis of N-substituted derivatives of 9-aminocarbazole. *Rev. Roum. Chim.* **1980**, *25* (5), 721-7; (c) Blom, A. V., Hydrazones of biphenylenehydrazine. *J. Prakt. Chem. (Leipzig)* **1916**, *94*, 77-84.
14. (a) Kyziol, J.; Tarnawski, J., Synthesis of N-substituted Derivatives of 9-aminocarbazole. *Rev. Roum. Chim.* **1980**, *25*, 721-727; (b) Kristen, M. O.; Gonioukh,

A.; Lilge, D.; Lehmann, S.; Bildstein, B.; Amort, C.; Malaun, M. Bisimidino compounds, their transition metal complexes, and use of the latter as polymerization catalysts. WO2001014391A1, 2001; (c) Jacobsen, P.; Madsen, P.; Westergaard, N. Preparation of hydrazones derivatives for treatment or prevention of diseases related to glucose metabolic pathways. WO9940062A1, 1999; (d) Goldfarb, D. S. Method using lifespan-altering compounds for altering the lifespan of eukaryotic organisms, and screening for such compounds. US20090163545A1, 2009.

15. (a) Wieland, H.; Susser, A., Ditertiary Hydrazines and Divalent Nitrogen. XIII. Some New Ditertiary Hydrazines and Tetrazines of the Aromatic Series. *Justus Liebigs Ann. Chem.* **1913**, 392, 169-85; (b) Koshimura, S.; Hamada, A.; Otaki, T.; Deguchi, K., Fundamental studies in chemotherapy of tuberculosis. L. The bacteriostatic action of various heterocyclic compounds upon tubercle bacilli. *Ann. Rept. Research Inst. Tuberc., Kanazawa Univ.* **1954**, 12 (No. 2), 9-12; (c) Kazami, T.; Sakai, K.; Hashimoto, M.; Sasaki, M.; Tsutsui, K.; Ahta, M. Electrophotographic plates. JP54081847A, 1979; (d) Akao, Y. Preparation of nitriles. JP01157922A, 1989; (e) Entwistle, I. D.; Johnstone, R. A. W.; Wilby, A. H., Metal-assisted reactions. Part 11. Rapid reduction of N-nitrosamines to N,N-disubstituted hydrazines; the utility of some low-valent titanium reagents. *Tetrahedron* **1982**, 38 (3), 419-23.

16. Abraham, R. J.; Mobli, M.; Smith, R. J., ¹H chemical shifts in NMR: part 19. Carbonyl anisotropies and steric effects in aromatic aldehydes and ketones. *Magn. Reson. Chem.* **2003**, 41 (1), 26-36.

17. Parakka, J. P.; Nugara, P. N.; Lakshmikantham, M. V.; Belmore, K. A.; Cava, M. P., The oxidation of 3-aminocarbazole and its N-ethyl derivative. *Synth. Met.* **1992**, 47 (2), 141-9.

18. Frisch, M. J.; Trucks, G. W.; Schlegel, H. B.; Scuseria, G. E.; Robb, M. A.; Cheeseman, J. R.; Zakrzewski, V. G.; Montgomery, J. A.; Stratmann, R. E.; Burant, J. C.; Dapprich, S.; Millam, J. M.; Daniels, A. D.; Kudin, K. N.; Strain, M. C.; Farkas, O.;

Tomasi, J.; Barone, V.; Cossi, M.; Cammi, R.; Mennucci, B.; Pomelli, C.; Adamo, C.; Clifford, S.; Ochterski, J.; Petersson, J. A.; Ayala, P. Y.; Cui, Q.; Morokuma, K.; Malick, D. K.; Rabuck, A. D.; Raghavachari, K.; Foresman, J. B.; Cioslowski, J.; Ortiz, J. V.; Stefanov, B. B.; Liu, G.; Liashenko, A.; Piskorz, P.; Kamaromi, L.; Gomperts, R.; Martin, R. L.; Fox, D. J.; Keith, T.; Al-Laham, M. A.; Peng, C. Y.; Nanayakkara, A.; Gonzalez, C.; Challacombe, M.; Gill, P. M. W.; Johnson, B. G.; Chen, W.; Wong, M. W.; Andres, J. L.; Head-Gordon, M.; Replogle, E. S.; Pople, J. A. *Gaussian 98*, Gaussian Inc.: Pittsburgh, PA, 1998.

19. Roothaan, C., New Developments in Molecular Orbital Theory. *Rev. Mod. Phys.* **1951**, *23* (2), 69-89.

20. (a) Becke, A. D., Density-functional thermochemistry. III. The role of exact exchange. *J. Chem. Phys.* **1993**, *98* (7), 5648-5652; (b) Lee, C.; Yang, W.; Parr, R., Development of the Colle-Salvetti correlation-energy formula into a functional of the electron density. *Phys. Rev. B* **1988**, *37* (2), 785-789.

6

Exploratory Reactions of Electron-Deficient 1,1-Diarylhydrazines to form Electron-Deficient Benzotriazoles and New Transition Metal Complexes

6.1 Preamble

Given the prior lack of successful preparations of 1,1-diarylhydrazines bearing electron-withdrawing groups (i.e. –nitro groups), there is little known about the chemistry of these compounds, specifically in their reactions with metals. Having established the stability of adducts of 2-nitrodiphenylhydrazine (NDPH) with various functional groups, we sought to explore the reactivity of these adducts and NDPH with metals. This reactivity is comprised of two essential aspects: the ability to alter the original NDPH to produce N-heterocycles and secondly, to assess the ability of NDPH adducts to form coordination compounds.

In the context of the current dissertation, our main interest was to try and use the electron-deficiency of NDPH as a more efficient route to the synthesis of 1-arylsubstituted benzotriazoles that maintained this electron deficiency. In addition, we sought to examine the effects of Schiff bases of these compounds upon metal coordination to see if the products would exhibit new properties since they have never to date been reported in the literature.

6.2 Introduction

To examine aromatic systems containing electron-deficient nitrogen that could potentially be used to form electron-deficient benzotriazoles as well as ligands, the 1,1-diarylhydrazines are a sensible starting point. As demonstrated in Chapters 4 and 5, the two phenyl rings ensure that any chemistry they engage in is limited to the nitrogen atoms and significant σ -withdrawing effects render their –diaryl nitrogen atoms electron-poor. The potential for novel reactivity of 1,1-diarylhydrazines was demonstrated by Aldeco-Pérez and co-workers who showed that 1,1-diphenylhydrazine could engage in rearrangements that the other phenylhydrazines did not¹.

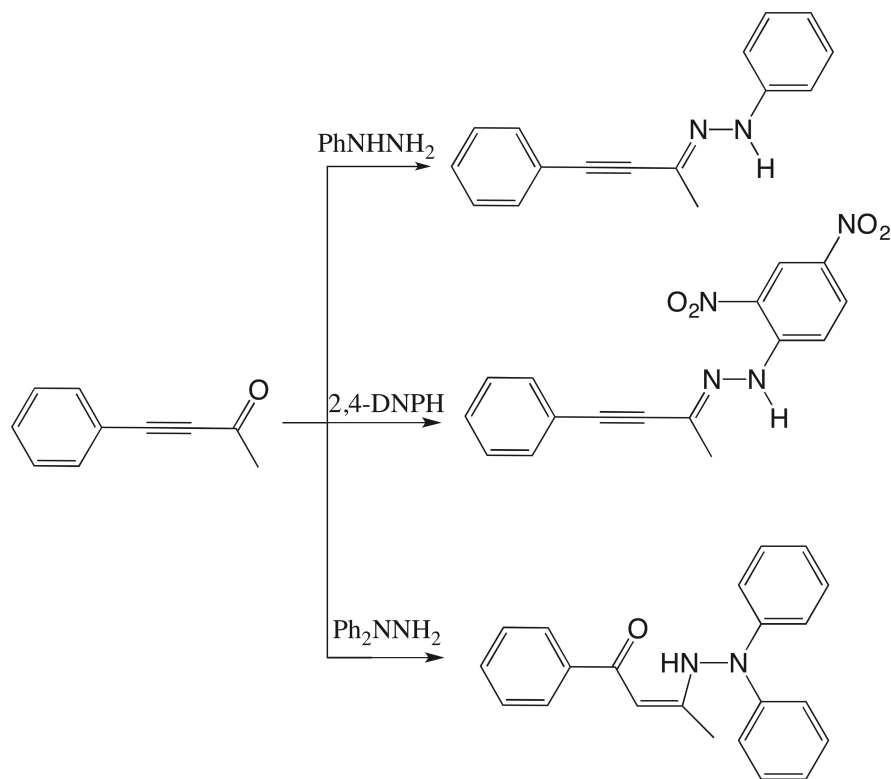


Figure 6-1: Reactivity of phenylhydrazines with carbonyl-containing alkynes¹.

While exhibiting unique reactivity, these hydrazines are also attractive for their potential use as ligands and as precursors to N-heterocyclic species. As ligands, 1,1-diarylhydrazines have been used to produce metal complexes with intriguing charge-transfer capability² owing to the ability to perturb the electronic environment of the NAr_2 moiety through aryl ring substitution (Figure 6-2). As a result of such perturbation, the hydrazine can adopt one of two possible bonding modes as either hydrazido- (2-) $\text{M}\equiv\text{N}-\text{NR}_2$ or formally neutral diazine $\text{M}=\text{N}=\text{NR}_2$ ligands (Figure 6-2). Salicylaldehyde derivatives of 1,1-diarylhydrazines are catalysts for the polymerization of olefins when complexed with nickel³.

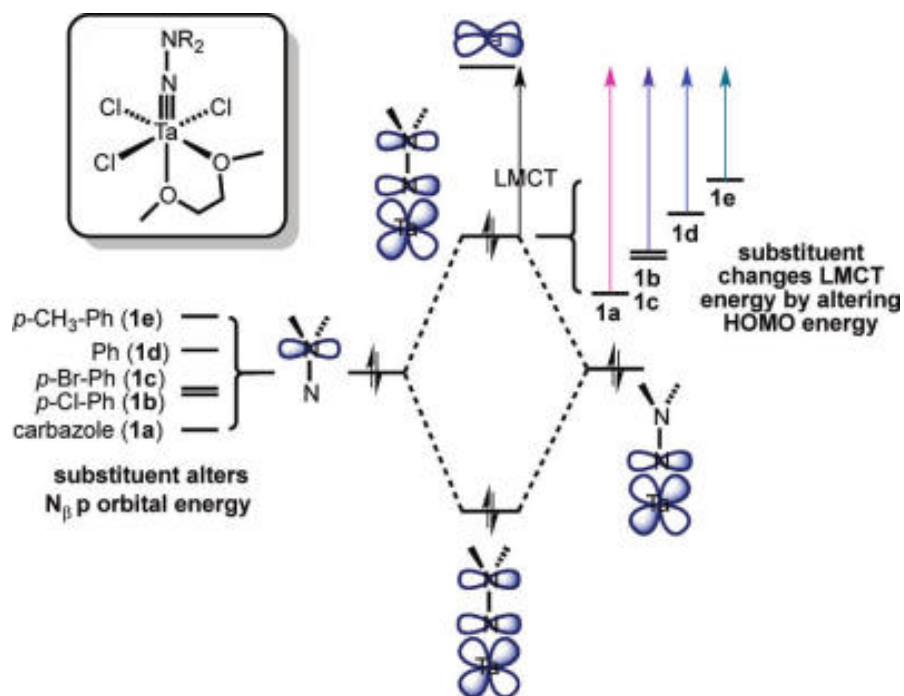


Figure 6-2: NAr_2 substituent effects on charge-transfer bands in hydrazido metal complexes. Reprinted with permission from Tonks, I. A.; Durrell, A. C.; Gray, H. B.; Bercaw, J. E., Groups 5 and 6 Terminal Hydrazido(2-) Complexes: $\text{N}\beta$ Substituent Effects on Ligand-to-Metal Charge-Transfer Energies and Oxidation States. *J. Am. Chem. Soc.* 2012, 134 (17), 7301-7304. Copyright 2012 American Chemical Society.

While demonstrating utility as ligands, the hydrazines are also useful reagents in organic synthesis, particularly in the synthesis of N-heterocycles. The synthesis of 1-hydroxybenzotriazole from *o*-chloronitrobenzene and hydrazine has been known since 1900 (Figure 6-3)⁴.

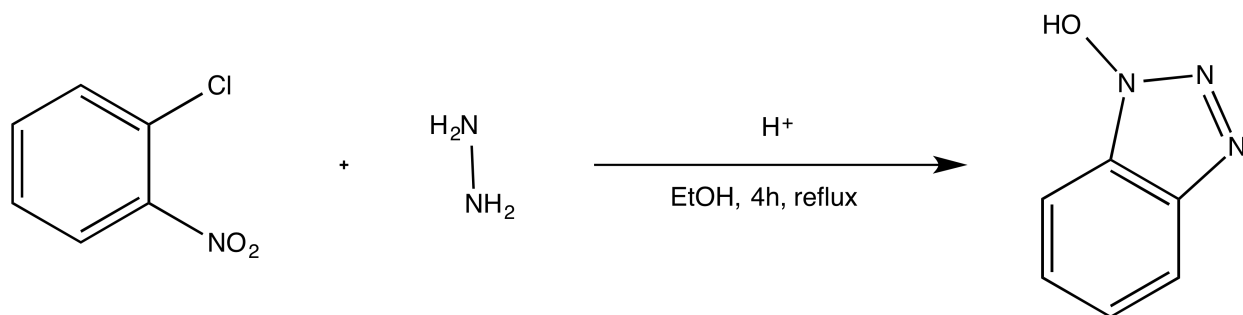


Figure 6-3: Synthesis of 1-hydroxybenzotriazole.

The above methodology has seen extensive use in the synthesis of substituted benzotriazoles by using analogously substituted halobenzenes⁵. While there is a comparatively vast literature of substituted benzotriazoles produced from substituted halobenzenes in reaction with hydrazine, there are also other more hazardous methods used to produce benzotriazoles, such as creation of an electrophilic nitrogen to mitigate the cyclization of *o*-phenylenediamines⁶. The benzotriazoles produced by this method still require additional reaction to achieve N-substitution. These reactions, which typically involve use of a base followed by nucleophilic substitution of a desired substituent bearing a halide, often result in the formation of substitution products at both the 1 and 2 positions, the separation of which is usually impossible without the use of chromatographic techniques. The simplest example of this methodology is the production of 1-methylbenzotriazole from benzotriazole and methyl iodide (Figure 1-32)⁷.

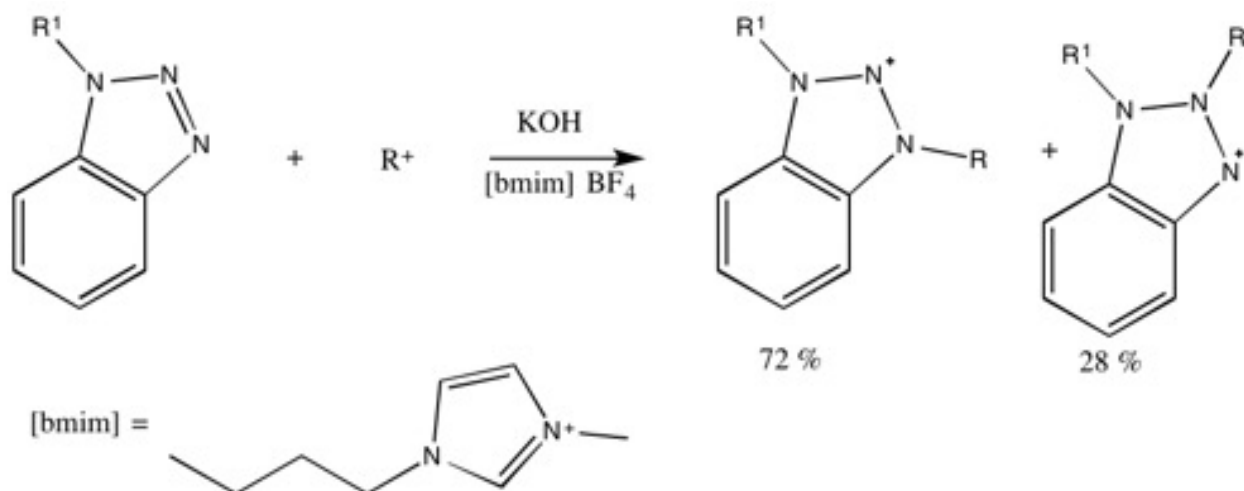
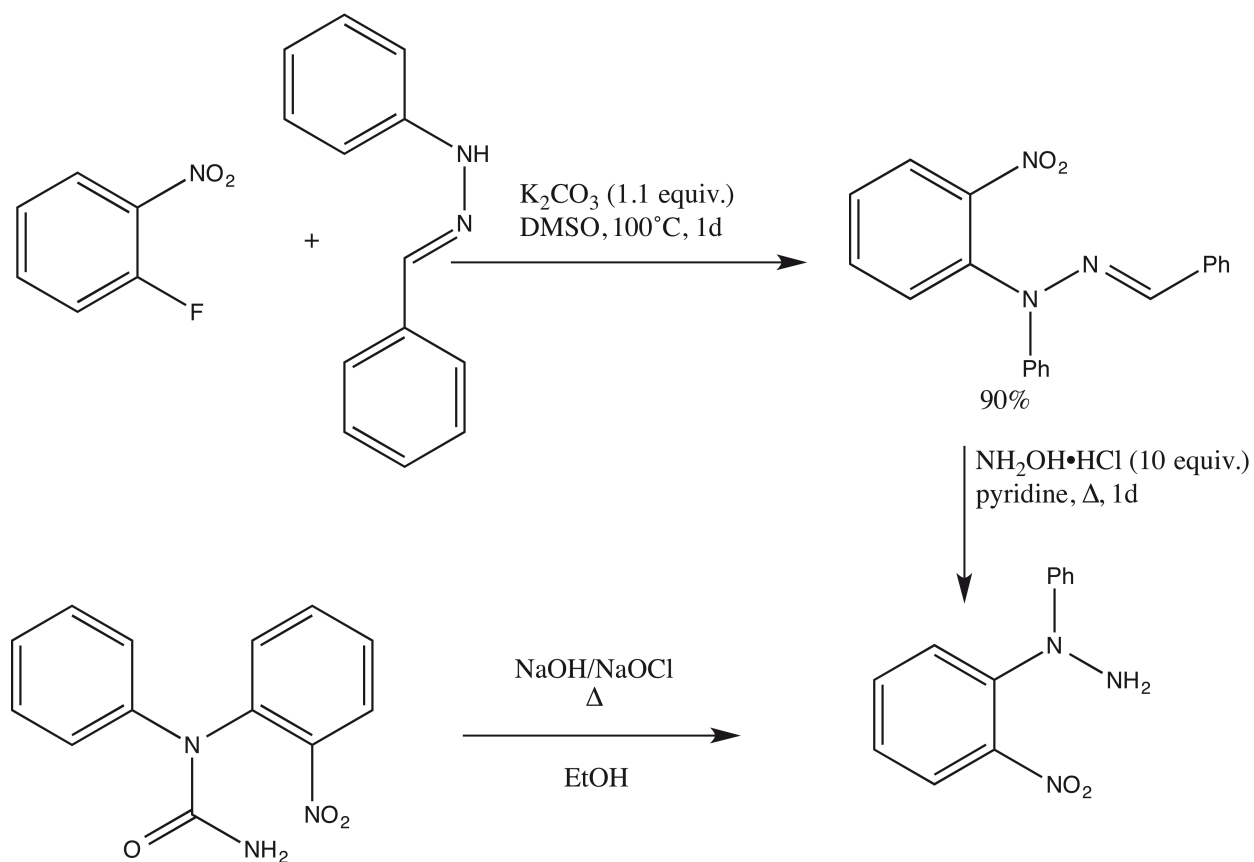


Figure 6-4: Typical N-alkylation of benzotriazole resulting in a mixture of 1- and 2-alkyl substitution products.

The analogous reaction to Figure 6-3 employing 1,1-diarylhydrazines to make benzotriazoles has seemingly never been successful. This is due to two important factors. First, the nucleophilicity of hydrazines is directly related to their substituents (Chapter 4). Consequently, the cyclization of the addition product of substituted hydrazines with *o*-halonitrobenzenes is hindered. Second and probably most importantly, is the sheer lack of methods to make hydrazine derivatives containing an *ortho*-nitro- substituent. There are currently only 12 references (SciFinder) to these species in the literature. Begtrup recently reviewed⁸ the synthetic routes to 1,1-diarylhydrazines with the synthesis of *o*-nitrophenyl derivatives only being achieved by Hofmann rearrangement in work by Murakami⁹ and by reaction with hydroxylamine hydrochloride as reported by Berezin¹⁰ and later by Bodzioch¹¹ using similar synthetic schemes (Figure 6-5).

ROUTE A



ROUTE B

Figure 6-5: Synthetic routes to 1-(2-nitrophenyl)-1-phenylhydrazine.

In the current chapter, I describe the reactions of NDPH and its Schiff's base with salicylaldehyde as a potential source of N-heterocycles and as an electron-deficient ligand for transition metals.

6.3 Results and Discussion

There is a myriad of methods described in the literature for the synthesis of 1-phenylbenzotriazole. Most of these methods, however, involve complicated starting materials such as the sulfonamides described by Liu¹² or exotic catalysts that require the use of expensive reagents and metals¹³. One method described here for the first time, which was inspired the reaction in Figure 6-3, is the Cadogan cyclization of suitable hydrazines (Figure 6-6).

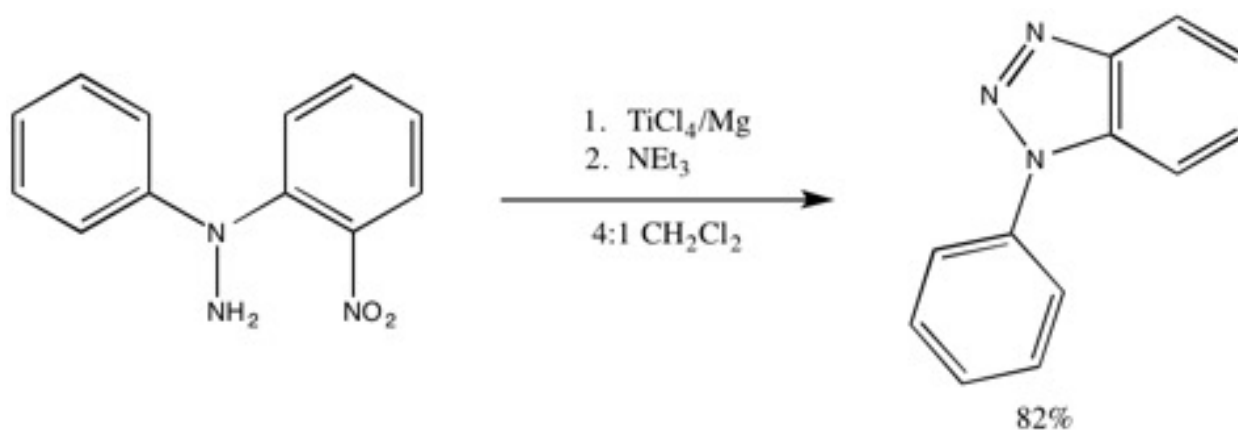


Figure 6-6: Synthesis of 1-phenylbenzotriazole via Cadogan cyclization of NDPH.

This reductive cyclization of -nitroarenes has shown promise in the formation of N-heterocycles. In this rearrangement, an oxygen scavenger deoxygenates a -nitro group to produce an electron deficient -nitroso or -nitreno species, which is then able to condense to form the final heterocyclic product. While phosphites are the usual reagents used as the oxygen scavengers in this reaction as shown by the in-depth work by Meriřor¹⁴ on the subject, studies by Entwistle¹⁵ have shown low-valent titanium reagents to be even more useful in the reduction of nitrosamines. Lin has also shown C-N bond formation when Ti(II) reagents are used in basic medium¹⁶. This procedure provides a more accessible route to the pure final product. The ionic impurities generated in this reaction can be removed by simple extraction from the reaction

mixture while the original phosphite-based methodologies require high temperatures and result in inevitable product degradation necessitating more complicated separation techniques¹⁷. Employing the mechanistic knowledge of Merișor to the Lin method yields two possible mechanistic routes for the reaction in Figure 6-7.

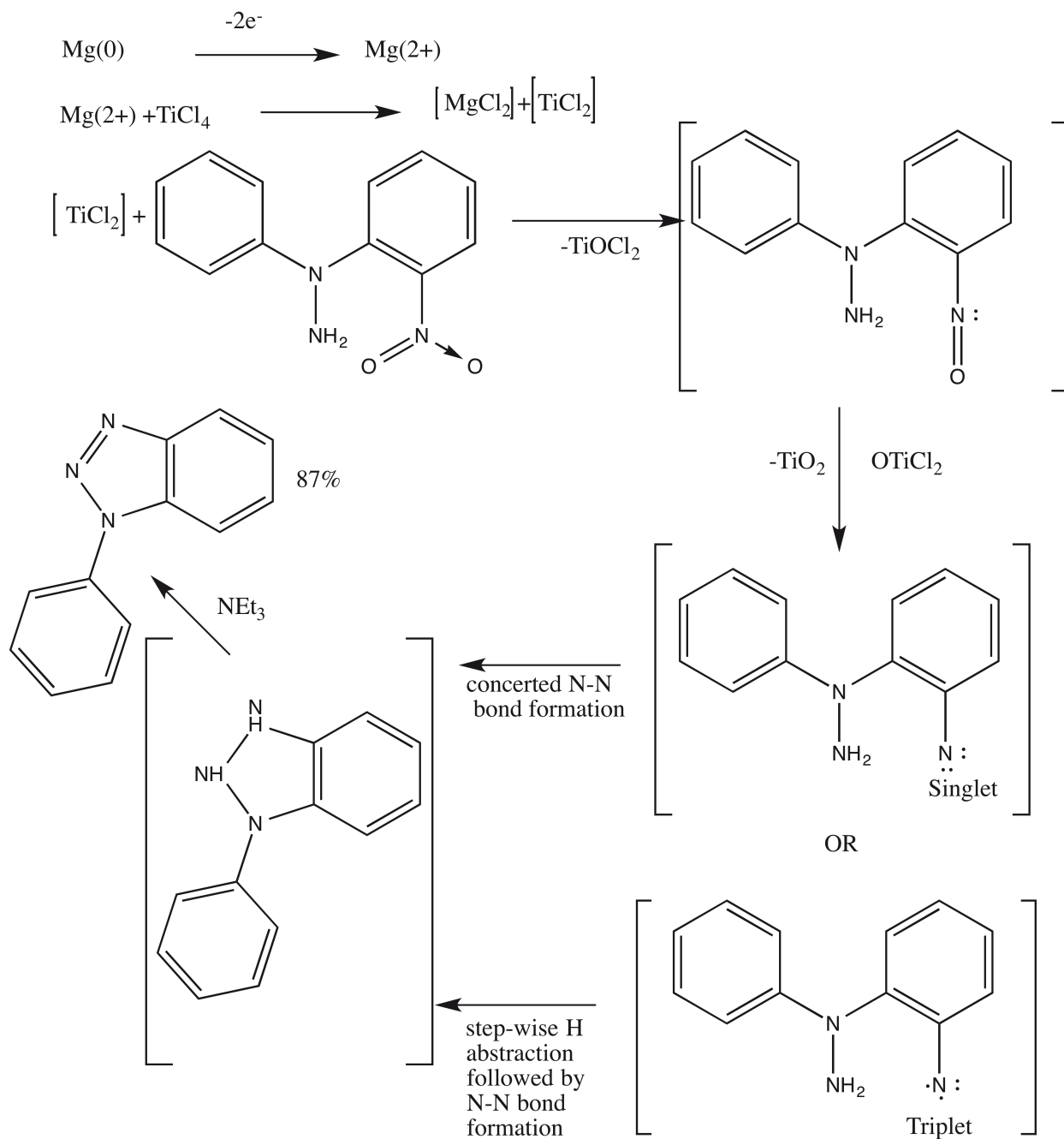


Figure 6-7: Possible mechanisms for benzotriazole formation from NDPH.

Indeed the reaction of NDPH under the conditions of Lin produces the desired product in high yield and purity. By simple extraction, without the need for chromatographic separation, the pure compound can be obtained with no trace of the 2-regioisomer. Analysis of the pure compound by single-crystal X-ray diffraction showed it to be a different polymorph from that which was reported previously¹⁸. The compound crystallized in the space group P_{212121} with 4 molecules per unit cell (Figure 6-8).

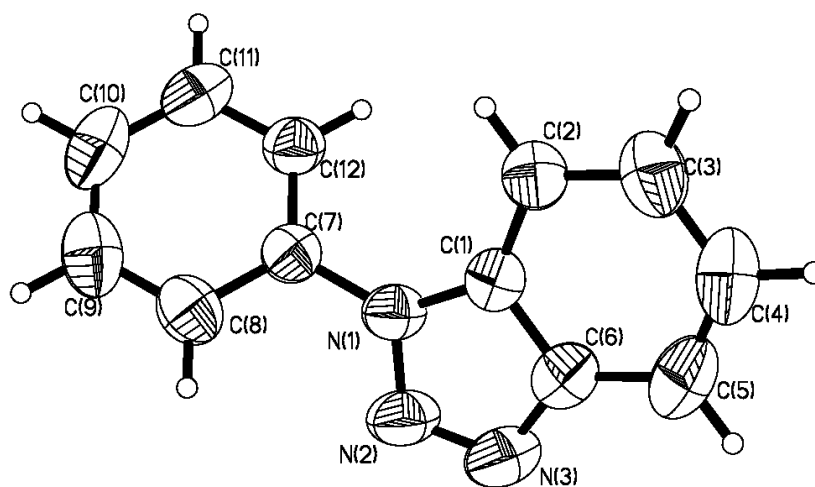
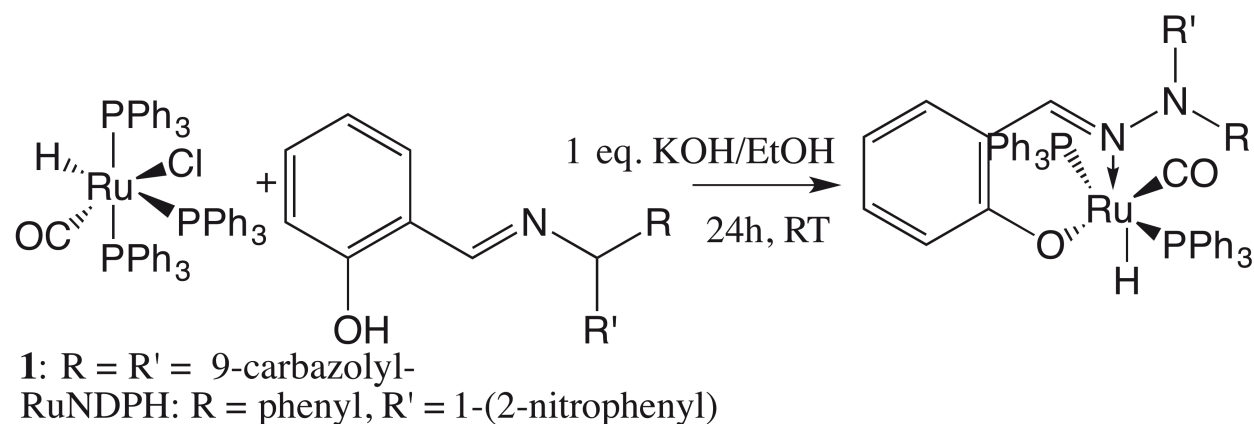


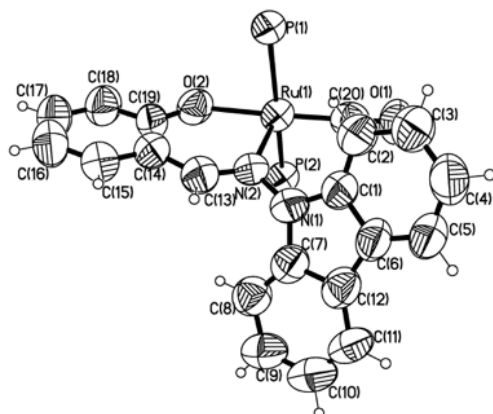
Figure 6-8: New polymorph of 1-phenylbenzotriazole. Selected metric parameters include N(1)-N(2) 1.363(2) Å, N(1)-C(7) 1.424(2) Å, N(1)-N(2)-N(3) 108.90(15)°, C(1)-N(1)-C(7)-C(8) -136.78(17)°.

To evaluate the ligand properties of the hydrazines described in this thesis, the adducts of AC and NDPH with salicylaldehyde were chosen as candidate compounds, since they would benefit from the chelate effect over the other derivatives and because a nickel compound of the AC-based compound was previously described as being useful in olefin polymerization reactions³. Based on the fact that nickel(II) complexes tend to form isolable polymers with N-heterocyclic ligands owing to the formation of supramolecular networks¹⁹, Ru(CO)(Cl)(H)(PPh₃)₃ was chosen as the candidate metal complex for the reaction with the hydrazine derivatives based on the strength of N-Ru bonds in characterized nitrenium ion complexes (Table 1-4). The reaction was carried out according to Scheme 6-1.

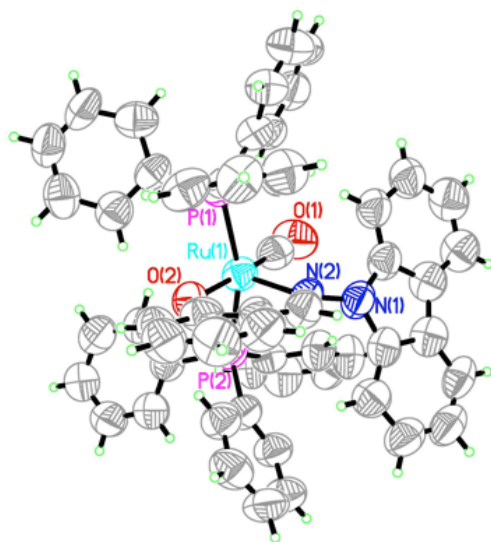


Scheme 6-1: Formation of salicylaldehyde ruthenium complexes of synthesized hydrazine derivatives.

Reaction of the carbazole-based derivative according to the above scheme yielded the corresponding complex in 86% yield. Recrystallization by slow-evaporation from a dichloromethane:methanol (1:20) solution yielded X-ray quality crystals (Figure 6-9).



(a)



(b)

Figure 6-9 (a): ORTEP representation of (1). Triphenylphosphine phenyl rings omitted for clarity. Selected geometric parameters are Ru(1) - N(1) 2.28(1) Å, Ru(1) - P(1) 2.437(8) Å, N(1) - N(2) 1.45(2) Å, Ru(1) - N(2) - N(1) - C(7) -108.5(9)°, Ru(1) - O(2) - C(19) - C(18) 174.3(7)°, distance of N(1) from plane 0.096 Å, distance of N(2) from plane 0.007 Å. (b) Full ORTEP of (1) showing steric crowding and bending of phosphines from ideal axial geometry.

This structure has several noteworthy features. First is the steric crowding about the metal centre as a result of the phosphine ligands and the rigidity of the carbazole ligand. The consequences of this crowding are bending of the phosphines from ideal 180° axial geometries to an angle of $160.98(9)^\circ$ toward the less encumbered region where the hydride is bound. Since N(2) is sp^2 -hybridized with the sum of the angles about it totalling $360(1)^\circ$, there must be only small N-Ru orbital overlap with no π -bonding. This is supported by the $\nu(\text{CO})$ value of 1919 cm^{-1} and a significant increase in shielding effect on the hydride NMR signal, consistent with decreased π -backbonding to the CO ligand and more electron density at ruthenium. There is also a dramatic increase in N-N bond length from $1.399(16)\text{ \AA}$ in the free ligand (Chapter 5) to $1.45(2)\text{ \AA}$ in this ruthenium complex. An explanation for these results is that the increased steric encumbrance at the metal does not allow the proper orientation of the ligands to engage in π -type bonding interactions. As a result, it can be concluded that these ligands are poor π -acceptors in the organometallic framework studied here. With diminished π -acceptor interactions, it is no surprise that the reaction of the NDPH-salicylaldehyde adduct was unsuccessful. As shown in Chapters 4 and 5, because of the mobility of its Ar_2 system, this compound is more sterically demanding than its analogue derived from AC. This increased bulk would hinder its reaction with the already crowded $\text{Ru}(\text{CO})(\text{Cl})(\text{H})(\text{PPh}_3)_3$ to form the desired chelate.

6.4 Conclusions

The condensation of NDPH to form 1-phenylbenzotriazole as well as the reactions of the salicylaldehyde condensation products of NDPH and AC with a ruthenium complex has been explored. NDPH is capable of forming 1-phenylbenzotriazole under Cadogan cyclization conditions using TiCl_4 and magnesium metal as an oxygen scavenger and reducing agent, respectively. This synthetic

methodology to produce 1-phenylbenzotriazole is advantageous in that it requires no chromatographic separation for the isolation of the pure product and no mixture of 1- and 2-regioisomers is produced.

Reaction of the salicylaldehyde Schiff bases of NDPH and AC, respectively, with $\text{Ru(H)(CO)(Cl)(PPh}_3)_3$ has shown these compounds to be very poor ligands, exhibiting very little σ -donor or π -acceptor capability. This behaviour contrasts that seen in metal complexes of triazolium species. This may, of course, be a result of the increased steric demand at the metal centre due to crowding by the phosphine ligands and studies would need to be carried out on equally crowded metal centres for adequate comparison. Such weak bi-dentate ligands may prove useful for catalytic applications and their evaluation as olefin polymerization catalysts could be interesting.

6.5 Experimental

6.5.1 General Methods

Dichloromethane and THF were continuously dried over a column of SiO_2 . All other reagents and solvents were obtained from commercial sources and were used as received. 9-nitrosocarbazole was synthesized following the method of Parakka²⁰ and was used without further purification. NDPH and salicylaldehyde derivatives of AC and NDPH were used from syntheses in previous chapters without further purification. ^1H - and ^{13}C -NMR spectra were recorded on 300 and 500 MHz Varian spectrometers. High-resolution mass spectra (HRMS) were measured by electrospray techniques with a time-of-flight detector (ESI/TOF). Melting points were determined using a micro-melting apparatus and are calibration-corrected.

6.5.2 Syntheses

1-Phenylbenzotriazole

A titanium(II) reagent was prepared according to the method of Lin as follows. To a 3-necked flask under $N_2(g)$ was added iron powder (.2330 g, 4.2 mmol) and dry THF (10mL). Titanium(IV) chloride (0.45 mL, 4.1 mmol) was added dropwise and a green solid was seen. The reaction was heated to reflux for 2 h. After 1 h, the solution had adopted a dark red colour. After the formation of the Ti(II) reagent, the reaction mixture was cooled to room temperature and NDPH (110 mg, 0.48 mmol) was added along with 10 mL of triethylamine. This mixture was then refluxed for an additional 2 h, cooled and left to stir at room temperature for 3 days. The solution was supplemented with 15 mL of 1:1 HCl : water (v:v) *CAUTION!* Violent reaction occurs! Add slowly. And the resulting solution was stirred for 2 hours at room temperature. Extraction (3 X 50 mL) with diethyl ether, drying ($MgSO_4$), evaporation under reduced pressure and recrystallization from 1:1 diethyl ether : hexanes furnished the pure crystalline compound. Yield: 82 mg (0.42 mol, 87.5%). m.p. 89–90 (lit.²¹ 89–90); Anal. Calcd. for $C_{12}H_9N_3$: C, 73.83%; H, 4.65%; N, 21.52%; Found: C, 73.75%; H, 4.62%; N, 21.57%.

Synthesis of (1)

To a solution of (0.11 mmol) in methanol (20 mL) was added 1 eq. of 0.1 M potassium hydroxide and the solution was stirred at room temperature for 1 h. $Ru(H)(CO)(Cl)(PPh_3)_3$ (0.101 g, 0.11 mmol) was added and the resulting suspension was stirred for 24 h at room temperature. Filtration of the resulting canary yellow solution yielded a crude product in 0.086 g (0.091 mmol, 83%). Recrystallization from dichloromethane-doped methanol at $-20^\circ C$ yielded the crystalline product as mustard yellow blocks. Yield 0.053 g (0.056 mmol, 54%). m.p. 150–151 $^\circ C$; 1H -NMR (400 MHz, C_6D_6) δ (ppm): 6.07 (t, 1H, J = 6.80 Hz), 6.10 (d, 1H, J = 8.00 Hz), 6.43 (d, 1H, J = 8.40 Hz), 6.84 – 6.95 (m, 20H), 7.12 (t, 2H, J = 7.20 Hz), 7.15 (s, 20H), 7.28 (d, 2H, J = 8.00

Hz), 7.67-7.72 (m, 12 H), 7.84 (s, 1H), 8.00 (d, 2H, $J = 7.60$ Hz); ^{31}P NMR (400 MHz, C_6D_6) δ (ppm): 37.45 (s).; IR (KBr, cm^{-1}): 517 (s), 735 (s), 743 (s), 841 (s), 999 (vw), 1024 (vw), 1070 (vw), 1092 (m), 1148 (w), 1186 (w), 1228 (w), 1264 (vw), 1314 (w), 1333 (m), 1361 (vw), 1433 (s), 1439 (s), 1462 (w), 1480 (m), 1526 (m), 1581 (w), 1604 (s), 1919 (vs), 2023 (w), 3053 (w); HRMS calcd. for $\text{C}_{56}\text{H}_{45}\text{N}_2\text{O}_2\text{P}_2\text{Ru}$: 941.19943, Found: 941.19864; Anal. Calcd. for $\text{C}_{56}\text{H}_{44}\text{N}_2\text{O}_2\text{P}_2\text{Ru}$: C, 71.56%; H, 4.72%; N, 2.98%; Found: C, 71.05%; H, 5.02%; N, 2.83%.

6.5.3 X-ray Crystallography

The X-ray diffraction data were measured with graphite monochromated Mo $\text{K}\alpha$ radiation ($\lambda = 0.71073$ Å) on crystals that were attached to a mitogen mount with viscous paratone N oil. The structures were solved by direct methods on an absorption-corrected model generated by SADABS. Refinement was achieved by a full-matrix least-squares procedure based on F^2 . The hydrogen atoms were located at calculated positions.

6.6 Acknowledgements

This research was supported by NSERC discovery grants to D.S.B. and I.S.B. The authors are grateful to Dr. Alexander Wahba and Nadim Saade for mass spectrometry analysis.

6.7 References

1. Aldeco-Perez, E. J.; Alvarez-Toledano, C.; Toscano, A.; Garcia-Estrada, J. G.; Penierres-Carrillo, J. G., Reaction of arylhydrazines with an α -alkynyl-carbonyl compound: an unexpected hydration reaction. *Tetrahedron Lett.* **2008**, *49* (18), 2942-2945.

2. Tonks, I. A.; Durrell, A. C.; Gray, H. B.; Bercaw, J. E., Groups 5 and 6 Terminal Hydrazido(2-) Complexes: N β Substituent Effects on Ligand-to-Metal Charge-Transfer Energies and Oxidation States. *J. Am. Chem. Soc.* **2012**, *134* (17), 7301-7304.
3. Kristen, M. O.; Bildstein, B.; Amort, C.; Malaun, M. Ligands, complex compounds and their use for polymerizing olefins. WO2002008236A1, 2002.
4. Zincke, T.; Schwarz, P., On Azimidole. [machine translation]. *Ann.* **1900**, *311*, 329-40.
5. (a) Convers, E.; Tye, H.; Whittaker, M., Preparation and evaluation of bipyridyl-tagged reagents and scavengers. *Tetrahedron* **2004**, *60* (39), 8729-8738; (b) Leonard, N. J.; Golankiewicz, K., Thermolysis of substituted 1-acetoxybenzotriazoles. Carbon-to-oxygen migration of an alkyl group. *J. Org. Chem.* **1969**, *34* (2), 359-65; (c) Takeda, K.; Tsuboyama, K.; Yamaguchi, K.; Ogura, H., 1,1'-Bis[6-(trifluoromethyl)benzotriazolyl] oxalate (BTBO): a new reactive coupling reagent for the synthesis of dipeptides, esters, and thio esters. *J. Org. Chem.* **1985**, *50* (2), 273-5; (d) Schiemann, K.; Showalter, H. D. H., Development of Polymer-Supported Benzotriazole as a Novel Traceless Linker for Solid-Phase Organic Synthesis. *J. Org. Chem.* **1999**, *64* (13), 4972-4975; (e) Scicinski, J. J.; Congreve, M. S.; Jamieson, C.; Ley, S. V.; Newman, E. S.; Vinader, V. M.; Carr, R. A. E., Solid-Phase Development of a 1-Hydroxybenzotriazole Linker for Heterocycle Synthesis Using Analytical Constructs. *J. Comb. Chem.* **2001**, *3* (4), 387-396; (f) Bhattacharya, S.; Kumar, V. P., Ester Cleavage Properties of Synthetic Hydroxybenzotriazoles in Cationic Monovalent and Gemini Surfactant Micelles. *Langmuir* **2005**, *21* (1), 71-78; (g) Augustynowicz-Kopec, E.; Zwolska, Z.; Orzeszko, A.; Kazimierzuk, Z., Synthesis and antimycobacterial activity of selected [(nitrobenzyl)oxy]benzotriazoles. *Acta Pol. Pharm.* **2008**, *65* (4), 435-439; (h) Fu, J.; Yang, Y.; Zhang, X.-W.; Mao, W.-J.; Zhang, Z.-M.; Zhu, H.-L., Discovery of 1H-benzo[d][1,2,3]triazol-1-yl 3,4,5-trimethoxybenzoate as a potential antiproliferative agent by inhibiting histone deacetylase. *Bioorg. Med. Chem.* **2010**, *18* (24), 8457-8462; (i)

Yu, B.; Huang, Z.; Zhang, M.; Dillard, D. R.; Ji, H., Rational Design of Small-Molecule Inhibitors for β -Catenin/T-Cell Factor Protein-Protein Interactions by Bioisostere Replacement. *ACS Chem. Biol.* **2013**, *8* (3), 524-529; (j) Carta, A.; Briguglio, I.; Piras, S.; Corona, P.; Boatto, G.; Nieddu, M.; Giunchedi, P.; Marongiu, M. E.; Giliberti, G.; Iuliano, F.; Blois, S.; Ibba, C.; Busonera, B.; La Colla, P., Quinoline tricyclic derivatives. Design, synthesis and evaluation of the antiviral activity of three new classes of RNA-dependent RNA polymerase inhibitors. *Bioorg. Med. Chem.* **2011**, *19* (23), 7070-7084; (k) Kumar, M.; Scobie, M.; Mashuta, M. S.; Hammond, G. B.; Xu, B., Gold-Catalyzed Addition of N-Hydroxy Heterocycles to Alkynes and Subsequent 3,3-Sigmatropic Rearrangement. *Org. Lett.* **2013**, *15* (4), 724-727; (l) Zhu, H.; Fu, J.; Zhang, Z. Preparation of benzotriazole derivatives as anti-proliferative agents. CN101928254A, 2010; (m) Tang, P.; Duan, Z.; Yang, Y., Synthesis of 1-hydroxy benzotriazole by phase-transfer catalysis. *Jingxi Huagong Zhongjianti* **2007**, *37* (1), 64-66; (n) Sehring, R.; Raddatz, E.; Drandarevski, C. Benzotriazoles and their use as biocidal substances. DE3238804A1, 1984; (o) Ochal, Z.; Kaminski, R., Transformations of bromodichloromethyl 4-chlorophenyl sulfone into new compounds with potential pesticidal activity. *Pol. J. Appl. Chem.* **2005**, *49* (3), 215-225; (p) Ochal, Z.; Bretner, M.; Wolinowska, R.; Tyski, S., Synthesis and in vitro Antibacterial Activity of 5-Halogenomethylsulfonyl- Benzimidazole and Benzotriazole Derivatives. *Med. Chem. (Sharjah, United Arab Emirates)* **2013**, *9* (8), 1129-1136; (q) Nardi, A.; Erichsen, H. K.; Peters, D.; Troelsen, K. d. L. L. Preparation of benzotriazole derivatives useful for the treatment of CNS disorders. WO2010081898A1, 2010; (r) Mizerski, A.; Ochal, Z.; Zalecki, S.; Ejmowski, Z., Transformations of 4-chlorophenyl difluoromethyl sulfone into new compounds with potential pesticidal activity. *Pestycydy (Warsaw)* **2001**, (1-2), 29-41; (s) McCall, J.; Kelly, R. C.; Romero, D. L. Pyrazolopyrimidinone compounds for the inhibition of PASK and their preparation. WO2014066795A1, 2014; (t) Liu, C.; Wang, W.; Ge, J., Improvement of solution synthesis of benzotriazole. *Huagong Jishu Yu Kaifa*

2010, 39 (10), 16-19; (u) Lakshman, M. K.; Bae, S. Preparation of convertible nucleoside derivatives for use in aryl nucleophilic substitution displacement reactions. WO2008045535A2, 2008; (v) Kehler, J.; Puschl, A.; Dahl, O., Improved syntheses of 1-hydroxy-4-nitro-6-trifluoromethylbenzotriazole and 1-hydroxy-4,6-dinitrobenzotriazole. *Acta Chem. Scand.* **1996**, 50 (12), 1171-1173; (w) Ji, H.; Yu, B.; Zhang, M.; Guo, W. Preparation of substituted 1H-indazol-1-ol analogs as inhibitors of beta-catenin/Tcf protein-protein interactions. WO2013120045A1, 2013; (x) Itoh, F.; Kunitomo, J.; Kobayashi, H.; Kimura, E.; Saitoh, M.; Kawamoto, T.; Iwashita, H.; Murase, K. Preparation of 2-heterocyclyl-1,3,4-oxadiazole derivatives as glycogen synthase kinase-3 β (GSK-3 β) inhibitors. WO2008016123A1, 2008; (y) Huang, H.; Huang, K.; Wang, H.; Huang, X. Process for synthesizing 1-hydroxy benzotriazole. CN103450103A, 2013; (z) Hael, N.; Austel, V.; Heider, J.; Reiffen, M.; Diederer, W.; Haarmann, W. Benzotriazoles and their use as drugs. DE3129447A1, 1983; (aa) Hagedorn, F.; Fiege, H.; Dorlars, A. Process for the preparation of 1-hydroxybenzotriazoles. DE19535244A1, 1997; (ab) Grigor'ev, E. I.; Zhil'tsov, O. S., Use of 1-hydroxybenzotriazole-based polymeric activated esters in peptide synthesis. *Zh. Org. Khim.* **1989**, 25 (9), 1963-7; (ac) Fathalla, M. F.; Khattab, S. N., Spectrophotometric determination of pKa's of 1-hydroxybenzotriazole and oxime derivatives in 95% acetonitrile-water. *J. Chem. Soc. Pak.* **2011**, 33 (3), 324-332; (ad) Dabhade, P. S.; Jain, N. P., Synthesis and evaluation of antifungal activity of benzotriazole derivatives. *Asian J. Biomed. Pharm. Sci.* **2013**, 3 (17), 29-34, 6 pp; (ae) Chen, S. A process for preparing benzotriazole. CN102875483A, 2013; (af) Carta, A.; Piras, S.; Boatto, G.; Paglietti, G., 1H,6H-Triazolo[4,5-e]benzotriazole 3-oxides and 5,5'-(Z)-diazene-1,2-diylbis(2-methyl-2H-1,2,3-benzotriazole) derived from chloronitrobenzotriazoles and hydrazine. *Heterocycles* **2005**, 65 (10), 2471-2481; (ag) Carta, A.; Paglietti, G., A new synthesis of triazolo[4,5-g]quinolines and unexpected ring reduced products by treatment with hydrazine hydrate. *ARKIVOC (Gainesville, FL, United States)* **2004**, (5), 66-75; (ah) Carta, A.;

- Boatto, G.; Paglietti, G.; Poni, G.; Setzu, M. G.; Caredda, P., Synthesis and biological evaluation of triazolo[4,5-g]quinolines, imidazo[4,5-g]quinolines and pyrido[2,3-g]quinoxaline. Part II. *Heterocycles* **2003**, *60* (4), 833-842; (ai) Bruncko, M.; Ding, H.; Doherty, G. A.; Elmore, S. W.; Hasvold, L.; Hexamer, L.; Kunzer, A. R.; Mantei, R. A.; McClellan, W. J.; Park, C. H.; Park, C.-M.; Petros, A. M.; Song, X.; Souers, A. J.; Sullivan, G. M.; Tao, Z.-F.; Wang, G. T.; Wang, L.; Wang, X.; Wendt, M. D.; Hansen, T. M. Preparation of N-acylsulfonamide Bcl-2-selective apoptosis-inducing agents for the treatment of cancer and immune diseases. US20100298321A1, 2010; (aj) Arnold, M. B.; Bender, D. M.; Cantrell, B. E.; Jones, W. D.; Ornstein, P. L.; Simon, R. L.; Smith, E. C. R.; Tromiczak, E. G.; Zarrinmayeh, H.; Zimmerman, D. M. Preparation of sulfonamides for potentiating of glutamate receptor function. WO2000006148A1, 2000; (ak) Anthony, N. J.; Gomez, R.; Jolly, S. M.; Su, D.-S.; Lim, J. Preparation of substituted indazoles, benzotriazoles and related bicyclic compounds as non-nucleoside reverse transcriptase inhibitors. WO2008076225A2, 2008; (al) Anthony, N. J.; Gomez, R.; Jolly, S. M. 1-(1H-Pyrazolo[3,4-b]pyridin-3-ylmethyl)-1H-indazole derivatives as non-nucleoside reverse transcriptase inhibitors and their preparation, pharmaceutical compositions and use in the treatment of HIV infection. WO2008076223A1, 2008.
6. Gomez, R.; Jolly, S. J.; Williams, T.; Vacca, J. P.; Torrent, M.; McGaughey, G.; Lai, M.-T.; Felock, P.; Munshi, V.; DiStefano, D.; Flynn, J.; Miller, M.; Yan, Y.; Reid, J.; Sanchez, R.; Liang, Y.; Paton, B.; Wan, B.-L.; Anthony, N., Design and Synthesis of Conformationally Constrained Non-Nucleoside Inhibitors of Reverse Transcriptase. *J. Med. Chem.* **2011**, *54* (22), 7920-7933.
7. Le, Z.-G.; Chen, Z.-C.; Hu, Y.; Zheng, Q.-G., Organic reactions in ionic liquids. An efficient method for the N-alkylation of benzotriazole. *J. Chem. Res.* **2004**, (5), 344-346.
8. Begtrup, M.; Rasmussen, L. K., Arylhydrazines. *Science of Synthesis*. **2007**, *31b*, 1773-1826.

9. Murakami, Y.; Yokoyama, Y.; Sasakura, C.; Tamagawa, M., An Efficient Synthesis of 1,1-Disubstituted Hydrazines. *Chem. Pharm. Bull.* **1983**, *31* (2), 423-423.
10. Berezin, A. A.; Zissimou, G.; Constantinides, C. P.; Beldjoudi, Y.; Rawson, J. M.; Koutentis, P. A., Route to Benzo- and Pyrido-Fused 1,2,4-Triazinyl Radicals via N'-(Het)aryl-N'-[2-nitro(het)aryl]hydrazides. *J. Org. Chem.* **2014**, *79* (1), 314-327.
11. Bodzioch, A.; Zheng, M.; Kaszynski, P.; Utecht, G., Functional Group Transformations in Derivatives of 1,4-Dihydrobenzo[1,2,4]triazinyl Radical. *J. Org. Chem.* **2014**, *79* (16), 7294-7310.
12. Liu, Z.; Larock, R. C., Facile N-Arylation of Amines and Sulfonamides and O-Arylation of Phenols and Arenecarboxylic Acids. *J. Org. Chem.* **2006**, *71* (8), 3198-3209.
13. (a) Beletskaya, I. P.; Davydov, D. V.; Moreno-Manas, M., Pd- and Cu-catalyzed selective arylation of benzotriazole by diaryliodonium salts in water. *Tetrahedron Lett.* **1998**, *39* (31), 5621-5622; (b) Buchwald, S. L.; Klapars, A.; Antilla, J. C.; Job, G. E.; Wolter, M.; Kwong, F. Y.; Nordmann, G.; Hennessy, E. J. Copper-catalyzed formation of carbon-heteroatom and carbon-carbon bonds by arylation and vinylation of amines, amides, hydrazides, heterocycles, alcohols, enolates, and malonates, using aryl, heteroaryl, and vinyl halides and analogs. WO2002085838A1, 2002; (c) Mukhopadhyay, C.; Tapaswi, P. K.; Butcher, R. J., A ligand-free copper (I) catalysed intramolecular N-arylation of diazoaminobenzenes in PEG-water: an expeditious protocol towards regiospecific 1-aryl benzotriazoles. *Org. Biomol. Chem.* **2010**, *8* (20), 4720-4729.
14. Merisor, E. Synthesis of N-heterocycles via intramolecular reductive cyclizations of ω -nitroalkenes. 2008.
15. Entwistle, I. D.; Johnstone, R. A. W.; Wilby, A. H., Metal-assisted reactions. Part 11. Rapid reduction of N-nitrosamines to N,N-disubstituted hydrazines; the utility of some low-valent titanium reagents. *Tetrahedron* **1982**, *38* (3), 419-23.

16. Lin, W.; Hu, M.-H.; Feng, X.; Cao, C.-P.; Huang, Z.-B.; Shi, D.-Q., An efficient and convenient synthesis of heterocycle-fused indazoles via the N–N bond forming reaction of nitroarenes induced by low-valent titanium reagent. *Tetrahedron* **2013**, *69* (32), 6721-6726.
17. Song, J. J.; Reeves, J. T.; Fandrick, D. R.; Tan, Z.; Yee, N. K.; Senanayake, C. H., Construction of the indole nucleus through C-H functionalization reactions. *ARKIVOC (Gainesville, FL, United States)* **2010**, (1), 390-449.
18. Takagi, K.; Al-Amin, M.; Hoshiya, N.; Wouters, J.; Sugimoto, H.; Shiro, Y.; Fukuda, H.; Shuto, S.; Arisawa, M., Palladium-Nanoparticle-Catalyzed 1,7-Palladium Migration Involving C–H Activation, Followed by Intramolecular Amination: Regioselective Synthesis of N1-Arylbenzotriazoles and an Evaluation of Their Inhibitory Activity toward Indoleamine 2,3-Dioxygenase. *J. Org. Chem.* **2014**, *79* (13), 6366-6371.
19. Wang, F.; Wu, X.-Y.; Yu, R.-M.; Zhao, Z.-G.; Lu, C.-Z., Supramolecular networks with 1-substituted benzotriazole ligands and transition metals. *J. Coord. Chem.* **2009**, *62* (20), 3296-3305.
20. Parakka, J. P.; Nugara, P. N.; Lakshmikantham, M. V.; Belmore, K. A.; Cava, M. P., The oxidation of 3-aminocarbazole and its N-ethyl derivative. *Synth. Met.* **1992**, *47* (2), 141-9.
21. Reynolds, G. A., Reaction of organic azides with benzyne. *J. Org. Chem.* **1964**, *29* (12), 3733-4.

Summary, Contribution to Original Knowledge and Future Research

7.1 Summary

The chemistry of electron-deficient nitrogen is a relatively unexplored field of chemistry. Specifically, N-heterocyclic triazolium cations have only been sparsely studied, since facile methods to produce them are still in the making. Likewise, nitrene intermediates are useful species but there is much debate as to their involvement in many of the reactions used to generate them and optimal conditions to control their reactivity are still being sought. These species are rare compounds that are able to engage in insertion reactions like their analogous carbenes, but also present the possibility for redox non-innocence, a facet not common to carbene chemistry.

The first structurally characterized N-heterocyclic nitrene complexes were reported in 2011 and it was hypothesized that similar triazolium-based ligand systems without chelating arms could be used to make similar metal complexes with short M-nitrene bonds. Later reports of similar complexes with other transition metals revealed the shortest such bonds were found in complexes of nickel and ruthenium (Table 1-4) and the weakest bonds were formed with molybdenum. We hypothesized that creation of a nitrene from reductive cyclization of 1-(2-nitrophenyl)-1-phenylhydrazine (NDPH) would yield N-phenylbenzotriazole-3-oxide in analogy to the reaction of hydrazine and benzotriazole (Figure 6-3). With this basic idea in mind, we set about the study of the synthesis of NDPH, which had only been poorly described, the electronic properties of its derivatives and its cyclization. The derivatives could be contrasted to the more electron-rich derivatives of 9-aminocarbazole (AC) to assess the effect of electron-

deficiency through conjugation with an aromatic system on nitrogen in comparison to the nitrenes.

In Chapter 2, we demonstrated the nucleophilicity of the single-nitrogen heterocycles pyrrole and indole and contrasted them to show the effect of conjugation of the pyrrole nitrogen with an extended aromatic system. The indole analogues did not show self-polymerization behaviour and were considerably more thermally stable than the pyrroles. We reported the first solid-state structure of $\text{Ph}_3\text{Si}(\text{pyrrole})$, which showed disordering of the pyrrole and aryl rings in the solid-state and were able to comment on the lability of the M-N bond in complexes of these heterocycles with the group 14 metals.

In Chapter 3, the reactivity of the pyrrolides and indolides could be contrasted with the chemistry of 1-(2-nitrophenyl)-phenylamine, where the nitrogen atom is sp^2 -hybridized owing to its conjugation with the proximal *ortho*-nitro group. We concretely demonstrated the probable involvement of nitrene intermediates in the conversion of the latter amine into NDPH. We also provided the first structural basis for the key intermediates involved in the transformation of an amine by chlorosulfonyl isocyanate into its corresponding urea and subsequent Hofmann rearrangement to yield the analogous 1,1-diarylhydrazine. These intermediates included an unusual sulfimidate, which could be isolated in the solid-state by increasing the ionic strength and then decomposed by inhibiting the network of hydrogen bonds that constitutes its crystal lattice. In addition, we determined the first crystal structure of a 1,1-diarylhydrazine containing an electron-withdrawing substituent.

In Chapter 4, we synthesized some new derivatives of NDPH. These derivatives showed considerable variation in N-N bond length. Through single-crystal diffraction studies on each derivative, we were able to advance a theory that bonding in these systems is dominated primarily by enhanced σ -based effects with little to no π -

contribution. This allowed an N-N bond ranging in length from long and sp^3-sp^3 to short and sp^2-sp^2 hybridization that are independent of intermolecular interactions.

Chapter 5 allowed the comparison of σ -based bonding in 1,1-diarylhydrazines with bonding where π -effects were also possible. Comparison of single-crystal diffraction data for analogous derivatives of AC with their NDPH analogues allowed the conclusion that steric encumbrance in NDPH prevents π -contribution to the N-N bond strength, which can be rectified by fusing the aryl rings. This comparison is likened to the fusion of pyrrole to a benzene ring to form indole, which echoes the behaviour of the pyrrolide and indolide metal complexes of chapter 2, despite the possibility of N-N lone pair repulsion.

Lastly, in Chapter 6 the ability to use NDPH as a route to sp^2 -hybridized N-heterocycles was explored using a titanium-mediated Cadogan cyclization. The condensation of NDPH in the presence of a base and an oxygen scavenger did indeed produce 1-phenylbenzotriazole in high yield and purity. In addition, the use of NDPH derivatives as ligands was explored using the salicylaldehyde Schiff base and these were contrasted with the analogue derived from AC. Again, the increased steric demand of the NDPH adduct precluded complex formation; however, the carbazole-derived product was characterized by spectroscopic techniques and by single-crystal X-ray diffraction. The N-N and N-Ru and Ru-O bond lengths in this derivative are longer than any other similar ruthenium chelates that have been reported, showing the detrimental effects of extended aromaticity on the σ -donating and π -accepting abilities of these compounds in comparison to the 1,2,3-triazolium cations.

7.2 Future work

Having developed techniques for the efficient synthesis of stable electron-poor sp^2 -hybridized 1,1-diarylhydrazines and derivatives that can be used as possible chelates in transition metal complexes as well as for the facile synthesis of 1-phenylbenzotriazole, there are 2 important research goals that could be pursued. The first is to utilize the methods of Katritzky¹ for the formation of N-oxides to make especially delocalized benzotriazolium derivatives that might be used as nitrenium-based ligands for transition metals that do not contain chelating arms. If successful, this would represent a method of nitrenium ion-based ligand synthesis with considerable versatility that employs relatively inexpensive reagents and might prove useful in the synthesis of various materials for optical and catalytic applications. The second future direction for this research concerns the metal complex formation of the ligands derived from NDPH. While binding to $Ru(CO)(Cl)(H)(PPh_3)_3$ was unsuccessful most likely due to steric encumbrance at the metal centre, perhaps less sterically crowded ruthenium derivatives such as $RuBr_2[(CH_3)_2SO]_4$ described by Riley². With more labile dimethylsulfoxide ligands that should minimize sterics, perhaps complex formation would be feasible. In addition, the catalytic activity of the AC-derived ruthenium chelate for olefin polymerization should be investigated to ascertain the effectiveness of these new hydrazine-based ligands for catalytic applications.

7.3 References

1. Katritzky, A. R.; Maimait, R.; Denisenko, S. N.; Steel, P. J.; Akhmedov, N. G., Conversions by Dimethyldioxirane of 1-Alkylbenzotriazoles into 2-Alkyl-trans-4,5,6,7-diepoxy-4,5,6,7-tetrahydrobenzotriazoles. *J. Org. Chem.* **2001**, *66* (16), 5585-5589.

2. Riley, D. P., trans-Dibromotetrakis(dimethyl sulfoxide)ruthenium(II): A versatile starting material for the synthesis of ruthenium(II) complexes for use as molecular oxygen oxidation catalysts. *Inorg. Chim. Acta* **1985**, 99 (1), 5-11.

APPENDIX A

Table S1

Comparison of Theoretical Isotopic Patterns for Pyrrolides and Indolides with Observed Values

Compound	m/Z	Theoretical Intensity (%)	Observed Intensity (%)	Difference (%)
1	417	52.60	49.84	2.76
	418	15.10	16.04	0.94
	419	71.60	70.64	0.96
	420	39.70	39.62	0.08
	421	100.00	100.00	0.00
	422	27.30	27.25	0.05
	423	22.90	24.43	1.53
	424	5.80	-	-
	425	0.80	-	-
	426	0.10	-	-
	427	0.00	-	-
2	374	0.00	8.83	8.83
	375	100.00	100.00	0.00
	376	33.80	33.96	0.16
	377	8.80	8.70	0.10
	378	1.50	-	1.50
	379	0.20	-	0.20
	380	0.00	-	0.00
3	459	2.70	-	2.70
	460	0.80	-	0.80
	461	1.90	-	1.90
	462	1.50	-	1.50
	463	40.70	40.80	0.10
	464	32.90	33.21	0.31
	465	74.90	76.00	1.10
	466	44.10	44.25	0.15
	467	100.00	100.00	0.00
	468	27.10	27.27	0.17
	469	16.50	16.61	0.11

	470	4.00	-	4.00
	471	16.60	16.82	0.22
	472	4.70	-	4.70
	473	0.60	-	0.60
	474	0.10	-	0.10
4				
	367	53.50	53.08	0.42
	368	13.00	14.88	1.88
	369	72.20	71.05	1.15
	370	37.20	38.14	0.94
	371	100.00	100.00	0.00
	372	23.40	24.28	0.88
	373	22.20	21.99	0.21
	374	5.00	-	-
	375	0.60	-	-
	376	0.00	-	-
5				
	324	52.60	45.37	7.23
	325	100.00	100.00	0.00
	326	29.40	30.54	1.14
	327	7.40	7.56	0.16
6				
	413	41.40	39.58	1.82
	414	31.70	30.77	0.93
	415	74.90	71.48	3.42
	416	41.60	40.37	1.23
	417	100.00	100.00	0.00
	418	23.20	24.25	1.05
	419	15.80	22.00	6.20
	420	3.40	7.17	3.77
	421	16.70	25.91	9.21
	422	4.00	6.47	2.47

Theoretical isotopic patterns based on molecular formulae of the compounds **1 – 6** were obtained using the Sheffield ChemPuter:
[\[http://winter.group.shef.ac.uk/chemputer/isotopes.html\]](http://winter.group.shef.ac.uk/chemputer/isotopes.html).

Experimental results obtained are within 10% of theoretical values.

APPENDIX B

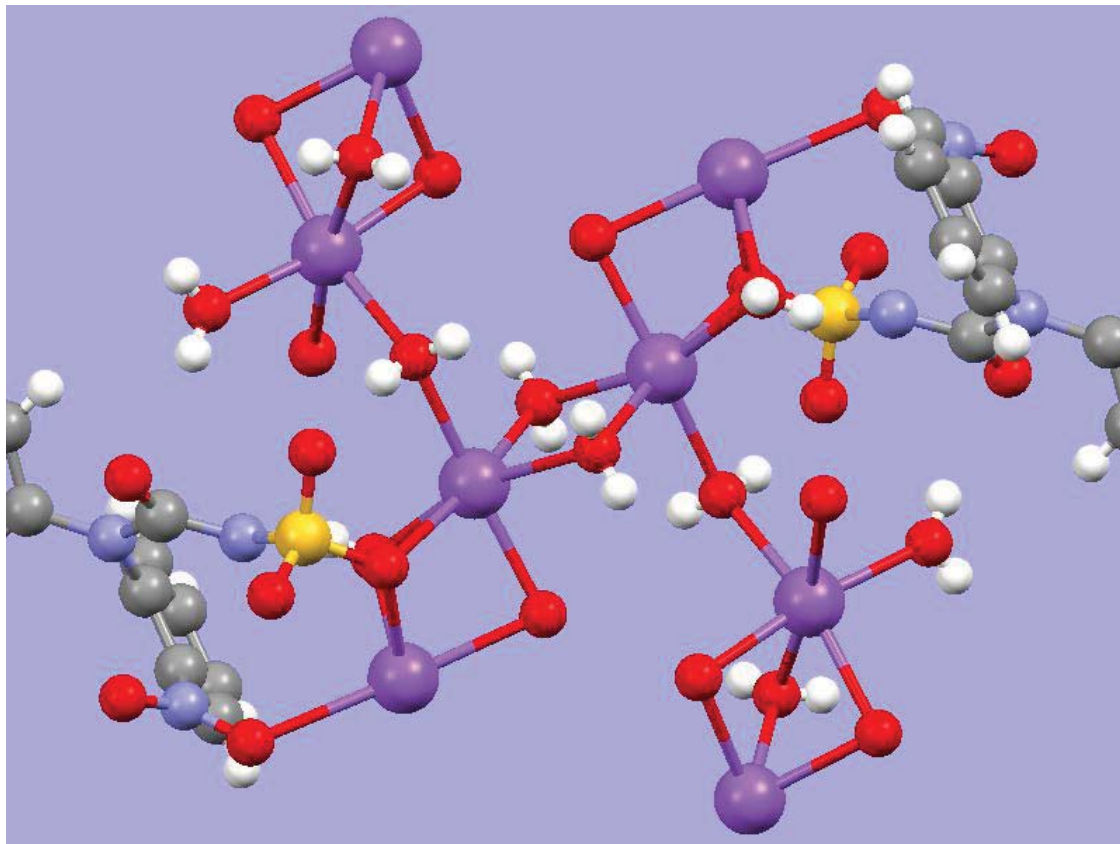


Figure S1 Hydrogen bonding and salt network for the sulfimide dianion in 1. Sodium cations are purple, and water as red with two hydrogens attached. The sulfimide dianions from adjacent cells also contribute as a chelate to one sodium and a bridge to an adjacent sodium. One of the waters also bridges two sodiums.

Density Functional Theoretical Results for the 2-NitrophenylPhenylAmine derivatives.

B3LYP/6-311++g** Results for the Optimized Ground State Structures.

Calculated Gas Phase Distance Matric for the Urea Derivative 2a

Distance matrix (angstroms):					
	1	2	3	4	5
1 N	0.000000				
2 N	2.350183	0.000000			
3 H	3.236996	1.008056	0.000000		
4 C	1.421755	2.775167	3.781645	0.000000	
5 C	2.497638	3.060078	4.004149	1.405684	0.000000
6 C	2.430878	3.788300	4.752357	1.401775	2.394395
7 C	3.768011	4.161198	5.052662	2.445879	1.393056
8 C	3.717553	4.738871	5.683719	2.435147	2.767516
9 H	2.612680	4.153588	5.045197	2.136608	3.373132
10 C	4.245862	4.894794	5.812828	2.825354	2.406550
11 H	4.629574	4.733507	5.527699	3.411367	2.135290
12 H	4.572600	5.633884	6.544876	3.409540	3.851230
13 H	5.328795	5.866067	6.743488	3.908396	3.388298
14 C	1.437888	3.673199	4.445923	2.446667	3.582612
15 C	2.445411	4.708367	5.529396	2.986929	3.809989
16 C	2.462196	4.302848	4.897833	3.566947	4.833396
17 C	3.722995	5.987860	6.753460	4.305112	5.164421
18 H	2.652297	4.725823	5.594829	2.813352	3.247984
19 C	3.732187	5.671870	6.243562	4.726493	5.957769
20 H	2.683116	3.988894	4.439063	3.827393	5.122227
21 C	4.228043	6.396445	7.062359	5.028867	6.100062
22 H	4.589210	6.836077	7.624765	4.996960	5.666887
23 H	4.603558	6.340066	6.809539	5.634457	6.916511
24 H	5.311980	7.467378	8.109541	6.082213	7.133475
25 C	1.406693	1.380167	2.010144	2.488542	3.181606
26 O	2.297621	2.276642	2.445534	3.593292	4.293374
27 H	2.574600	1.007982	1.712955	2.515123	2.755863
28 N	2.990833	3.072380	3.824097	2.524845	1.480778
29 O	2.877464	3.392047	4.078890	2.896035	2.316428
30 O	4.063570	3.519507	4.071757	3.527435	2.310010
6 C	0.000000				
7 C	2.779129	0.000000			
8 C	1.389434	2.404264	0.000000		
9 H	1.083181	3.862162	2.151985	0.000000	
10 C	2.415002	1.388484	1.395134	3.399140	0.000000
11 H	3.860659	1.081936	3.396542	4.943565	2.160287
12 H	2.142191	3.388912	1.083766	2.473054	2.154368
13 H	3.399145	2.144772	2.158469	4.298585	1.083046
14 C	3.026701	4.767139	4.346409	2.839171	5.076257
15 C	3.528022	4.864771	4.618298	3.509292	5.201142
16 C	3.846500	5.982666	5.202405	3.283881	6.137601
17 C	4.611211	6.130770	5.639253	4.379642	6.333019
18 H	3.519313	4.218363	4.400498	3.811698	4.708853
19 C	4.864525	7.050594	6.132639	4.209816	7.125343
20 H	4.062949	6.266946	5.428446	3.429822	6.398727
21 C	5.188488	7.117915	6.324222	4.683071	7.212796
22 H	5.290056	6.515241	6.152938	5.164227	6.726774
23 H	5.677822	8.002546	6.940447	4.903193	8.013627
24 H	6.166747	8.107408	7.239408	5.614947	8.151083
25 C	3.558237	4.490028	4.769204	3.719096	5.152343
26 O	4.618506	5.642825	5.896886	4.616789	6.332261
27 H	3.278270	3.610608	4.045189	3.730269	4.184889
28 N	3.776049	2.439311	4.244321	4.652926	3.727333
29 O	4.233385	3.444155	4.934235	4.945009	4.623433
30 O	4.668025	2.763294	4.915788	5.606654	4.134931
11 H	0.000000				
12 H	4.299952	0.000000			
13 H	2.493172	2.491796	0.000000		
14 C	5.658146	5.034729	6.131248	0.000000	
15 C	5.662920	5.298550	6.184276	1.395503	0.000000
16 C	6.924583	5.707534	7.174842	1.396153	2.418134
17 C	6.926696	6.152714	7.254502	2.413392	1.392893
18 H	4.894105	5.187840	5.646133	2.147014	1.082955
19 C	7.989797	6.516564	8.119208	2.411367	2.785319
20 H	7.217981	5.899131	7.434126	2.149720	3.397017
21 C	7.995115	6.716195	8.156490	2.790500	2.416165
22 H	7.220663	6.644434	7.568130	3.393259	2.145751
23 H	8.965915	7.232481	8.995640	3.391452	3.869380

24 H	8.973827	7.549899	9.054800	3.874457	3.398777
25 C	5.196791	5.640236	6.210889	2.452310	3.557060
26 O	6.307671	6.728517	7.398968	2.770178	3.846933
27 H	4.233974	4.895929	5.101252	3.973364	4.985383
28 N	2.594133	5.327672	4.581977	4.039865	4.154947
29 O	3.669804	5.993915	5.529633	3.596793	3.524865
30 O	2.475661	5.978295	4.805656	5.214830	5.377112
16 C	0.000000				
17 C	2.788447	0.000000			
18 H	3.395881	2.155887	0.000000		
19 C	1.391822	2.410199	3.867884	0.000000	
20 H	1.082354	3.870728	4.285858	2.153285	0.000000
21 C	2.418124	1.393314	3.400267	1.394688	3.400850
22 H	3.872498	1.084094	2.478396	3.395134	4.954736
23 H	2.144159	3.394454	4.951843	1.084093	2.474256
24 H	3.399760	2.153038	4.297332	2.153809	4.296267
25 C	3.043715	4.747818	3.768417	4.372515	2.871362
26 O	2.985201	4.815937	4.224746	4.153422	2.735681
27 H	4.639477	6.293881	4.951769	6.023335	4.318852
28 N	5.328842	5.502365	3.464700	6.429306	5.637731
29 O	4.885596	4.782059	2.831187	5.849412	5.325514
30 O	6.457932	6.718627	4.662096	7.605479	6.668541
21 C	0.000000				
22 H	2.153059	0.000000			
23 H	2.153514	4.293996	0.000000		
24 H	1.083959	2.483662	2.483096	0.000000	
25 C	5.081524	5.643602	5.077267	6.140915	0.000000
26 O	4.945790	5.734353	4.725946	5.930556	1.213323
27 H	6.737296	7.127024	6.698798	7.815966	2.086572
28 N	6.508414	5.927064	7.406740	7.528433	3.225995
29 O	5.813824	5.157194	6.844486	6.790087	3.101091
30 O	7.724001	7.111962	8.558338	8.744968	4.045495
26 O	0.000000				
27 H	3.145570	0.000000			
28 N	4.112271	3.148756	0.000000		
29 O	3.697167	3.763807	1.221508	0.000000	
30 O	4.902044	3.513437	1.223777	2.171378	0.000000

APPENDIX C

Figure S1: NOESY SPECTRUM OF COMPOUND 1. Using NOESY, the through-space interactions of nearby protons are detected during the mixing time due to Nuclear Overhauser cross relaxation. The cross peaks identify the coupled nuclei and hence can be used to distinguish between *Z* and *E* isomers. The arrow in the spectrum below is pointing at the very faint cross-peak between the methyl signal and the amide N-H signal of the *Z* isomer.

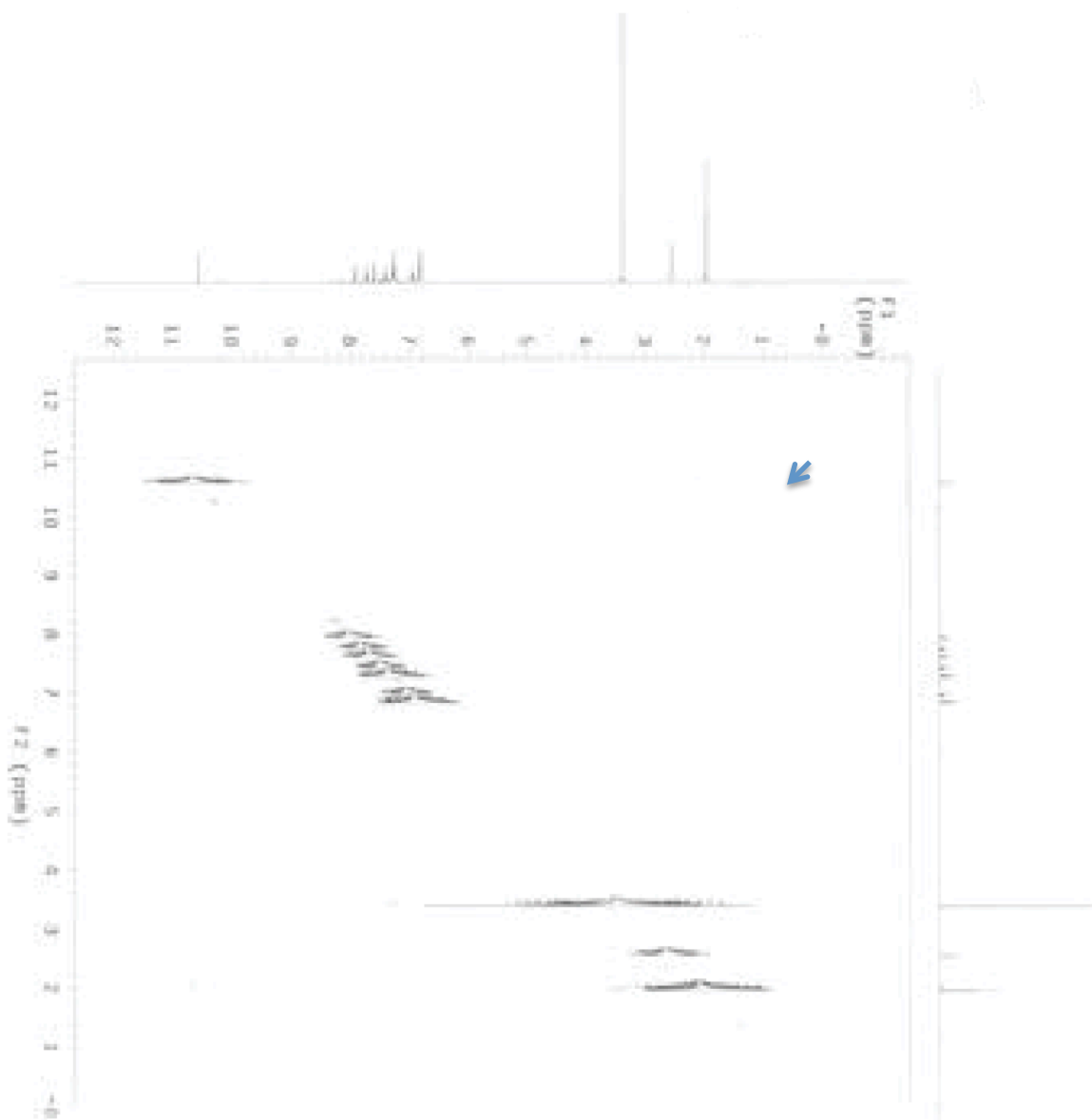
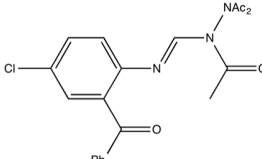
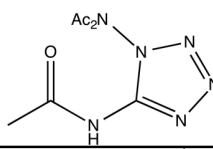
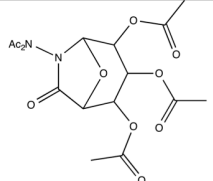
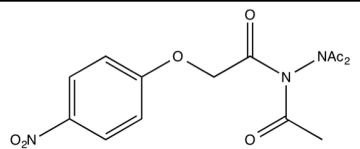
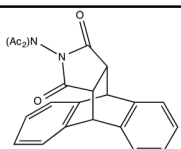
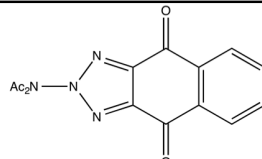
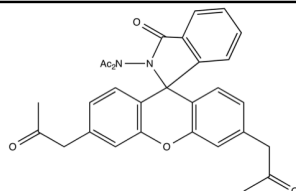
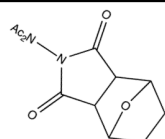


Table S1: Parameters for the N(C(O)Me)₂ Nitrogen of Structurally Characterized N,N-Diacetylhydrazines

Substituents on adjacent N atom to the N(C(O)Me) ₂ Group	N-N (Å)	sum about N(COME) ₂ (°)	Distance of N(COME) ₂ from its plane (Å)	Reference
	1.3883	358.22(1)	0.109	12
	1.381(2)	358.8(1)	0.089	13
	1.400(3)	359.8(1)	0.035	14
	1.398(3) and 1.402(3)	359.1(5) and 359.3(5)	0.077 and 0.071	15 ^a
	1.388(2)	360.0(3)	0.003	16
	1.388(7)	359(1)	0.044	17
	1.391(5)	358.0(6)	0.115	18
	1.383(2)	N/A	N/A	19 ^b
^a Two independent molecules				
^b Incomplete structural data available				

Crystallographic data for compounds 1 – 5.

Table S1: Crystallographic data for compounds 1.

Compound	1
Empirical Formula	C ₁₄ H ₁₃ N ₃ O ₃
T (K)	298
fw (g/mol)	271.27
Crystal System	Triclinic
Space Group	<i>P</i> -1
a (Å)	8.9615(9)
b (Å)	9.1136(9)
c (Å)	17.2404(17)
α (deg)	104.308(1)
β (deg)	90.356(2)
γ (deg)	91.495(2)
V (Å ³)	1363.8(2)
Z	4
density (g/cm ³)	1.321
Reflections collected	8623
Independent reflections	2633
Data/restraints/parameters	2633/0/362
Final R indices [<i>I</i> > 2s(<i>I</i>)] R1	0.042
wR2	0.114
Goodness of fit on F ²	1.04

Table S2: Crystallographic data for compounds **2**.

Compound	2
Empirical Formula	C ₁₆ H ₁₅ N ₃ O ₄
T (K)	298
fw (g/mol)	313.31
Crystal System	Monoclinic
Space Group	<i>P2₁/c</i>
a (Å)	11.0898(9)
b (Å)	9.186(7)
c (Å)	15.4627(12)
α (deg)	90
β (deg)	93.121(1)
γ (deg)	90
V (Å ³)	1575.0(2)
Z	4
density (g/cm ³)	1.321
Reflections collected	17400
Independent reflections	3376
Data/restraints/parameters	3376/0/209
Final R indices [<i>I</i> > 2σ(<i>I</i>)] R1	0.049
wR2	0.154
Goodness of fit on F ²	1.06

Table S3: Crystallographic data for compounds **3**.

Compound	3
Empirical Formula	C ₁₅ H ₁₅ N ₃ O ₂
T (K)	298
fw (g/mol)	269.3
Crystal System	Monoclinic
Space Group	<i>P2₁/c</i>
a (Å)	8.2058()
b (Å)	18.202(2)
c (Å)	9.9424(11)
α (deg)	90
β (deg)	102.588(1)
γ (deg)	90
V (Å ³)	1449.4(3)
Z	4
density (g/cm ³)	1.234
Reflections collected	16396
Independent reflections	3416
Data/restraints/parameters	3416/0/182
Final R indices [<i>I</i> > 2s(<i>I</i>)] R1	0.047
wR2	0.151
Goodness of fit on F ²	1.17

Table S4: Crystallographic data for compounds **4**.

Compound	4
Empirical Formula	C ₁₉ H ₁₅ N ₃ O ₃
T (K)	298
fw (g/mol)	333.34
Crystal System	Monoclinic
Space Group	<i>P2₁/n</i>
a (Å)	9.9767(16)
b (Å)	14.657(2)
c (Å)	12.178(2)
α (deg)	90
β (deg)	112.064(2)
γ (deg)	90
V (Å ³)	1650.4(5)
Z	4
density (g/cm ³)	1.342
Reflections collected	19220
Independent reflections	3971
Data/restraints/parameters	3971/0/230
Final R indices [<i>I</i> > 2σ(<i>I</i>)] R1	0.04
wR2	0.115
Goodness of fit on F ²	1.04

Table S5: Crystallographic data for compounds **5**.

Compound	5
Empirical Formula	C ₁₉ H ₁₅ N ₃ O ₂
T (K)	298
fw (g/mol)	317.34
Crystal System	Triclinic
Space Group	<i>P</i> -1
a (Å)	10.372(4)
b (Å)	11.700(5)
c (Å)	14.688(6)
α (deg)	93.534(5)
β (deg)	102.257(5)
γ (deg)	109.276(5)
V (Å ³)	1627.2(11)
Z	4
density (g/cm ³)	1.295
Reflections collected	14352
Independent reflections	7481
Data/restraints/parameters	7481/0/433
Final R indices [<i>I</i> > 2σ(<i>I</i>)] R1	0.045
wR2	0.138
Goodness of fit on F ²	1.03

Calculated Gas Phase Distance Matrix for the Hydrazine Derivative 3

Distance matrix (angstroms):					
	1	2	3	4	5
1 N	0.000000				
2 N	1.404281	0.000000			
3 H	2.002371	1.017214	0.000000		
4 C	1.411673	2.450708	2.674225	0.000000	
5 C	2.441832	2.897997	2.934645	1.403461	0.000000
6 C	2.453082	3.691511	3.838347	1.405006	2.414099
7 C	3.716796	4.271254	4.189732	2.426972	1.392564
8 H	2.677693	2.611869	2.647527	2.162267	1.082403
9 C	3.721559	4.840390	4.862762	2.425404	2.779340
10 H	2.687174	4.007048	4.218088	2.158392	3.398042
11 C	4.228914	5.089290	5.021585	2.817296	2.421663
12 H	4.580629	4.912626	4.768302	3.402434	2.140733
13 H	4.588784	5.779352	5.796066	3.401312	3.863610
14 H	5.312244	6.146299	6.032142	3.900632	3.404345
15 C	1.404857	2.373523	3.052205	2.477826	3.727855
16 C	2.430229	3.549045	4.326112	3.066801	4.282951
17 C	2.472439	2.902716	3.396594	3.649490	4.876173
18 C	3.708012	4.690996	5.467441	4.416852	5.666142
19 H	2.630159	3.828270	4.613364	2.851574	3.876424
20 C	3.744794	4.219692	4.767996	4.857457	6.139369
21 C	4.230923	4.968775	5.657112	5.170671	6.475293
22 H	4.567132	5.606873	6.418415	5.102265	6.279784
23 H	4.602278	4.873732	5.306749	5.753379	7.009197
24 H	5.313267	6.016616	6.701605	6.234420	7.543289
25 H	1.996725	1.015018	1.669584	2.783480	2.830487
26 N	2.960137	2.857163	2.942888	4.087898	5.134711
27 O	2.851025	2.754888	2.454610	3.654817	4.584837
28 O	4.040317	3.675996	3.746601	5.250559	6.223418
	6	7	8	9	10
6 C	0.000000				
7 C	2.780829	0.000000			
8 H	3.401955	2.140645	0.000000		
9 C	1.389899	2.399817	3.861597	0.000000	
10 H	1.082053	3.862460	4.303455	2.143399	0.000000
11 C	2.422414	1.392303	3.394180	1.394772	3.398075
12 H	3.865130	1.084371	2.447877	3.387279	4.946706
13 H	2.138177	3.386397	4.945872	1.084426	2.453153
14 H	3.404312	2.155556	4.287360	2.157620	4.291626
15 C	2.937809	4.889702	4.047388	4.317771	2.636911
16 C	3.182660	5.266084	4.715794	4.417216	2.760483
17 C	4.019690	6.064099	5.103596	5.401609	3.517022
18 C	4.349684	6.613634	6.091694	5.528604	3.693036
19 H	2.934105	4.708726	4.367245	3.966176	2.774958
20 C	5.024807	7.282824	6.401057	6.374509	4.325160
21 C	5.160921	7.522215	6.827111	6.428189	4.396036
22 H	4.910678	7.107714	6.745326	5.933308	4.274746
23 H	5.931085	8.171979	7.219626	7.272190	5.208140
24 H	6.147939	8.564288	7.899680	7.367984	5.323257
25 H	4.152441	4.194712	2.231041	5.171960	4.623486
26 N	4.583790	6.329183	5.240413	5.894044	4.213128
27 O	4.102995	5.658022	4.760581	5.279635	3.874785
28 O	5.803904	7.460981	6.203330	7.117242	5.411375
	11	12	13	14	15
11 C	0.000000				
12 H	2.151495	0.000000			
13 H	2.153040	4.289836	0.000000		
14 H	1.083337	2.487208	2.488366	0.000000	
15 C	5.141098	5.830581	4.960718	6.201490	0.000000
16 C	5.333545	6.225211	4.911563	6.324220	1.404236
17 C	6.297876	6.993783	5.944923	7.349551	1.406489
18 C	6.566862	7.587965	5.840163	7.512057	2.434505
19 H	4.756410	5.624952	4.494974	5.694306	2.141912
20 C	7.397523	8.244821	6.769587	8.421119	2.448367
21 C	7.514932	8.508334	6.720991	8.493152	2.829410
22 H	6.967254	8.062081	6.142448	7.837506	3.408641
23 H	8.300809	9.120459	7.638815	9.321508	3.412741
24 H	8.500116	9.557169	7.572614	9.450553	3.912274
25 H	5.204686	4.671449	6.180579	6.225312	3.030436
26 N	6.667596	7.180349	6.481962	7.703622	2.516905
27 O	5.969505	6.481746	5.878371	6.958432	2.880510
28 O	7.865921	8.262998	7.699281	8.904089	3.536544
	16	17	18	19	20
16 C	0.000000				
17 C	2.395491	0.000000			
18 C	1.387695	2.764414	0.000000		
19 H	1.082923	3.376232	2.147879	0.000000	
20 C	2.780624	1.394110	2.401858	3.862838	0.000000
21 C	2.418408	2.407030	1.396944	3.399691	1.386935
22 H	2.138967	3.848422	1.084056	2.464877	3.386401
23 H	3.862036	2.135176	3.395096	4.944091	1.081856
24 H	3.401470	3.389681	2.160530	4.296878	2.144959
25 H	3.959364	3.725516	5.140799	4.030715	4.953377
26 N	3.768580	1.474128	4.233016	4.649279	2.436048
27 O	4.218419	2.317466	4.922382	4.933367	3.454728
28 O	4.679462	2.309881	4.918794	5.621761	2.757018

	21	22	23	24	25
21 C	0.000000				
22 H	2.154945	0.000000			
23 H	2.158945	4.298636	0.000000		
24 H	1.082889	2.492574	2.494337	0.000000	
25 H	5.561320	5.952624	5.646309	6.592122	0.000000
26 N	3.720959	5.316713	2.593062	4.577881	3.804797
27 O	4.625811	5.982282	3.688662	5.537265	3.758915
28 O	4.132768	5.981664	2.457049	4.801680	4.514392
	26	27	28		
26 N	0.000000				
27 O	1.226069	0.000000			
28 O	1.223902	2.168133	0.000000		

Calculated Gas Phase Vibrational Modes for
the Urea Derivative **2a**

Mode	Frequencies (cm ⁻¹)	Frc Consts	IR Inten
1	33.1457	0.0039	2.2108
2	38.4349	0.0039	0.2093
3	64.3345	0.0187	0.784
4	68.0946	0.022	1.5011
5	80.2043	0.0244	1.2365
6	100.1316	0.0326	5.9019
7	123.4009	0.0458	0.1623
8	138.5151	0.0683	3.3771
9	198.8808	0.1589	3.8207
10	243.3459	0.1641	3.1234
11	255.4305	0.2321	3.3194
12	323.6117	0.3969	1.7486
13	328.2752	0.3999	2.1313
14	370.2607	0.1977	31.477
15	384.7676	0.1475	67.1731
16	415.9735	0.3823	2.3067
17	418.794	0.3055	0.2676
18	433.8224	0.6147	13.2076
19	466.1839	0.3967	35.8015
20	507.3131	0.2505	26.9998
21	515.6367	0.3979	22.3714
22	531.4043	0.6321	6.1133
23	584.3634	0.9602	0.6807
24	616.2613	0.8463	37.443
25	633.1772	1.4828	0.3174
26	651.892	1.5463	11.6701
27	683.9214	1.8029	9.5837
28	705.5586	0.5275	40.0973
29	720.2328	1.2422	27.3554
30	738.266	1.6459	5.7824
31	755.03	2.6285	7.7777
32	764.5916	0.7009	24.4731
33	778.1948	0.7547	23.2642
34	797.8669	0.8513	20.1845
35	842.4012	0.5244	1.2133
36	865.9117	4.5015	27.3036
37	890.1216	0.699	1.5938
38	921.0488	0.7428	1.6006
39	949.2307	2.5843	3.0281
40	978.1886	0.7962	0.1836
41	980.6263	0.7761	0.3854
42	998.5901	0.7689	0.0728
43	1006.3017	0.7907	0.6588
44	1018.7516	3.5354	0.7312
45	1028.3964	3.723	3.2721
46	1050.576	1.3498	6.6502
47	1066.3821	1.6686	4.7467
48	1094.972	1.4164	39.344
49	1104.443	1.1603	10.6652
50	1111.4669	1.7136	3.4867
51	1163.9597	1.4208	6.8377
52	1181.9515	0.9152	0.0935
53	1186.6196	0.9267	2.3494
54	1198.6031	0.9636	0.8969
55	1241.7655	2.9236	16.7522
56	1288.4742	1.7897	4.2672
57	1299.0096	4.6394	83.4441
58	1332.1323	5.4077	16.4989
59	1339.5035	4.5319	4.7395
60	1352.7371	2.2188	141.5114
61	1358.6276	2.8989	207.9538
62	1384.3488	12.8384	301.9484
63	1472.7932	2.8547	9.2505
64	1484.307	2.9507	1.082
65	1510.7736	3.5347	52.1435
66	1525.1567	3.0833	62.1991
67	1588.8226	14.6256	182.6518
68	1612.6193	9.3564	77.4964
69	1617.7555	1.9246	131.0926
70	1626.8477	9.2426	3.2786
71	1636.1733	8.7968	72.8357
72	1644.3373	9.672	74.0599
73	1771.8003	15.1847	446.2022
74	3165.9639	6.4108	0.2988
75	3175.7622	6.474	10.2451
76	3178.5867	6.472	2.2588
77	3187.5242	6.5479	23.5252
78	3193.0227	6.5523	4.8508
79	3198.511	6.5963	4.3086
80	3200.0515	6.6093	2.9027
81	3202.3691	6.6171	2.3901
82	3213.7229	6.6603	2.0054
83	3585.4053	7.9241	37.7605
84	3702.4248	8.9074	52.5395

Calculated Gas Phase Vibrational Modes for
the Hydrazine Derivative **3**

Mode	Frequencies (cm ⁻¹)	Force Consts	IR Inten
1	29.9344	0.0035	2.8088
2	48.9481	0.0059	1.1145
3	66.8574	0.0251	0.8321
4	83.3668	0.0199	1.3562
5	141.0308	0.0507	5.9462
6	145.4759	0.0558	5.7413
7	193.1974	0.1121	2.5333
8	236.7136	0.1787	0.7106
9	242.6209	0.1879	0.822
10	323.2783	0.3888	0.7835
11	346.7466	0.3689	1.327
12	353.9113	0.4498	2.9718
13	398.4064	0.1239	18.6046
14	415.8366	0.365	8.8475
15	421.8721	0.3283	4.0254
16	436.021	0.4462	3.7756
17	474.0007	0.5442	1.736
18	516.2391	0.4935	14.0764
19	573.6873	0.8537	1.8949
20	597.4318	1.0069	7.0507
21	625.5101	1.2228	4.0419
22	632.0955	1.495	0.2251
23	669.7276	1.5987	5.3605
24	704.9406	0.5596	31.2273
25	720.7612	1.2292	19.6301
26	744.9294	1.7803	6.862
27	762.0113	0.6292	63.4828
28	773.6458	0.6794	30.2121
29	796.7335	1.0055	7.3504
30	831.9942	0.5204	14.0194
31	843.2208	0.7232	131.3471
32	868.465	3.1845	23.458
33	884.6169	0.6966	0.5464
34	904.4206	0.7049	4.4631
35	950.4088	2.2429	16.2939
36	973.8085	0.7962	0.9876
37	977.446	0.7615	0.0735
38	994.2583	0.7485	0.4091
39	998.5518	0.7703	0.629
40	1008.559	3.3529	2.9137
41	1051.733	1.4495	1.1687
42	1059.438	1.6123	12.7545
43	1098.841	2.5873	2.2417
44	1107.582	1.3082	5.7731
45	1141.044	1.8532	19.5599
46	1165.119	1.3482	8.1451
47	1182.799	0.9098	2.0202
48	1185.861	0.9309	5.3307
49	1207.924	0.9821	14.2232
50	1269.323	2.1067	77.4721
51	1294.852	2.2233	64.2708
52	1310.237	2.347	151.2378
53	1325.458	1.6171	28.183
54	1342.614	7.5329	18.3937
55	1353.922	2.8495	6.65
56	1368.114	2.5236	64.1853
57	1381.227	6.6052	186.6205
58	1471.334	2.8744	2.8909
59	1488.945	3.1591	1.5436
60	1512.518	3.5991	60.3306
61	1523.222	3.0007	134.8012
62	1576.234	12.8026	242.4371
63	1610.043	9.4056	66.105
64	1619.602	8.9406	6.3976
65	1634.965	8.9664	217.2894
66	1644.416	8.2401	34.0393
67	1678.308	1.955	38.701
68	3165.501	6.4088	4.6339
69	3172.359	6.4588	9.0463
70	3174.897	6.4568	4.431
71	3189.696	6.5472	23.0365
72	3192.307	6.5475	7.8574
73	3196.945	6.5846	10.2336
74	3198.572	6.6008	3.4361
75	3201.59	6.6079	1.6184
76	3214.093	6.6609	2.1503
77	3461.604	7.3752	2.0777
78	3552.286	8.1758	5.2846

Supplementary Table 1 Solvation Effects for Hofmann Intermediates and Transition States

	Gas Phase		In water	
	Absolute Energy A.U.	Relative energy (kcal/mol)	Absolute Energy A.U.	Relative Energy (kcal/mol)
2-Nitrophenylphenyl				
Singlet Nitrene	-890.743836	0	-890.7665396	0
Transition State	-890.7314099	+7.80	-890.7499343	+10.4
Isocyanate	-891.810805	-42.1	-890.8240544	-36.1
Triplet Nitrene	-890.759988	-10.1	-890.776478	-6.24

Energies are not zero point corrected.

Crystallographic data for compounds 1 – 3.

Table S2: Crystallographic data for compound 1.

Compound	1
Empirical Formula	C ₁₃ H ₁₉ N ₃ Na ₂ O ₁₁ S
T (K)	293
fw (g/mol)	471.35
Crystal System	Monoclinic
Space Group	<i>P21/c</i>
a (Å)	20.144(3)
b (Å)	7.7678(10)
c (Å)	13.2545(17)
α (deg)	90
β (deg)	106.5670(10)
γ (deg)	90
V (Å ³)	1987.9(4)
Z	4
density (g/cm ³)	1.575
Reflections collected	4673
Independent reflections	2191
Data/restraints/parameters	4673/0/311
Final R indices [<i>I</i> > 2 σ (<i>I</i>)] R1	0.032
wR2	0.105
Goodness of fit on F ²	1.07

Table S3: Crystallographic data for compound 2a.

Compound	2a
Empirical Formula	C ₁₃ H ₁₁ N ₃ O ₃
T (K)	100
fw (g/mol)	257.25
Crystal System	Triclinic
Space Group	<i>P</i> -1
a (Å)	6.9053(11)
b (Å)	8.1316(13)
c (Å)	11.2989(17)
α (deg)	79.233(2)
β (deg)	85.084(2)
γ (deg)	74.963(2)
V (Å ³)	601.47(16)
Z	2
density (g/cm ³)	1.42
Reflections collected	6906
Independent reflections	2728
Data/restraints/parameters	2728/0/172
Final R indices [<i>I</i> > 2σ(<i>I</i>)] R1	0.038
wR2	0.101
Goodness of fit on F ²	1.04

Table S4: Crystallographic data for compound 2b.

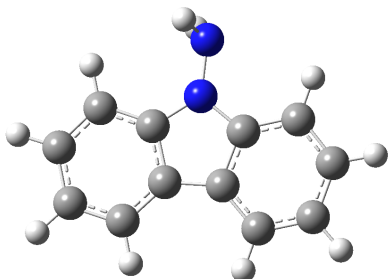
Compound	2b
Empirical Formula	C ₁₅ H ₁₃ N ₃ O ₅
T (K)	100
fw (g/mol)	315.28
Crystal System	Triclinic
Space Group	<i>P</i> -1
a (Å)	7.7722(8)
b (Å)	10.1203(11)
c (Å)	10.6799(11)
α (deg)	102.479(1)
β (deg)	103.182(1)
γ (deg)	105.813(1)
V (Å ³)	751.45
Z	2
density (g/cm ³)	1.393
Reflections collected	8662
Independent reflections	3406
Data/restraints/parameters	3406/0/208
Final R indices [<i>I</i> > 2σ(<i>I</i>)] R1	0.041
wR2	0.115
Goodness of fit on F ²	1.05

Table S5: Crystallographic data for compound 3.

Compound	3
Empirical Formula	C ₁₂ H ₁₁ N ₃ O ₂
T (K)	100
fw (g/mol)	229.24
Crystal System	Orthorhombic
Space Group	<i>Pna2₁</i>
a (Å)	9.9468(10)
b (Å)	14.1301(13)
c (Å)	7.8945(8)
α (deg)	90
β (deg)	90
γ (deg)	90
V (Å ³)	1109.57
Z	4
density (g/cm ³)	1.372
Reflections collected	12091
Independent reflections	2583
Data/restraints/parameters	2583/1/162
Final R indices [<i>I</i> > 2 σ (<i>I</i>)] R1	0.034
wR2	0.087
Goodness of fit on F ²	1.02

APPENDIX D

Figure S1: Calculated structure of 9-aminocarbazole in the gas phase.



N-N = 1.39320 Ang. N-H = 1.01654 Ang N-N-H = 110.16201, 110.16151 H-N-H = 109.30506

C-N-N-H = 60.35514

		55		56		57					
		A		A		A					
Frequencies --		1656.3516				1693.2437				3163.0079	
Red. masses --		5.3918				1.2076				1.0854	
Frc consts --		8.7154				2.0399				6.3981	
IR Inten --		8.6131				27.2234				0.6086	
Atom	AN	X	Y	Z	X	Y	Z	X	Y	Z	
1	6	-0.11	0.02	0.00	0.00	-0.01	0.00	0.02	0.02	0.00	
2	6	0.20	0.05	0.00	0.00	0.00	0.00	0.01	-0.03	0.00	
3	6	-0.20	-0.05	0.00	-0.01	-0.01	0.00	0.00	0.00	0.00	
4	6	0.24	-0.01	0.00	0.00	0.02	0.00	0.00	0.00	0.00	
5	6	-0.21	-0.04	0.00	-0.01	-0.01	0.00	0.01	-0.03	0.00	
6	6	0.08	0.06	0.00	0.01	0.01	0.00	-0.04	0.01	0.00	
7	1	0.03	-0.12	0.00	0.00	0.00	0.00	-0.29	-0.29	0.00	
8	1	-0.28	-0.09	0.00	-0.01	0.00	0.00	-0.10	0.38	0.00	
9	1	0.24	0.10	0.00	0.02	0.00	0.00	-0.10	0.33	0.00	
10	1	0.06	-0.08	0.00	0.00	-0.02	0.00	0.45	-0.11	0.00	
11	6	0.19	-0.06	0.00	0.03	0.00	0.00	0.00	0.00	0.00	
12	6	-0.19	0.05	0.00	-0.03	0.00	0.00	0.01	0.03	0.00	
13	6	-0.20	0.00	0.00	-0.07	0.00	0.00	0.00	0.00	0.00	
14	6	0.10	0.01	0.00	0.02	0.01	0.00	0.02	-0.02	0.00	
15	1	0.26	-0.07	0.00	0.04	-0.02	0.00	-0.09	-0.34	0.00	
16	6	0.20	-0.05	0.00	0.04	0.00	0.00	0.00	0.01	0.00	
17	6	-0.08	0.07	0.00	-0.01	0.00	0.00	-0.02	-0.01	0.00	

18	1	-0.02	-0.12	0.00	-0.01	-0.02	0.00	-0.24	0.24	0.00
19	1	-0.23	0.08	0.00	-0.04	0.02	0.00	-0.02	-0.07	0.00
20	1	-0.05	-0.10	0.00	-0.01	0.00	0.00	0.29	0.07	0.00
21	7	-0.02	0.00	0.00	0.05	-0.03	0.00	0.00	0.00	0.00
22	7	-0.01	0.04	0.00	0.01	-0.06	0.00	0.00	0.00	0.00
23	1	0.15	-0.27	-0.20	-0.25	0.53	0.37	0.00	0.00	0.00
24	1	0.15	-0.27	0.20	-0.25	0.53	-0.37	0.00	0.00	0.00

58

59

60

A

A

A

Frequencies -- 3163.7531

3169.7971

3172.4073

Red. masses -- 1.0856

1.0885

1.0899

Frc consts -- 6.4020

6.4441

6.4624

IR Inten -- 0.1384

4.6753

7.7225

Atom	AN	X	Y	Z	X	Y	Z	X	Y	Z
1	6	0.02	0.02	0.00	0.01	0.02	0.00	0.01	0.01	0.00
2	6	0.00	-0.02	0.00	0.01	-0.06	0.00	0.00	-0.02	0.00
3	6	0.00	0.00	0.00	0.00	0.00	0.00	0.00	0.00	0.00
4	6	0.00	0.00	0.00	0.00	0.00	0.00	0.00	0.00	0.00
5	6	0.01	-0.02	0.00	-0.01	0.04	0.00	0.00	0.01	0.00
6	6	-0.03	0.01	0.00	0.03	-0.01	0.00	0.01	0.00	0.00
7	1	-0.19	-0.20	0.00	-0.19	-0.20	0.00	-0.10	-0.10	0.00
8	1	-0.05	0.19	0.00	-0.18	0.64	0.00	-0.05	0.19	0.00
9	1	-0.09	0.28	0.00	0.15	-0.50	0.00	0.05	-0.17	0.00
10	1	0.36	-0.08	0.00	-0.32	0.08	0.00	-0.07	0.02	0.00
11	6	0.00	0.00	0.00	0.00	0.00	0.00	0.00	0.00	0.00
12	6	-0.01	-0.04	0.00	0.00	0.01	0.00	-0.01	-0.06	0.00
13	6	0.00	0.00	0.00	0.00	0.00	0.00	0.00	0.00	0.00
14	6	-0.03	0.03	0.00	0.00	0.00	0.00	0.00	0.00	0.00
15	1	0.11	0.43	0.00	-0.05	-0.17	0.00	0.17	0.64	0.00
16	6	0.00	-0.01	0.00	0.00	0.00	0.00	0.01	0.01	0.00
17	6	0.04	0.01	0.00	0.02	0.00	0.00	-0.05	-0.01	0.00
18	1	0.34	-0.34	0.00	0.04	-0.04	0.00	0.02	-0.03	0.00
19	1	0.03	0.10	0.00	0.02	0.06	0.00	-0.05	-0.16	0.00
20	1	-0.44	-0.11	0.00	-0.24	-0.06	0.00	0.63	0.16	0.00
21	7	0.00	0.00	0.00	0.00	0.00	0.00	0.00	0.00	0.00
22	7	0.00	0.00	0.00	0.00	0.00	0.00	0.00	0.00	0.00
23	1	0.00	0.00	0.00	0.00	0.00	0.00	0.00	0.00	0.00
24	1	0.00	0.00	0.00	0.00	0.00	0.00	0.00	0.00	0.00

61

62

63

A

A

A

Frequencies --	3179.6731	3187.4364	3190.9406
Red. masses --	1.0932	1.0949	1.0969
Frc consts --	6.5117	6.5543	6.5802
IR Inten --	20.8432	25.5245	19.5325

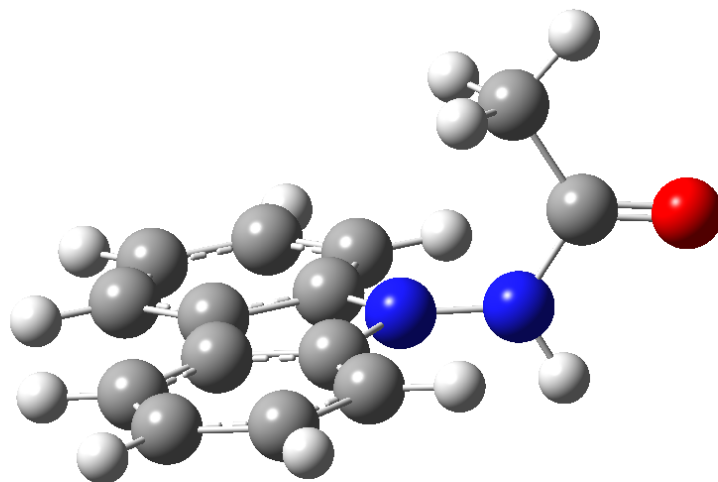
Atom	AN	X	Y	Z	X	Y	Z	X	Y	Z
1	6	-0.03	-0.02	0.00	0.00	0.00	0.00	-0.04	-0.04	0.00
2	6	0.01	-0.04	0.00	0.00	0.00	0.00	0.01	-0.03	0.00
3	6	0.00	0.00	0.00	0.00	0.00	0.00	0.00	0.00	0.00
4	6	0.00	0.00	0.00	0.00	0.00	0.00	0.00	0.00	0.00
5	6	0.02	-0.05	0.00	0.00	0.00	0.00	-0.01	0.03	0.00
6	6	0.04	-0.01	0.00	-0.01	0.00	0.00	-0.05	0.01	0.00
7	1	0.29	0.29	0.00	0.04	0.04	0.00	0.49	0.50	0.00
8	1	-0.12	0.44	0.00	0.00	-0.01	0.00	-0.10	0.33	0.00
9	1	-0.18	0.60	0.00	0.01	-0.03	0.00	0.08	-0.28	0.00
10	1	-0.46	0.10	0.00	0.06	-0.01	0.00	0.53	-0.13	0.00
11	6	0.00	0.00	0.00	0.00	0.00	0.00	0.00	0.00	0.00
12	6	0.00	0.00	0.00	0.01	0.04	0.00	0.00	0.00	0.00
13	6	0.00	0.00	0.00	0.00	0.00	0.00	0.00	0.00	0.00
14	6	0.00	0.00	0.00	-0.05	0.05	0.00	0.00	0.00	0.00
15	1	0.01	0.03	0.00	-0.11	-0.42	0.00	0.01	0.05	0.00
16	6	0.00	0.00	0.00	0.01	0.02	0.00	0.00	0.00	0.00
17	6	0.00	0.00	0.00	-0.03	-0.01	0.00	0.00	0.00	0.00
18	1	0.03	-0.03	0.00	0.55	-0.55	0.00	-0.04	0.04	0.00
19	1	0.00	-0.02	0.00	-0.07	-0.24	0.00	0.01	0.03	0.00
20	1	0.03	0.01	0.00	0.33	0.09	0.00	-0.01	0.00	0.00
21	7	0.00	0.00	0.00	0.00	0.00	0.00	0.00	0.00	0.00
22	7	0.00	0.00	0.00	0.00	0.00	0.00	0.00	0.00	0.00
23	1	0.00	0.00	0.00	0.00	0.00	0.00	0.00	0.00	0.00
24	1	0.00	0.00	0.00	0.00	0.00	0.00	0.00	0.00	0.00

	64	65	66
	A	A	A

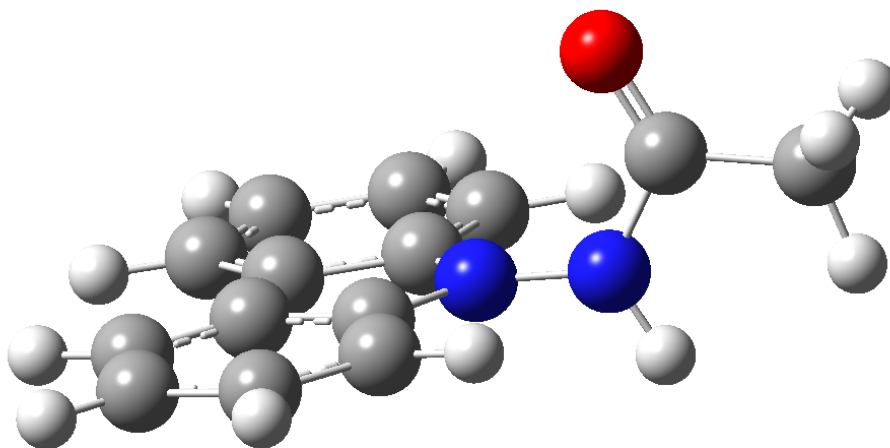
Frequencies --	3201.6935	3463.7582	3541.9821
Red. masses --	1.0939	1.0449	1.0993
Frc consts --	6.6069	7.3864	8.1257
IR Inten --	6.1253	3.4808	3.3023

The calculated values of the N-N bond and the IR frequencies associated with the -NH_2 group are smaller than those experimentally determined.

Figure S2: Calculated structure for *N*-(9*H*-carbazol-9-yl)acetamide (1) E and Z isomers with relative energies.



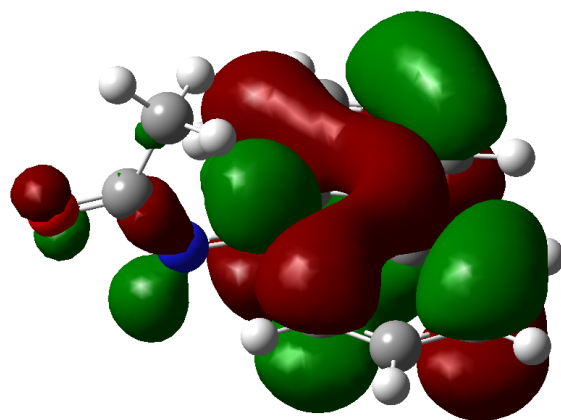
E = -725.6410542 AU, Rel E = 0



E = -725.6383073 AU, Rel E. = +1.72 kcal/mol

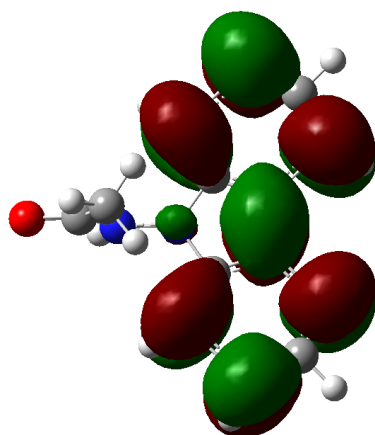
Figure S3: Calculated frontier molecular orbitals for *N*-(9*H*-carbazol-9-yl)acetamide (1). Interpretations of the results are below each diagram.

HOMO



π -character for carbazole, antibonding with respect to N-N bond, large N carbazole component and weakly N lone pair and N-C.

LUMO



Carbazole anti-bonding with N-lone pair.

Crystallographic data for AC and compounds 1 – 3.

Table S1: Crystallographic data for AC.

Compound	AC
Empirical Formula	C ₁₂ H ₁₀ N ₂
T (K)	298
fw (g/mol)	182.22
Crystal System	Orthorhombic
Space Group	<i>Pca2₁</i>
a (Å)	17.647(4)
b (Å)	9.271(2)
c (Å)	5.8002(13)
α (deg)	90
β (deg)	90
γ (deg)	90
V (Å ³)	949.0(4)
Z	4
density (g/cm ³)	1.275
Reflections collected	4370
Independent reflections	680
Data/restraints/parameters	1529/1/156
Final R indices [<i>I</i> > 2s(<i>I</i>)] R1	0.056
wR2	0.145
Goodness of fit on F ²	1.08

Table S2: Crystallographic data for compounds 1.

Compound	1
Empirical Formula	C ₁₄ H ₁₂ N ₂ O
T (K)	298
fw (g/mol)	224.26
Crystal System	Orthorhombic
Space Group	<i>Pbca</i>
a (Å)	15.601(11)
b (Å)	9.134(6)
c (Å)	16.882(12)
α (deg)	90
β (deg)	90
γ (deg)	90
V (Å ³)	2406(3)
Z	8
density (g/cm ³)	1.238
Reflections collected	16263
Independent reflections	1529
Data/restraints/parameters	1529/0/156
Final R indices [<i>I</i> > 2s(<i>I</i>)] R1	0.055
wR2	0.166
Goodness of fit on F ²	1.03

Table S3: Crystallographic data for compounds 2.

Compound	2
Empirical Formula	C ₁₆ H ₁₄ N ₂ O ₂
T (K)	298
fw (g/mol)	266.29
Crystal System	Monoclinic
Space Group	<i>P2₁/c</i>
a (Å)	9.1176(18)
b (Å)	26.396(5)
c (Å)	11.475(2)
α (deg)	90
β (deg)	89.97(2)
γ (deg)	90
V (Å ³)	2761.6(9)
Z	8
density (g/cm ³)	1.281
Reflections collected	20051
Independent reflections	3536
Data/restraints/parameters	3536/0/362
Final R indices [<i>I</i> > 2s(<i>I</i>)] R1	0.066
wR2	0.205
Goodness of fit on F ²	0.90

Table S4: Crystallographic data for compounds 3.

Compound	3
Empirical Formula	C ₁₉ H ₁₄ N ₂ O
T (K)	298
fw (g/mol)	286.32
Crystal System	Monoclinic
Space Group	<i>P2₁/n</i>
a (Å)	9.4449(11)
b (Å)	18.122(2)
c (Å)	9.6388(16)
α (deg)	90
β (deg)	119.308(1)
γ (deg)	90
V (Å ³)	1438.6(3)
Z	4
density (g/cm ³)	1.322
Reflections collected	8952
Independent reflections	1415
Data/restraints/parameters	1415/0/143
Final R indices [<i>I</i> > 2s(<i>I</i>)] R1	0.053
wR2	0.131
Goodness of fit on F ²	1.09

APPENDIX E

Table S1: Crystallographic data for 1-Phenylbenzotriazole.

Compound	1-Phenylbenzotriazole
Empirical Formula	C ₁₂ H ₉ N ₃
T (K)	298
fw (g/mol)	195.22
Crystal System	Orthorhombic
Space Group	<i>P2₁2₁2₁</i>
a (Å)	6.4825(9)
b (Å)	10.7002(15)
c (Å)	14.492(2)
α (deg)	90
β (deg)	90
γ (deg)	90
V (Å ³)	1005.2(2)
Z	4
density (g/cm ³)	1.29
Reflections collected	11874
Independent reflections	2411
Data/restraints/parameters	2411/0/137
Final R indices [<i>I</i> > 2s(<i>I</i>)] R1	0.032
wR2	0.08
Goodness of fit on F ²	1.04

Table S2: Crystallographic data for compound 1.

Compound	1
Empirical Formula	C ₅₆ H ₄₄ N ₂ O ₂ P ₂ Ru
T (K)	298
fw (g/mol)	939.94
Crystal System	Triclinic
Space Group	<i>P</i> -1
a (Å)	12.71(4)
b (Å)	12.91(4)
c (Å)	18.01(5)
α (deg)	73.71(4)
β (deg)	83.07(4)
γ (deg)	63.21(3)
V (Å ³)	2532(12)
Z	2
density (g/cm ³)	1.29
Reflections collected	16133
Independent reflections	5494
Data/restraints/parameters	5494/0/570
Final R indices [<i>I</i> > 2σ(<i>I</i>)] R1	0.076
wR2	0.266
Goodness of fit on F ²	1.06